Optimizing Growth of Iron-Oxidizing Bacteria for Acid Mine Drainage Remediation

A thesis presented to

the faculty of

the Russ College of Engineering and Technology of Ohio University

In partial fulfillment

of the requirements for the degree

Master of Science

Anan Almomani

August 2023

This thesis titled

Optimizing Growth of Iron-Oxidizing Bacteria for Acid Mine Drainage Remediation

by

ANAN ALMOMANI

has been approved for

the Civil and Environmental Engineering

and the Russ College of Engineering and Technology by

Guy Riefler

Professor of Civil and Environmental Engineering

Patrick Fox

Dean, Russ College of Engineering and Technology

Abstract

ALMOMANI, ANAN. M.S., August 2023, Master of Science in Civil and Environmental Engineering.

Optimizing Growth of Iron-Oxidizing Bacteria for Acid Mine Drainage Remediation

Director of Thesis: Dr. Guy Riefler

The effects of pH, nutrients, and organic carbon on iron oxidation rates by mixed cultures of iron-oxidizing bacteria collected from three different extremely acidic AMD sites were investigated for the possibility of remediating the Truetown AMD at the Sunday creek, OH. Four values of pH (2.0, 2.5, 3.0, and 4.0), four concentrations of ammonium (0.01 M, 0.05 M, 0.1 M, and 0.5 M), five concentrations of phosphate (0.1 mM, 0.5 mM, 1.0 mM, 5.0 mM, and 10.0 mM), and three concentrations of glucose (0.05 M, 0.1 M, and 0.2 M) were tested. The best pH, ammonium concentration, and phosphate concentration were found to be 2.5, 0.1 M, and 5.0 mM, respectively, resulting in an iron oxidation rate of 0.570 hr^{-1}, while the organic carbon resulted in approximately 52% inhibition after only one sub-culture. The iron oxidation rates achieved in this study surpassed the maximum iron oxidation rate achieved in most studies reported in the literature except for two studies where they adopted significantly different operation conditions. The best culture was found to be the one collected from Wolf Run site of predominantly *A. ferrooxidans.* Applying these results to Truetown AMD achieved a 12-fold increase in biotic iron oxidation rates, and a 1327-fold increase compared to the abiotic iron oxidation rates at Truetown site. In conclusion, iron-oxidizing bacteria, and nutrient addition significantly enhanced iron oxidation rates at very low pH. With further economical and operational optimization,

AMD remediation by microorganisms can become a fast, sustainable, and low-cost treatment method exceeding other available AMD remediation techniques.

Dedication

To the curious kid in me, who lives on learning and asking questions. To the dreaming soul in my heart, striving to leave the world a better place. To my mom, for her unconditional love and support. To my undergrad advisor, for believing in me when no one else did, for making me believe that this journey was possible.

Acknowledgments

I want to thank Dr. Karen Coschigano and her team for conducting the DNA extraction for further species analysis.

A sincere appreciation for Hannah Schulz, an undergraduate researcher, who helped me with washing more than 3000 iron measurement vials throughout this study.

Last but never least, Dr. Riefler, I want to deeply thank you for giving me this opportunity and allowing me to live the best 2 years of my life doing what I love. Learning from you was a unique experience full of joy and passion! I enjoyed every single class, course, meeting, lab work, and field trip I took/had with you. Thank you for your amazing mentoring, humbleness, patience, and most importantly, thank you for your contagious passion! You are one of greatest teachers I have ever met in my life. I was, and always will be, honored to work with you!

Table of Contents

Page

List of Tables

Page

List of Figures

Chapter 1: Introduction

In the past 200 years, humanity dedicated their efforts and intelligence to create a better and easier version of life; the life we know today. Although life has become more convenient, this evolution has come with a cost, a cost that was not addressed at the beginning, causing the planet to pay the price.

"What is the price of ignorance?" A question that I ended up asking myself while I was trying to find the reason behind this work. They say what you do not know cannot hurt you. Well, when it comes to environmental disasters, you always wish that you have known better.

This is why we learn; this is why I did this work; and this is why you are reading this now. Knowledge is the most powerful tool anyone can obtain. It helps us build a better world, avoid regretful mistakes, and sometimes, if we got lucky, fix the past ones.

Generation of Acid Mine Drainage

Background for this work goes back to one of the most well-known industries in the United States for over two centuries, coal mining. Coal mining began in the early 1700s in Ohio and Pennsylvania before the rapid spread of this industry to other states (National Academies of Sciences et al., 2018). By 1980, more than 5200 coal mines were documented in the US with more than 2400 underground mines and 2800 surface mines (National Academies of Sciences et al., 2018). The lack of environmental knowledge in the 1700s led to the lack of awareness about the environmental impacts of this industry and therefore lack of environmental regulations. Before any environmental regulations, surface coal mining, involving scraping the topsoil layer, and underground coal mining, involving opening shafts into the earth that followed the coal seams, did not follow any restrictions

or protocols regarding operation and closure, and were later called abandoned mine lands (Sheoran et al., 2010; Underground Coal Mining, DEP). The improper closure of these mines caused groundwater to fill in the cavities and react with the mine walls and exposed minerals, dissolving several pollutants and toxic metals in excessive concentrations (Akcil & Koldas, 2006). The water resulting in this process is called acid mine drainage (AMD). AMD formed when the exposed sulfide minerals react with water and oxygen (Akcil & Koldas, 2006).

Acid Mine Drainage Characteristics

Low pH and a high concentration of metals are two unique characteristics associated with AMD formation, and while AMD characteristics vary from site to site, it is commonly associated with high concentrations of iron and manganese (Peppas et al., 2000). Due to these characteristics, the formation of AMD contaminates surface and ground water, as well as soil. This contamination harms the natural biodiversity and makes it impossible for most habitats to function properly. The impairment of the streams due to AMD happens through acidification, high concentrations of metals pollution, and sedimentation (Herlihy et al., 1990). The degree of this contamination relies on the concentrations of oxidized sulfide minerals, and the composition of these metals (Akcil & Koldas, 2006). In addition to the mentioned chemical characteristics, AMD is also known with high acidity and low total alkalinity (Acharya & Kharel, 2020). “The acidity level, metal composition and concentrations of a given AMD source depend on the type and quantity of sulfide minerals present (acid-producing) and acid-neutralizing (carbonate) minerals contained in the exposed rock” (J. G. Skousen et al., 2019) According to Akcil & Koldas, the primary documented factors that affect the AMD generation rate are pH,

temperature, oxygen when it's below the saturation concentration, the chemical activity of the ferric iron, the surface area of exposed metal sulfides, and bacterial cultures and their bioactivity(Akcil & Koldas, 2006).

While more than 100 minerals have been identified in coal, iron sulfide remains the major concern (Holland & Turekian, 2004). The oxidation of iron sulfide (pyrite) in water is the main cause of pH reduction and AMD production, and it exists in high concentrations compared to other minerals. Moreover, toxic metals can be leached out of other minerals by the low pH water. Other oxidation-susceptible sulfide minerals that can be found in AMD waters are aluminum, mercury, lead, nickel, arsenic, cobalt, copper, cadmium, and zinc. The chemical oxidation reaction occurs when the pyrite (FeS_2) gets exposed to oxygen and water as follows:

$$FeS_2 + {}^{7}/_{2}\, O_2 + H_2O \rightarrow Fe^{2+} + 2SO_4^{2-} + 2H^+ \qquad (1)$$

This reaction results in increased acidity and dissolved solids, which leads to a decrease in pH (Akcil & Koldas, 2006; Holland & Turekian, 2004). With the continuous presence of dissolved oxygen, the ferrous iron can be further oxidized to ferric iron accordingly:

$$Fe^{2+} + {}^{1}/_{4}\, O_2 + H^+ \rightarrow Fe^{3+} + {}^{1}/_{2}\, H_2O \qquad (2)$$

Step (2) is a very slow reaction and is usually referred to as the “rate-limiting” step (Hallberg, 2010; Sahoo et al., 2013). The ferric iron can further oxidize pyrite or hydrolyze into Fe-oxides. Within a certain pH range and saturated concentrations, the ferric hydroxide will precipitate resulting in a net increase in hydrogen concentration and therefore lower the pH further:

$$Fe^{3+} + 3H_2O \rightarrow Fe(OH)_{3_{(S)}} + 3H^+ \quad (3)$$

The overall reaction step is shown in Eqn.4.

$$FeS_2 + {}^{15}/_4\, O_2 + {}^{7}/_2\, H_2O \rightarrow Fe(OH)_3 + 2SO_4^{2-} + 4H^+ \quad (4)$$

The overall reaction step shows that for each mole of pyrite oxidized, 4 moles of acidity are generated. This drastic reduction in pH explains the origin of the word “acid” in acid mine drainage.

Impacts of Acid Mine Drainage

Many negative environmental impacts have been studied due to AMD production. Acharya and Kharel (2020) summarized these impacts, as adopted, and modified from (Gray, 1997) in **Figure 1. 1**. An AMD identification strategy and detailed effects were thoroughly discussed in (Gray, 1997).

Figure 1. 1

Impacts of Acid Mine Drainage (Acharya & Kharel, 2020)

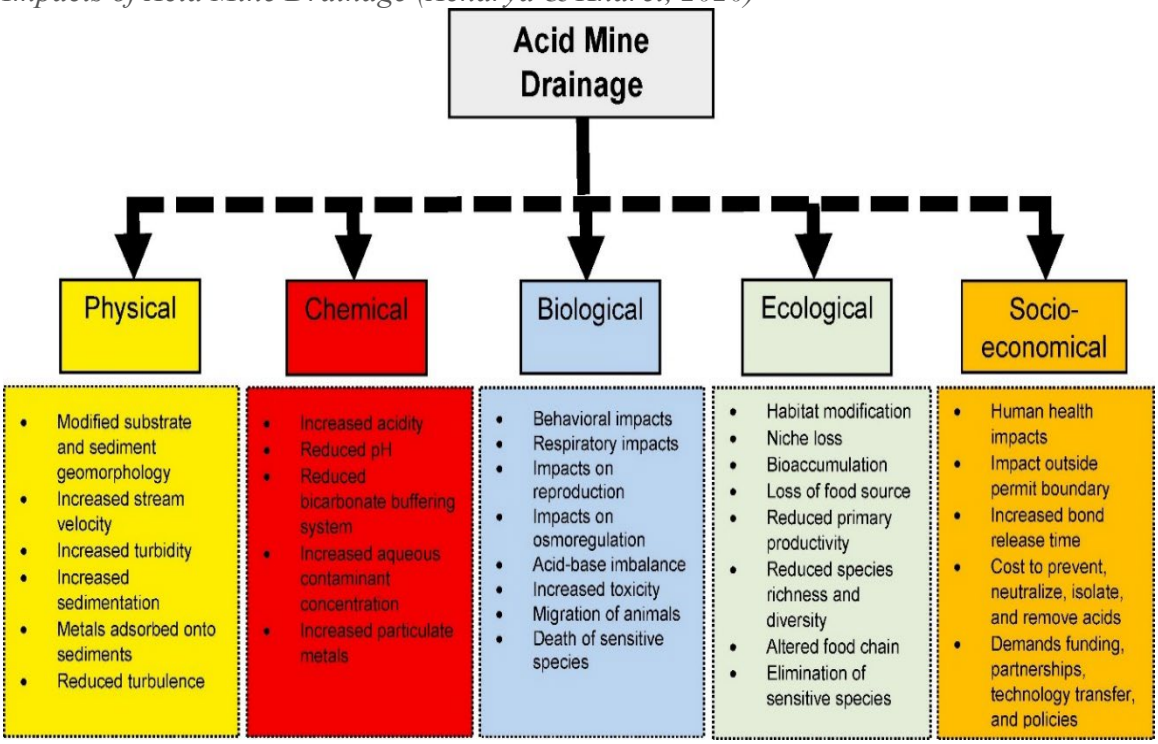

As can be interpreted from the figure, AMD has acute negative environmental impacts. These impacts make the affected streams unsuitable for recreational, domestic, agriculture, or even industrial uses (J. G. Skousen et al., 2019). Moreover, the dissolved toxic metals can move up the food chain and pose a serious threat to plants, animals, and humans (Chen et al., 2021). In eastern US alone, more than 10,000 km of streams and 72,000 ha of lakes were contaminated with AMD by 1990 (Herlihy et al., 1990). According to the same study, around 4600 km of streams were acidic (pH<5.0), and another 5800 km of streams were not acidic but significantly impacted by AMD in the mid-Atlantic and south-eastern region of the US. In the US alone, AMD is continuously polluting over 20,000 km of streams (J. G. Skousen et al., 2019). The largest portion of this pollution

comes from abandoned mine lands, the lands that were mined and left without any reclamation prior to the passage of the Surface Mining and Reclamation Act in 1977 (J. Skousen et al., 2017; J. G. Skousen et al., 2019). These concerning numbers have raised the need for a low-cost and efficient treatment technology (Herlihy et al., 1990).

Acid Mine Drainage Treatment

"Under the Clean Water Act, every state must adopt water quality standards to protect, maintain and improve the quality of the nation's surface waters. These standards represent a level of water quality that will support the goal of "swimmable/fishable" waters." (Ohio EPA, 2023). According to rule 3745-1-04 of the Ohio Administrative Code (OAC), "all surface waters shall be free from sludge, floating debris, oil and scum, color and odor producing materials, substances that are harmful to human, animal or aquatic life, and nutrients in concentrations that may cause algal blooms." Ohio EPA regulates aquatic life health in the form of "Designated Aquatic Life Uses" using the biological integrity of the stream. Then, the contaminants affecting the biological health of a certain stream are identified and targeted for restoration. Ohio EPA categorizes streams into five designated uses in a descending order: Exceptional Warm Water Habitat (EWH), Warmwater Habitat (WWH), Modified Warmwater Habitat (MWH), Limited Resource Water (LRW), and Coldwater Habitat (CWH), where streams designated as EWH are the most diverse and healthy streams. In order to determine aquatic life uses, the Ohio EPA surveys fish and macro-invertebrate populations as well as chemical and physical water quality parameters for a given stream. The results from the bio-survey are then used to establish a metric score for both fish (IBI) and macro-invertebrate (ICI) that indicates the biological integrity of that stream. The Index of Biologic Integrity (IBI) metric is a measure of fish species

diversity and species populations. The score of this index helps to understand the severity of pollutants effects on stream habitat. Moreover, when combined with the chemical characteristics of the stream, the IBI index can tell the types of occupying fish. The Invertebrate Community Index (ICI) metric is based on measurements of macro-invertebrate communities living in a stream. Identifying certain species in the stream can give an idea about the level of pollution stressing this stream. Ohio EPA requires achieving the highest "designated use" wherever possible. Therefore, the Sunday Creek restoration goal is to meet the WWH criteria, while most of the creek sites are designated in the MWH and LRH criteria with 45% of these sites receiving a fair to very poor macro-invertebrate ranking. Continuous release of untreated AMD is the primary cause for the poor biological rating of Sunday Creek (AMDAT, 2003). Many aquatic species are sensitive to the resulting low pH and the overabundance of iron precipitates that destroy habitat.

Many treatment methods, approaches, and techniques have been thoroughly discussed in (Akcil & Koldas, 2006; Chemical Aspects of Acid Mine Drainage on JSTOR, 2023; Gray, 1997; Johnson & Hallberg, 2005; Sahoo et al., 2013; Simate & Ndlovu, 2014; J. G. Skousen et al., 2019). Although many of these treatment methods have been used at mining sites, only the minority of them were sustainable and cost-effective (Chen et al., 2021). According to (J. Skousen et al., 2017), regardless of the adopted technique, the AMD chemistry, and the site condition (active operation or abandoned mine land), all AMD treatment methods aim to neutralize the water acidity, oxidize (or reduce) the dissolved metals, and eliminate these metals from the water through precipitation. The remediation of AMD relies on increasing the pH and removing the dissolved metals of concern. The remediation pathway can either be geochemical (abiotic) or biological

(biotic). Geochemical treatment aims to increase the water pH by adding alkalinity-generating materials, in addition to chemical oxidants to allow the oxidation and precipitation of dissolved metals as hydroxides (Johnson & Hallberg, 2005). The addition of these materials relies on the acid-base chemistry of a given AMD to calculate the required mass of alkalinity needed to neutralize the acidity. The most common and readily used material to generate alkalinity in AMD treatment is the limestone because of its low cost and availability (J. G. Skousen et al., 2019). Moreover, it is very safe for use and has a neutralization potential between 75% - 100% (J. G. Skousen et al., 2019). However, one major disadvantage for using limestone is the massive doses required to increase and maintain a higher pH (Matlock et al., 2002). Moreover, the limestone dissociation is relatively slow and therefore it must be supplied with a very large surface area (fine-grained) to serve its purpose. In addition, limestone produces a secondary waste (gypsum) that is highly regulated, not easily handled, and has costly disposal requirements (Wang et al., 1996). Lime can also adsorb high concentrations of metals hydroxides and gypsum to form agglomerates that can block the whole treatment system resulting in increased operation and maintenance costs (Bologo et al., 2012). Other chemicals that are used to neutralize the AMD acidity are calcium oxide (CaO), magnesium hydroxide ($Mg(OH)_2$), slaked lime ($Ca(OH)_2$), and sodium hydroxide (NaOH). Sodium hydroxide has proven to be better in terms of efficiency and the secondary waste volume and composition (Chen et al., 2021). It has a 100% neutralization potential; however, it needs special safety and handling precautions, and it is about nine times more expensive than the limestone (Acharya & Kharel, 2020).

Oxidation of the ferrous iron is necessary to lower the solubility of the element, so that it can be removed from the AMD by settling. Ferrous iron can be oxidized biologically by microorganisms, or abiotically by oxygen or the addition of chemical oxidants such as hydrogen peroxide. Oxygen is typically provided by forcing the water to cascade over steps and reach equilibrium with atmospheric oxygen. However, sites need appropriate land and elevation drop for that to be possible. Air bubbling is another alternative. Under acidic conditions (below pH 4), however, Stumm and Morgan (1981) proved that the abiotic ferrous iron oxidation by oxygen is negligible. Hydrogen peroxide, on the other hand, is a very strong oxidant and can readily oxidize iron even under acidic conditions. However, hydrogen peroxide sterilizes the water, making it a less favorable option to the projects aiming for recreational surface water remediation and habitat restoration. Moreover, hydrogen peroxide is relatively expensive, dangerous, and requires special handling and extended safety precautions that come at a high cost. Biological treatment, on the other hand, relies on microorganisms to immobilize the dissolved metals by oxidation. It is much faster than the abiotic oxidation by oxygen, especially under acidic conditions, and significantly cheaper and safer than hydrogen peroxide. The biological oxidation remediation phenomenon will be discussed in the iron oxidation chemistry and microbiology section.

Choosing the suitable treatment method is critically affected by mineralogy, geochemistry, hydrology, and microbiology. These characteristics drastically differ from site to site, making it hard to generalize one treatment method for all contaminated sites (J. Skousen et al., 2017). Moreover, economics plays a major role in choosing the suitable remediation method and technique (Johnson & Hallberg, 2005). The high costs associated

with treating copious amounts of AMD water continuously raised the desperate need for more sustainable and cost-effective remediation strategy (Chen et al., 2021; Kefeni et al., 2017). Because of the massive amount of the exposed minerals, AMD flow is predicted to contain high concentrations of metals and acidity for hundreds of years requiring a long-term treatment operational cost. Moreover, the adopted treatment methods require expensive pH neutralizing chemicals and chemical oxidants. Also, the resulting sludge requires special collection and disposal techniques at a cost. For these reasons, reducing operational costs is essential to affordably continue treatment. Therefore, recent research is now focusing on using the AMD as a sustainable resource by recovering valuable resources such as water, metals, sulfuric acid, and rare earth elements during the treatment process (Chen et al., 2021). Chen *et al.* have also noted that metals precipitation has been well-explored, but recovering these metals from AMD treatment and reusing them is still a new and promising strategy that needs further investigation. Depending on the AMD chemistry, the outcome sludge of the treatment process is usually an iron-rich material, making its recovery from AMD waters into a marketable precipitates and pigments of a special interest (Johnson & Hallberg, 2005). Some studies have investigated the efficiency and feasibility of metals and iron removal from AMD waters using various treatment methods and recovery techniques (Bologo et al., 2012; Hedin et al., 2003; Hu et al., 2022; Mogashane et al., 2023; Ryan et al., 2017; Silva et al., 2019; Tabak et al., 2003). These studies have proven the possibility of recovering iron with up to 98% efficiency. The recovered iron was then used to produce colorants. This pigment can then be sold resulting in considerable yearly revenues that can help reduce the operation costs.

The Chemistry and Microbiology of Iron Oxidation

Iron can be oxidized either geochemically in the presence of chemical oxidants, or biogeochemically in the presence of bacteria and oxygen (Acharya & Kharel, 2020). Iron serves as the electron donor while the oxygen (or the chemical oxidant) serves as the electron acceptor. Under acidic conditions, however, Singer and Stumm (1970) suggested that the primary oxidant of the pyrite is the ferric iron (Fe^{3+}), and it occurs at a faster rate than oxygen, which can accelerate the ferrous iron oxidation as illustrated in Equation (5) (Vengosh, 2005). This cycle continues until the pyrite, or the ferric iron, is depleted. The rate of this reaction is directly proportional to the Fe^{3+}/Fe^{2+} ratio and it is significantly enhanced by the presence of iron-oxidizing bacteria as they help maintain a high Fe^{3+}/Fe^{2+} ratio (Boon & Heijnen, 1998).

$$14Fe^{3+} + FeS_2 + 8H_2O \rightarrow 15Fe^{2+} + 16H^+ + 2SO_4^{2-} \qquad (5)$$

Luther (1987) argued that the reason the ferric iron is a stronger and faster oxidant than the oxygen is that the former adopts a mechanism where it chemically binds to the sulfide surface and oxidize it, while the latter can't.

Stumm and Morgan (1981) have also found that both reaction pathways (chemical and biological) can occur when the pH is above 4. However, when the pH is below 4, only the biological reaction takes place, while the abiotic reaction becomes negligible. They have also stated that under these acidic conditions, ferrous iron oxidation can be significantly enhanced by the presence of acidophilic iron-oxidizing microorganism with a rate factor larger than 10^6. The degree of this enhancement has been directly associated with the number of iron-oxidizing microorganisms, the bioactivity of these

microorganisms, and pH (Edwards et al., 2000). Therefore, the improvement of bacterial growth was suggested to be crucial for achieving higher oxidation rates.

Stumm and Morgan (1981) have also described the abiotic ferrous iron oxidation in aqueous systems. They stated that the iron oxidation rate is mainly affected by both pH and oxygen concentration:

$$\frac{d[Fe^{2+}]}{dt} = \frac{k\,[O_{2(aq)}]\cdot[Fe^{2+}]}{[H^{+}]^{2}} \quad (6)$$

However, they have noted that below pH 4, the iron oxidation rate is independent of pH. They found that at this oxidation independence range of pH, and oxygen is in excess, the oxidation rate can be represented as:

$$-k[Fe^{2+}] = \frac{d[Fe^{2+}]}{dt} \quad (7)$$

Where k is the first-order oxidation rate in (t^{-1})

By integrating and rearranging, we get:

$$[Fe^{2+}] = [Fe^{2+}]_o e^{-kt} \quad (8)$$

Where $[Fe^{2+}]_o$ is the initial ferrous iron concentration.

They have also proven that the ferrous iron oxidation rate (by oxygen) is significantly decreased below pH 6, and this may be the reason why the abiotic effects can be neglected in very acidic conditions (below pH 4). At this acidic range, the iron oxidation rate is significantly enhanced by iron-oxidizing bacteria (Johnson & Hallberg, 2005).

However, adopting a biologically based remediation approach requires a comprehensive understanding of the microorganisms' role in the oxidation process. Schippers *et al.* (2010) investigated the microbial diversity in more than 70 mine dumps and heaps. They found that iron-oxidizing bacteria and archaea were the most dominant

microorganisms in these sites. These predominant microorganisms were extremely acidophilic, and they thrived at pH below 3.0 (Vera et al., 2013). Iron-oxidizing bacteria were found to belong to four phyla: "Proteobacteria (*Acidithiobacillus, Acidiphilium, Acidiferrobacter, Ferrovum*); Nitrospirae (*Leptospirillum*); Firmicutes (*Alicyclobacillus, Sulfobacillus*); and Actinobacteria (*Ferrimicrobium, Acidimicrobium, Ferrithrix*)" (Ortiz-Castillo et al., 2021).

Acidithiobacillus ferrooxidans (A. ferrooxidans), an obligate chemolithoautotrophy acidophile, is the first-isolated and the most well-studied species of iron-oxidizing bacteria. A chemolithoautotrophs are microorganisms that obligately obtains energy by oxidizing inorganic compounds (using inorganic matter as an electron donor). Research has been able to identify 23 strains of this species categorized into 7 subgroups. *Acidithiobacillus ferrivorans*, a species categorized under one of these subgroups, has been suggested to be the predominant species in low-temperatures environments (Hallberg et al., 2010; Liljeqvist et al., 2011, 2013). Gene sequencing of some of the strains of *A. ferrooxidans* showed that they have a putative pho regulon, that is suggested to be responsible of assimilating inorganic phosphorus from the environment, and a functional C-P lyase system, that is responsible of the degradation of other phosphorus sources such as phosphonate, allowing these tested strains to survive under extreme nutrients scarcity (Avdalović et al., 2015; Vera et al., 2003, 2008). However, under phosphate limitation, *T. ferrooxidans* (currently named *A. ferrooxidans*) showed a reduction in growth rates and iron oxidation capacity (Seeger & Jerez, 1993), proving the necessity of this nutrient for efficient growth and enhanced iron oxidation. Unfortunately,

research in this area is focused exclusively on this single species of iron oxidizers despite the considerable biodiversity of iron-oxidizing bacteria (Johnson & Hallberg, 2005).

Leptospirillum spp*.,* with its two recognized species, *L. ferrooxidans* and *L. thermoferrooxidans*, have been identified in mine sites and AMD worldwide (Hallberg & Johnson, 2003; Johnson & Hallberg, 2005). These bacteria were found to be obligatory aerobic iron oxidizers, as they don't use other substances either as electron donor (ferrous iron) or acceptor (oxygen). The mesophilic strains of these bacteria have been found to be strictly aerobic, and obligately chemolithotrophic. Some other acidophilic mesophilic iron-oxidizing species found were *Ferrimicrobium acidiphilum*, and *Ferroplasma acidiphilum* (Ortiz-Castillo et al., 2021). While some species of iron-oxidizing bacteria like *Leptospirillum* spp. and *Acidithiobacillus* spp. are obligately chemolithoautotrophic, other species of iron-oxidizers like *Acidiphilium acidophilum* and *Acidimicrobium ferrooxidans* can grow autotrophically on ferrous iron, heterotrophically on organic matter, or mixotrophically on all these substrates (Vera et al., 2013). Heterotrophic iron-oxidizers were found to be able to reduce iron under anoxic/anaerobic conditions using glucose as a carbon and energy source and the ferric iron as the terminal electron acceptor (Johnson & McGinness, 1991). Therefore, having mixed cultures of iron-oxidizers can result in iron cycling (between ferric and ferrous) with changed conditions or in microenvironments.

For archaea, most species were found to belong to *Sulfolobales*, including genera such as *Sulfolobus*, *Metallosphaera*, *Acidianus*, and *Sulfurisphaera* (Norris et al., 2000) as cited in (Vera et al., 2013).

It was found that the microbial community and biodiversity crucially depend on the site mineralogy along with other factors such as pH, temperature, the availability of a

carbon source, and energy source (Ortiz-Castillo et al., 2021). A study conducted by Jones & Bennett (2017) found that 70-90 percent of the phylogenetic diversity and composition is associated with the type of the mineral surface rather than the other mentioned environmental factors.

Kinetics (Temperature, pH, Nutrients)

Many researchers have investigated the kinetics of iron oxidation by microorganisms. It is difficult to draw general conclusions or even compare studies, because researchers fit the data to different models (e.g. zero-order. First-order, Monod), report specific rates according to different measures of biomass (e.g. per cell, per total C), and test a range of pH, temperature, iron concentration, and species.

Many studies investigated the effect of temperature on iron oxidation rates by many iron-oxidizing species. Ojumu *et al.* (2009) investigated the effects of temperature on ferrous-iron oxidation rates by *L. ferriphilium* in a continuous system. The tested temperature range was 18 – 45 °C. The pH was maintained at 1.3. Results have shown that the oxidation rate increases with increased temperature up to 42 °C with a maximum ferrous iron oxidation rate of 16.25 mol Fe^{2+} $(mol\ C\ h)^{-1}$ at 42 °C which was equivalent to 77.34 hr^{-1} after converting to first-order kinetics. The bacterial growth rate was found to be inhibited below 18 °C and above 45 °C with a maximum growth yield at 25 °C. The iron oxidation rates achieved in this study were the highest among all other studies reported in the literature.

Özkaya et al. (2007), on the other hand, investigated a wider temperature range (2 – 50 °C) by predominantly *L. ferriphilium* culture in a fluidized bed reactor system. The pH was maintained at 0.9. The study has suggested that the lag phase was dependent on

temperature, in which at the optimum temperature, the bacteria experienced the minimum lag phase of 1 d. They also found that iron oxidation and bacterial growth were inhibited below 10 °C and above 42 °C, which was consistent with Ojumu *et al.* findings. The optimum temperature was found to be around 35° C with a maximum oxidation rate of 0.6 g Fe^{2+}/g VS.h which was equivalent to 0.0743 hr^{-1} using first-order kinetics. Although Özkaya *et al.* investigated the same species, temperature ranges, and close pH conditions to Ojumu *et al*. study, the iron oxidation rates achieved in this study were approximately 1000-fold slower. The significantly high oxidation rates achieved by Ojumu *et al.* are likely because of the significantly high influent-iron concentrations.

One of the few studies investigated the effect of temperature by a mixed culture in a batch system (Ahonen't And & Tuovinen2, 1989). The enrichment was achieved by a sequence of subculturing at different temperatures ranging between 4 °C and 46 °C (46 °C was later dropped due to complete inhibition of growth). After enrichment, each enrichment culture was tested at a temperature range of 4 °C – 37 °C. A pH of 5.2 was maintained over all enrichments and tests temperatures. Results showed that among all incubation temperatures, the culture enriched at 19 °C achieved the highest oxidation rate with an increasing rate as the test temperature increases. However, this culture was not tested at 28 °C incubation temperature and as a result, the highest oxidation rate achieved in this study was for 28 °C culture incubated at 28 °C with a growth rate constant of 0.0998 hr^{-1}.

Breed *et al.* (1999) , however, tested a narrow temperature range (30 – 40 °C) using different species of iron oxidizers, a predominantly *L. ferrooxidans* culture, in a continuous system. The pH was maintained at 1.75. It was found that ferrous iron oxidation rates

increase as the temperature increases with a maximum ferrous iron oxidation rate of 13.62 mmol Fe^{2+} (mmol C h)$^{-1}$ at 40 °C. Overall, literature agrees that higher iron oxidation rates can be achieved at higher temperatures (up to ~40 °C). This could be due to increased biological activity or the enhanced abiotic effects. In general, Stumm and Morgan (1981) reported that the ferrous iron oxidation rate increases by tenfold for 15 °C degrees increase at constant pH for abiotic systems.

Many other studies have investigated the effect of pH on the growth and activity of iron-oxidizing microorganisms as well as iron oxidation rates. A later study was published by Ojumu & Peterson (2011) following the temperature test with a pH test by the same species of the mesophilic *L. ferriphilium* in a continuous system. The tested range of pH was 0.8 – 2.0, and the best temperature (42 °C) from the previous temperature test was maintained. It was found that the maximum ferrous iron oxidation rate of 14.54 mol Fe^{2+} (mol C h)$^{-1}$ occurred at pH 1.3.

Breed & Hansford (1999a) also investigated the effect of pH on iron oxidation rates by *Leptospirillum ferrooxidans*. pH values ranging from 1.1 to 1.7 were tested in a continuous culture system, and the temperature was maintained at 40 °C. They found that the increase of pH from 1.1 to 1.7 did not have a significant effect on the biomass yield or the iron oxidation rates. The highest reported iron oxidation rate was found 19.02 mmol Fe^{2+} (mmol C h)$^{-1}$ at pH 1.5, which was 1.4-fold higher than the rate achieved by Breed & Hansford for almost similar conditions but with different microorganisms. These results were found consistent with Sheng *et al.* (2016) as they found that *Leptospirillum* is the dominant species in extremely acidic environments where pH is below 2.0.

Plumb *et al.* (2008) also tested the effects of pH on ferrous iron oxidation by three strains of bioleaching microorganisms including *Leptospirillum ferriphilum, Sulfobacillus thermosulfidooxidans,* and *Metallosphaera hakonensis* using a batch stirred tank reactor system. The tested pH range was 0.5 – 3.5. The overall optimal pH for most stains was found to be in pH 1.5 – 2.0 range, and that ferrous iron oxidation was completely inhibited at pH 0.5. The maximum reported iron oxidation rate for each species was 0.072 hr^{-1} at pH 2.0, 0.140 hr^{-1} at pH 1.5, and about 0.25 hr^{-1} at pH 2.5, respectively. However, a portion of the high oxidation rate achieved by the 3rd species was likely to occur due to the addition of KOH and the high incubation temperature (>70 °C), making the comparison unreliable.

Overall, it was proven that microorganisms respond and function differently at different ranges of pH. This finding was further explained by Sheng *et al.* (2016, 2017). They investigated the effects of pH and ferrous iron concentration on the microbial community structure and iron oxidation rates within pH 2.1 - 4.2 range and 60 – 2400 mg/L ferrous iron concentration range. It was found that the microbial community structure and the relative abundance are significantly correlated with pH and ferrous iron concentration. Some tested species of bacteria were found to be restricted within a certain bound of pH. For example, *Acidothiobacillus* was found to be predominant at pH < 3.0 with a peak at pH 2.9 and iron concentration between 300 and 600 mg/L. Although the highest oxidation rates occurred at the lowest pH with a rate of 2.44×10^{-7} mol Fe(II) L^{-1} s^{-1} at pH 2.4, the highest iron removal efficiency occurred between pH 2.9 and 3.3. It was also found that both iron oxidation rate and total iron removal efficiency decreased at the higher bound of the tested pH (pH 4.2). Moreover, it was found that higher ferrous iron oxidation rates were achieved at higher influent ferrous iron concentrations with a maximum rate of 7.7 ×

10^{-7} mol Fe(II) L^{-1} s^{-1} at 2400 mg/L iron concentration. The study has also shown that the alpha microbial biodiversity decreased with lower pH values while the relative abundance of acidophilic iron-oxidizing bacteria increased. This may explain why higher ferrous iron oxidation rates were achieved at lower pH, and that because with lower biodiversity, more energy would be available for iron-oxidizing bacteria to utilize. In contrast, Sand (1989) found in their study that ferrous iron oxidation by *T. ferrooxidans* was inhibited at pH below 1.3 and the oxidation was resumed when the pH went above 1.8. From a thermodynamic perspective, Gibbs free energy of ferrous iron oxidation becomes less negative as pH increases. This can explain why overall, higher ferrous iron oxidation rates can be obtained at lower pH (Sheng et al., 2017).

In addition to the study conducted by Sheng *et al.* (2016, 2017), Edward *et al.* (2022) also investigated the effect of the initial ferrous iron concentration on iron oxidation rates and bacterial growth. Ferrous iron oxidation by *Acidiplasma cupricumulans* archaea was investigated in a batch system. The tested range of initial ferrous iron concentration was 0.3 g/L – 5.0 g/L. It was found that above 1.0 g/L of ferrous iron concentration, iron oxidation was incomplete, and the maximum biomass concentration remained constant. These findings suggested that the biological iron oxidation was limited by a secondary nutrient. This suggestion was later proven when growth rates and iron oxidation rates experienced an improvement after switching to 0K media (a nutrient richer media). The maximum Fe^{2+} oxidation rate achieved in this study was 0.114 hr^{-1}, which was within the range of the rates found by (Breed & Hansford, 1999b; Nemati & Harrison, 2000). **Table 1** summarizes these studies with the reported conditions and kinetic

Table 1

Summary of the Studies Investigated Ferrous Iron Oxidation Rates in the Literature.

Study	Species	pH	T (°C)	Reactor system	Tested iron concentration	Iron oxidation rate (unit reported)	First order iron oxidation rate (hr^{-1})	Maximum rate
(Ojumu et al., 2009)	*L. ferriphilum*	1.3	18-45	Continuous culture	12.0 g/L	16.25 mol Fe^{2+} (mol C h)$^{-1}$	40.82 - 77.34	77.34 hr^{-1} at 42 °C
(Ojumu & Petersen, 2011)	*L. ferriphilum*	0.8-2.0	42	Continuous culture	12.0 g/L	14.54 mol Fe^{2+} (mol C h)$^{-1}$	-	14.54 mol Fe^{2+} (mol C h)$^{-1}$ at pH 1.3
(Özkaya et al., 2007)	*L. ferriphilium*	0.9	2-50	Fluidized-bed reactor	4.0 g/L	0.6 g Fe^{2+}/g VS.h	0.0111 - 0.0743	0.0743 hr^{-1} at 35 °C
(Breed et al., 1999)	Predominantly *L. ferrooxidans*	1.75	30-40	Continuous culture	12.0 g/L	13.62 mmol Fe^{2+} (mmol C h)$^{-1}$	-	13.62 mmol Fe^{2+} (mmol C h)$^{-1}$at 40 °C
(Breed & Hansford, 1999a)	*L. ferrooxidans*	1.1-1.7	40	Continuous culture	12.0 g/L	19.02 mmol Fe^{2+} (mmol C h)$^{-1}$	-	19.02 mmol Fe^{2+} (mmol C h)$^{-1}$at pH 1.5
(Ahonen't And & Tuovinen2, 1989)	Mixed culture	5.2	4-37	Batch system	6.0 g/L	0.0998 hr^{-1}	0.00963 - 0.0998	0.0998 hr^{-1} at 28 °C
(Edward et al., 2022)	*Acidiplasma cupricumulans*	1.4	45	Batch system	0.3 – 5.0 g/L	4.088 x 10^{-10} mg Fe^{2+} $cell^{-1}$ h^{-1}	0.0856	0.0856 hr^{-1} at < 1.0 g/L Fe^{2+}
(Sheng et al., 2017)	Mixed culture 1	2.1-4.2	20	Continuous system	60 – 2400 mg/L	7.7×10^{-7} mol Fe^{2+}/ L^{-1} s^{-1}	0.593 – 1.50	1.50 hr^{-1} at pH 2.4
	Mixed culture 2	2.3-4.1	20	Continuous system	80 – 2400 mg/L		1.25 – 3.62	3.62 hr^{-1} at pH 2.3

Multiple studies suggested that ferrous iron oxidation by microorganisms is dependent on a secondary nutrient (Edward et al., 2022), but very few studies investigated these nutrients and their optimal concentrations. One of those studies (Tuovinen et al., 1971) investigated the effects of inorganic nutrients and some organic compounds on ferrous iron oxidation by *T. ferrooxidans* in a continuous system supplied with 2000 mg Fe^{2+}/L. pH was kept at 2.5 – 3.0 range. It was found that ammonium, phosphorus, sulfate, and magnesium all enhanced iron oxidation rates. While no optimal concentrations for ammonium or phosphorus were documented, sulfate and magnesium had a minimum unlimited concentration of 2.0 g SO^{2-}/L and 2.0 mg Mg^{2+}/L, respectively. Moreover, it was found that nitrate and chloride had inhibitory effects at high concentrations, while no effects were observed for calcium and potassium addition. Lastly, the effects of adding organic carbon compounds varied from increasing the lag phase to complete inhibition, suggesting that this strain of *T. ferrooxidans* was unable to utilize organic carbon as an energy source, which was also proven by (Plumb et al., 2008).

The toxicity of organic carbon on ferrous iron oxidation by *A. ferrooxidans* was also investigated by (Fang & Zhou, 2006). They found that ferrous iron oxidation was completely inhibited at organic carbon concentrations higher than 150 mg/L. The inhibition of organic compounds including glucose was also proven by multiple other studies (Frattini et al., 2000; Marchand & Silverstein, 2010) tested variable strains of *T. ferrooxidans* but with different inhibition concentrations that were found to be dependent on the bacterial strain. In these studies, organic carbon (including glucose) had the potential to completely inhibit bacterial growth.

Another study investigated the effects of Aluminum and nitrate on iron-oxidizing bacterial growth in batch system (Blight & Ralph, 2008). Inhibitory effects were observed by both tested minerals. For aluminum, 85 mM caused a 15% reduction in bacterial growth, while more acute effects were observed by nitrate, as 15 mM caused 35% reduction in bacterial growth, and complete inhibition occurred after 3 subculturing cycles (Truetown site has 0.074 mM aluminum and negligible nitrate concentration).

Although literature agreed on the inhibitory effects of high concentrations of chloride, a study conducted by Korehi *et al.* proved the existence of some species of the extremophile iron-oxidizers that can tolerate concentrations of chloride as high as 1 M (Korehi et al., 2013).

Sand (1989) also found that in acute acidic environments, and after ferrous iron depletion, the bacterial cells of *T. ferrooxidans* use the energy resulting from sulfur oxidation to maintain a neutral pH range in the cytoplasm. This may explain why *T. ferrooxidans* bacteria achieved higher oxidation rates with the presence of excess sulfate/sulfur (Tuovinen et al., 1971).

In conclusion, the literature thoroughly investigated the effect of temperature and pH on iron oxidation rates. Higher iron oxidation rates were achieved at lower pH values and higher temperatures. Moreover, higher oxidation rates were achieved in continuous systems. However, the literature is lacking information about the effects of nutrients like nitrogen and phosphorus on a mixed culture of iron-oxidizers and iron oxidation rates. Therefore, this study aims to fill this gap.

Truetown Seep and Chemistry

The Sunday Creek watershed in south-eastern Ohio witnessed intensive deep coal mining since the early 1800s (with about 38% of the area mined). These mined lands were then abandoned prior to the environmental regulations governing mining and water quality (AMDAT, 2003). Around 18 room-and-pillars coal mines were found in the area forming a mine complex that is informally known as "Truetown mine complex" that encompasses 25 mi^2. The improper closure of these mines led to groundwater filling these rooms, reacting with the exposed sulfide minerals producing AMD. A failure in the seal of a pumping station of the abandoned mine in the area (39°26'48.5"N, 82°06'27.6"W) in 1983 caused the discharge of this AMD into the Sunday Creek 7 mi upstream of its junction with the Hocking River. For several years, research was conducted to develop technology to remediate this discharge with the goal of removing metals, increasing alkalinity, and as a result, restoring wildlife habitat in Sunday Creek, and meeting the WWH criteria wherever possible. The selected treatment method relied on oxidation and precipitation of the ferrous iron by pumping the discharge into a treatment facility. The novel part in this project was the recovery of ferric hydroxide sludge to be processed and sold as paint pigment. The recovery of this resource will offset the operational costs and overcome the financial burdens of this project. The discharge produces on average 5.3 million L/d of AMD with an average ferrous iron concentration of 252 mg/L. This can yield around 2.6 tonnes/d of dry pigment.

Chemical characteristics of Truetown AMD collected from "watershedata.com" website as the average of the results of all the samples from 2018 to 2023. The location ID on the website is "SCTR016" (See **Table 2**).

Table 2

Average Chemical Characteristics of Truetown Seep from 2018-2023.

Parameter	Value	Unit
Discharge	5.285	10^6 L/d
pH	5.26	N/A
Conductivity	2480	uScm
Acidity	430	mg/L
Alkalinity	22.3	mg/L
TDS	2315	mg/L
TSS	5.3	mg/L
Iron (Fe)	252	mg/L
Sulfate	1511	mg/L
Manganese (Mn)	5	mg/L
Aluminum (Al)	2.1	mg/L
Chloride (Cl)	20.6	mg/L
Calcium (Ca)	178	mg/L
Magnesium (Mg)	56	mg/L
Sodium (Na)	190	mg/L
Potassium (K)	11	mg/L

Objective of the Study

This study aimed to enhance iron oxidation rates by optimizing growth of a mixed culture of iron-oxidizing bacteria. Multiple mixed cultures were collected from extremely acidophilic environments contaminated with AMD. The study aimed to find the best culture, to find the best pH value, to enrich this culture in a modified 9K growth media, to find the best nutrients concentrations, and to apply the results to Truetown AMD. The study investigated the effects of different ammonium, phosphorus, and organic carbon (glucose) concentrations on iron oxidation rates. The culture and nutrients concentrations with the highest achieved iron oxidation rates were then supplied to Truetown AMD to investigate the degree of enhancement. Enhancing oxidation and growth rates will play a major role in adopting the microbial treatment pathway as an efficient and feasible treatment method.

Chapter 2: Methodology

Site Selection

Three sites were selected for this study. Two of these sites were selected using the chemical database that is available on "watersheddata.com" for all surface streams and watersheds in Ohio. Because previous studies showed higher oxidation rates at low pH, sites with pH < 4.0 and high iron concentrations were selected. Because Truetown site had a relatively high pH of 5.26, it was not selected for this study. Other considered factors were the sulfate concentration and recently reported sampling results. High sulfate and iron concentrations strengthened the belief that the sampled stream remained an active AMD source. The age of the last documented sample was important to determine whether the site was still contaminated with AMD and had not been remediated. The sites' detailed information is summarized in **Table 3**, and a picture of the sites' locations is shown in **Figure 2. 1**.

Table 3

Selected Sites Information

Sample ID in the study	FR	WR	PA
Location	Jackson, Milton, Ohio	Jefferson, Springfield, Ohio	Gallitzin state park, Somerset, Pennsylvania
Sub watershed	Flint Run	Wolf Run	Paint Creek
Sample ID (website Ref.)	FR0126	WRMS027	NA
Maps coordinates	39°03'43.2"N 82°30'18.5"W	40°27'16.7"N 80°52'01.0"W	40°14'28.3"N 78°44'27.4"W
Field pH	2.5 – 2.7	3.0 – 3.5	2.0 – 4.0
[Fe^{2+}]	130 mg/L	125 mg/L	~100 mg/L
Tested pH in the study	One set at pH 2.5	Two sets: pH 2.5 and pH 3.0	Two sets: pH 2.0 and pH 4.0

Figure 2. 1

Sites Location: a) Flint Run Location b) Wolf Run Location c) PA Location

Sampling

Samples were collected from different spots within 100 ft downstream of the documented sampling spot which explains the range of pH readings at each site. Sediment samples were collected from the top 2 cm of the streambed using sterilized Teflon spoons and autoclaved sediment jars. At WR location, the streambed consisted of rock, and the sediment samples were collected by scraping the surface crust off of the rocks. Water samples were collected from the same locations before collecting the sediment samples using sterilized 1.0 L plastic bottles filled with no headspace. Samples were transported back to the laboratory on ice and were processed within 6 hr of collection.

Bacterial Extraction

The bacteria were extracted from the sediment using 3.8 mM sodium pyrophosphate solution. Sodium pyrophosphate ($Na_4P_2O_7$) solution was prepared by mixing 1.0 g of sodium pyrophosphate in 1.0 L of DI water. Sodium pyrophosphate has been shown effective at mobilizing bacteria from sediment into the solution (Bonmati et al., 1998). pH was adjusted according to the final incubation pH of the sample. The solution was autoclaved at 121 °C and 15 psi for 30 min. 60 g of sediment were mixed with 500 mL of the solution, put on a shaker table at 300 rpm for 40 min, allowed to settle, and the supernatant (inoculum) was used for this study.

pH Test

Two sets of inoculums were investigated for each tested pH. One set consisted of 50% sediment supernatant and 50% AMD from the same site. The second set consisted of 100% AMD without any sediment supernatant addition. All sets were conducted in triplicate with one negative control by adding 2.0% formaldehyde. The negative control

was important to determine the abiotic effects on iron oxidation. Formaldehyde has been proved to be effective in inactivating bacteria with minimal chemical alteration (Sharma et al., 2020). A fed-batch reactor system was adopted using Erlenmeyer flasks. The flasks were soaked with nitric acid, scrubbed, washed thoroughly, and autoclaved at 121 °C and 15 psi for 30 min prior to use. The ratio of solution to empty flask was 1:5 by adding 100 ml of solution to 500 ml flask volume. The flasks were capped with a sponge cap to prevent dust and particles from contaminating the sample and allowing the oxygen to diffuse freely. The flasks were put on a shaker table at 200 rpm. pH and dissolved ferrous iron concentration were monitored with time. Ferrous iron was added separately using 10,000 mg/L iron sulfate stock solution. The ferrous iron concentration was brought up to approximately 250 mg/L whenever it dropped below 10 mg/L. Multiple cycles of ferrous iron addition were conducted until stable oxidation rates were reached or a decline was observed likely due to nutrient limitation or accumulation of inhibitory chemicals. Samples were incubated at room temperature (~22° C). The tested pH values were chosen according to the original environment's pH where the samples were collected from and varied between pH 2.0 and pH 4.0. The chosen pH values took into consideration the lower and upper bound of the measured pH at the site, except for the WR culture, where one of the two sets was tested at pH 2.5 (less than the lower bound), as the literature suggested higher biological oxidation rates in extremely acidic conditions below pH 3.0. Moreover, the pH value of 2.5 for the WR culture was chosen to match the FR culture incubation pH for further comparison purposes. **Table 4** summarizes the pH test methodology.

Table 4

Summary of the Methodology of the pH Test

	WR			FR		PA	
Incubation pH	2.5		3.0	2.5		2.0	4.0
Composition	A*	B**	B**	A*	B**	B**	B**
Number of trials	3	3	3	3	3	3	3
Negative control	-	1	1	-	1	1	1
Total number of trials	11			7		8	
	26 Total flasks						

*Composition A: 100% AMD from the site location.
**Composition B: 50% inoculum extracted from the sediment, 50% AMD from the site location.

Bacteria Enrichment and Nutrients Test

Following the pH evaluation, the cultures with the highest resulting iron oxidation rates were enriched in a defined media, and experiments were conducted to evaluate the nutritional needs of the organisms and at what concentrations iron oxidation rates were maximal. The tested nutrients were nitrogen, phosphorus, and organic carbon. The nutrients were supplied in the form of ammonium sulfate, potassium phosphate dibasic, and glucose, respectively. No information in the literature was available for the best nutrients concentration except for the ammonium and phosphorus concentrations provided by the original 9K media of 0.045 M and 2.87 mM, respectively. Therefore, these concentrations were used as a mean guide and lower and higher concentrations were tested. A summary of the of the nutrients tested concentrations is shown in **Table 5**.

Table 5

A Summary of the Nutrients Tested Concentrations

	N (M)	P (mM)	C (M)
Low	0.01	0.1 and 0.5	0.05
Average	0.05	1.0 and 5.0	0.1
High	0.1 and 0.5	10.0	0.2
Number of tested cultures	2	1	1
Control	1 for each culture at 0.05 M	1 at 5.0 mM	1 at 0.05 M
# of tests in triplicate	7	5	3
Total # of flasks	23	16	10

9K Medium

Following the pH testing in the cultures original media, the bacterial cultures with the best pH values (WR and FR cultures at pH 2.5) were enriched in a defined media for further nutrients testing while the PA culture was omitted due to unsatisfactory iron oxidation rates. The defined media used was a modified version of the 9K medium. The 9K medium is a common defined growth medium used for enriching iron-oxidizing bacterial cultures and pure strains. The original recipe of the 9K medium is provided by "ATCC.org" for every 1.0 L of DI water:

$(NH_4)_2SO_4$……..…….. 3.0 g

K_2HPO_4……...…….…... 0.5 g

$MgSO_4.7H_2O$……..……..0.5 g

KCl…….....0.1 g

$Ca(NO_3)_2$……..….0.01 g

$FeSO_4.7H_2O$……..44.2 g (adjusted to the desired final concentration)

However, some adjustments were made to comply with some literature findings (Tuovinen et al., 1971) and with what best fits the chemistry of the Truetown AMD. These adjustments were made as follows:

1. The potassium chloride (KCl) added in the original recipe would result a final Cl^- concentration of 48 mg/L. Cl^- was proven to be inhibitory for the growth of iron-oxidizing bacteria (Tuovinen et al., 1971). Moreover, Truetown AMD has Cl^- concentration that does not exceed 25 mg/L. Therefore, the KCl addition was adjusted to match the concentration in Truetown AMD with a final Cl^- concentration of 25 mg/L.
2. To control the nitrogen source, calcium nitrate was replaced with calcium sulfate. The calcium concentration in the original 9k medium was 2.44 mg/L, and 178 mg/L in Truetown AMD. Literature has suggested no inhibitory effects for calcium (Tuovinen et al., 1971), and therefore, a mid-way concentration of 100 mg/L Ca^{2+} was adopted for this study.
3. Literature has suggested that sulfate has beneficial effects on iron oxidation with lowest unlimited concentrations of 2 g/L (Tuovinen et al., 1971). The concentration of SO_4^{2-} at Truetown AMD was found to be around 1500 mg/L. Because the ammonium was supplied in the form of ammonium sulfate, the sulfate concentration was not fixed throughout the nitrogen source evaluation, as higher ammonium concentrations carried higher sulfate concentrations as well. Therefore, the concentration of SO_4^{2-} was kept at or higher than 1500 mg/L throughout the nitrogen source evaluation set, and at 5000 mg/L throughout the phosphorus source and carbon source evaluation sets.

4. Literature has suggested that magnesium has beneficial effects on iron oxidation with lowest unlimited concentrations of 2 mg/L (Tuovinen et al., 1971). Truetown AMD has a magnesium concentration of about 60 mg/L. However, because the magnesium was supplied in the form of magnesium sulfate, and in order to meet the minimum adopted sulfate concentration of 1500 mg/L at low tested ammonium concentrations, the magnesium concentration was fixed at 75 mg/L throughout the study.
5. The hydrated form of magnesium sulfate ($MgSO_4.7H_2O$) was not available in the laboratory. Therefore, the dehydrate form was used instead ($MgSO_4$).

The resulted modified 9K medium recipe was prepared as follows:

$(NH_4)_2SO_4$…….…….. different tested concentrations
K_2HPO_4……... different tested concentrations
$MgSO_4$…….……..0.376 g
KCl…….....0.04206 g
$CaSO_4.2H_2O$…….….0.4296 g

- This recipe is for each 1L of solution. pH was adjusted to 2.5 using sulfuric acid.
- The solution was prepared with DI water in glass media bottles, and it was autoclaved at 121° C and 15 psi for 30 min.

This part of the study was conducted in stages. In other words, the methodology of one stage heavily relies on the results from the previous stage. Therefore, some parts of the methodology will be justified in the results section.

Iron Sulfate Addition

A stock solution of iron sulfate was prepared separately. 25 g of iron sulfate heptahydrate was added to 500 ml autoclaved DI water in a glass media bottle (adjusted to pH 2.5) using a sterilized spoon to reach a final concentration of 10,000 mg/L. The ferrous iron concentration was brought up to approximately 250 mg/L, whenever it dropped below 10 mg/L by adding the stock solution. The solution was preserved in the fridge at low pH to prevent iron oxidation and precipitation. Multiple cycles of ferrous iron addition were conducted until stable oxidation rates were reached or a decline in the oxidation rates was observed.

Nitrogen Test

For the nitrogen source evaluation, nitrogen was supplied in the form of ammonium sulfate. No study in literature has tested ammonium as a nitrogen source for iron-oxidizing bacteria. Therefore, the decision was made to test the following concentrations of ammonium: 0.01 M, 0.05 M, 0.1 M, and 0.5 M.

Both the FR and the WR cultures enriched at pH 2.5 were tested for the best ammonium concentration. The PA culture was not tested due to unsatisfactory oxidation rates. All concentrations were tested in triplicate, and only the WR culture was tested for 0.5 M of ammonium. One negative control was prepared for each culture at 0.05 M ammonium by adding 2.0% formaldehyde. The test was conducted using 500 ml Erlenmeyer flasks with 100 ml of test sample. The flasks were soaked in nitric acid, scrubbed, washed thoroughly, and autoclaved at 121° C and 15 psi for 30 min. The cultures with the best pH were used as inoculum for this stage. The inoculum from the previous stage was prepared by increasing the pH to approximately 4.2, allowing the oxidized iron

to settle, pouring the supernatant in a sterilized flask, reducing the pH back to 2.5, and using this supernatant as inoculum. Each flask was prepared by adding 10% inoculum and 90% modified 9K media. The flasks were capped with a sponge cap to prevent dust and particles from contaminating the sample and allowing the oxygen to diffuse freely. The flasks were put on a shaker table at 200 rpm.

At this stage, no information was available for the optimum phosphate concentration for iron-oxidizing bacteria. Therefore, the phosphate concentration was fixed at the concentration provided in the original 9K recipe. The final recipe for this stage was prepared as follows:

$(NH_4)_2SO_4$…….……..0.6607 g, 3.3035 g, 6.607 g, and 33.035 g
K_2HPO_4……....0.5 g
$MgSO_4$……..0.376 g
KCl……....0.04206 g
$CaSO_4.2H_2O$……...…..0.4296 g

- This recipe is for each 1.0 L of solution. pH was adjusted to 2.5 using sulfuric acid.
- Each ammonium concentration was prepared in a separate solution.
- The solution was prepared with DI water in glass media bottles, and it was autoclaved at 121° C and 15 psi for 30 min.
- Ferrous iron was added separately using the iron sulfate stock solution.

pH and ferrous iron concentration were monitored with time. Ferrous iron concentration was brought back up to 250 mg/L, whenever it dropped below 10 mg/L. Multiple cycles of ferrous iron additions were conducted until stable oxidation rates were

reached or a decline was observed. The nitrogen evaluation methodology is summarized in **Table 6**.

Table 6

A Summary of the Nitrogen Test Methodology

Tested cultures	WR	FR
Tested ammonium concentrations in triplicate	0.01 M, 0.05 M, 0.1 M, 0.5 M	0.01 M, 0.05 M, 0.1 M
Control	1 at 0.05 M	1 at 0.05 M
Sample composition	10% inoculum, 90% modified 9K medium	10% inoculum, 90% modified 9K medium
Total # of flasks	13	10

Phosphorus Test

For the phosphorus source evaluation, phosphorus was supplied in the form of potassium phosphate dibasic. Five concentrations of phosphate were tested: 0.1 mM, 0.5 mM, 1.0 mM, 5.0 mM, and 10.0 mM. Only the WR culture was carried out to this stage. The FR culture was omitted due to unsatisfactory oxidation rates. All concentrations were tested in triplicate. One negative control was prepared at 5.0 mM phosphate by adding 2.0% formaldehyde. The test was conducted using 500 ml Erlenmeyer flasks with 100 ml of test sample. The flasks were soaked in nitric acid, scrubbed, washed thoroughly, and autoclaved at 121° C and 15 psi for 30 min. The cultures with the best pH and ammonium concentration were used as inoculum for this stage. The inoculum from the previous stage was prepared by increasing the pH to approximately 4.2, allowing the oxidized iron to settle, pouring the supernatant to a sterilized flask, reducing the pH back to 2.5, and using

this supernatant as inoculum. Each flask was prepared by adding 10% inoculum and 90% modified 9K media. The flasks were capped with a sponge cap to prevent dust and particles from contaminating the sample and allowing the oxygen to diffuse freely. The flasks were put on a shaker table at 200 rpm.

The best ammonium concentration was found to be 0.1M. Therefore, 0.1M ammonium concentration was fixed at this stage, resulting the following modified 9K medium recipe:

$(NH_4)_2SO_4$……..……..6.607g

K_2HPO_4……....0.0174g, 0.0871g, 0.1742g, 0.871g, and 1.742g
$MgSO_4$……..0.376 g
KCl……....0.04206 g
$CaSO_4.2H_2O$…….0.4296 g

- This recipe is for each 1.0 L of solution. pH was adjusted to 2.5 using sulfuric acid.
- Each phosphate concentration was prepared in a separate solution.
- The solution was prepared with DI water in glass media bottles, and it was autoclaved at 121° C and 15 psi for 30 min.
- Ferrous iron was added separately using the iron sulfate stock solution.

pH and ferrous iron concentration were monitored with time. Ferrous iron concentration was brought back up to approximately 250 mg/L, whenever it dropped below 10 mg/L. Multiple cycles of ferrous iron addition were conducted until stable oxidation rates were reached or a decline was observed. The phosphorus evaluation methodology is summarized in **Table 7**.

Table 7

A Summary of the Phosphorus Test Methodology

Tested cultures	WR
Tested phosphorus concentrations in triplicate	0.1 mM, 0.5 mM, 1.0 mM, 5.0 mM, 10.0 mM
Control	1 at 5.0 mM
Sample composition	10% inoculum, 90% modified 9K medium
Total # of flasks	16

Organic Carbon Test

For the organic carbon evaluation, the organic carbon source was supplied in the form of glucose. Three concentrations of glucose were tested: 0.05 M, 0.1 M, and 0.2 M. Only WR culture was carried out to this stage. All other cultures were omitted due to unsatisfactory oxidation rates. All concentrations were tested in triplicate, and the test was conducted in duplicate. One negative control was prepared at 0.05 M glucose by adding 2.0% formaldehyde. The test was conducted using 500 ml Erlenmeyer flasks with 100 ml of test sample. The flasks were soaked in nitric acid, scrubbed, washed thoroughly, and autoclaved at 121° C and 15 psi for 30 min. The cultures with the best pH, ammonium concentration, and phosphate concentration were used as inoculum for this stage. The inoculum from the previous stage was prepared by increasing the pH to approximately 4.2, allowing the oxidized iron to settle, pouring the supernatant to a sterilized flask, reducing the pH back to 2.5, and using this supernatant as inoculum. Each flask was prepared by adding 10% inoculum and 90% modified 9K media. The flasks were capped with a sponge cap to prevent dust and particles from contaminating the sample and allowing the oxygen

to diffuse freely. The flasks were put on a shaker table at 200 rpm. **Figure 2. 2** shows the organic carbon test setup.

Figure 2. 2

Organic Carbon Test Setup

The best phosphate concentration was found to be 5.0 mM. Therefore, 5.0 mM phosphate concentration was fixed at this stage, resulting the following modified 9K medium recipe:

$(NH_4)_2SO_4$……..……..6.607g

K_2HPO_4……....0.871g

$MgSO_4$……..0.376 g

KCl……....0.04206 g

$CaSO_4.2H_2O$…….0.4296 g

Glucose ($C_6O_6H_{12}$)……..9.0g, 18.0g, and 36.0g

- This recipe is for each 1.0 L of solution. pH was adjusted to 2.5 using sulfuric acid.
- Each glucose concentration was prepared separately.
- The solution was prepared with DI water in glass media bottles, and it was autoclaved at 121° C and 15 psi for 30 min.
- Ferrous iron was added separately using the iron sulfate stock solution.

pH and ferrous iron concentration were monitored with time. Ferrous iron concentration was brought back up to approximately 250 mg/L, whenever it dropped below 10 mg/L. Multiple cycles of ferrous iron addition were conducted until stable oxidation rates were reached or a decline was observed. The organic carbon evaluation methodology is summarized in **Table 8**.

Table 8

A Summary of the Organic Carbon Methodology

Tested cultures	**WR**
Tested organic carbon concentrations in triplicate	0.05 M, 0.1 M, 0.2 M
Control	1 at 0.05 M
Sample composition	10% inoculum, 90% modified 9K medium
Total # of flasks	10

Applying the Results

Wolf Run and Truetown AMD Water Analysis

Wolf Run and Truetown AMD water was analyzed for nitrogen and phosphorus concentrations to keep track of the final concentration after the nutrient supply. Fresh water samples were collected from WR and TT sites and transported on ice within 24 hr to the lab for the analysis. Two sterilized bottles were collected for each site: one bottle contained sulfuric acid to preserve the sample for the nitrogen test, and the other bottle was collected for the phosphorus test. The nitrogen was analyzed for total nitrogen, nitrite, and nitrate, while the phosphorus was analyzed for orthophosphate and total phosphorous. The samples were analyzed at Alloway Labs-Marion (1776 Marion-Waldo Rd #7428, Marion, OH 43302).

Wolf Run Culture Enrichment

Successive sub-culturing in different mediums may result in major changes in the bacterial culture composition. Therefore, fresh field cultures were collected to test their performance with the best nutrients combination. The same sampling methodology was adopted to collect sediment samples from the same spot that the WR culture was collected from, and the same bacterial extraction methodology was adopted to prepare the inoculum for this stage. Sediment samples were collected from the top 2 cm of the streambed using sterilized Teflon spoons and autoclaved sediment jars. Water samples were collected from the same locations before collecting the sediment sample using sterilized 1.0 L plastic bottles filled with no headspace. Samples were transported back to the laboratory on ice and were processed within 6 hr of collection. The bacteria were extracted from the sediment using 3.8 mM sodium pyrophosphate solution. Sodium pyrophosphate ($Na_4P_2O_7$) solution

was prepared by mixing 1.0 g of sodium pyrophosphate in 1.0 L of DI water. pH was adjusted to 2.5 using sulfuric acid. The solution was autoclaved at 121° C and 15 psi for 30 min. 60-80 g of sediment were mixed with each 500 mL of the solution, put on a shaker table at 300 rpm for 40 min, allowed to settle, and the supernatant (inoculum) was used for this stage.

500 ml Erlenmeyer flasks were used for incubation. Flasks were soaked in nitric acid, scrubbed, washed thoroughly, and autoclaved at 121° C and 15 psi for 30 min prior to use. The flasks were capped with a sponge cap to prevent dust and particles from contaminating the sample while allowing the oxygen to diffuse freely. The flasks were put on a shaker table at 200 rpm. **Figure 2. 3** shows the WR enrichment test setup.

Figure 2. 3

Wolf Run Enrichment Test Setup

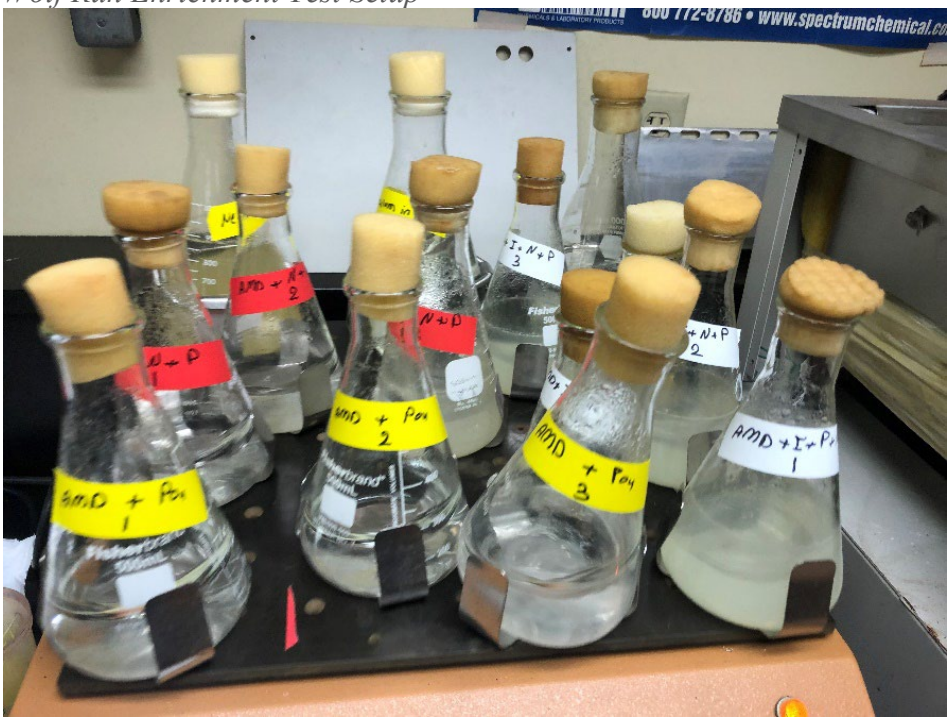

The best pH, phosphorus concentration, and ammonium concentration were found to be 2.5, 5.0 mM, and 0.1 M, respectively. Organic carbon was proven to have no beneficial effect on the oxidation rates. The pH was adjusted to 2.5 for all samples using sulfuric acid. The phosphorus was added in the form of potassium phosphate dibasic, and the ammonium was added in the form of ammonium sulfate. Different combinations of nutrients and inoculum additions were investigated. The tested combinations and the samples composition for WR AMD enrichment are illustrated in **Table 9**.

Table 9

A Summary of the Wolf Run Enrichment Test Methodology

Trial abbreviation	Sample Composition	Nutrients final Concentration	Test conducted in:
WR-AMD	100% AMD	None	Triplicate
WR-AMD + N + P	100% AMD	0.1 M NH_4^+ 5.0 mM PO_4^{3-}	Triplicate
WR-AMD + I	90% AMD, 10% inoculum	None	Triplicate
WR-AMD + N + P + I	90% AMD, 10% inoculum	0.1 M NH_4^+ 5.0 mM PO_4^{3-}	Triplicate
WR-AMD + N + I	90% AMD, 10% inoculum	0.1 M NH_4^+	Triplicate
WR-AMD + P + I	90% AMD, 10% inoculum	5.0 mM PO_4^{3-}	Triplicate

Total of 18 flasks

pH and ferrous iron concentration were monitored with time. Ferrous iron concentration was brought back up to approximately 250 mg/L whenever it dropped below 10 mg/L. Ferrous iron was added separately using the iron sulfate stock solution. Multiple

cycles of ferrous iron addition were conducted until stable oxidation rates were reached or a decline was observed.

Truetown AMD Enrichment

Enriching Truetown AMD with WR cultures was conducted to allow us to investigate the performance of the bacterial culture in different environments, and the possibility of using the tested culture to remediate a site like Truetown. The inoculum from the previous stage (WR AMD enrichment) was prepared by increasing the pH to approximately 4.2, allowing the oxidized ferric iron to settle, pouring the supernatant to a sterilized flask, reducing the pH back to 2.5, and using this supernatant as inoculum. 500 ml Erlenmeyer flasks were used for incubation. Flasks were soaked in nitric acid, scrubbed, washed thoroughly, and autoclaved at 121° C and 15 psi for 30 min prior to use. The flasks were capped with a sponge cap to prevent dust and particles from contaminating the sample while allowing the oxygen to diffuse freely. The flasks were put on a shaker table at 200 rpm. The tested combinations and the samples composition for Truetown AMD enrichment are illustrated in **Table 10**.

Table 10

A Summary of the Truetown Enrichment Test Methodology

Trial abbreviation	Solution Composition	Nutrients final Concentration	Test conducted in:
TT-AMD	100% AMD	None	Triplicate + 1 negative control*
TT-AMD + N + P	100% AMD	0.1 M NH_4^+ 5.0 mM PO_4^-	Triplicate
TT-AMD + P	100% AMD	5.0 mM PO_4^-	Triplicate
TT-AMD + I	90% AMD, 10% inoculum	None	Triplicate
TT-AMD + I + N + P	90% AMD, 10% inoculum	0.1 M NH_4^+ 5.0 mM PO_4^-	Triplicate + 1 negative control*
TT-AMD + I + N	90% AMD, 10% inoculum	0.1 M NH_4^+	Triplicate
TT-AMD + I + P	90% AMD, 10% inoculum	5.0 mM PO_4^-	Triplicate

***The negative control achieved by adding 2.0% formaldehyde** **Total of 23 flasks**

pH and ferrous iron concentration were monitored with time. Ferrous iron concentration was brought back up to approximately 250 mg/L whenever it dropped below 10 mg/L. Ferrous iron was added separately using the iron sulfate stock solution. Multiple cycles of ferrous iron addition were conducted until stable oxidation rates were reached or a decline was observed.

Wolf Run Inoculum Species Analysis

The species analysis was conducted on the WR inoculum that was used in this study. This is the inoculum that was sub-cultured in the growth media multiple times and tested on Truetown AMD. DNA extraction was conducted by Dr. Karen Coschigano's team at the Biomedical Sciences department at Ohio University following the protocol provided by

MR DNA Lab and modified according to Dr. Coschigano's experience. The extracted sample was then delivered to MR DNA Lab (Shallowater, TX 79363) for further species analysis.

Iron Measurement and Calibration

The dissolved ferrous iron was measured using colorimetry (Standard Methods 3500B). A Hach spectrophotometer measured the amount of light absorbed by the sample, which then can be converted to dissolved ferrous iron concentration using a calibration curve. The calibration curve was initiated using 250 mg/L iron sulfate, 5.549 mM 1,10-phenanthroline, and ammonium acetate stock solutions. The ammonium acetate solution was prepared by dissolving 25.0 g of ammonium acetate in 15.0 mL of ultrapure water, and then mixing it with 70 mL of glacial acetic acid. 5.0 mL of sample diluted with ultrapure water, 2.0 ml of 1,10 phenanthroline, 1.0 ml of ammonium acetate solution, and 2.0 ml of DI water were added to a 10.0 mL glass vial. The vial was then closed, shaken well, cleaned from any stains or air bubbles (as this can affect the reading accuracy), put in the spectrophotometer, and the reading was taken. The zero sample was prepared with 5.0 ml of ultrapure water (without any iron addition) followed by all the previously listed steps and was used to zero the Hach device. Linear regression was then conducted to find the curve of the best fit. The equation of the curve was then used to find the dissolved ferrous iron concentration of all the samples throughout this study. The calibration curve was then redone whenever new stock solutions were mixed for use. **Table 11** shows the samples prepared to initiate the calibration curve followed by **Figure 2. 4** showing sample calibration curve and the best fit equation.

Table 11

The Spectrophotometer Calibration Samples Preparation

Stock soln (µL)	DI water (µL)	Dilution factor (DF)	1,10-phenanthroline (µL)	Ammonium acetate solution (µL)	DI water (µL)	Final iron concentration (mg/L)	Absorption factor (Abs)
0	5000	-	2000	1000	2000	0	0
25.0	4975	200	2000	1000	2000	1.0	0.124
50.0	4950	100	2000	1000	2000	2.0	0.256
100.0	4900	50	2000	1000	2000	4.0	0.528
200.0	4800	25	2000	1000	2000	6.0	0.772

Figure 2. 4

Sample Spectrophotometer Calibration Curve

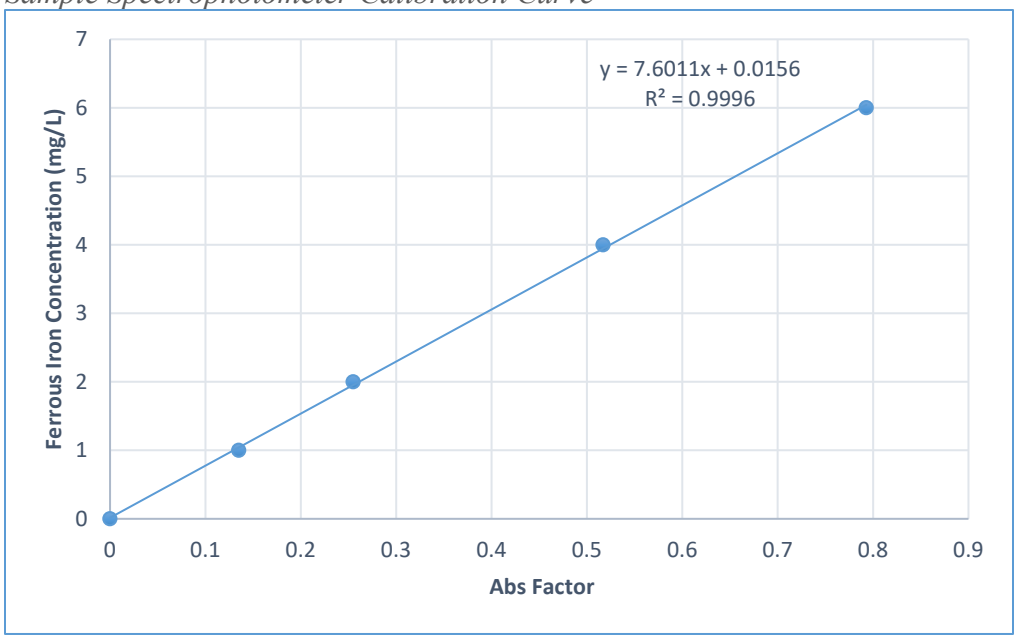

The dissolved ferrous iron concentration of any given sample was measured using the following equation:

$$Y = 7.6011X + 0.0156 \quad (9)$$

where Y is the dissolved ferrous iron concentration in mg/L,

and X is the absorption factor.

Absorbance was linear up to a Fe^{2+} concentration of 6 mg/L. Samples were diluted until the absorbance was within the calibration range.

Reaction Kinetics and Modeling

The iron oxidation rate in AMD waters with no oxygen limitation in a fed-batch reactor is expected to follow the first order kinetics. For a steady-state, first order reaction:

$$C = C_o e^{-kt} \quad (10)$$

Where C is the concentration at time t,

C_o is the initial concentration at time zero,

and k is the reaction rate constant.

The ferrous iron concentration was plotted versus time and points were fitted with an exponential curve. The constant of the exponent represented the reaction rate constant. The reaction rate constant was then used to determine the best pH, ammonium concentration, phosphorus concentration, organic carbon concentration, and the best nutrient combination in this study.

The effect of nitrogen and phosphorus concentrations on iron oxidation rates were modeled using Andrew's Equation and Monod Equation. The kinetics modeling was used to estimate the iron oxidation parameters constants. The concept, derivation, use, and limitations of each equation have been well studied and can be found in (Grady et al., 1998,

pg.78) Non-linear regression was used to fit the model by minimizing the square error between the experimental data and the model estimated data. For the first trial, Andrew's Equation was used assuming inhibitory effects at high substrate concentrations:

$$\mu = K_m \frac{C}{K_s + C + C^2/K_i} \quad (11)$$

Where μ is the model estimated iron oxidation rate,

C is the iron concentration,

K_m is the maximum iron oxidation rate.

K_s is the half-saturation coefficient (the substrate concentration at which the iron oxidation rate is half K_m),

And K_i is the inhibition coefficient.

However, if the non-linear regression modelling resulted in a high K_i value estimate, the model can be simplified back to Monod Equation, indicating no inhibitory effects at high substrate concentrations. When this case was confirmed, the non-linear regression was repeated using Monod Equation:

$$\mu = K_m \frac{C}{K_s + C} \quad (12)$$

Literature Kinetics Conversion

Due to the inconsistency of the documented units of iron oxidation rates, converting these oxidation rates to first-order kinetics was necessary to compare the results of this study.

Most of the studies in the literature measured kinetics in a flow through chemostat and assumed steady-state, zero-order kinetics:

$$k_0 = \frac{C_o - C}{\theta} \quad (13)$$

By knowing the influent and effluent concentrations/ratio, and interpreting the θ values from the dilution rates (1/ θ*),* the first-order kinetics assuming steady-state can be found as follows:

$$k_1 = \frac{C_o - C}{C\,\theta} \quad (14)$$

The continuous system mass balance can be found in reference (Schnoor, J.L. 1996.). For papers that provided enough raw data, first-order reaction rates were calculated from their data for comparison with the results reported here.

Statistical Analysis

The statistical analysis was conducted using SPSS statistics software. Any comparison between only two groups was conducted using an independent sample T-test. For multiple groups, the comparison was conducted using one-way ANOVA and the follow up Post Hoc tests. For homogenous variances, the Bonferroni Post Hoc test was adopted, while for non-homogenous variances, Games Howell Post Hoc test was adopted. Despite the adopted test, the Bonferroni correction for alpha value was achieved by dividing the alpha value by the number of tested groups participating in the Post Hoc test. New variables were defined for the independent sample T-test to avoid further correction of the alpha value and increasing the risk of the family-wise error. All tests were conducted at 95% level of confidence.

Chapter 3: Results

pH Test

Different cultures and media conditions were tested for iron oxidation kinetics under fed-batch growth system. The ferrous iron concentration was brought back up to approximately 250 mg/L, whenever it dropped below 10 mg/L, and Fe^{2+} oxidation rates were measured after each iron addition. Because the goal was to find conditions and cultures with the fastest kinetics, the average oxidation rate from the best batch for each trial was compared. In most cases, iron oxidation rates increased with repeated additions then declined again by the $3^{rd}/4^{th}$ addition. This trend is illustrated in **Figure 3. 2** through **Figure 3. 5** for the WR tested cultures. Average oxidation rates went from 0.0458 hr^{-1} to 0.0793 hr^{-1} to 0.138 hr^{-1} to 0.129 hr^{-1} with successive feedings. A rate of 0.138 hr^{-1} from the 3^{rd} feeding was used as representative for this trial. The rest of the cycles for other cultures are provided in the appendix.

Wolf Run (WR) Culture

WR AMD had an average pH of 3.25. Two culture trials were tested from Wolf Run site at pH 2.5, one using bacterial inoculum extracted from WR sediment (WR W + I), and the other using only WR AMD (WR W). One other trial was tested at pH 3 using bacterial inoculum extracted from WR sediment (WR W + I). The test was conducted in triplicate for each trial with negative controls by adding 2.0% formaldehyde at pH 2.5 and pH 3.0. The data of ferrous iron concentration with time were fitted exponentially as shown in **Figure 3. 1**, **Figure 3. 2** through **Figure 3. 5**, and **Figure 3. 6** for (WR W) and (WR W + I) at pH 2.5, and for (WR W + I) at pH 3.0, respectively.

Figure 3. 1

Ferrous Iron Oxidation with WR AMD at pH 2.5, No Nutrient Addition (2nd Iron Addition)

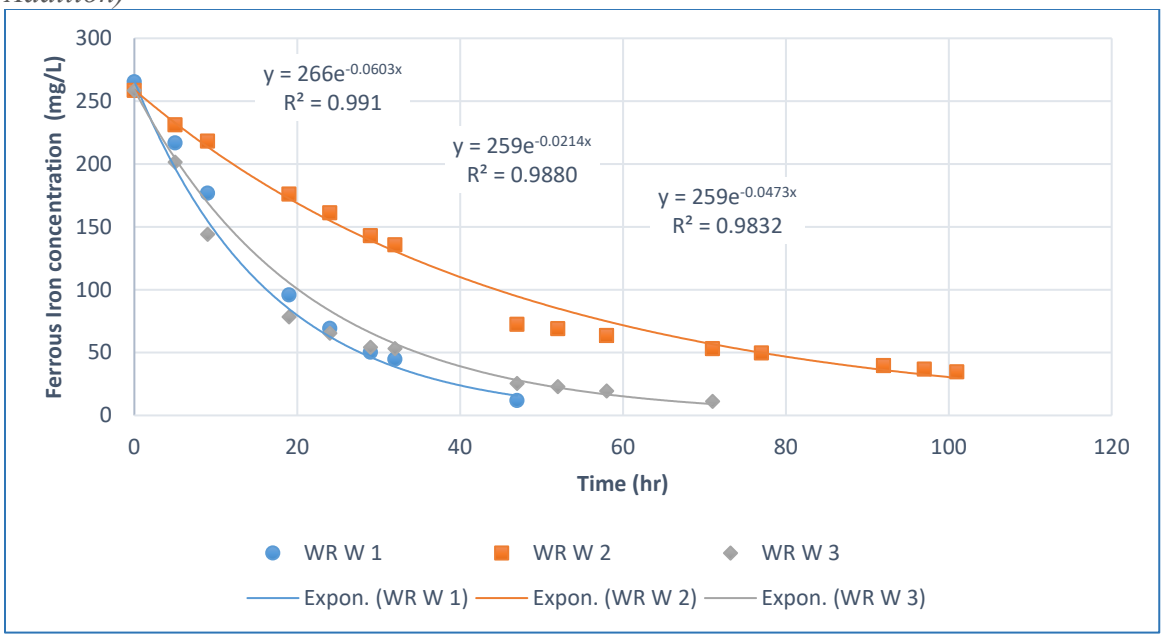

Figure 3. 2

Ferrous Iron Oxidation with WR AMD and Bacterial Inoculum Extracted from WR Sediment at pH 2.5, No Nutrient Addition (1st Iron Addition)

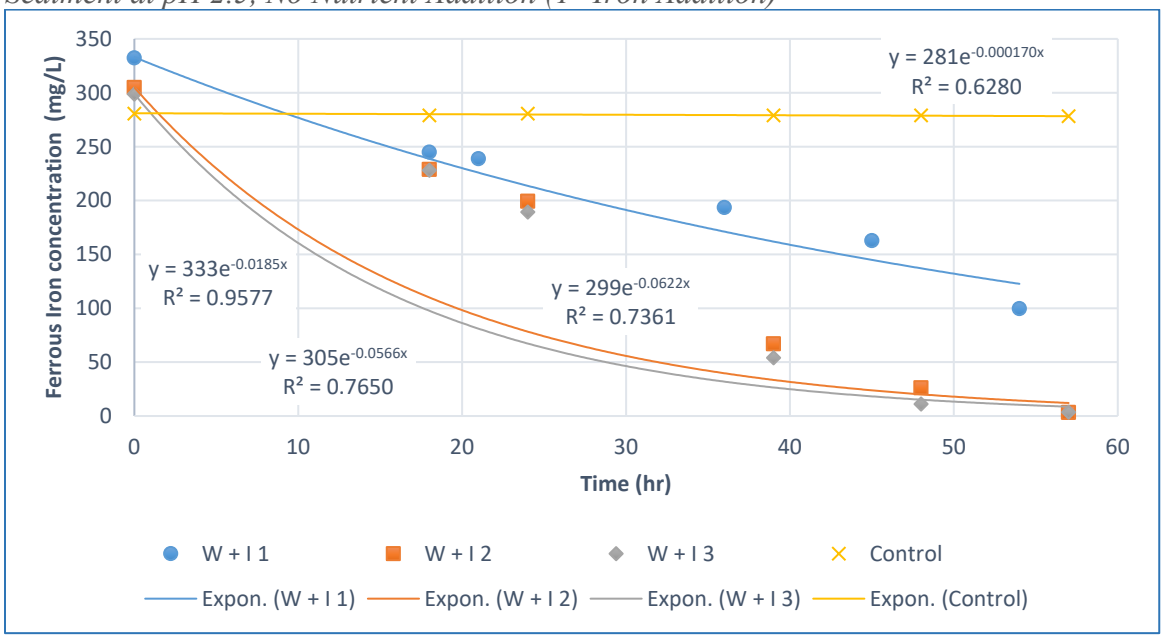

Figure 3. 3

Ferrous Iron Oxidation with WR AMD and Bacterial Inoculum Extracted from WR Sediment at pH 2.5, No Nutrient Addition (2nd Iron Addition)

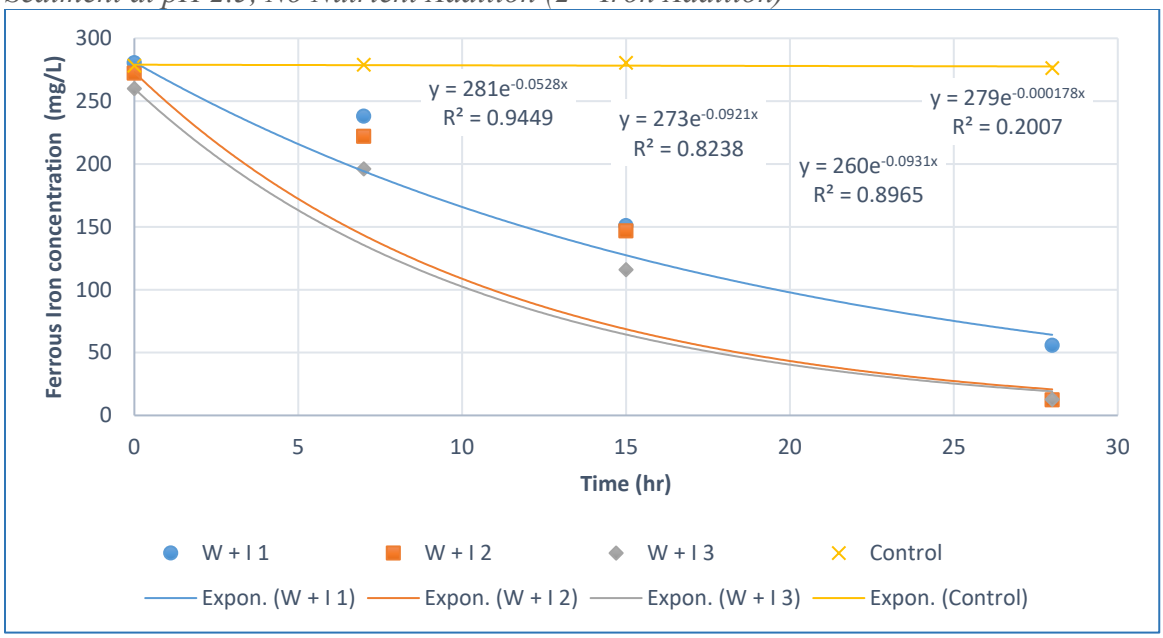

Figure 3. 4

Ferrous Iron Oxidation with WR AMD and Bacterial Inoculum Extracted from WR Sediment at pH 2.5, No Nutrient Addition (3rd Iron Addition)

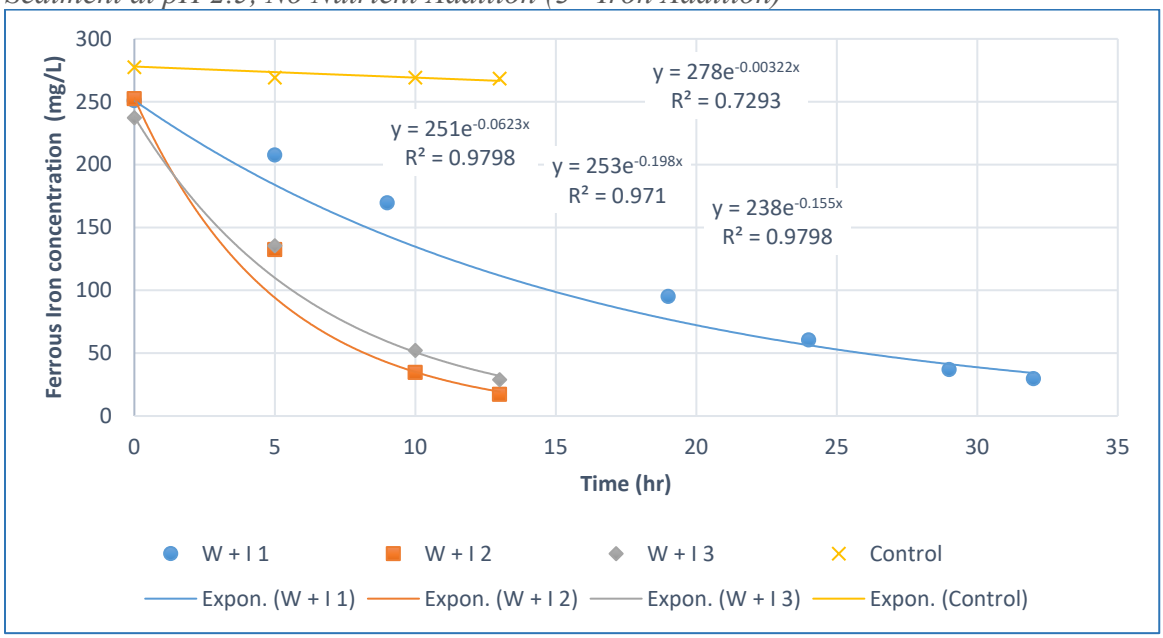

Figure 3. 5

Ferrous Iron Oxidation with WR AMD and Bacterial Inoculum Extracted from WR Sediment at pH 2.5, No Nutrient Addition (4th Iron Addition)

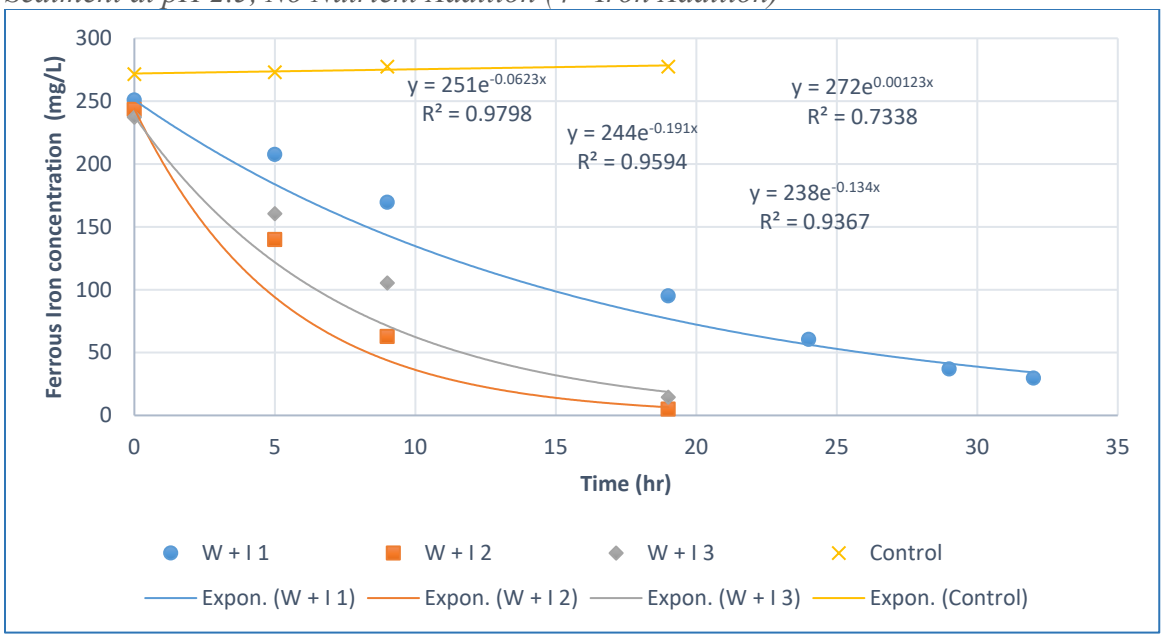

Figure 3. 6

Ferrous Iron Oxidation with WR AMD and Bacterial Inoculum Extracted from WR Sediment at pH 3.0, No Nutrient Addition (2nd Iron Addition)

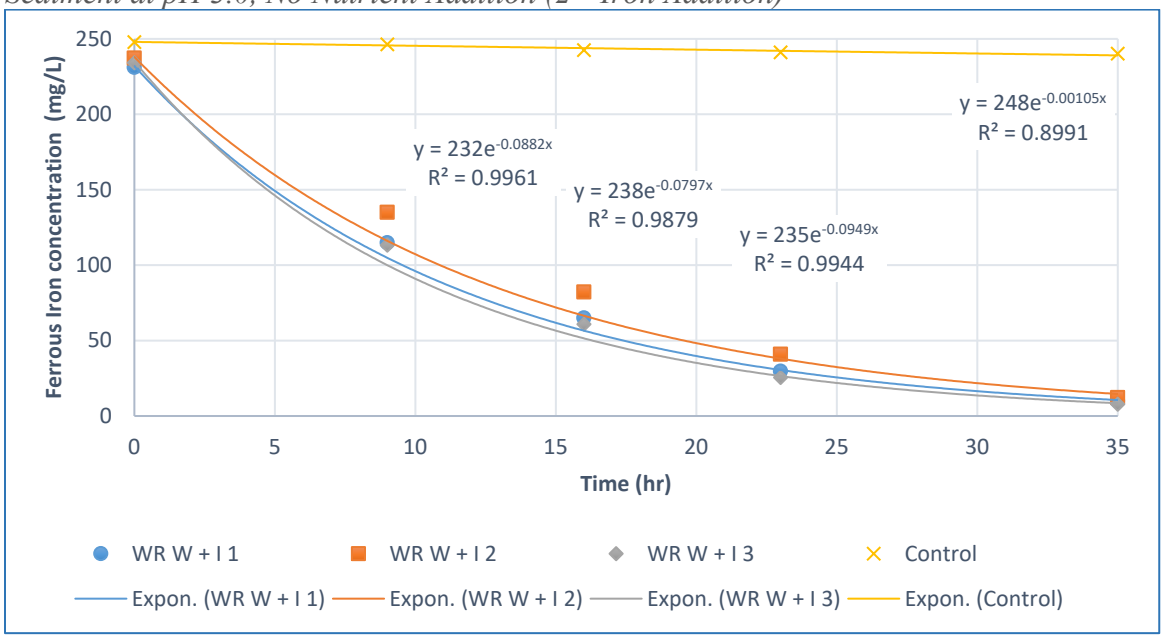

The iron oxidation rates increased with inoculum addition at both pH values. At pH 2.5, the oxidation rate increased by 3.2-fold from an average of 0.0427 hr^{-1} for WR W, to an average of 0.138 hr^{-1} for WR W+I. However, at pH 3.0, the average iron oxidation rate with inoculum addition was 1.57-fold less than the iron oxidation rate achieved at pH 2.5 (with an average of 0.0876 hr^{-1}). Moreover, at pH 2.5, the detention time decreased from an average of 73 hr for WR W, to an average of 20 hr for WR W+I. At pH 3.0, the detention time was consistent for the 3 trials with a value of 35 hr. The ferrous iron oxidation was minimal in all the negative controls with a maximum rate of 3.22 x 10^{-3} hr^{-1} being 13.2-fold less than the slowest achieved biotic oxidation rate at this stage.

Flint Run (FR) Culture

Two culture trials were tested from the Flint Run site, one using FR AMD and bacterial inoculum extracted from FR sediments (FR W + I) and the other one using only FR AMD (FR W). FR AMD water had a pH of 2.5 – 2.7 and the incubation pH was 2.5. The test was conducted in triplicate for each trial with one negative control achieved by adding 2.0% formaldehyde. The ferrous iron concentrations with time were fitted exponentially as shown in **Figure 3. 7** for (FR W) and **Figure 3. 8** for (FR W + I). The iron oxidation rates increased 10-fold with sediment inoculum addition from an average of 0.0142 hr^{-1} for FR W, to an average of 0.144 hr^{-1} for FR W+I. Moreover, the reaction time decreased from approximately 105 hr for FR W to 20 hr for FR W+I. ferrous iron oxidation was minimal in the negative control with a rate of 5.03×10^{-5} hr^{-1}.

Figure 3. 7

Ferrous Iron Oxidation with FR AMD at pH 2.5, No Nutrient Addition (1st Iron Addition)

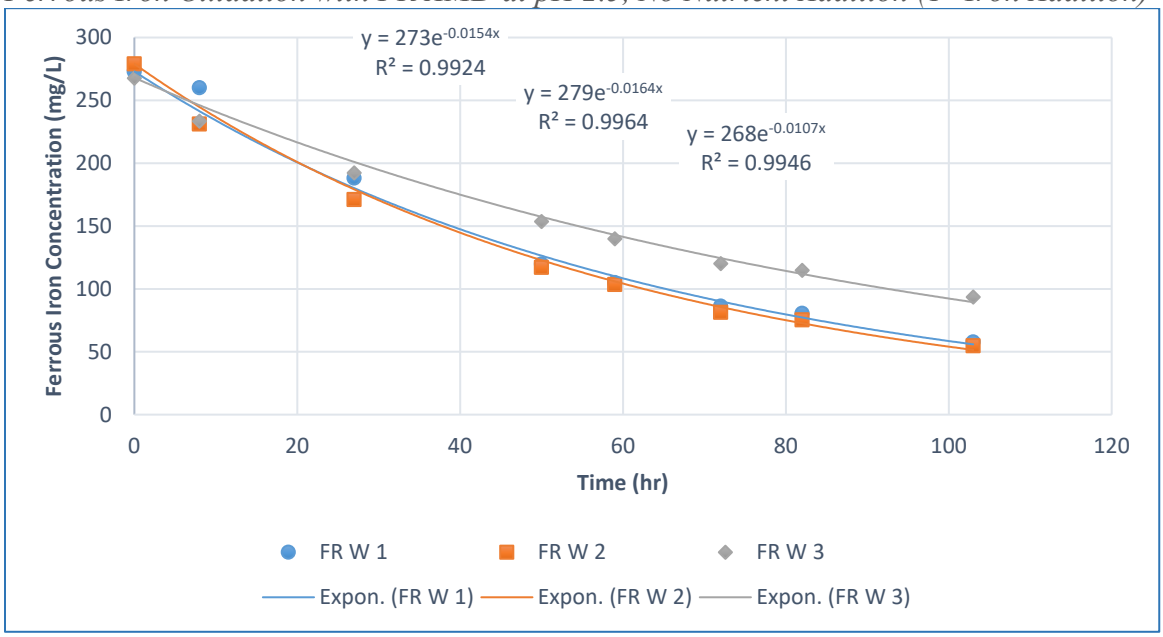

Figure 3. 8

Ferrous Iron Oxidation with FR AMD and Bacterial Inoculum Extracted from FR Sediment at pH 2.5, No Nutrient Addition (2nd Iron Addition)

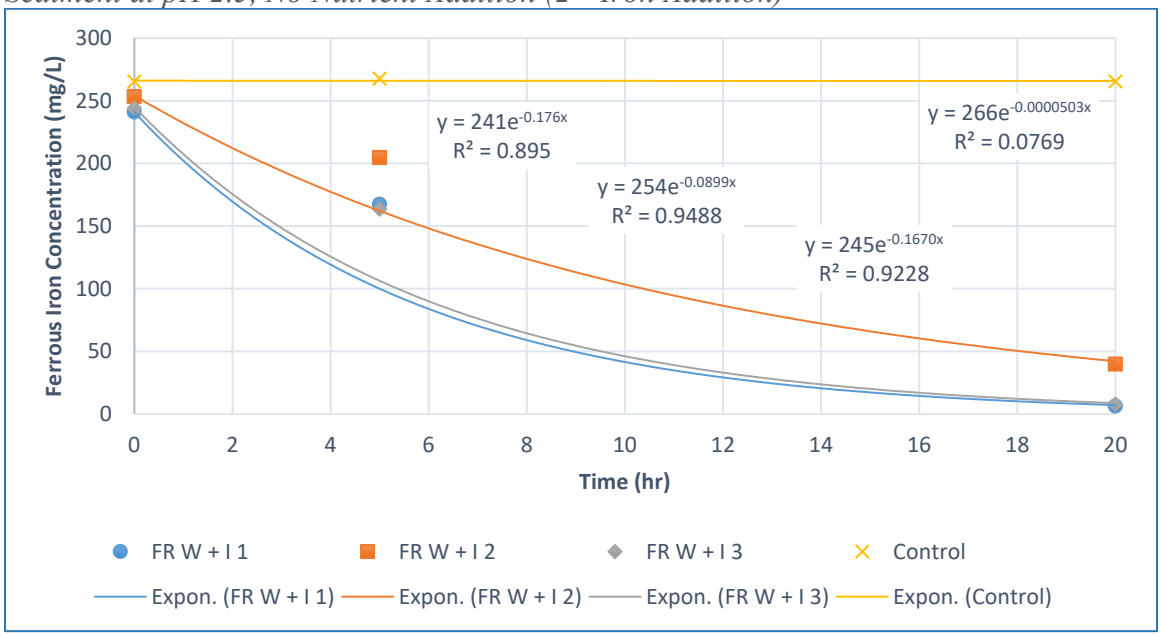

PA Culture

One culture trial (PA W + I) was tested from a Pennsylvania site at two different pH values, pH 2.0 and pH 4.0, using PA AMD and bacterial inoculum extracted from PA sediment. The test was conducted in triplicate for each trial with one negative control at each pH value. The data of ferrous iron concentration with time were fitted exponentially as shown in **Figure 3. 9** and **Figure 3. 10** for (PA W + I) at pH 2.0 and (PA W + I) at pH 4.0, respectively.

Figure 3. 9

Ferrous Iron Oxidation with PA AMD And Bacterial Inoculum Extracted from PA Sediment at pH 2.0, No Nutrient Addition (1st Iron Addition)

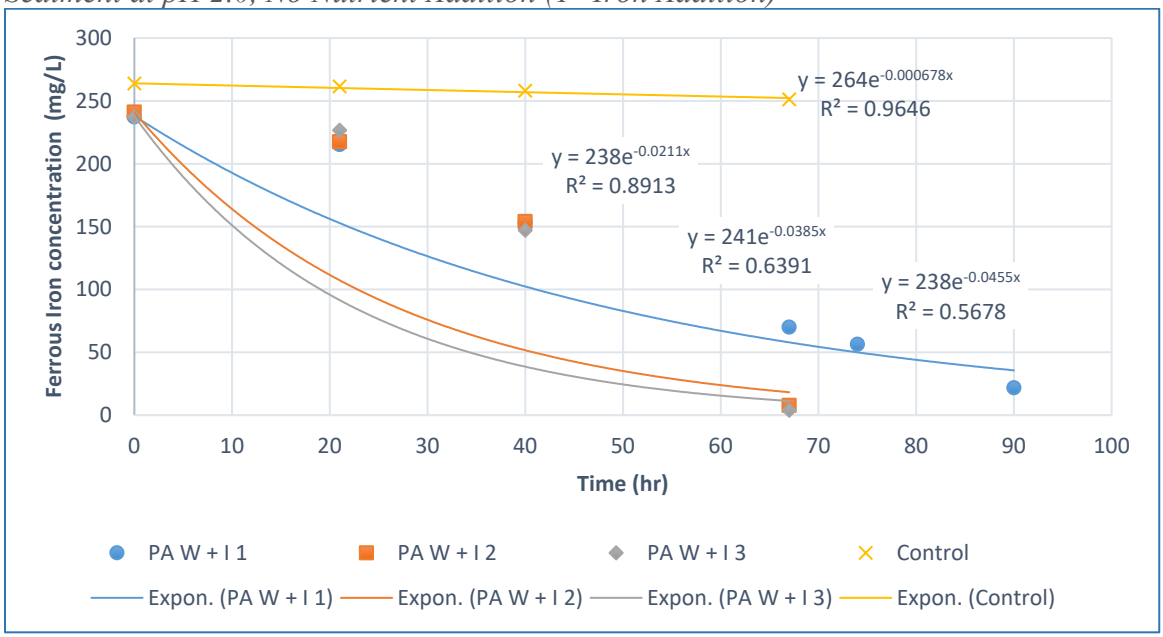

Figure 3. 10

Ferrous Iron Oxidation with PA AMD and Bacterial Inoculum Extracted from PA Sediment at pH 4.0, No Nutrient Addition (2nd Iron Addition)

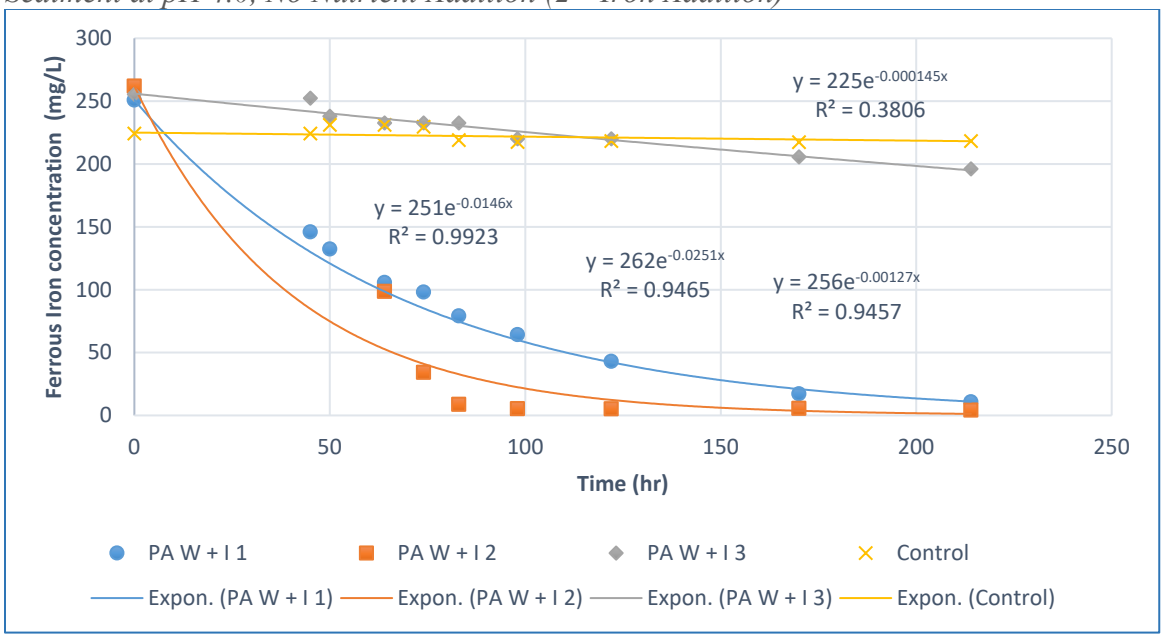

At pH 2.0, the oxidation rates had an average of 0.0353 hr^{-1} with an average detention time of 75 hr. However, at pH 4.0, the average oxidation rate was 2.5-fold lower with a value of 0.0137 hr^{-1} and an average detention time of 214 hrs. The ferrous iron oxidation decreased substantially by the 3rd iron addition. The ferrous iron oxidation was minimal in all the negative controls with a maximum rate of of 6.78×10^{-4} hr^{-1} at pH 2.0 being 20-fold less than the slowest achieved biotic oxidation rate at this stage. Because of the significantly lower iron oxidation rates compared with the WR and the FR cultures, no further testing was done with the PA culture. The summary descriptive statistics for the pH test is shown in **Figure 3. 11**.

Figure 3. 11

Summary Descriptive Statistics of the pH Test

Descriptive Statistics

	N	Mean		Std. Deviation	Variance
	Statistic	Statistic	Std. Error	Statistic	Statistic
FR_WI_pH_2.5	3	.14430	.027324	.047326	.002
FR_W_pH_2.5	3	.01417	.001757	.003044	.000
WR_WI_pH_2.5	3	.13840	.040071	.069405	.005
WR_W_pH_2.5	3	.04267	.011465	.019858	.000
WR_WI_pH_3.0	3	.08760	.004398	.007618	.000
PA_WI_pH_2.0	3	.03533	.007446	.012897	.000
PA_WI_pH_4.0	3	.01367	.006960	.012055	.000
Valid N (listwise)	3				

Nutrients Test

Nitrogen, phosphorus, and organic carbon (glucose) concentrations were investigated with the WR and the FR cultures. The bacteria were cultured in a modified 9K media. Ferrous iron oxidation rates were measured and compared statistically. The tests were conducted in a fed-batch system. Because the highest oxidation rates were found to occur at pH 2.5, this pH was maintained throughout all conducted nutrients tests.

Nitrogen Test

The nitrogen source was supplied in the form of ammonium sulfate. Two culture inoculums were tested separately for nitrogen. One using FR AMD and bacterial inoculum extracted from FR sediments (FR) and the other one using WR AMD, and bacterial inoculum extracted from WR sediments (WR) that were enriched at pH 2.5. The inoculum accounted for 10% of the sample while the modified 9K media accounted for the remaining 90%. The phosphate concentration was fixed at 0.00287 M as suggested in the original 9K recipe and no organic carbon was added. The incubation pH was 2.5. Four ammonium

concentrations were tested for the WR inoculum, 0.01 M, 0.05 M, 0.1 M, and 0.5 M, while three ammonium concentrations were tested for the FR inoculum, 0.01 M, 0.05 M, and 0.1 M. The tests were conducted in triplicate for each concentration with one negative control for each culture at 0.05 M of ammonium achieved by adding 2.0% formaldehyde. Ferrous iron concentration was brought back up to approximately 250 mg/L whenever it dropped below 10 mg/L, and Fe^{2+} oxidation rates were measured after each iron addition by exponentially fitting ferrous iron concentrations with time data points. Because the goal was to find conditions and cultures with the fastest kinetics, the average oxidation rate from the best batch for each trial was plotted here for comparison. **Figure 3. 12** through **Figure 3. 18** show ferrous iron oxidation rates for WR inoculum at 0.01 M, 0.05 M, 0.1 M, and 0.5 M of ammonium and for FR inoculum at 0.01 M, 0.05 M, and 0.1 M of ammonium, respectively. Figures showing ferrous iron oxidation rates at other ferrous iron addition cycles are listed in the appendix.

Figure 3. 12

Ferrous Iron Oxidation Rates with WR Inoculum in Modified 9K Media, 0.01 M N, 2.87 mM P, No C (3rd Iron Addition)

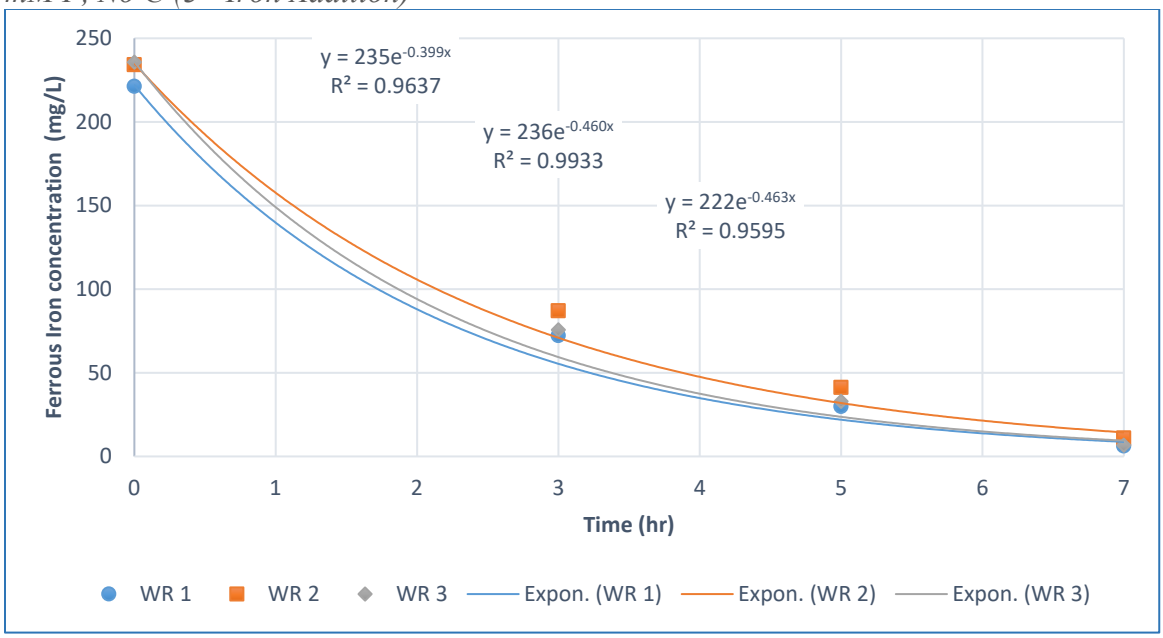

Figure 3. 13

Ferrous Iron Oxidation Rates with WR Inoculum in Modified 9K Media, 0.05 M N, 2.87 mM P, No C (2nd Iron Addition)

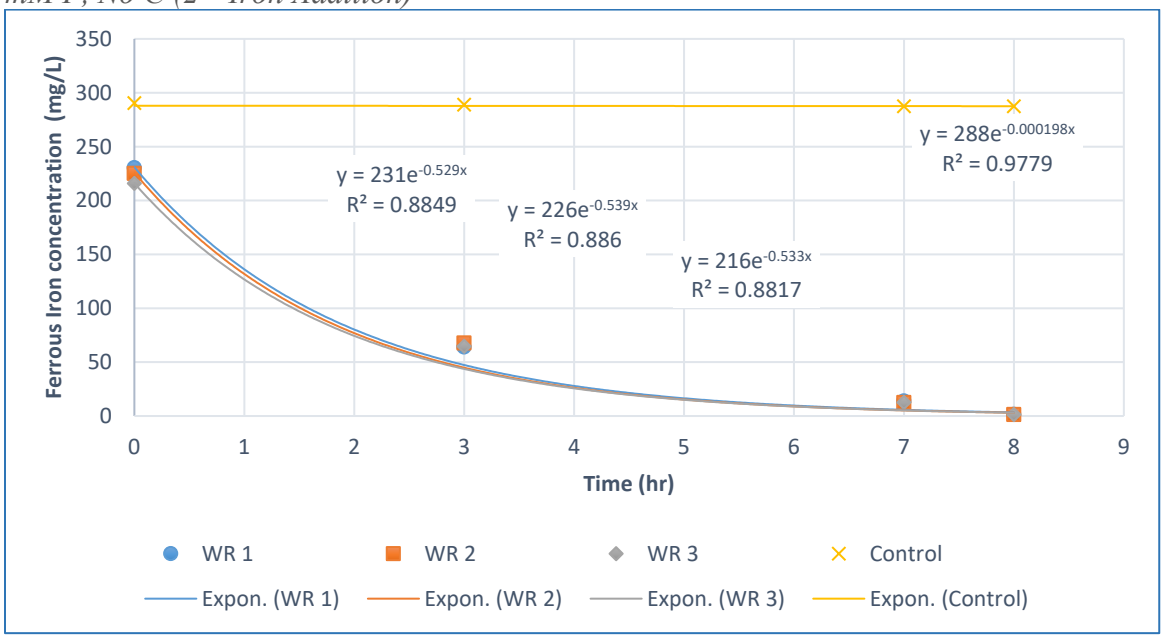

Figure 3. 14

Ferrous Iron Oxidation Rates with WR Inoculum in Modified 9K Media, 0.1 M N, 2.87 mM P, No C (3rd Iron Addition)

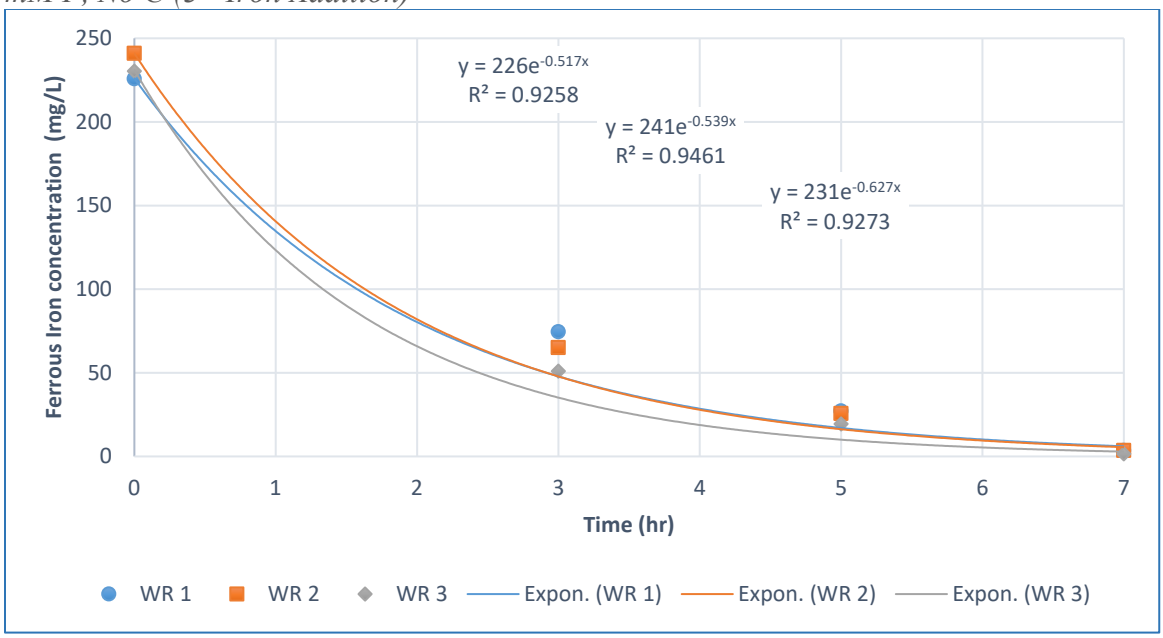

Figure 3. 15

Ferrous Iron Oxidation Rates with WR Inoculum in Modified 9K Media, 0.5 M N, 2.87 mM P, No C (2nd Iron Addition)

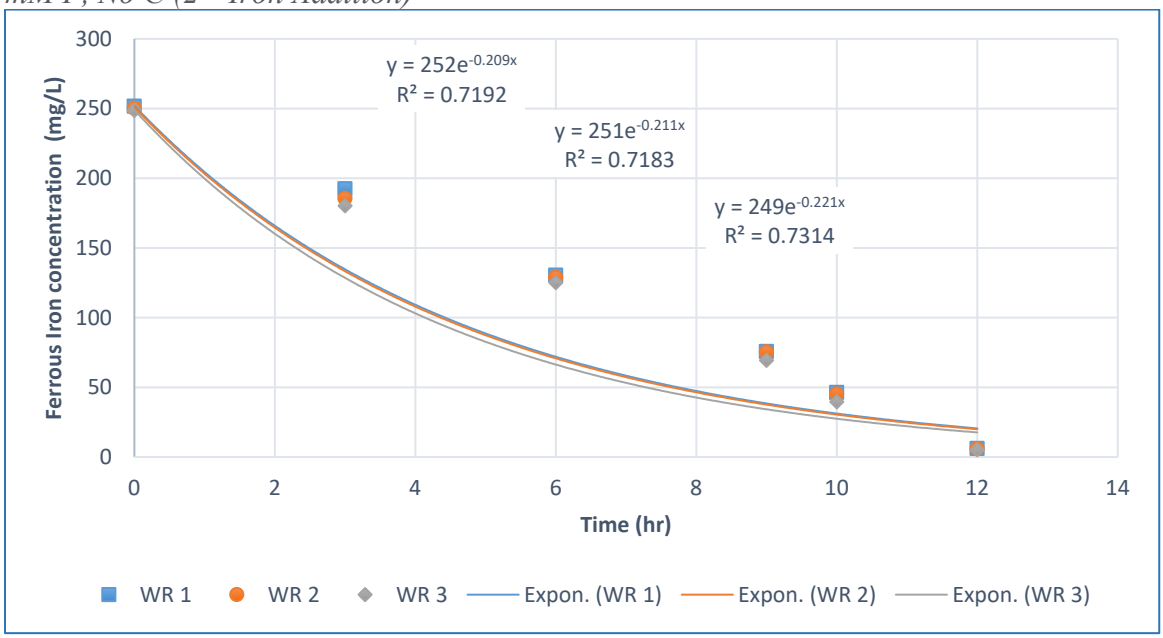

Figure 3. 16

Ferrous Iron Oxidation Rates with FR Inoculum in Modified 9K Media, 0.01 M N, 2.87 mM P, No C (1st Iron Addition)

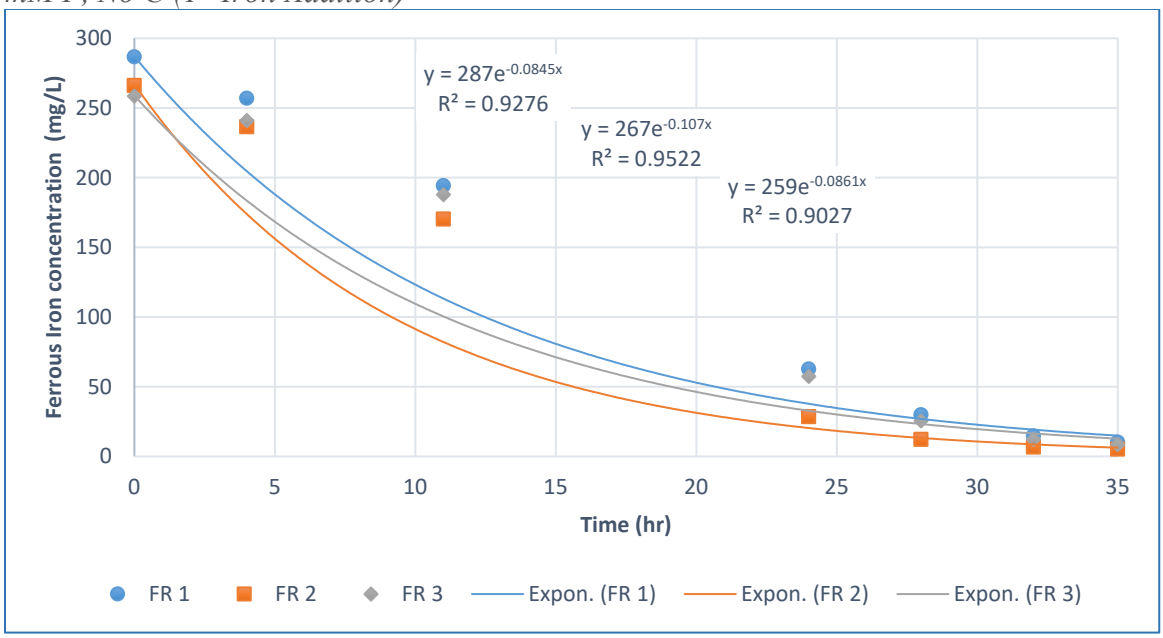

Figure 3. 17

Ferrous Iron Oxidation Rates with FR Inoculum in Modified 9K Media, 0.05 M N, 2.87 mM P, No C (1st Iron Addition)

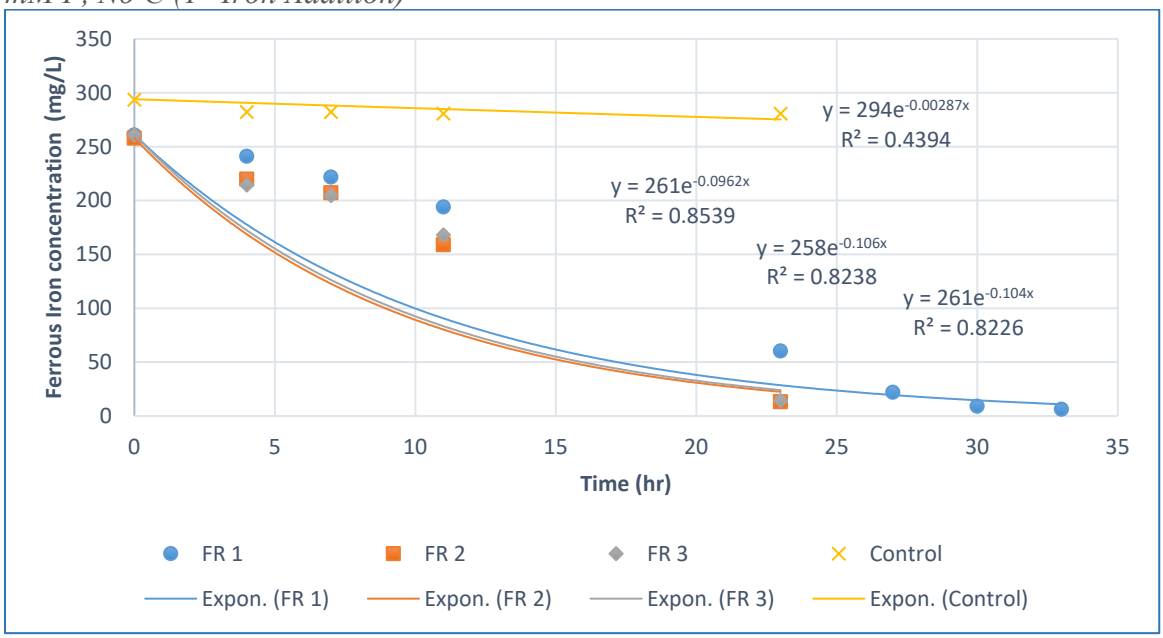

Figure 3. 18

Ferrous Iron Oxidation Rates with FR Inoculum in Modified 9K Media, 0.1 M N, 2.87 mM P, No C (1st Iron Addition)

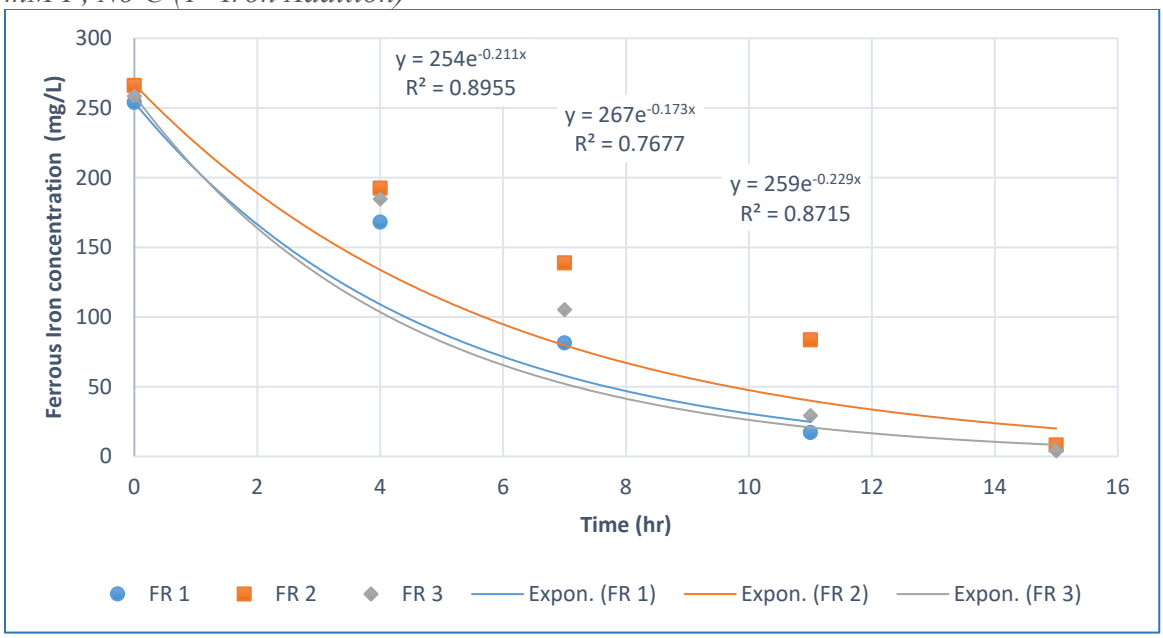

For both the WR and the FR cultures, the highest oxidation rates occurred at 0.1 M of ammonium while ferrous iron oxidation was minimal in all the negative controls with a maximum rate of 2.87 x 10^{-3} hr^{-1}. The average oxidation rate at 0.5 M of ammonium was 2.62 times slower than at 0.1 M showing inhibitory effects. The WR culture experienced an extended lag phase, and the highest average oxidation rates were delayed until the 3rd iron addition cycle in some of the tested ammonium concentrations. For the FR culture, on the other hand, the highest average oxidation rates occurred at the 1st iron addition regardless of the ammonium concentration. Overall, the average oxidation rates of the FR culture were significantly lower than the WR culture regardless of the ammonium concentration. In terms of the goodness of fit (R^2), the WR culture achieved an R^2 value higher than 0.98 when the ammonium concentration was less than or equal to 0.1 M,

indicating that iron oxidation followed first-order kinetics. In contrast, iron oxidation by the FR culture resulted in R^2 values less than 0.90, indicating less compliance with first order kinetics. Because of the significantly lower iron oxidation rates in the FR trials, these cultures were not used for further testing. The summary descriptive statistics is shown in **Figure 3. 19**.

Figure 3. 19

Summary Descriptive Statistics of the Ammonium Test

Descriptive Statistics

	N	Mean		Std. Deviation	Variance
	Statistic	Statistic	Std. Error	Statistic	Statistic
WR_0.01_M_NH4	3	.44067	.020851	.036116	.001
WR_0.05_M_NH4	3	.53367	.002906	.005033	.000
WR_0.1_M_NH4	3	.56100	.033606	.058207	.003
WR_0.5_M_NH4	3	.21367	.003712	.006429	.000
FR_0.01_M_NH4	3	.09253	.007248	.012554	.000
FR_0.05_M_NH4	3	.10207	.002990	.005178	.000
FR_0.1_M_NH4	3	.20433	.016506	.028589	.001
Valid N (listwise)	3				

Phosphorus Test

The phosphorous source was supplied in the form of potassium phosphate. One culture inoculum was tested for phosphorous using WR culture that was previously enriched in the modified 9K media at 0.1 M of ammonium (WR). The inoculum accounted for 10% of the sample while the modified 9K media accounted for the remaining 90%. The ammonium concentration was fixed at 0.1 M, as it resulted in the highest oxidation rates among the tested concentrations for both cultures, and no organic carbon was added. The incubation pH was 2.5. Five phosphate concentrations were tested at this stage, 0.1 mM,

0.5 mM, 1.0 mM, 5.0 mM, and 10.0 mM. The test was conducted in triplicate for each concentration with one negative control at 5.0 mM of phosphate achieved by adding 2.0% formaldehyde. The ferrous iron concentration was brought back up to approximately 250 mg/L whenever it dropped below 10 mg/L, and Fe^{2+} oxidation rates were measured after each iron addition by exponentially fitting ferrous iron concentrations with time data points. Because the goal was to find conditions and cultures with the fastest kinetics, the average oxidation rate from the best batch for each trial was plotted here for comparison. In all cases, the best average oxidation rates were achieved at the 2^{nd} iron addition cycle. Ferrous iron oxidation rates for WR culture at 0.1 mM, 0.5 mM, 1.0 mM, 5.0 mM, and 10.0 mM of phosphate are shown in **Figure 3. 20** through **Figure 3. 24**, respectively. Figures showing ferrous iron oxidation rates at other ferrous iron addition cycles are provided in the appendix.

Figure 3. 20

Ferrous Iron Oxidation Rates with WR Inoculum in Modified 9K Media, 0.1 M N, 0.1 mM P, No C (2nd Iron Addition)

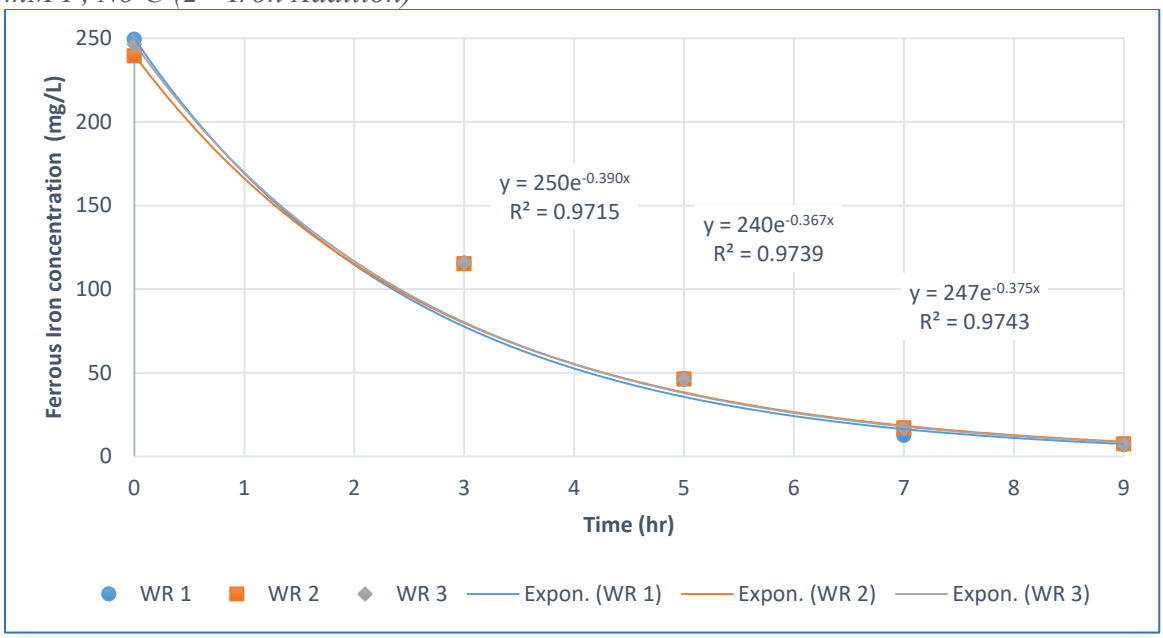

Figure 3. 21

Ferrous Iron Oxidation Rates with WR Inoculum in Modified 9K Media, 0.1 M N, 0.5 Mm P, No C (2nd Iron Addition)

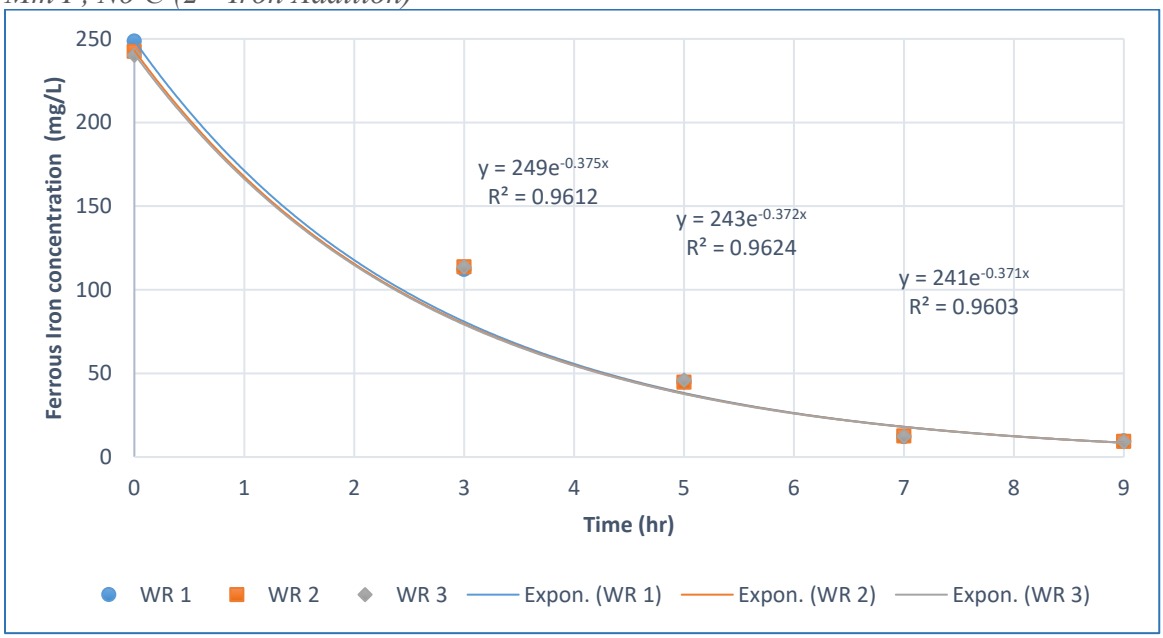

Figure 3. 22

Ferrous Iron Oxidation Rates with WR Inoculum in Modified 9K Media, 0.1 M N, 1.0 mM P, No C (2nd Iron Addition)

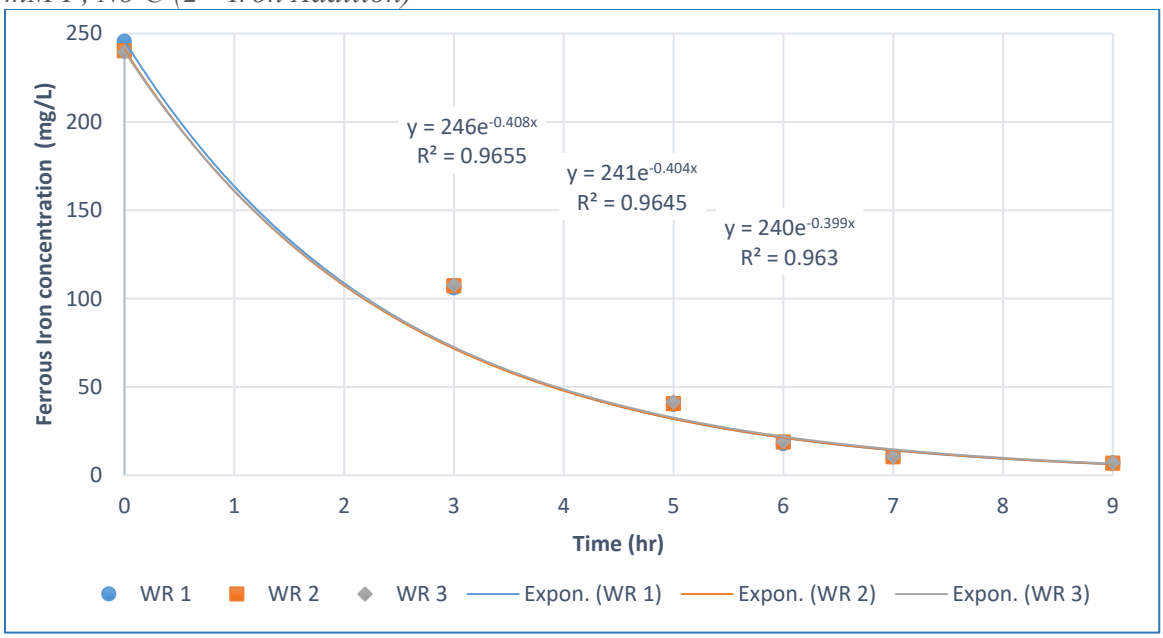

Figure 3. 23

Ferrous Iron Oxidation Rates with WR Inoculum in Modified 9K Media, 0.1 M N, 5.0 mM P, No C (2nd Iron Addition)

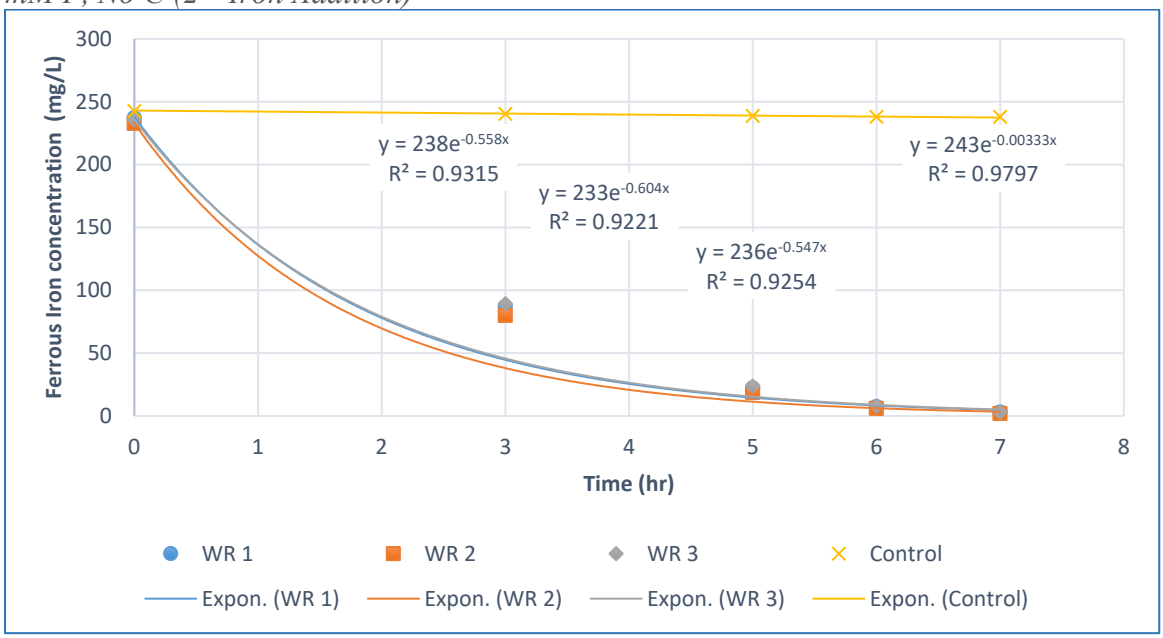

Figure 3. 24

Ferrous Iron Oxidation Rates with WR Inoculum in Modified 9K Media, 0.1 M N, 10.0 mM P, No C (2nd Iron Addition)

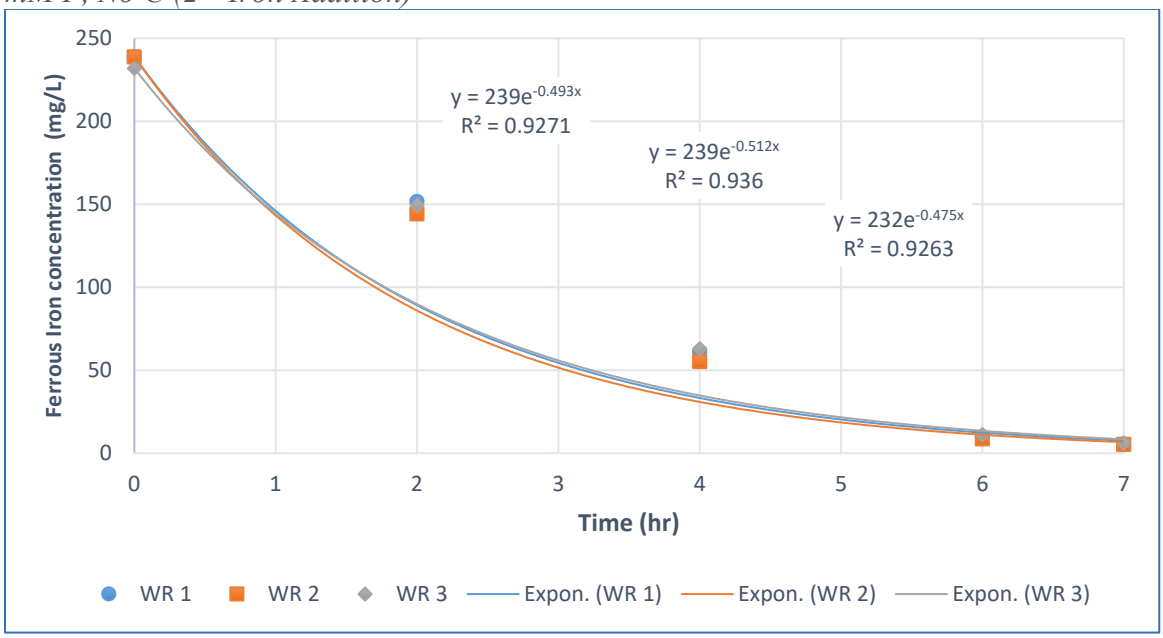

Ferrous iron oxidation rates increased with increasing phosphate concentration up to 5.0 mM and then slightly decreased at 10.0 mM of phosphate. The highest average oxidation rate was achieved at 5.0 mM phosphate. Ferrous iron oxidation was minimal in the negative control with a rate of 3.33 $x10^{-3}$ hr^{-1}. Regardless of the phosphate concentration, the highest oxidation rates were achieved at the 2nd iron addition. In terms of the goodness of fit (R^2), the WR culture achieved R^2 value higher than 0.92 at all tested phosphate concentrations, indicating that iron oxidation followed the first order kinetics. The summary descriptive statistics is shown in **Figure 3. 25**.

Figure 3. 25

Summary Descriptive Statistics of the Phosphorus Test

Descriptive Statistics

	N	Mean		Std. Deviation	Variance
	Statistic	Statistic	Std. Error	Statistic	Statistic
WR_0.1_mM_PO4	3	.37733	.006741	.011676	.000
WR_0.5_mM_PO4	3	.37267	.001202	.002082	.000
WR_1.0_mM_PO4	3	.40367	.002603	.004509	.000
WR_5.0_mM_PO4	3	.56967	.017458	.030238	.001
WR_10.0_mM_PO4	3	.49333	.010682	.018502	.000
Valid N (listwise)	3				

Organic Carbon Test

The organic carbon source was supplied in the form of glucose. One culture inoculum was tested for organic carbon using WR culture that was previously enriched in the modified 9K media at 0.1 M of ammonium and 5.0 mM of phosphorus (WRI). The inoculum accounted for 10% of the sample while the modified 9K media accounted for the remaining 90%. The ammonium concentration was fixed at 0.1 M and the phosphorous concentration was fixed at 5.0 mM as these concentrations resulted in the highest oxidation rates among the tested concentrations. The incubation pH was 2.5. Three glucose concentrations were tested at this stage, 0.05 M, 0.1 M, and 0.2 M. The test was conducted in triplicate for each concentration with one negative control at 0.05 M of glucose achieved by adding 2.0% formaldehyde. After three feedings, a second set of trials was performed by sub-culturing the inoculum from the first run. The ferrous iron concentration was brought back up to approximately 250 mg/L whenever it dropped below 10 mg/L, and Fe^{2+} oxidation rates were measured after each iron addition by exponentially fitting ferrous iron concentrations with time data points. Because the goal was to find conditions and cultures

with the fastest kinetics, the average oxidation rate from the best batch for each trial was plotted here for comparison. Regardless of the glucose concentration, the best average oxidation rates were achieved at the 2nd iron addition cycle. Ferrous iron oxidation rates for WR culture at 0.05 M, 0.1 M, and 0.2 M of glucose are shown in **Figure 3. 26** through **Figure 3. 28** for the first run, and **Figure 3. 29** through **Figure 3. 31** for the sub-culture run, respectively. Figures showing ferrous iron oxidation rates at other ferrous iron addition cycles are listed in the appendix.

Figure 3. 26

Ferrous Iron Oxidation Rates with WR Inoculum in Modified 9K Media, 0.1 M N, 5.0 mM P, 0.05 M Glucose, First Enrichment (2nd Iron Addition)

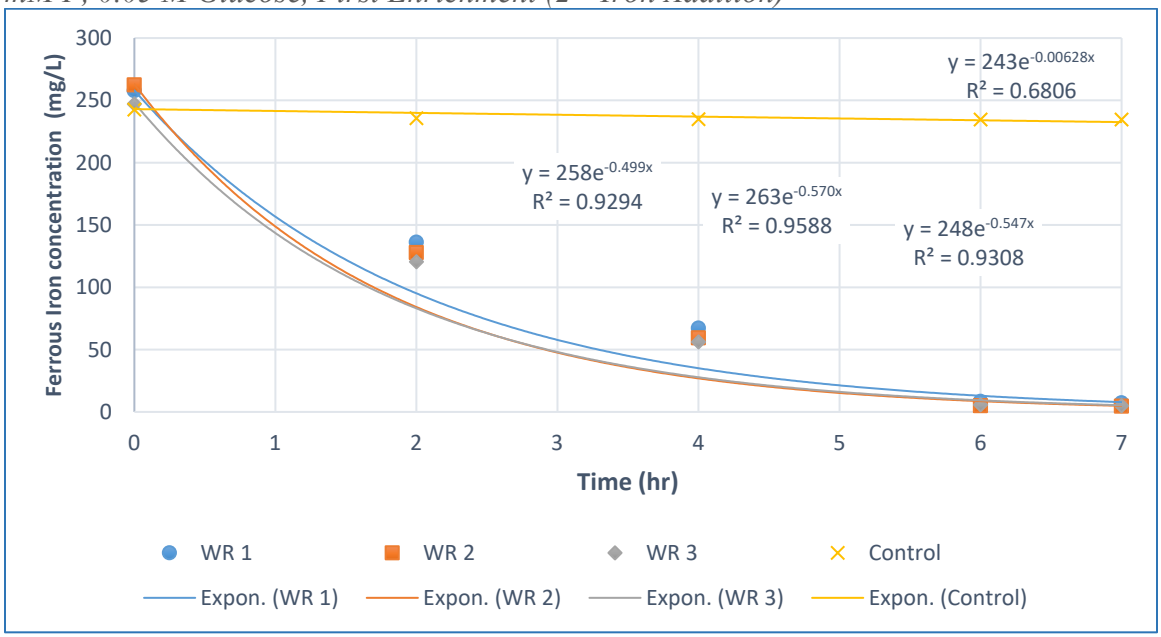

Figure 3. 27

Ferrous Iron Oxidation Rates with WR Inoculum in Modified 9K Media, 0.1 M N, 5.0 mM P, 0.1 M Glucose, First Enrichment (2nd Iron Addition)

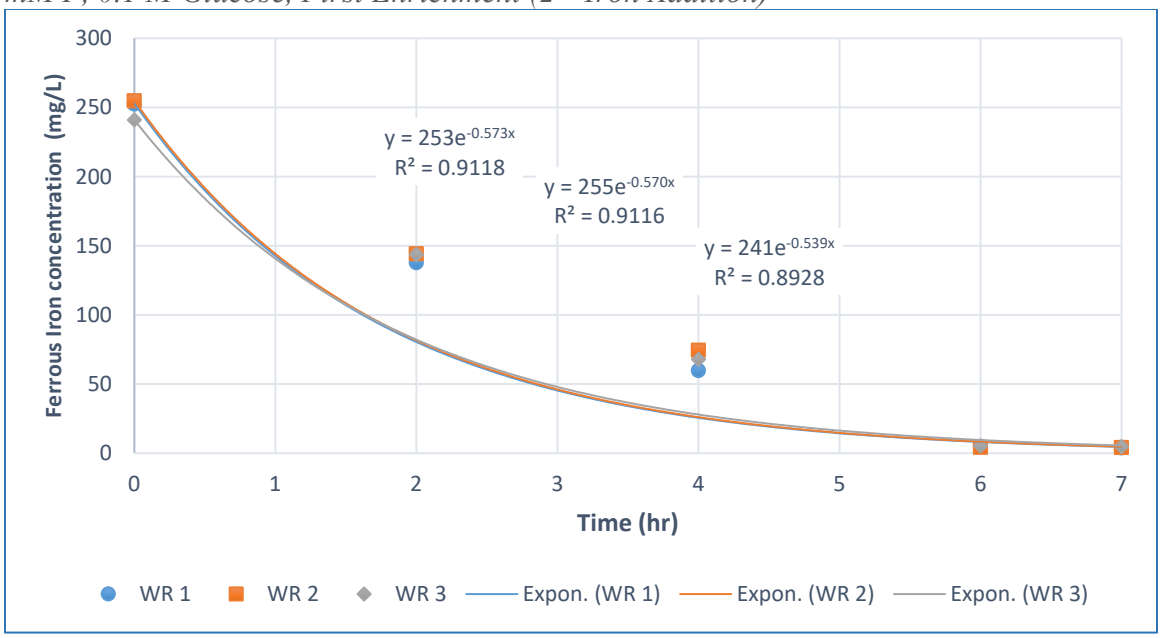

Figure 3. 28

Ferrous Iron Oxidation Rates with WR Inoculum in Modified 9K Media, 0.1 M N, 5.0 mM P, 0.2 M Glucose, First Enrichment (2nd Iron Addition)

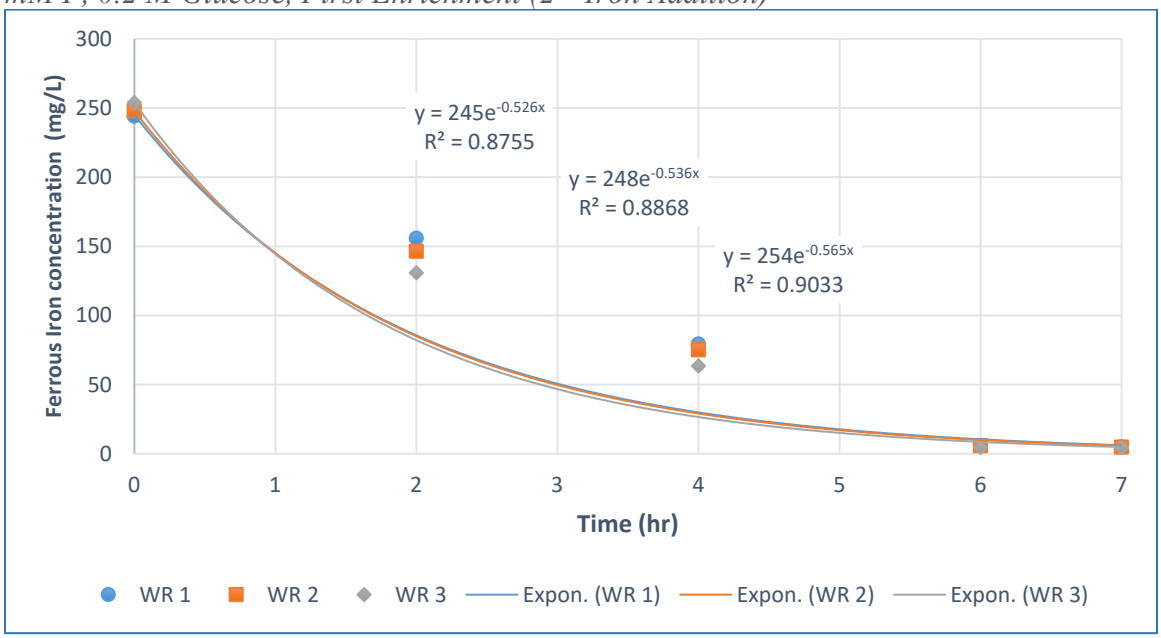

Figure 3. 29

Ferrous Iron Oxidation Rates with WR Inoculum in Modified 9K Media, 0.1 M N, 5.0 mM P, 0.05 M Glucose, Sub-Culture (2nd Iron Addition)

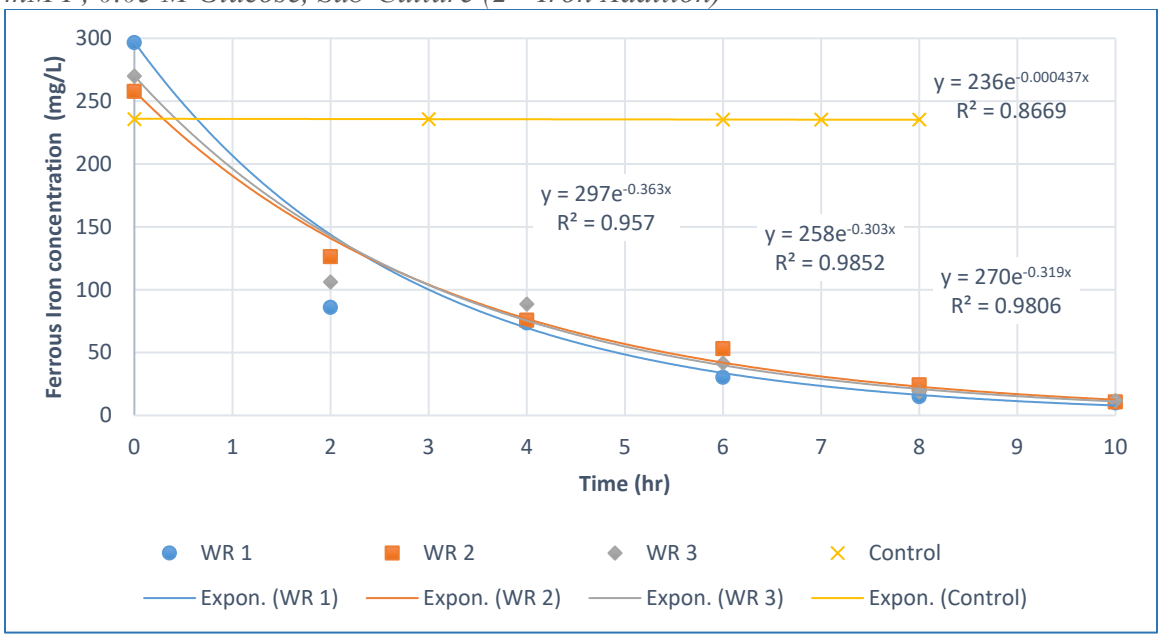

Figure 3. 30

Ferrous Iron Oxidation Rates with WR Inoculum in Modified 9K Media, 0.1 M N, 5.0 mM P, 0.1 M Glucose, Sub-Culture (2nd Iron Addition)

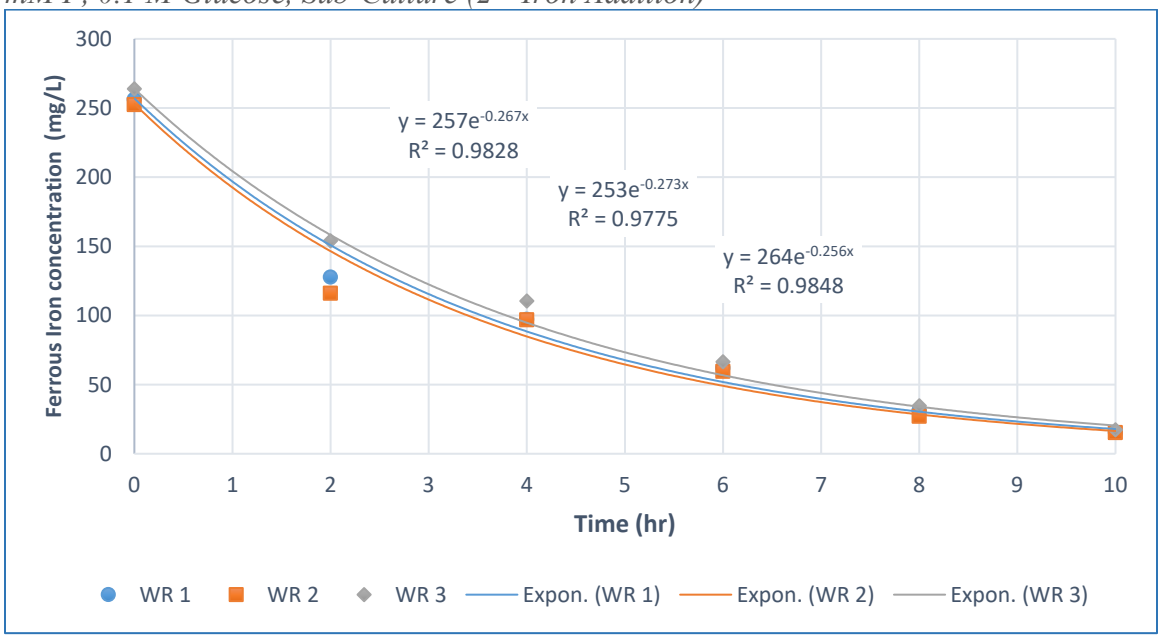

Figure 3. 31

Ferrous Iron Oxidation Rates with WR Inoculum in Modified 9K Media, 0.1 M N, 5.0 mM P, 0.2 M Glucose, Sub-Culture (2nd Iron Addition)

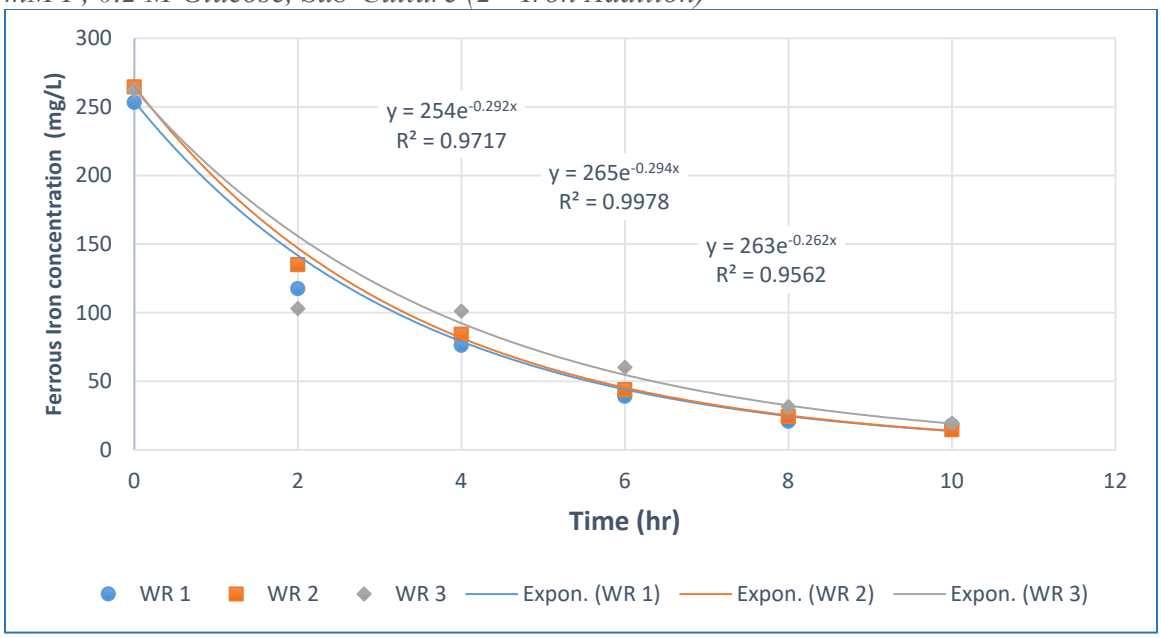

For the first enrichment, the average oxidation rates at all tested glucose concentrations were almost equal with the highest value at 0.1 M glucose. Ferrous iron oxidation was minimal in the negative control with a maximum rate of 6.28 $x10^{-3}$ hr^{-1}. Regardless of the glucose concentration, the highest oxidation rates were achieved at the 2nd iron addition. In terms of the goodness of fit (R^2), the WR culture achieved R^2 value higher than 0.90 at all tested glucose concentrations, indicating that iron oxidation followed the first order kinetics. The summary descriptive statistics for the first enrichment is shown in **Figure 3. 32**.

Figure 3. 32

Summary Descriptive Statistics of the Organic Carbon (Glucose) Test.

Descriptive Statistics

	N	Mean		Std. Deviation	Variance
	Statistic	Statistic	Std. Error	Statistic	Statistic
WR_0.05_M_Glucose	3	.53867	.020915	.036226	.001
WR_0.1_M_Glucose	3	.56067	.010868	.018824	.000
WR_0.2_M_Glucose	3	.54233	.011695	.020257	.000
Valid N (listwise)	3				

For the second enrichment after subculturing, however, and regardless of the glucose concentration, the average oxidation rates decreased substantially. At 0.1 M glucose, for example, the average iron oxidation rate was inhibited by 52% after one subculture only. The highest oxidation rate was achieved at 0.05 M glucose in the duplicate run. The summary descriptive statistics for the second enrichment is shown in **Figure 3. 33**.

Figure 3. 33

Summary Descriptive Statistics of the Organic Carbon (Glucose) Sub-Culture Test

Descriptive Statistics

	N	Mean		Std. Deviation	Variance
	Statistic	Statistic	Std. Error	Statistic	Statistic
WR_0.05_M_Glucose_duplicate	3	.32833	.017938	.031070	.001
WR_0.1_M_Glucose_duplicate	3	.26533	.004978	.008622	.000
WR_0.2_M_Glucose_duplicate	3	.28267	.010349	.017926	.000
Valid N (listwise)	3				

Applying the Results

Wolf Run and Truetown AMD Water Analysis

Fresh samples of Wolf Run and Truetown AMD water were analyzed for nitrite, nitrate, total nitrogen, orthophosphate, and total phosphate. The nitrite, orthophosphate, and total phosphate concentrations in WR sample were below the practical quantitation limit (PQL), while the total nitrogen found in the sample was 1.28 mg/L (9.14×10^{-5} M). For TT AMD, nitrite, nitrate, and phosphate concentrations were below PQL, while the total nitrogen found in the sample was 2.02 mg/L (1.44×10^{-4} M), and the orthophosphate concentration was 0.04 mg/L (4.21×10^{-4} mM). Both concentrations were significantly below the 0.1 M nitrogen, and 5.0 mM phosphorous concentrations tested in this study. For this reason, the initial concentrations of nitrogen and phosphorus in WR and TT waters were neglected. **Figure 3. 34** and **Figure 3. 35** show the analysis report for WR AMD and TT AMD, respectively.

Figure 3. 34

WR AMD Water Analysis for Nitrogen and Phosphorus Concentrations

Analyte	Results	Units	PQL	Preparation Method	Analytical Method	Analyst
Nitrite-N	<0.10	mg/L	0.10		EPA 353.2 Rev. 2.0/SM4500-NO3 F-00,16	TLL
Nitrate/Nitrite-N	0.14	mg/L	0.10		EPA 353.2 Rev. 2.0/SM4500-NO3 F-00,16	TLL
Nitrate-N	0.14	mg/L	0.10		EPA 353.2 Rev. 2.0/SM4500-NO3 F-00,16	TLL
Orthophosphate as P, Lab Filtered (Estimate)	<0.01	mg/L	0.01	SM 4500P-B(1)-11	SM 4500 P, E-99, 11	CAB
Orthophosphate as PO4, Lab Filtered (Estimate)	<0.03	mg/L	0.03	SM 4500P-B(1)-11	SM 4500 P, E-99, 11	CAB
Phosphate, Total as P	<0.04	mg/L	0.04	SM 4500P-B(5)-11	SM 4500-P E-11	TLL
Phosphate, Total as PO4	<0.12	mg/L	0.12	SM 4500P-B(5)-11	SM 4500-P E-11	TLL
Total Kjeldahl Nitrogen	1.14	mg/L	0.50		EPA 351.2 Rev. 2.0	JDS
Total Nitrogen, Calculation	1.28	mg/L	0.60		SM 4500 NO3 F-11/EPA 351.2 Rev. 2.0	ELH

Figure 3. 35

TT AMD Water Analysis for Nitrogen and Phosphorus Concentrations

Analyte	Results	Units	PQL	Preparation Method	Analytical Method	Analyst
Nitrite-N	<0.10	mg/L	0.10		EPA 353.2 Rev. 2.0/SM4500-NO3 F-00,16	TLL
Nitrate/Nitrite-N	<0.10	mg/L	0.10		EPA 353.2 Rev. 2.0/SM4500-NO3 F-00,16	TLL
Nitrate-N	<0.10	mg/L	0.10		EPA 353.2 Rev. 2.0/SM4500-NO3 F-00,16	TLL
Orthophosphate as P, Lab Filtered (Estimate)	0.01	mg/L	0.01	SM 4500P-B(1)-11	SM 4500 P, E-99, 11	CAB
Orthophosphate as PO4, Lab Filtered (Estimate)	0.04	mg/L	0.03	SM 4500P-B(1)-11	SM 4500 P, E-99, 11	CAB
Phosphate, Total as P	<0.04	mg/L	0.04	SM 4500P-B(5)-11	SM 4500-P E-11	TLL
Phosphate, Total as PO4	<0.12	mg/L	0.12	SM 4500P-B(5)-11	SM 4500-P E-11	TLL
Total Kjeldahl Nitrogen	2.02	mg/L	0.50		EPA 351.2 Rev. 2.0	JDS
Total Nitrogen, Calculation	2.02	mg/L	0.60		SM 4500 NO3 F-11/EPA 351.2 Rev. 2.0	ELH

Wolf Run Culture Enrichment

Different combinations of the best nutrients concentrations that resulted in the highest oxidation rates were investigated using WR AMD and WR inoculum extracted from the sediments. The AMD accounted for 90% of the sample while the inoculum accounted for the remaining 10%. The nutrients were added in the form of concentrated solution with different combinations to track the effect of each possible nutrient addition. The nitrogen (N) was added in the form of ammonium sulfate to achieve a final concentration of 0.1 M, the phosphorous (P) was added in the form of potassium phosphate to achieve a final concentration of 5.0 mM, and no organic carbon was added. The incubation pH for all conducted tests at this stage was 2.5. The summary of the tested combinations and their composition is listed in **Table 9** in the methodology chapter. Six combinations of possible inoculum and nutrients additions were tested. The test was conducted in triplicate for each combination. The ferrous iron concentration was brought back up to approximately 250 mg/L whenever it dropped below 10 mg/L, and Fe^{2+} oxidation rates were measured after each iron addition by exponentially fitting ferrous iron concentrations with time data points. Because the goal was to find conditions and cultures with the fastest kinetics, the average oxidation rate from the best batch for each trial was plotted here for comparison. Ferrous iron oxidation rates for six combinations are shown in **Figure 3. 36** through **Figure 3. 41**. Figures showing ferrous iron oxidation rates at other ferrous iron addition cycles are listed in the appendix.

Figure 3. 36

Ferrous Iron Oxidation Rates with WR AMD Only at pH 2.5, No Nutrient Addition (1st Iron Addition)

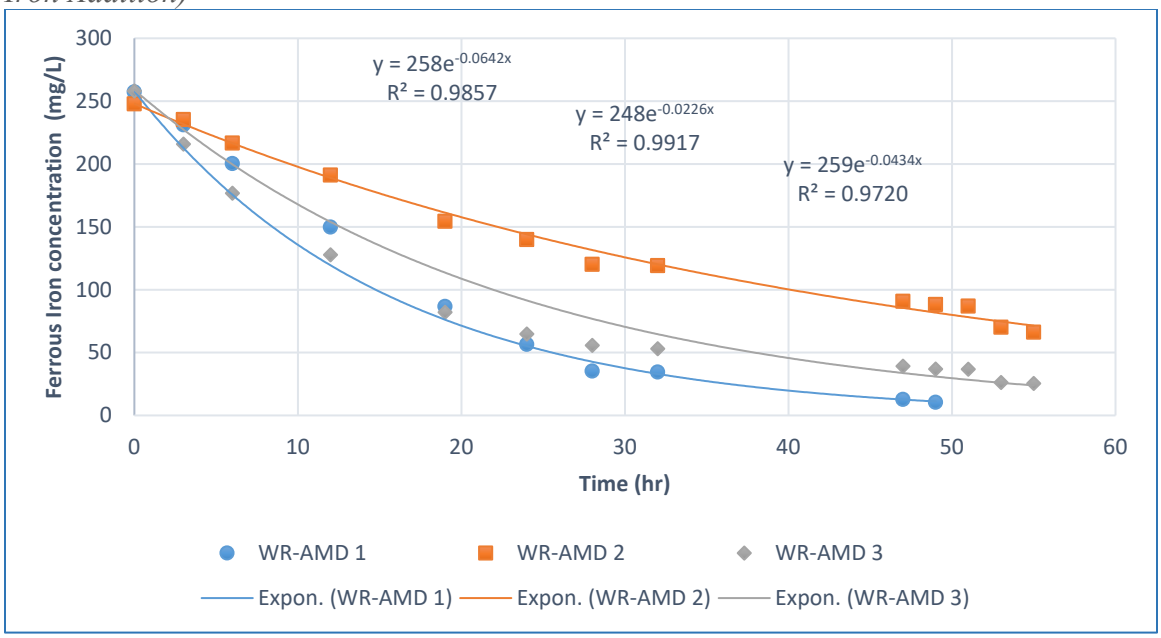

Figure 3. 37

Ferrous Iron Oxidation with WR AMD and Bacterial Inoculum Extracted from WR Sediment at pH 2.5, No Nutrient Addition (3rd Iron Addition)

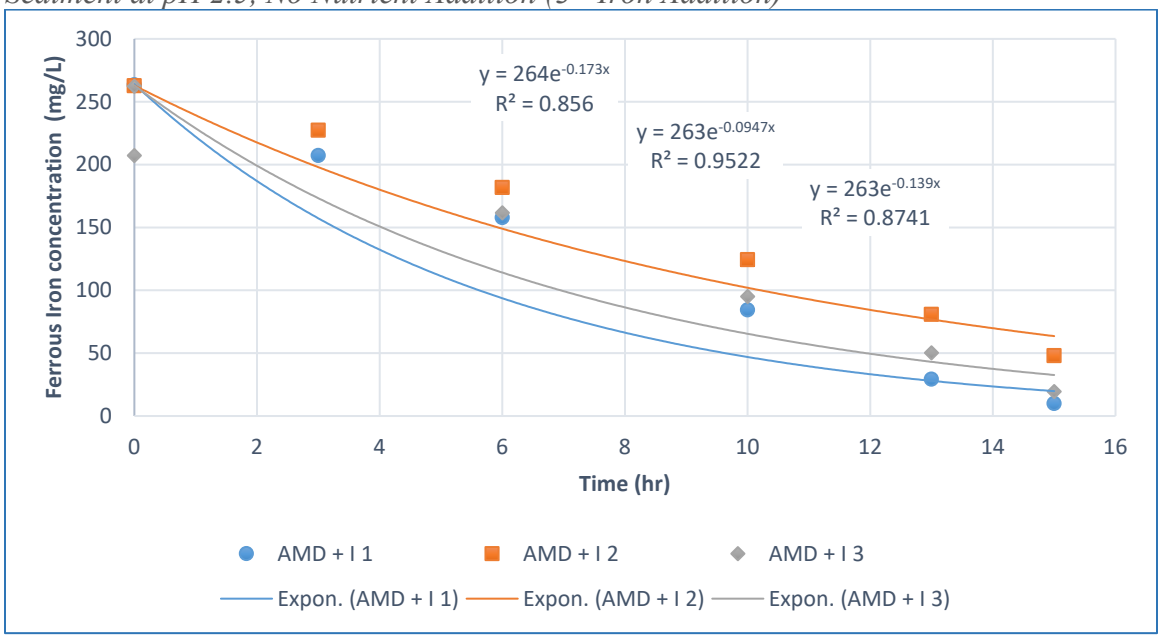

Figure 3. 38

Ferrous Iron Oxidation with WR AMD and Bacterial Inoculum Extracted from WR Sediment at pH 2.5, 0.1 M N, No P, No C (2nd Iron Addition)

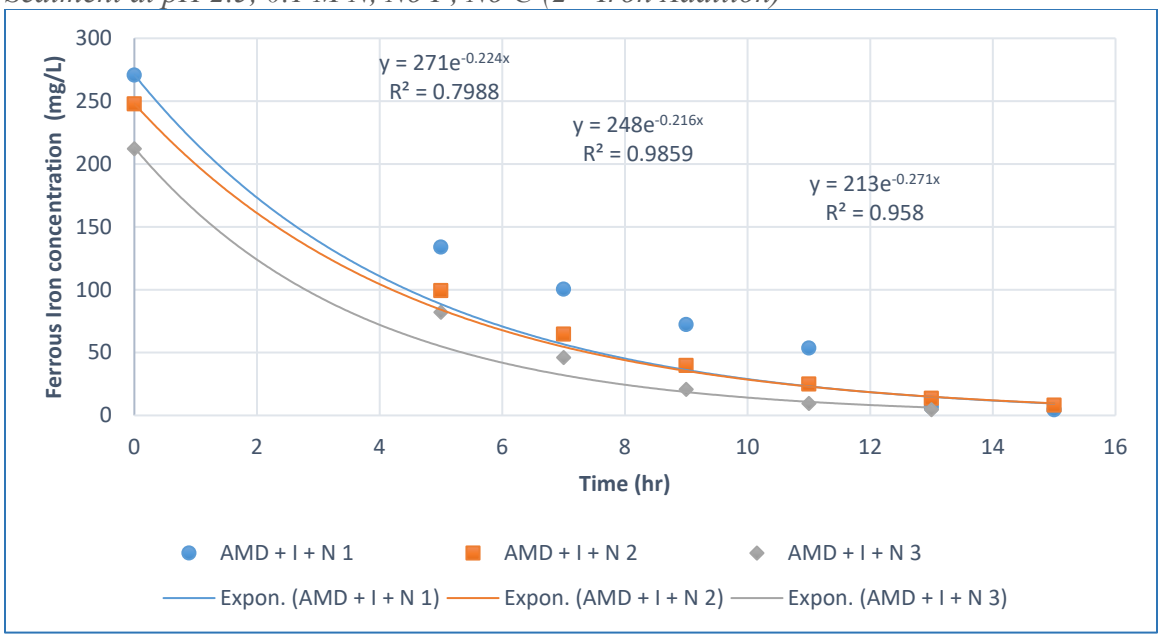

Figure 3. 39

Ferrous Iron Oxidation with WR AMD and Bacterial Inoculum Extracted from WR Sediment at pH 2.5, 5.0 mM P, No N, No C (3rd Iron Addition)

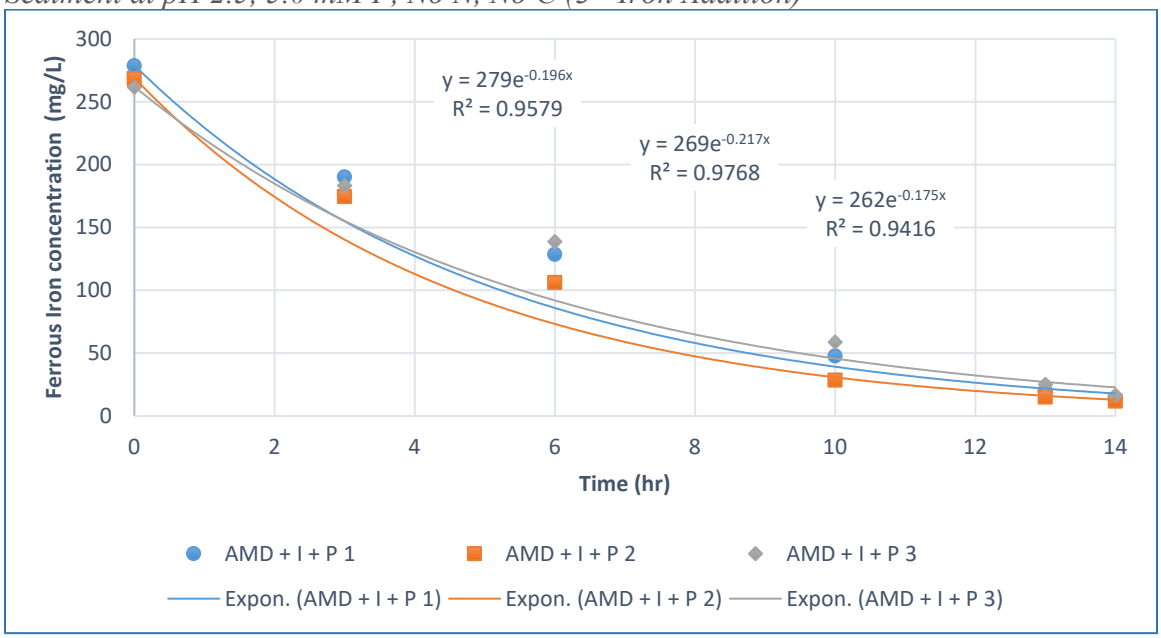

Figure 3. 40

Ferrous Iron Oxidation with WR AMD at pH 2.5, 5.0 mM P, 0.1 M N, No C, No Inoculum Addition (2nd Iron Addition)

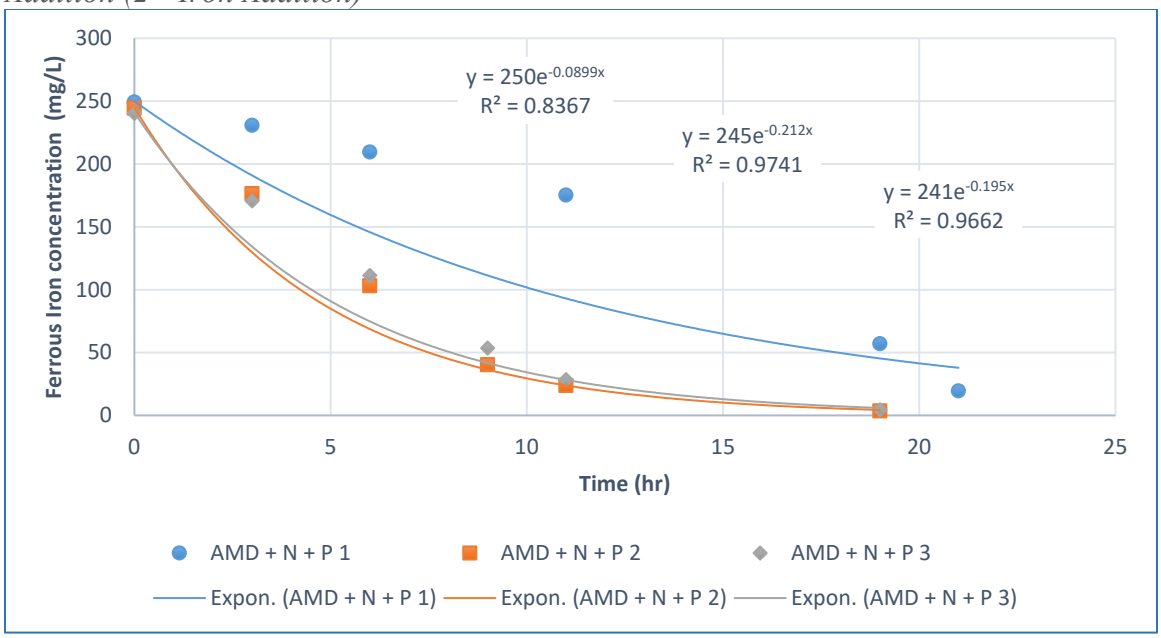

Figure 3. 41

Ferrous Iron Oxidation with WR AMD and Bacterial Inoculum Extracted from WR Sediment at pH 2.5, 0.1 M N, 5.0 mM P, No C (3rd Iron Addition)

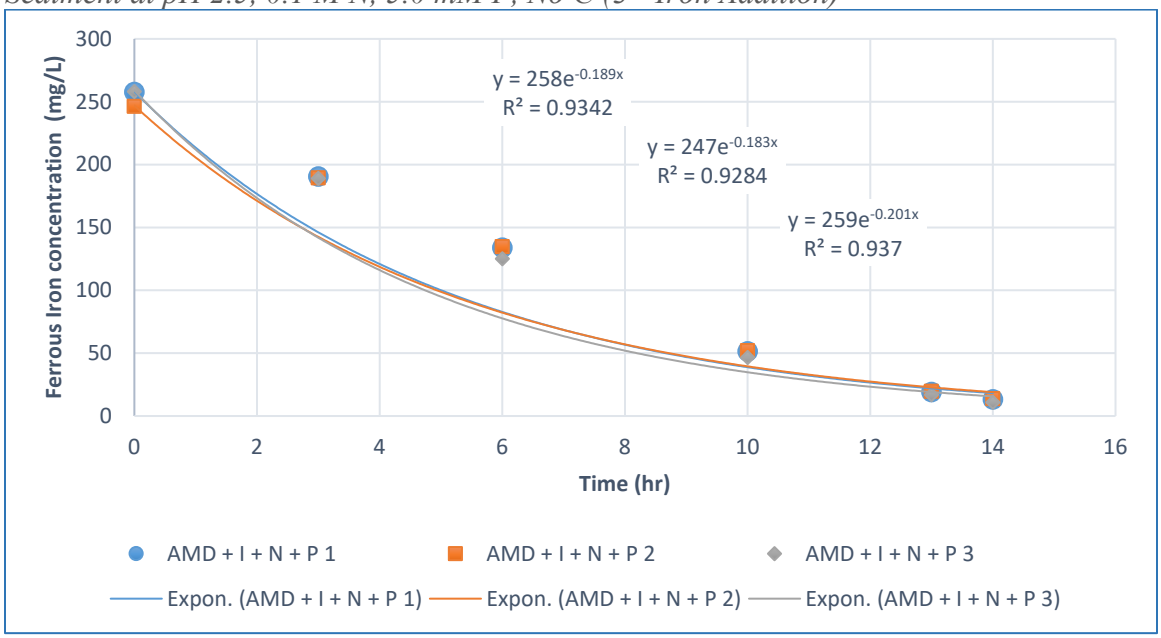

For the 1st trial, only WR AMD water was tested with no extracted inoculum or nutrient addition where the initial nutrient concentration in the water was below the practical quantitation limit. The highest achieved average oxidation rate was 0.0430 hr^{-1} at the 1st iron addition. After the addition of the extracted inoculum from the WR sediments in the second combination, the average iron oxidation rate substantially increased by 3.2-fold with a rate of 0.136 hr^{-1} at the 3rd iron addition. The addition of inoculum this time experienced an extended lag phase (illustrated in the 1st and 2nd iron additions figures in the appendix) likely due to the difference in the media composition. In the first set (the pH-test set), the inoculum accounted for 50% of the sample composition, while in this set, the inoculum accounted for only 10% of the sample composition.

For the 3rd trial, a final concentration of 0.1 M of NH_4^+ was added to the WR AMD water and the WR inoculum extracted from the sediments. This combination resulted in the highest achieved iron oxidation rates at this stage with a rate of 0.237 hr^{-1} at the 2nd iron addition. The addition of ammonium increased iron oxidation rates of the inoculated trials by 1.75-fold.

For the 4th trial, a final concentration of 5.0 mM of PO_4^{-2} was added to the WR AMD water and the WR inoculum extracted from the sediments. This combination resulted in the second highest achieved iron oxidation rates at this stage with a rate of 0.196 hr^{-1} at the 3rd iron addition. The addition of phosphorus increased average iron oxidation rate by 1.45-fold making it less effective than the addition of ammonium only.

For the 5th trial, both nutrients were added without the inoculum with a final concentration of 0.1 M ammonium and 5.0 mM phosphorus. The addition of nutrients to the existent planktonic bacteria substantially increased iron oxidation rates by 3.9-fold at

the 2nd iron addition. However, the addition of nutrients only achieved a rate of 0.166 hr^{-1} which was only 18% higher than the rate achieved by the addition of the extracted inoculum without any nutrients.

For the 6th and last trial at this stage, both the extracted inoculum and the nutrients were added. The final concentration of the ammonium was 0.1 M and 5.0 mM for phosphorus. Surprisingly, the resulting average oxidation rate was 0.191 hr^{-1}, very close to the inoculum and phosphorus trial and they were both less than the average oxidation rate resulted from the inoculum and ammonium trial. Adding both nutrients to the AMD water and extracted inoculum substantially increased iron oxidation rate from no addition by 4.44-fold.

Regardless of the tested combination, the addition of the extracted inoculum and/or nutrients substantially increased iron oxidation rates with a minimum of 3.2 folds. The best iron oxidation rates were achieved when both the extracted inoculum and one of the nutrients were added. In terms of the goodness of fit (R^2), the WR culture achieved R^2 values higher than 0.90 at all tested combinations, indicating that iron oxidation followed first-order kinetics. The summary descriptive statistics for the WR enrichment test is shown in **Figure 3. 42**.

Figure 3. 42

Summary Descriptive Statistics of the WR AMD Enrichment Test

Descriptive Statistics

	N	Mean		Std. Deviation	Variance
	Statistic	Statistic	Std. Error	Statistic	Statistic
WR_AMD_only	3	.04300	.011547	.020000	.000
WR_AMD_N_P	3	.16567	.038150	.066078	.004
WR_AMD_I	3	.13567	.022578	.039107	.002
WR_AMD_N_I	3	.23700	.017156	.029715	.001
WR_AMD_P_I	3	.19600	.012124	.021000	.000
WR_AMD_N_P_I	3	.19100	.005292	.009165	.000
Valid N (listwise)	3				

Truetown AMD Enrichment

Different combinations of the best nutrients concentrations that resulted in the highest oxidation rates were investigated using TT AMD and WR inoculum extracted from the sediments. The AMD accounted for 90% of the sample while the inoculum accounted for the remaining 10%. The nutrients were added in the form of concentrated solution with different combinations to track the effect of each possible nutrient addition. The nitrogen (N) was added in the form of ammonium sulfate to achieve a final concentration of 0.1 M, the phosphorous (P) was added in the form of potassium phosphate to achieve a final concentration of 5.0 mM, and no organic carbon was added. The incubation pH for all conducted tests at this stage was 2.5. The summary of the tested combinations and their composition is listed in **Table 10** in the methodology chapter. Seven combinations of possible inoculum and nutrients additions were tested in triplicate. The ferrous iron concentration was brought back up to approximately 250 mg/L whenever it dropped below 10 mg/L, and Fe^{2+} oxidation rates were measured after each iron addition by exponentially

fitting ferrous iron concentrations with time data points Because the goal was to find conditions and cultures with the fastest kinetics, the average oxidation rate from the best batch for each trial was plotted here for comparison. Ferrous iron oxidation rates for the seven combinations are shown in **Figure 3. 43** through **Figure 3. 49**. Figures showing ferrous iron oxidation rates at other ferrous iron addition cycles are listed in the appendix.

Figure 3. 43

Ferrous Iron Oxidation Rates with TT AMD Only at pH 2.5, No Nutrient Addition (1st Iron Addition)

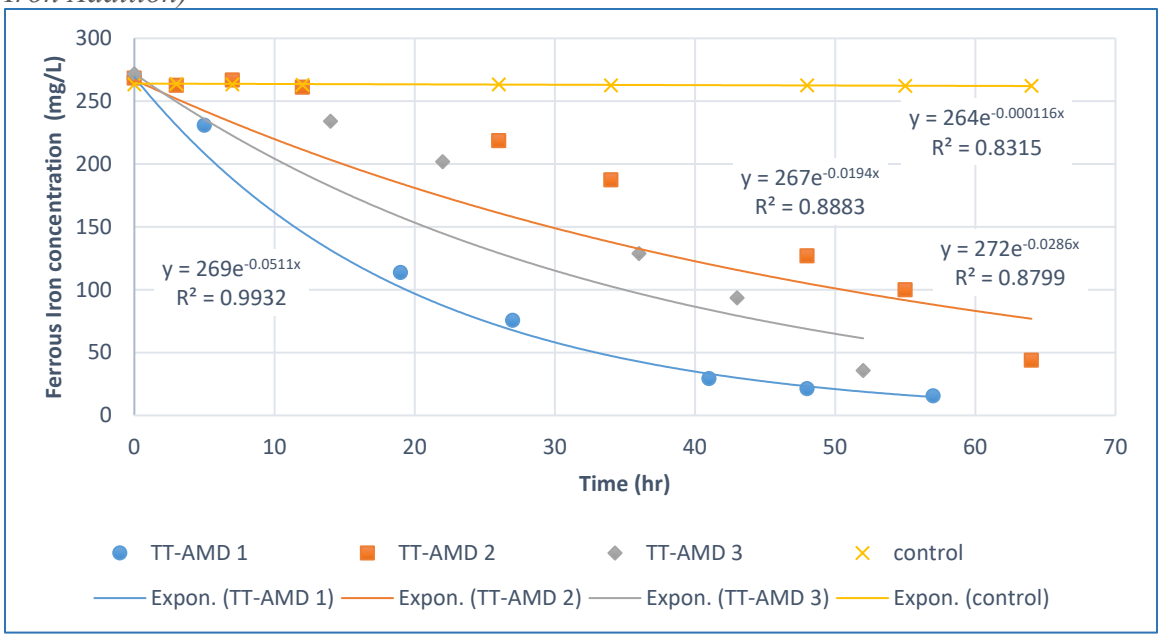

Figure 3. 44

Ferrous Iron Oxidation with TT AMD and Bacterial Inoculum Extracted from WR Sediment at pH 2.5, No Nutrients Addition (1st Iron Addition)

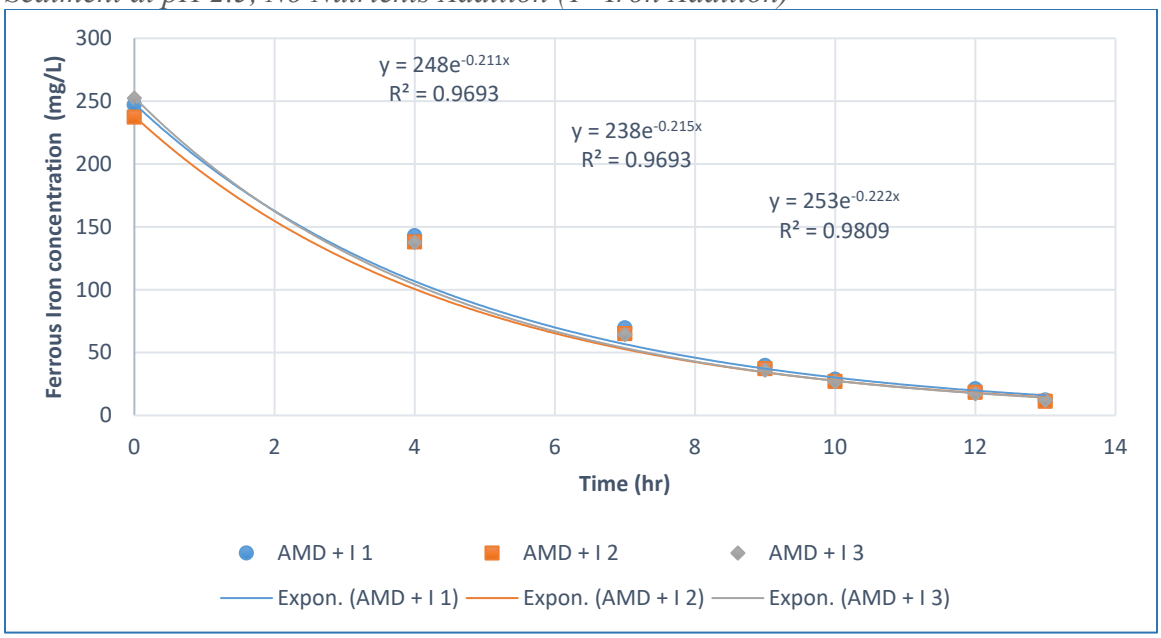

Figure 3. 45

Ferrous Iron Oxidation with TT AMD and Bacterial Inoculum Extracted from WR Sediment at pH 2.5, 0.1 M N, No P, No C (1st Iron Addition)

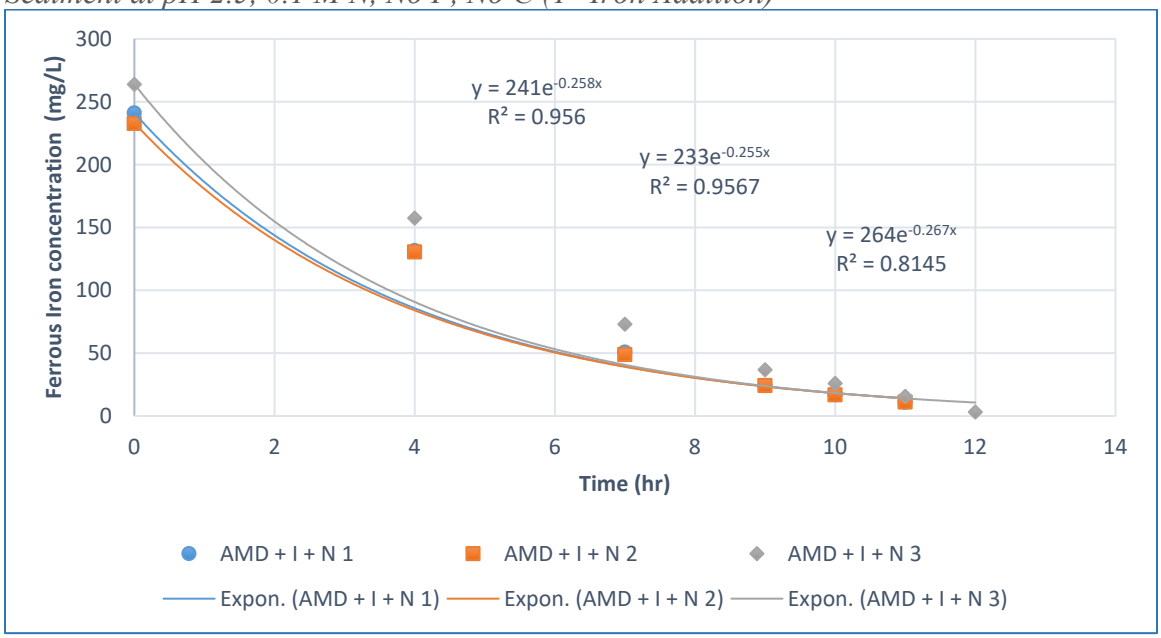

Figure 3. 46

Ferrous Iron Oxidation with TT AMD and Bacterial Inoculum Extracted from WR Sediment at pH 2.5, 5.0 mM P, No N, No C (2nd Iron Addition)

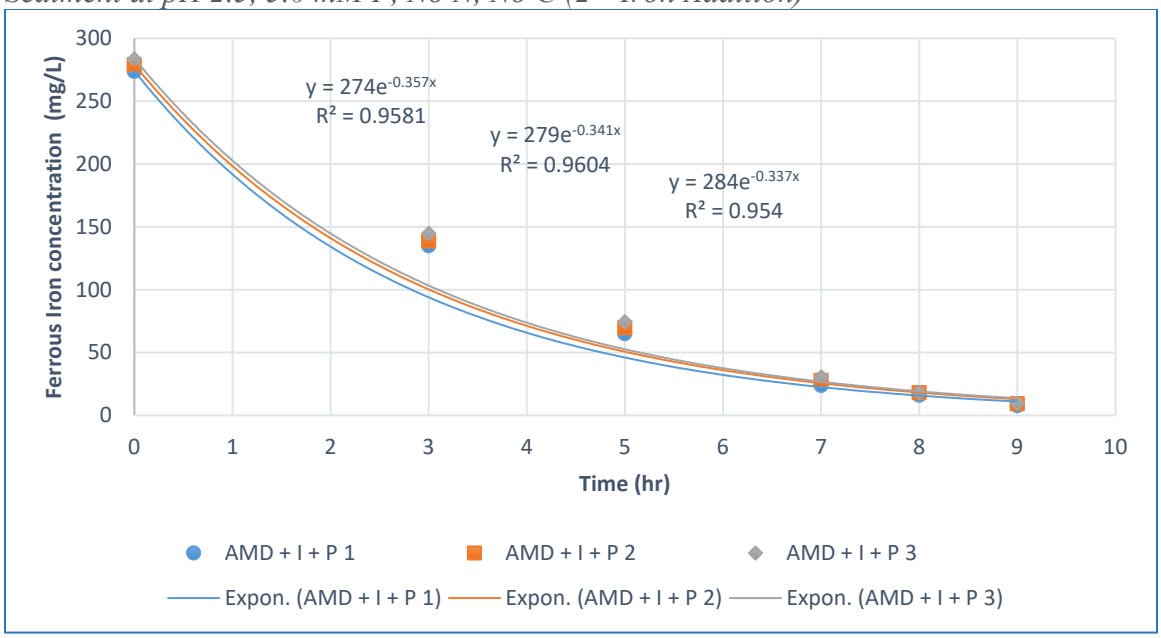

Figure 3. 47

Ferrous Iron Oxidation Rates with TT AMD at pH 2.5, 5.0 mM P, No N, No C, No Inoculum Addition (3rd Iron Addition)

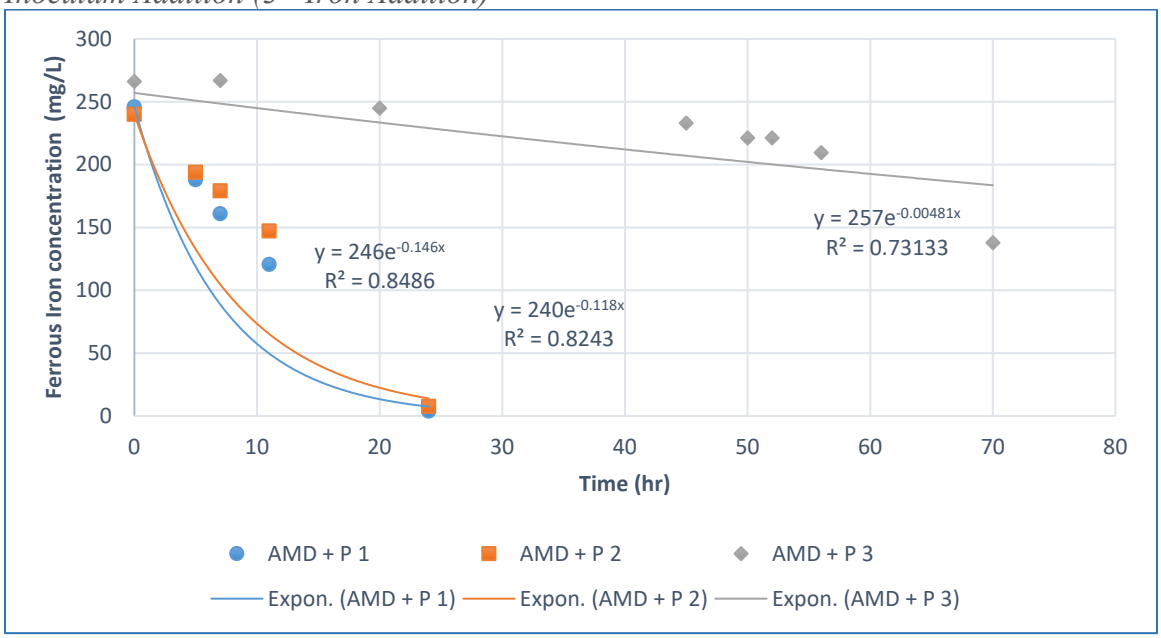

Figure 3. 48

Ferrous Iron Oxidation Rates with TT AMD at pH 2.5, 0.1 M N, 5.0 mM P, No C, No Inoculum Addition (3rd Iron Addition)

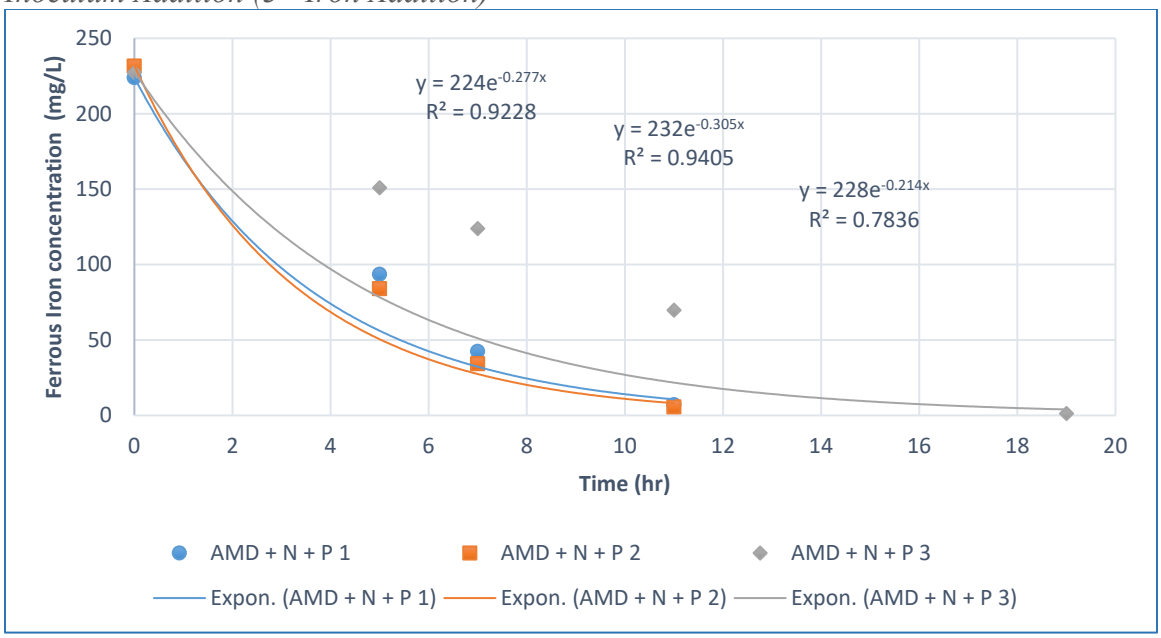

Figure 3. 49

Ferrous Iron Oxidation with TT AMD and Bacterial Inoculum Extracted from WR Sediment at pH 2.5, 0.1 M N, 5.0 mM P, No C (1st Iron Addition)

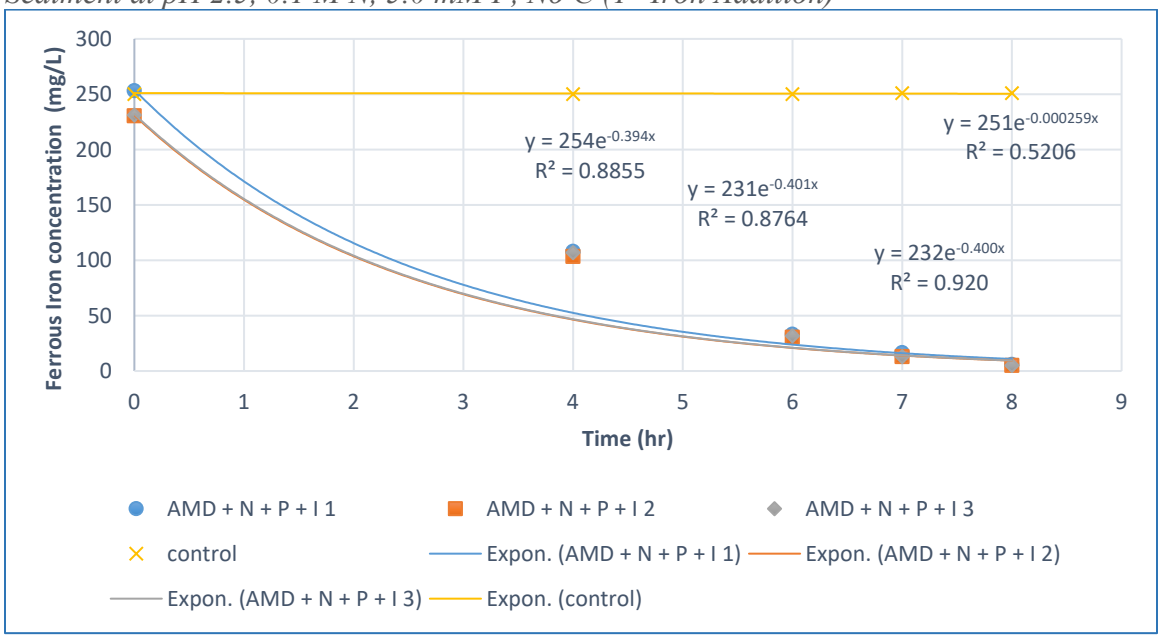

For the 1st trial, when only the AMD water collected from TT with neglected initial nutrient concentrations was tested, the best average oxidation rate achieved was 0.0330 hr^{-1} at the 1st iron addition. This rate was one of slowest among the tested AMD waters. Moreover, the iron oxidation rate was inconsistent between the three trials. For example, the replicate "W2" in **Figure 3. 43** was observed in a relatively drastic lag phase compared to the other two replicates. Regardless of the very slow biotic oxidation by the existent planktonic bacteria without any nutrient or extracted inoculum addition, the average achieved biotic oxidation rate was 330-fold faster than the abiotic oxidation rate.

For the 2nd trial, when the extracted inoculum from the WR sediments was added to TT AMD water without any nutrients addition, the best average oxidation rate achieved was 0.216 hr^{-1} at the 1st iron addition. The addition of WR inoculum to TT water substantially increased the iron oxidation rates by 6.55-fold. Moreover, the addition of the WR inoculum resulted in more consistent rates among the three trials. Also, the reaction time drastically decreased from +60 hr to 13 hr.

For the 3rd trial, the effect of 0.1 M ammonium addition to TT water and WR inoculum was investigated. The best average iron oxidation rate achieved was 0.260 hr^{-1} at the 1st iron addition. The addition of ammonium further enhanced the iron oxidation rates by 20%.

For the 4th trial, the effect of phosphorus addition to TT water only with a final concentration of 5.0 mM was investigated. The best average iron oxidation rate achieved was 0.0897 hr^{-1} at the 1st iron addition. When compared to TT AMD water only, the addition of phosphorus enhanced the iron oxidation rates by 2.7-fold. However, without

the inoculum addition, the bacterial growth experienced approximately 15 d of lag phase where iron oxidation was negligible, while with the inoculum addition, the maximum lag phase period was approximately 2 d. Moreover, the oxidation rates and reaction times among the three replicates had substantial differences, indicating fundamental differences in the cultures.

For the 5th trial, the addition of both the WR inoculum and 5.0 mM was investigated. The best average iron oxidation rate achieved was 0.345 hr^{-1} at the 2nd iron addition. The addition of phosphorus and WR inoculum substantially enhanced the iron oxidation rates by 10.5-fold (compared to TT AMD water only). The addition of the WR inoculum, on the other hand, accounted for a 3.85-fold increase in iron oxidation rates. Moreover, once again, the addition of inoculum achieved more consistent iron oxidation rates among the three replicates and substantially reduced the lag phase period.

For the 6th trial, the addition of both ammonium (0.1 M) and phosphorus (5.0 mM) to the TT AMD water was investigated. For this set, no WR inoculum was added. The best average iron oxidation rate achieved was 0.249 hr^{-1} at the 1st iron addition. When compared to TT AMD water only, the addition of phosphorus enhanced the iron oxidation rates by 7.5-fold. However, without the inoculum addition, the bacterial growth experienced around 15 d of lag phase where iron oxidation was negligible, while with the inoculum addition, the maximum lag phase period was about 2 d. Moreover, the oxidation rates and reaction times among the three trials had substantial differences, indicating fundamental differences in the bacterial composition.

For the 7th and last trial at this stage, WR inoculum, ammonium, and phosphorus were added to TT water. This combination resulted in the highest achieved oxidation rates

with an average rate of 0.398 hr^{-1} at the 1st iron addition. This rate was the highest achieved oxidation rate among all tested AMD waters and compositions in this study. This addition enhanced the iron oxidation rate by 12-fold. The addition of the WR inoculum, on the other hand, accounted for a 1.6-fold increase in iron oxidation rates. Moreover, once again, the addition of inoculum achieved more consistent iron oxidation rates among the three replicates and substantially reduced the lag phase period. In addition, the average biotic oxidation rate achieved by the addition of the WR inoculum and both nutrients, was 1327-fold faster than the maximum abiotic oxidation rate (2.59×10^{-4} hr^{-1}).

Regardless of the tested combination, the addition of the extracted inoculum and/or nutrients substantially increased iron oxidation rates with a minimum of 2.7-fold. The best iron oxidation rates were achieved when the WR extracted inoculum and both nutrients were added. In terms of the goodness of fit (R^2), the achieved R^2 value was higher than 0.90 with all trials that included inoculum, indicating that iron oxidation followed the first order kinetics with inoculum addition. However, without the inoculum addition, the achieved R^2 value was lower than 0.90, indicating less compliance with first-order kinetics. **Figure 3. 50** shows the summary descriptive statistics of the TT AMD enrichment test.

Figure 3. 50

Summary Descriptive Statistics of the TT AMD Enrichment Test

Descriptive Statistics

	N	Mean		Std. Deviation	Variance
	Statistic	Statistic	Std. Error	Statistic	Statistic
TT_AMD_only	3	.03303	.009416	.016308	.000
TT_AMD_I	3	.21600	.003215	.005568	.000
TT_AMD_N_I	3	.26000	.003606	.006245	.000
TT_AMD_P_I	3	.34500	.006110	.010583	.000
TT_AMD_P	3	.08967	.043098	.074648	.006
TT_AMD_N_P	3	.24867	.028416	.049217	.002
TT_AMD_N_P_I	3	.39833	.002186	.003786	.000
Valid N (listwise)	3				

WR Enriched Culture Species Identification

The WR inoculum enriched in the modified 9K medium at the best ammonium (0.1 M) and phosphorus (5.0 mM) concentrations was analyzed for bacteria and archaea species. Surprisingly, the archaea count was zero, as no archaea of any species was found in the sample. For bacteria, however, over 15 species were identified in the water with a significant bias towards iron-oxidizing bacteria. **Figure 3. 51** shows the bacteria species relative abundance for the top 12 species found in the WR inoculum sample.

Figure 3. 51

Relative Abundance of the Bacteria Species Found in the WR Enriched Culture

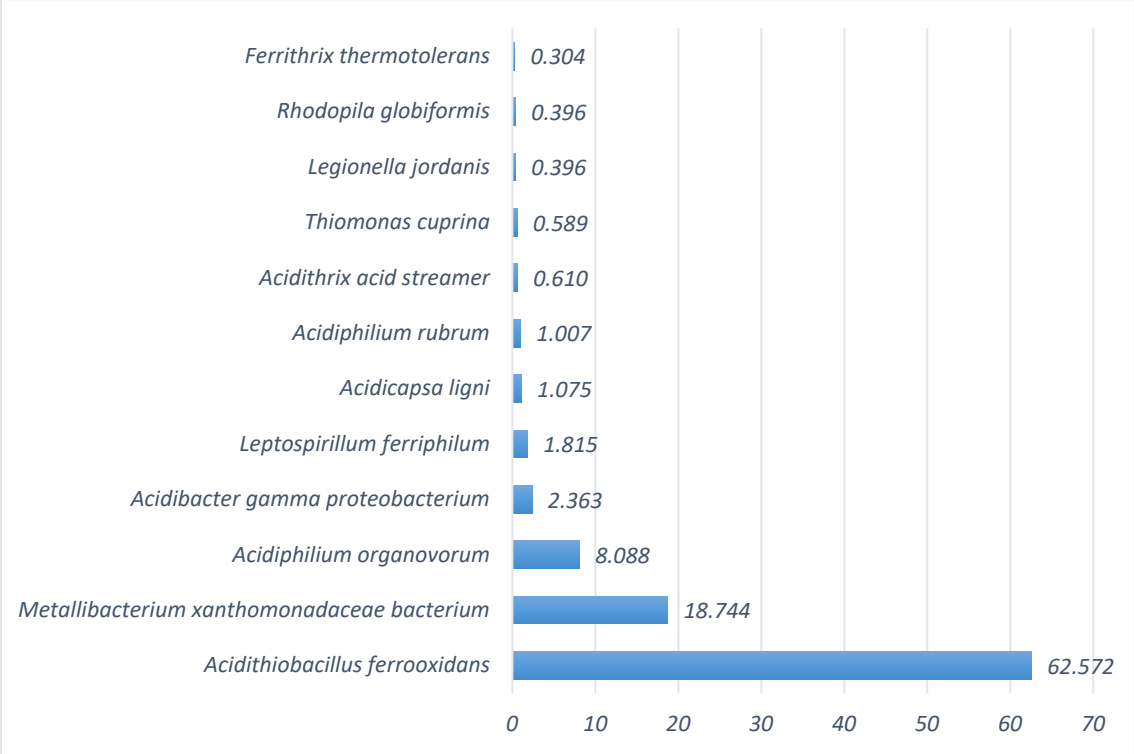

As expected, *Acidithiobacillus ferrooxidans* was the dominant species and accounted for 62.56% of the bacterial community. Interestingly, a recently recognized species, *Metallibacterium xanthomonadaceae* bacterium, accounted for 18.7% of the inoculum sample, being approximately 15 times higher than other well recognized iron-oxidizing bacteria like *Leptospirillum ferriphilum. Acidiphilium organovorum* accounted for 8.09% of the bacterial community. Those top 3 species were the most dominant species in the WR inoculum with a combined relative abundance of approximately 90% of the sample. All other species (not shown in the graph) accounted for approximately 2% of the sample. many of these were known acidophiles.

Kinetics Modeling

The effect of the tested nutrients concentrations (ammonium and phosphorus) on iron oxidation rates was modeled using the Monod Equation and the Andrew's Equation. At first, the iron oxidation rates with nutrient concentration graphs were fitted using the Andrew's Equation assuming inhibitory effects of the tested nutrient at high concentrations. The model curve-fitting was achieved using non-linear regression. **Figure 3. 52** shows the non-linear regression of iron oxidation rates as a function of ammonium concentrations with WR culture using the Andrew's Equation, while **Table 12** reports the resulting estimated model parameters.

Figure 3. 52

Iron Oxidation Rates as a Function of Ammonium Concentration

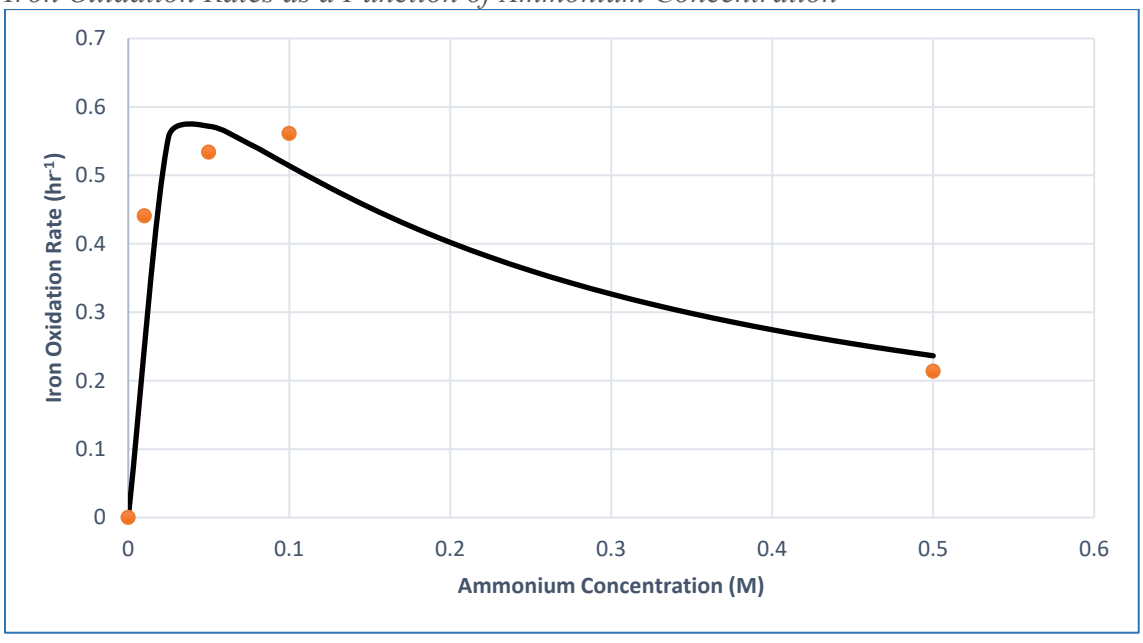

Table 12

Estimated Model Parameters of the Ammonium Concentration Effect on Iron Oxidation Rates

Model parameters	
K_m	0.796 hr^{-1}
K_s	0.00788 M
K_i	0.212 M

According to the model, the highest possible iron oxidation rate resulting from ammonium addition is 0.796 hr^{-1} while the ammonium concentration at which the iron oxidation rate is equal to half the maximum possible rate is 0.0079 M. Moreover, inhibitory effects were detected at higher ammonium concentrations.

Modeling the effect of phosphorus on iron oxidation rates using the Andrew's Equation, resulted in a K_i estimated value of 501,643.8. according to (Grady *et al.*, 1998), a large K_i value indicates that the substrate (phosphorus) has no inhibitory effects, and the model can be simplified to the Monod Equation. Therefore, the curve-fitting was repeated using the Monod Equation and the parameter estimates were reported. **Figure 3. 53** shows the non-linear regression of iron oxidation rates as a function of phosphorus concentrations with WR culture using the Monod Equation, while **Table 13** reports the resulting estimated model parameters.

Figure 3. 53

Iron Oxidation Rates as a Function of Phosphorus Concentration

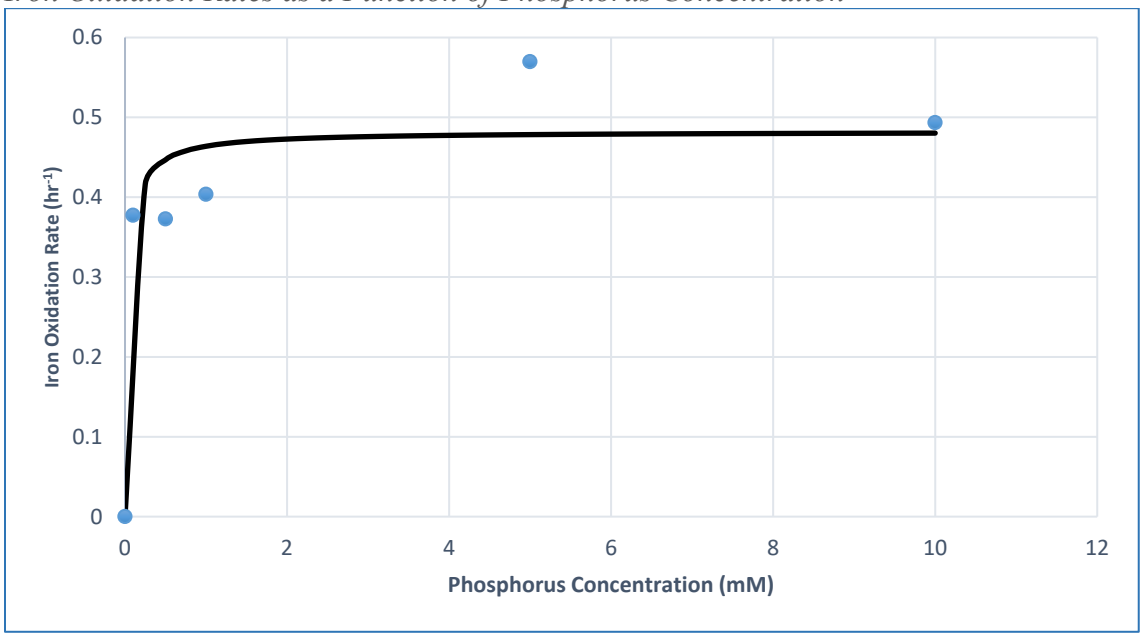

Table 13

Estimated Model Parameters of the Phosphorus Concentration Effect on Iron Oxidation Rates

Model parameters	
K_m	0.482 hr^{-1}
K_s	0.0396 mM

According to the model, the highest possible iron oxidation rate resulting from phosphorus addition is 0.482 hr^{-1} while the ammonium concentration at which the iron oxidation rate is equal to half the maximum possible rate is 0.0396 mM. Although iron

oxidation rates slightly decreased at higher phosphorus concentrations, no inhibitory effects were detected by the model at higher phosphorus concentrations.

Chapter 4: Discussion

pH Test

The best oxidation rates were achieved at the second dissolved ferrous iron feeding cycle for almost all cultures with all compositions. The lower oxidation rates at the first cycle were likely due to the lag phase and low bacteria counts. On the other hand, the reduction in oxidation rates after the second cycle was likely because of nutrients limitations or by-products accumulation causing the reaction to cease in the forward direction. On average, the lag phase for these tested cultures was less than a day. Processing the samples within 6 hr of collection played a major role in reducing the lag phase.

For all tested cultures, and despite the bacterial composition, the negative control showed a significantly lower oxidation rate. This suggested that the organisms substantially enhanced the iron oxidation rates, and at these tested pH values, the abiotic effects can be neglected.

The one-way ANOVA test was conducted to compare the three groups of WR and FR cultures with inoculum only. The test showed insignificant differences between the groups. This means that with inoculum addition, the average oxidation rates for FR culture and WR culture at both pH values were equal. For all tested cultures, the inoculum addition significantly increased the iron oxidation rates. The addition of inoculum increased the iron oxidation rates by 10.2-fold for FR culture and 3.2-fold for WR culture. This suggested that the extracted bacteria from the sediments from these sites were more efficient at oxidizing iron than the existing planktonic bacteria. For the WR and PA cultures, the oxidation rates increased with lower pH values. For WR culture, the average oxidation rate at pH 2.5 was 1.58 times higher than the one at pH 3.0. for PA culture, the average

oxidation rate at pH 2.0 was 2.58 times higher than the one at pH 4.0. Many studies in the literature have focused on testing very low ranges of pH (below 2.0) (Ojumu & Petersen, 2011). Sheng *et al.* (2016, 2017) have tested a similar range of pH using continuous mixed culture. They found that the highest oxidation rates were achieved at the lowest pH values (pH 2.1 – 2.3) which was consistent with the results found in this study. They have also found that the bacterial composition was strongly dependent on pH. It is worth it to investigate the species analysis under these different values of pH to compare the bacterial community composition that resulted in the highest oxidation rates. The study has also shown that the alpha microbial biodiversity decreased with lower pH values while the relative abundance of acidophilic iron-oxidizing bacteria increased. This may explain why higher ferrous iron oxidation rates were achieved at lower pH, and that because with lower biodiversity, more energy would be available for iron-oxidizing bacteria to utilize.(Sheng *et al.*, 2016). Minimal pH adjustment was needed throughout the study. pH was persistent with iron oxidation and did not go below 2.4. This is likely due to Fe^{3+} solubility at this low pH, as the $Fe(OH)_{3(s)}$ precipitates (Equation (3)) cannot form below pH 2.4. The PA culture had significantly lower oxidation rates at both pH values. Due to these unsatisfactory oxidation rates, the PA culture was dropped from further testing. The average oxidation rates and the statistical results are illustrated in **Figure 4. 1**. The y-axis shows the mean iron oxidation rate of the replicates and the tested groups are shown on the x-axis. The letters refer to the statistical grouping, as the groups with the same letters are statistically equal (n = 3, alpha = 0.05). The error bars illustrate one standard deviation of the associated groups. SPSS output tables are shown in the appendix.

Figure 4. 1

Average Oxidation Rates and Statistical Analysis Summary - pH Test, AMD Media, No Nutrients Addition

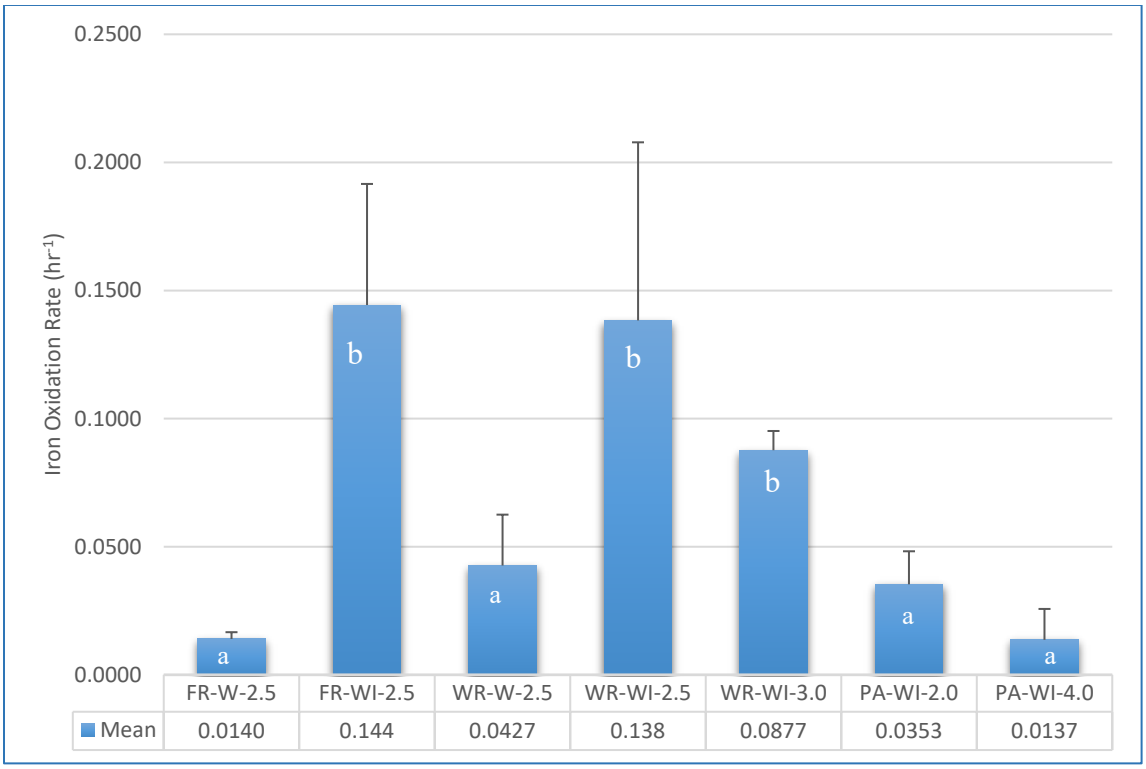

Nutrients Test

Nitrogen Test

The best oxidation rates were achieved at 0.1 M of NH_4^+ in both cultures. Overall, iron oxidation rates by the WR culture were significantly higher than the FR culture at each tested ammonium concentration. At the best ammonium concentration (0.1 M), the average iron oxidation rate by the WR culture was 2.75 times higher than the rate achieved by the FR culture, and therefore, the FR culture was omitted from further testing. For the WR culture, although the highest oxidation rates were achieved at 0.1 M ammonium, the statistical analysis showed insignificant difference when the ammonium concentration was

less than or equal to 0.1 M, $F(3,8) = 62.7$, $p < 0.001$, while for the FR culture, the iron oxidation rate at 0.1 M NH_4^+ was significantly higher than lower two concentrations, $F(2,6) = 33.6$, $p < 0.001$. The statistical analysis also proved that iron oxidation by the WR culture at 0.5 M NH_4^+ was significantly lower than the rate at 0.1 M NH_4^+ which indicated the occurrence of significant inhibition at higher ammonium concentrations. This result is consistent with Tuovinen *et al.* (1971), where they found that high concentrations of nitrate inhibited iron oxidation by *Thiobacillus ferrooxidans*. In terms of iron additions, the WR culture experienced an extended lag phase and the best achieved oxidation rates occurred at the $2^{nd}/3^{rd}$ iron addition. This is likely due to changing the media from the original culture AMD to the modified 9K media. The FR culture, however, achieved the highest iron oxidation rates at the first iron addition and decreased slightly afterwards. The reduction in iron oxidation rates after successive iron additions is likely to occur due to secondary nutrient limitation or by-products accumulation causing the reaction to cease in the forward direction. The negative controls showed a significantly lower ferrous iron oxidation rates with a maximum rate of 2.87×10^{-3} hr^{-1} which was 32-fold slower than the slowest achieved biotic oxidation rate (0.092 hr^{-1}). This, once again, proved that the bacteria drastically enhance iron oxidation rates. No study was found in the literature testing ammonium as a nitrogen supply for iron-oxidizing bacteria. Therefore, comparing iron oxidation rates with the literature was not possible. (Tuovinen et al., 1971) tested the growth of *T. ferrooxidans* on ferrous iron with 0.001 M ammonium. No iron oxidation rates were reported but a ten-fold increase in the cell count was observed. However, the ammonium was supplied in the form of ammonium phosphate, and considering the potential effects of phosphorus supply, tying the increase in bacteria numbers to ammonium concentration only was not possible.

The summary of the ammonium test and the statistical analysis are shown in **Figure 4. 2**. The y-axis shows the mean iron oxidation rate of the replicates and the tested groups are shown on the x-axis. The letters refer to the statistical grouping, as the groups with the same letters are statistically equal. The error bars illustrate the standard deviation of the associated groups. The SPSS output tables are shown in the appendix.

Figure 4. 2

Average Oxidation Rates and the Statistical Analysis - Ammonium Test, Modified 9K Media at pH 2.5, 2.87 mM P, No C

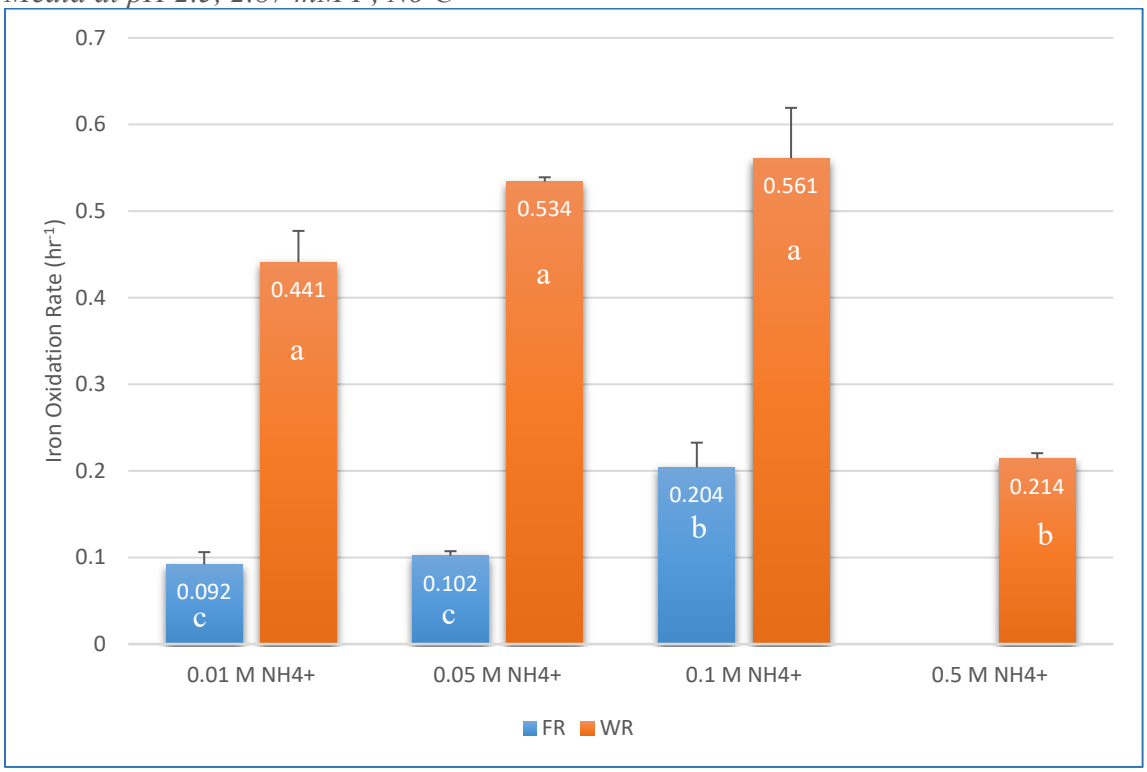

Phosphorus Test

Iron oxidation rates generally increased with phosphorus addition. Although literature have stated that iron-oxidizing bacteria have enzymes that are efficient in scavenging and assimilating phosphorous from the surrounding environment allowing the bacteria to survive in phosphorus-scarce environments (Avdalović et al., 2015; Seeger & Jerez, 1993; Vera et al., 2003, 2008), these results show that phosphorus availability significantly enhanced iron oxidation rates. The best iron oxidation rates were achieved at 5.0 mM of phosphate and were significantly higher than the rates at lower phosphate concentrations. Although the average oxidation rate at 10.0 mM was lower than the one at 5.0 mM, the statistical analysis showed insignificant difference between the two concentrations, $F(3,8) = 74.7$, $p < 0.001$. Regardless of the phosphate concentration, the best iron oxidation rates were achieved at the 2nd iron addition. The slower oxidation rates at the 1st iron addition are likely to occur due to the lag phase. Ferrous iron oxidation was significantly slower in the negative control with a rate of 3.33×10^{-3} hr^{-1} which was 112-fold slower than the slowest achieved biotic oxidation rate (0.373 hr^{-1}). This demonstrates the major role that the bacteria play in the oxidation process. No study found in the literature reported iron oxidation rate by iron-oxidizing bacteria as a function of phosphorus concentration. However, Seeger & Jerez (1993) investigated the response of *T. ferrooxidans* to phosphate limitation by monitoring the bacterial growth in phosphate-deficit and 23 mM phosphate media. The phosphate addition resulted in a four-fold increase in the bacteria numbers and increased the iron oxidation capacity (no rates were reported). Moreover, Tuovinen (1971) reported a ten-fold increase in *T. ferrooxidans* bacteria numbers when a 0.526 mM phosphate was supplied to a large-scale

sulfide ore. However, it was argued that this significant increase might have occurred due to the potential ability of phosphate to mobilize *T. ferrooxidans* from the surface of the ore. Nonetheless, the beneficial effects of phosphorus supply on iron-oxidizing bacterial growth were proven in the literature, but no study reported those effects on iron oxidation rates. The summary of the phosphorus test and the statistical analysis are shown in **Figure 4. 3**. The y-axis shows the mean iron oxidation rate of the replicates and the tested groups are shown on the x-axis. The letters refer to the statistical grouping, as the groups with the same letters are statistically equal. The error bars illustrate the standard deviation of the associated groups. The SPSS output tables are shown in the appendix.

Figure 4. 3

Average Oxidation Rates and the Statistical Analysis - Phosphorus Test, Modified 9K Media at pH 2.5, 0.1M N, No C

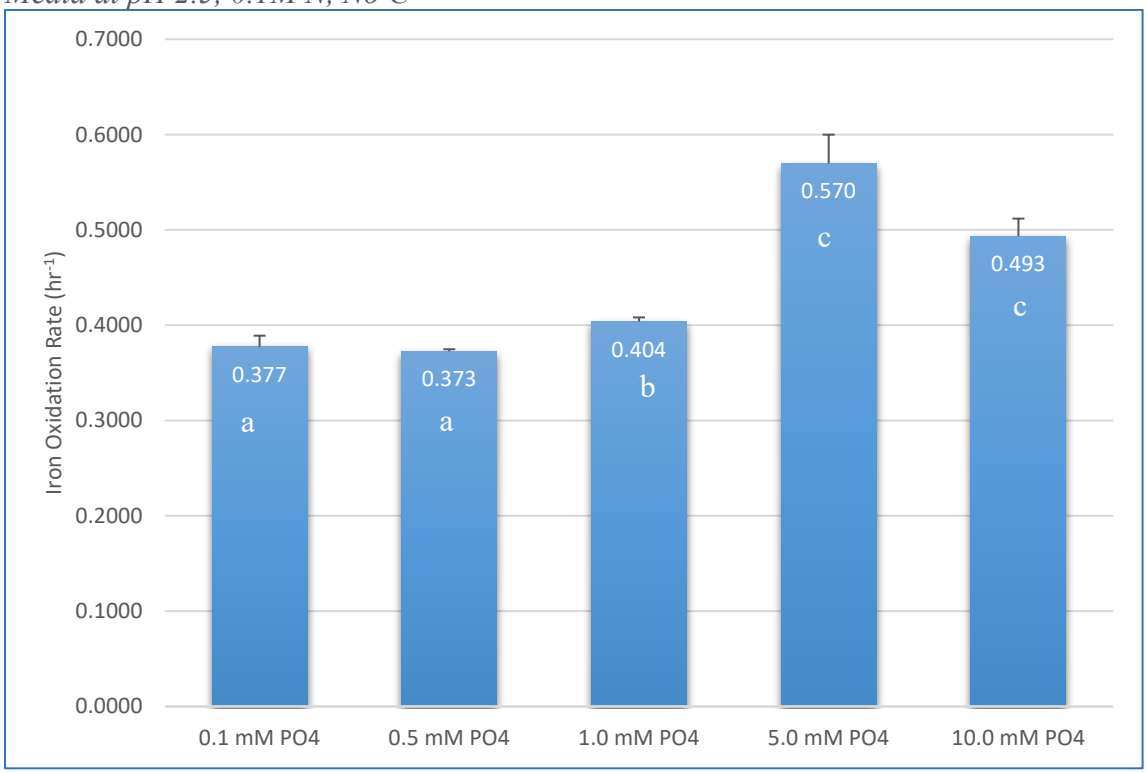

Organic Carbon Test

For the first enrichment, and regardless of the concentration, the addition of organic carbon did not significantly affect the iron oxidation rates (from 0.57 hr^{-1} without organic carbon to 0.56 hr^{-1} with 0.1 M organic carbon), $F(3,8) = 0.877$, $p = 0.512$. Overall, the addition of organic carbon caused a slight drop in iron oxidation rates.

For the second enrichment, however, iron oxidation rates were significantly and drastically inhibited by more than 52% after only one subculture enrichment. Moreover, the highest oxidation rate after sub-culturing was achieved at the lowest glucose concentration. This strongly indicates that glucose has significant inhibitory effects with successive sub-culturing. This finding is consistent with other studies that investigated the effect of other forms of organic carbon on iron oxidation and the growth of iron-oxidizing bacteria (Fang & Zhou, 2006; Frattini et al., 2000; Marchand & Silverstein, 2010). These results indicate that the species existing in the inoculum are mostly obligate chemolithoautotrophs, with very small relative abundance to no heterotrophs, which was later proven by the species analysis.

Despite the occurrence of these inhibitory effects, ferrous iron oxidation was still significantly slower in the negative control with a maximum rate of 6.28×10^{-3} hr^{-1} which was 43-fold slower than the slowest achieved biotic oxidation rate in the second enrichment (0.265 hr^{-1}). This illustrates the ability of iron-oxidizing bacteria to surpass the abiotic oxidation even when the conditions are not ideal. Literature have documented four possible mechanisms for organic carbon inhibition: “by directly affecting the iron-oxidizing system; by reacting abiologically with ferrous iron outside the cell; by interfering with the role of sulfate in iron oxidation; or by non-selectively disrupting the cell envelope or membrane”

(Frattini et al., 2000). Frattini *et al.* (2000) have also proven that the inhibitory organic carbon concentration is strongly strain-dependent. This might explain the inconsistency in the results as the tested culture was a mix of multiple species and strains with different relative abundance. However, organic carbon has been found necessary for the growth of iron-oxidizing archaea, while several iron-oxidizing bacteria couldn't grow on organic carbon like yeast extract (Plumb et al., 2008). This suggested that the tested mixed culture in this study had significantly low numbers of iron-oxidizing archaea, which was later proved by the species analysis. The summary of the organic carbon test and the statistical analysis are shown in **Figure 4. 4**. The y-axis shows the mean iron oxidation rate of the replicates and the tested groups are shown on the x-axis. The letters refer to the statistical grouping, as the groups with the same letters are statistically equal. The error bars illustrate the standard deviation of the associated groups. The SPSS output tables are shown in the appendix.

Figure 4. 4

Average Oxidation Rates and the Statistical Analysis - Glucose Test, Modified 9K Media at pH 2.5, 0.1 M N, 5.0 mM P

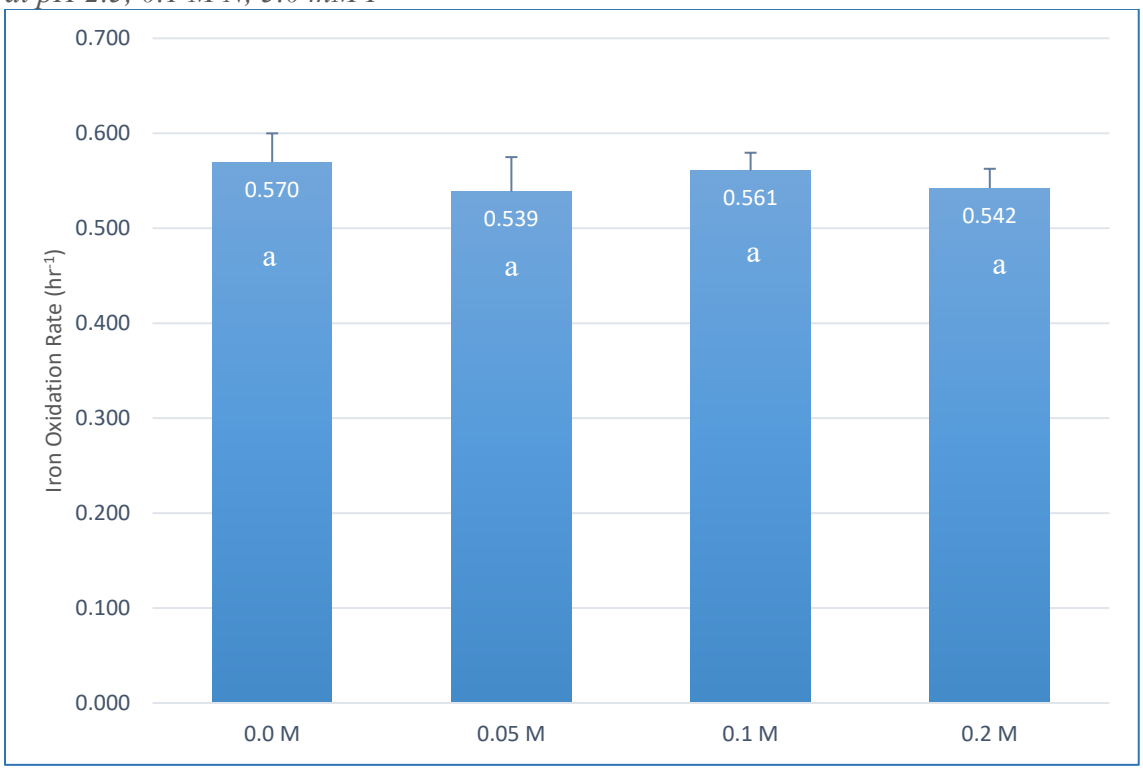

Wolf Run Culture Enrichment

When only the WR AMD water was tested, with no extracted inoculum or nutrients additions, the best average oxidation rate achieved was 0.0430 hr^{-1} at the first iron addition. This repeatedly observed behavior of iron-oxidizing bacteria, where iron oxidation rates significantly degrade by the second iron addition, indicates that the iron-oxidizing bacteria may rely on the low nutrient concentrations in the WR AMD for growth.

Both the extracted inoculum and/or nutrients addition significantly enhanced iron oxidation rates by a minimum of 3.2-fold, $t(4) = -2.386$, $p = 0.038$. The best average oxidation rate achieved was 0.237 hr^{-1} when both the extracted inoculum and 0.1 M of

ammonium were added. This addition increased iron oxidation rates by 5.5-fold. Although the addition of the extracted inoculum and ammonium resulted in a higher average oxidation rate (0.237 hr^{-1}) than the addition of the extracted inoculum and phosphorus (0.196 hr^{-1}), the difference was insignificant, $t(4) = 1.952$, $p = 0.061$. Moreover, the addition of phosphorus maintained consistently high oxidation rates over a higher number of iron additions, while for the ammonium addition only, iron oxidation rates degraded significantly by the 3rd run. This indicates that phosphorus is a more important nutrient for bacterial growth in the long run.

Although the addition of the extracted inoculum to the AMD water and nutrients further enhanced iron oxidation rates compared with AMD water with only nutrients added, the statistical analysis showed insignificant difference between the two groups, $t(4) = -.658$, $p = 0.288$. However, the addition of the extracted inoculum significantly decreased the lag phase and resulted in more consistent rates between the three trials.

Regardless of the composition of the nutrients added, all combinations of nutrients significantly enhanced iron oxidation rates when added to WR AMD and extracted inoculum. The addition of both the extracted inoculum and nutrients was necessary to achieve the highest oxidation rates. However, further economic analysis is necessary to determine the most efficient combination. The summary of the WR enrichment test is shown in **Figure 4. 5**. Because of the high number of groups, the one-way ANOVA was inefficient in detecting the differences between the groups, $F(4,10) = 2.910$, $p = 0.078$. Therefore, four independent T-tests were conducted to interpret the data. For this reason, a comprehensive statistical grouping for this stage is not available. Four different variables were defined to avoid further correction of the alpha value. The y-axis shows the mean iron

oxidation rate of the replicates and the tested groups are shown on the x-axis. The letters refer to the statistical grouping, as the groups with the same letters are statistically equal. The error bars illustrate the standard deviation of the associated groups. The SPSS output tables are shown in the appendix.

Figure 4. 5

Average Oxidation Rates and the Statistical Analysis - the WR AMD Enrichment Test, pH 2.5, 0.1 M N, 5.0 mM P

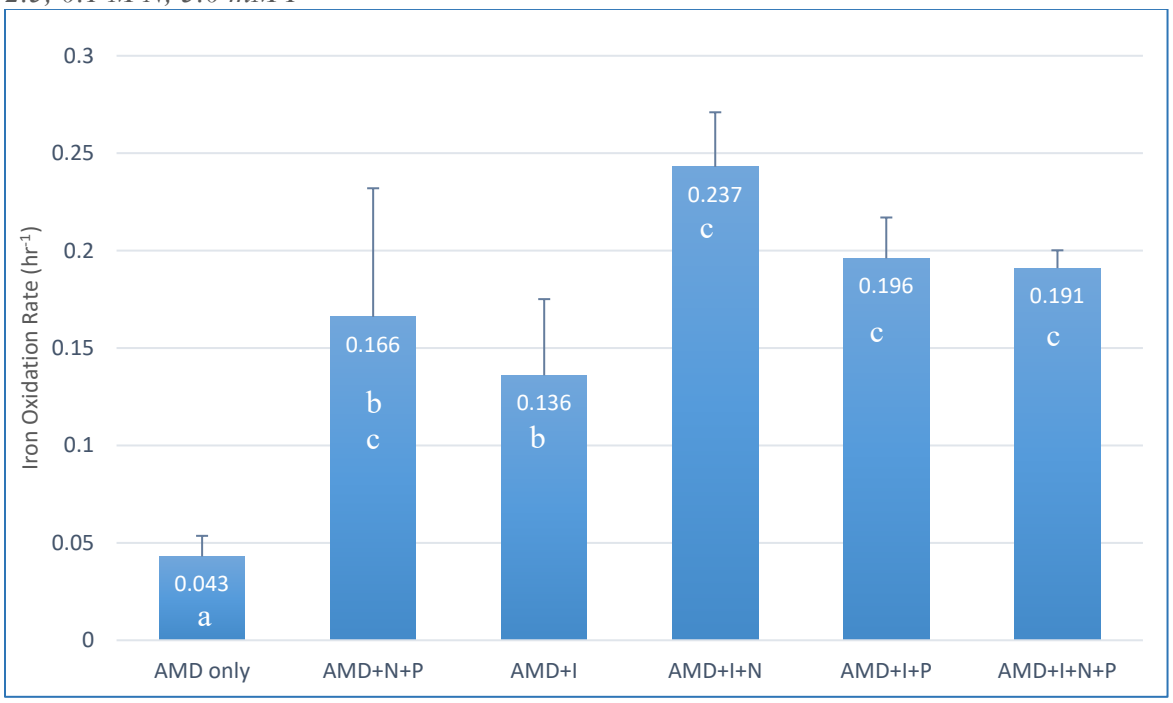

Figure 4. 6 shows the average oxidation rates of the tested combinations with successive iron additions. The addition of the extracted inoculum was very effective in reducing the lag phase, while the addition of nutrients was necessary to achieve relatively high oxidation rates. Moreover, the addition of both the extracted inoculum and the nutrients maintained consistent and high oxidation rates.

Figure 4. 6

Average Oxidation Rates of the Tested Trials with Successive Iron Additions, WR AMD Enrichment, pH 2.5, 0.1 M N, 5.0 mM P

Truetown AMD Enrichment

Regardless of the combination tested, the addition of inoculum and nutrients significantly enhanced iron oxidation rates. Surprisingly, the bacteria extracted from the WR sediments achieved higher oxidation rates in TT AMD than their original environment media (WR AMD). Overall, the iron oxidation rates resulting from enriching the WR culture in TT water were the highest among all tested AMD in the study.

When only the TT AMD water was tested, with no extracted inoculum or nutrients additions, the best average oxidation rate achieved was 0.0330 hr^{-1} at the first iron addition. This repetitive observed behavior, where iron oxidation rates significantly decreased by

the second iron addition, indicates that iron-oxidizing bacteria may rely on a secondary nutrient for growth and iron oxidation. Moreover, it was observed that iron oxidation rates fluctuate drastically among the three replicates when only the existent planktonic TT bacteria were tested (with no WR inoculum addition). Because of this inconsistency in the results, relying on the existent TT culture was not preferable.

Regardless of the nutrients composition, the addition of the extracted WR inoculum was significantly important to reduce the lag phase, achieve higher oxidation rates, and provide consistency in the results among the trials. Moreover, when the inoculum was added, the nutrients became more efficient in enhancing iron oxidation rates. For example, when only the phosphorus was added, a 2.7-fold increase in iron oxidation rates was achieved, but with further addition of the extracted inoculum, a 10.5-fold increase in iron oxidation rates was achieved. Moreover, it was found that regardless of the nutrients composition, adding the nutrients solely to the TT AMD was not efficient, as the reported oxidation rates were delayed for about 15 d, where iron oxidation was negligible. The addition of the WR inoculum was necessary to overcome the long lag phase period. In addition, results among the three replicates varied significantly resulting in high standard deviation in the average oxidation rate. For these reasons, the combinations that did not contain the WR inoculum were omitted from the statistical analysis and further comparisons. However, it is worth noting that despite the inconsistent results and the prolonged lag phase, adding the nutrients to the TT AMD eventually resulted in a high average oxidation rate (0.249 hr^{-1}). Therefore, repeated enrichments using ammonium, phosphorus and the native planktonic TT bacteria may produce a suitable culture with high

oxidation rates and as a result, no inoculum addition will be needed. The efficiency of this theory is worth further testing.

The statistical analysis showed significant differences between all the tested groups that contained the WR culture regardless of the nutrient composition, $F(3,8) = 412.706$, $p < 0.001$. The best average iron oxidation rate achieved (0.398 hr^{-1}) was when the WR inoculum and both nutrients were added. This addition resulted in a 12-fold increase in iron oxidation rates. The addition of phosphorus had a more significant impact than the addition of ammonium, indicating that phosphorus is more important for bacterial growth and iron oxidation.

The best biotic average oxidation rate achieved (0.398 hr^{-1}) was 1327 folds faster than the abiotic oxidation rate (0.0003 hr^{-1}). This illustrates the significance of the biological impact on remediation and iron oxidation. The summary of the TT enrichment is shown in **Figure 4. 7**. The y-axis shows the mean iron oxidation rate of the replicates and the tested groups are shown on the x-axis. The letters refer to the statistical grouping, as the groups with the same letters are statistically equal. The error bars illustrate the standard deviation of the associated groups.

Figure 4. 7

Average Oxidation Rates and the Statistical Analysis - the TT AMD Enrichment Test, pH 2.5, 0.1 M N, 5.0 mM P

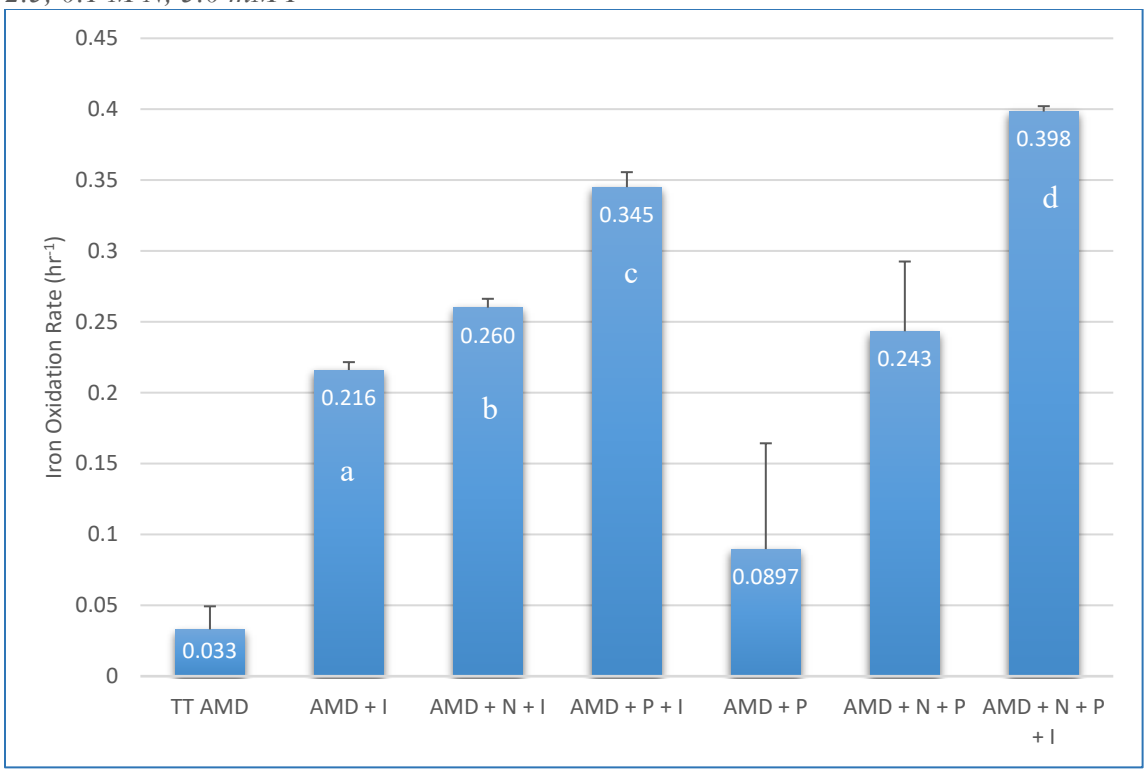

In terms of iron additions, the beneficial effect of the addition of the WR inoculum quickly diminished by the 3rd iron addition. This illustrates that iron-oxidizing bacterial growth depended on a secondary nutrient. This result was also observed from the addition of the WR inoculum and ammonium. The addition of ammonium seemed effective at the 1st iron addition but then quickly decreased with successive additions. This indicated that the iron-oxidizing bacteria required other nutrients as well to maintain growth and consistent iron oxidation rates. For the last two combinations, however, when phosphorus was added, iron oxidation rates were the highest and remained relatively high and consistent over the three runs. This indicated that the addition of phosphorus was necessary

to maintain high and consistent iron oxidation rates. Regardless of the combination, the iron oxidation rates experienced a considerable reduction by the 3rd iron addition. This was likely due to by-products accumulation that cause the reaction to cease in the forward direction. **Figure 4. 8** shows the average oxidation rates of the tested combinations with successive iron additions.

Figure 4. 8

Average Oxidation Rates of the Tested Trials with Successive Iron Additions, TT AMD Enrichment, pH 2.5, 0.1 M N, 5.0 mM P

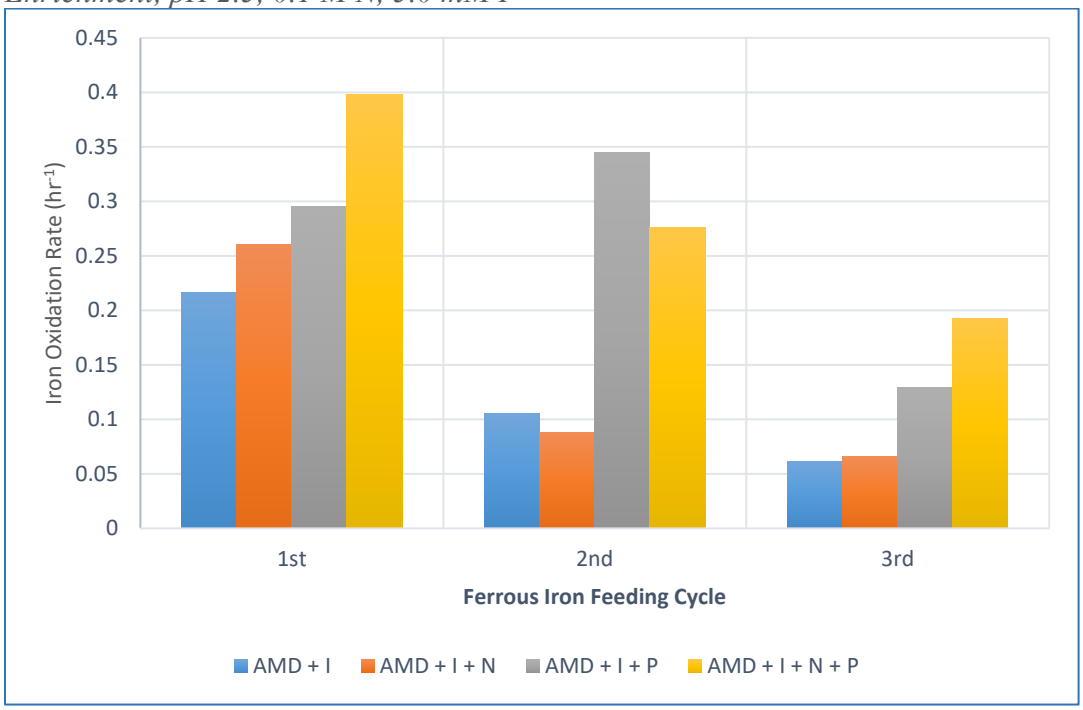

Iron Oxidation Rates Summary and Comparison

To summarize the iron oxidation rates achieved in this study, **Table 14** list the biotic iron oxidation rates for each trial with its composition.

Table 14

Summary of the Biotic Iron Oxidation Rates

Abbreviation	pH	Inoculum	Media	N (M)	P (mM)	C (M)	Avg. rate	Std. dev.
FR-W	2.5	N/A	100% FR AMD	N/A	N/A	N/A	0.0142	0.00304
FR-W+I	2.5	50% FR	50% FR AMD	N/A	N/A	N/A	0.144	0.0473
WR-W	2.5	N/A	100% WR AMD	N/A	N/A	N/A	0.427	0.0199
WR-W+I	2.5	50% WR	50% WR AMD	N/A	N/A	N/A	0.138	0.0694
WR-W+I	3.0	50% WR	50% WR AMD	N/A	N/A	N/A	0.0876	0.00762
PA-W+I	2.0	50% PA	50% PA AMD	N/A	N/A	N/A	0.0353	0.0129
PA-W+I	4.0	50% PA	50% PA AMD	N/A	N/A	N/A	0.0137	0.0121
WR_0.01M_N	2.5	10% WR	90% 9K*	0.01	2.87	N/A	0.441	0.0361
WR_0.05M_N	2.5	10% WR	90% 9K*	0.05	2.87	N/A	0.534	0.00503
WR_0.1M_N	2.5	10% WR	90% 9K*	0.1	2.87	N/A	0.561	0.0582
WR_0.5M_N	2.5	10% WR	90% 9K*	0.5	2.87	N/A	0.214	0.00643
FR_0.01M_N	2.5	10% FR	90% 9K*	0.01	2.87	N/A	0.0925	0.0126
FR_0.05M_N	2.5	10% FR	90% 9K*	0.05	2.87	N/A	0.102	0.00518
FR_0.1M_N	2.5	10% FR	90% 9K*	0.1	2.87	N/A	0.204	0.0286
WR_0.1_mM_P	2.5	10% WR	90% 9K*	0.1	0.1	N/A	0.377	0.0117
WR_0.5_mM_P	2.5	10% WR	90% 9K*	0.1	0.5	N/A	0.373	0.00208
WR_1.0_mM_P	2.5	10% WR	90% 9K*	0.1	1.0	N/A	0.404	0.00451
WR_5.0_mM_P	**2.5**	**10% WR**	**90% 9K***	**0.1**	**5.0**	**N/A**	**0.570**	**0.0302**

Abbreviation	pH	Inoculum	Media	N (M)	P (mM)	C (M)	Avg. rate	Std. dev.
WR_10.0_mM_P	2.5	10% WR	90% 9K*	0.1	10.0	N/A	0.493	0.0185
WR_0.05M_Glucose	2.5	10% WR	90% 9K*	0.1	5.0	0.05	0.539	0.0362
WR_0.1M_Glucose	2.5	10% WR	90% 9K*	0.1	5.0	0.1	0.561	0.0188
WR_0.2M_Glucose	2.5	10% WR	90% 9K*	0.1	5.0	0.2	0.542	0.0203
WR_AMD_only	2.5	N/A	100% WR AMD	N/A	N/A	N/A	0.043	0.020
WR_AMD_N_P	2.5	N/A	100% WR AMD	0.1	5.0	N/A	0.166	0.0661
WR_AMD_I	2.5	10% WR	90% WR AMD	N/A	N/A	N/A	0.136	0.0391
WR_AMD_N_I	2.5	10% WR	90% WR AMD	0.1	N/A	N/A	0.237	0.0297
WR_AMD_P_I	2.5	10% WR	90% WR AMD	N/A	5.0	N/A	0.196	0.0210
WR_AMD_N_P_I	2.5	10% WR	90% WR AMD	0.1	5.0	N/A	0.191	0.00917
TT_AMD_only	2.5	N/A	100% TT AMD	N/A	N/A	N/A	0.0330	0.0163
TT_AMD_I	2.5	10% WR	90% TT AMD	N/A	N/A	N/A	0.216	0.00557
TT_AMD_N_I	2.5	10% WR	90% TT AMD	0.1	N/A	N/A	0.260	0.00625
TT_AMD_P_I	2.5	10% WR	90% TT AMD	N/A	5.0	N/A	0.345	0.0156
TT_AMD_P	2.5	N/A	100% TT AMD	N/A	5.0	N/A	0.0897	0.0746
TT_AMD_N_P	2.5	N/A	100% TT AMD	0.1	5.0	N/A	0.249	0.0492
TT_AMD_N_P_I	2.5	10% WR	90% TT AMD	0.1	5.0	N/A	0.398	0.00379

***Modified 9K medium recipe provided in the methods section for each trial.**

Due to the difference in the adopted kinetics model and the order of the reaction in some studies, iron oxidation rates comparison was not possible in some cases. Overall, regardless of the tested media, the species of the bacteria, pH, temperature, or even iron concentration, the best iron oxidation rates achieved in this study surpassed most of the iron oxidation rates reported in the literature with a minimum of 5.7-fold (Ahonen't And & Tuovinen2, 1989; Edward et al., 2022; Özkaya et al., 2007; Plumb et al., 2008), (see **Table 1**). However, the iron oxidation rates achieved by Ojumu *et al*. (2009) and Sheng *et al*. (2017) surpassed the iron oxidation rates achieved in this study by a maximum of 135-fold and 6.3-fold, respectively. The high oxidation rates achieved in both studies are likely due to the higher growth yield in the continuous system resulting from the extremely high influent iron concentrations. For example, in Sheng et al. study, the maximum iron oxidation rate increased from 2.44×10^{-7} mol Fe(II) L^{-1} s^{-1} to 7.7×10^{-7} mol Fe(II) L^{-1} s^{-1} for the same operational conditions when the influent ferrous iron concentration increased from 300 mg/L to 2400 mg/L. Moreover, literature found that higher specific iron oxidation rates can be achieved in continuous systems, which was the system adopted by both studies (Boon et al., 1999).

The highest achieved iron oxidation rate in this study was 0.570 hr^{-1} using the Wolf Run mixed culture enriched in a defined growth medium at ~20° C and pH 2.5. The addition of nutrients was proven to significantly enhance iron oxidation rates in both WR AMD and TT AMD. The inoculum and nutrients addition to TT AMD achieved a 12-fold increase in biotic oxidation rates. With this being noted, it would be interesting to combine the operational conditions adopted by Sheng *et al.* and Ojumu *et al.* studies, with the results found in this study. Switching to a continuous system with further pH and nutrients

optimization may result in further faster iron oxidation rates at Truetown site. This is a very promising outcome showing that the addition of nutrients and operational conditions optimization can significantly enhance iron-oxidizing bacterial growth and as a result achieve higher iron oxidation rates.

WR Enriched Culture Species Analysis

Approximately 62.6% of the inoculum consisted of *Acidithiobacillus ferrooxidans*. *At. ferrooxidans* are obligatory chemolithoautotrophs with a remarkable broad metabolic capacity. This species is one of the most flexible species among iron-oxidizers as it has a relatively broad list of potential electron donors and acceptors. *At. ferrooxidans* can grow aerobically on iron and reduced inorganic sulfur compounds or anaerobically on hydrogen and many other inorganic compounds as an electron donor. They can also utilize a wide range of electron acceptors like oxygen, ferric iron, and elemental sulfur. This unique wide range of metabolic capacity provides this species with more available energy for growth than other iron-oxidizing species. This may be one of the main reasons why *At. ferrooxidans* were found to be the dominant species in this inoculum and many other tested cultures in the literature. Many studies in literature have found that *At. ferrooxidans* are the dominant species below pH 3.0, optimally at pH 2.0, and with a lowest boundary at pH 1.3 - 1.5 (Clapa et al., 2019; Hallberg & Johnson, 2001; Ingledew, 1982; Sheng et al., 2016). This may explain why the highest iron oxidation rate for the WR culture was achieved at pH 2.5 and not pH 3.0 although the pH at the site ranged between 3.0 – 3.5. The lower pH may have provided this species with more favorable growth conditions and as a result achieved higher oxidation rates. However, it was found that *At. ferrooxidans* are more sensitive to ferric iron inhibition than other species of iron-oxidizing bacteria like

L.ferriphilum (Ojumu et al., 2009). This might explain the significant inhibition of iron oxidation rates by the 3rd iron addition in most cases throughout this study.

Metallibacterium xanthomonadaceae bacterium accounted for approximately 18.5% of the inoculum. Some case studies have found this species in acid mine drainage in extremely acidic environments below pH 3.0 with high metals concentration (Clapa et al., 2019). Not much information was found about the metabolic mechanisms or optimal conditions for this species.

Acidiphilium organovorum was the 3rd highest dominant species with a relative abundance of 8.08%. this species was found in other extremely acidic AMD sites across the world where the pH is below 3.0 (Aytar et al., 2015). Although the pH condition was ideal for this species, *Acidiphilium* spp. are obligate heterotrophs that cannot oxidize iron and their growth is significantly enhanced by some organic compounds like glucose (Aytar et al., 2015; Lobos et al., 1986). This came contradictory with the inoculum enrichment conditions as it was enriched in a modified 9K medium with the best nutrients concentration without any organic carbon addition. This indicates that this species might have a higher relative abundance in the natural environment before the modified 9K media enrichment.

Some strains of *Acidibacter gamma proteobacterium* were also recognized in the literature (e.g. *Acidibacter ferrireducens*) growing naturally in AMD. They are obligate heterotrophs growing in the 2.5 – 4.5 pH range (Falagán & Johnson, 2014).

The low relative abundance of *Leptospirillum ferriphilum* was expected as literature found that this species grows at pH below 2.0 optimally around pH 1.3 (Ojumu

& Petersen, 2011; Özkaya et al., 2007; Plumb et al., 2008). Therefore, the pH conditions were not ideal for this species to thrive.

Overall, iron-oxidizing bacteria accounted for approximately 86% of the sample. Sheng *et al.* (2016) have found that the alpha microbial biodiversity decreased with lower pH values while the relative abundance of acidophilic iron-oxidizing bacteria increased. This may explain why higher ferrous iron oxidation rates were achieved at lower pH, and that because with lower biodiversity, more energy would be available for iron-oxidizing bacteria to utilize. This has also been proven by the species analysis in this study. No archaea were found in the media and biodiversity among the bacteria was relatively low considering a mixed culture environment.

Moreover, organic carbon has been found necessary for the growth of archaea, while several iron-oxidizing bacteria couldn't grow on organic carbon like yeast extract (Plumb et al., 2008). A complete inhibition was observed for some species like *A. ferrooxidans* after the addition of glucose (Fang & Zhou, 2006). This came consistent with the results found in this study, as the dominant species was *A. ferrooxidans,* an obligate chemolithoautotrophy that is unable to assimilate organic carbon.

Chapter 5: Conclusions

The effect of pH, nutrients, and organic carbon on iron oxidation rates by mixed cultures of iron-oxidizing bacteria collected from three different extremely acidic AMD sites was investigated for the possibility of remediating the Truetown AMD at the Sunday creek, OH. Lower pH values achieved higher oxidation rates. The best culture was found to be the one collected from the WR site with the inoculum extracted from the WR sediment and enriched at pH 2.5. This culture was found to be predominantly *A. ferrooxidans.* Mobilizing the bacteria from the sediment achieved significantly higher oxidation rates than the existing planktonic bacteria alone at all tested cultures. The addition of ammonium and phosphorus significantly enhanced iron oxidation rates at all tested media. The best ammonium and phosphorus concentrations were found to be 0.1 M and 5.0 mM, respectively. The addition of organic carbon significantly inhibited iron oxidation rates by 52% after only one sub-culture. This result was expected for a predominantly chemolithoautotrophic culture that is unable to grow on organic matter. The iron oxidation rates achieved in this study surpassed the maximum iron oxidation rate achieved in most studies reported in the literature except for two studies where they adopted significantly different operation conditions. Phosphorus availability was necessary to achieve higher oxidation rates and sustain these rates over a higher number of iron feedings. The addition of the inoculum extracted from the WR sediment and the best nutrients concentrations to TT AMD achieved a 12-fold increase in iron oxidation rates and 1327-fold increase compared to abiotic oxidation rates at TT site. This significant increase is very promising and strengthens the possibility of adopting the biological treatment pathway as an efficient and sustainable treatment method.

Chapter 6: Recommendations

For the lab-scale experiments, it would be interesting to investigate the bacterial culture composition and the relative abundance changes with different nutrients concentrations. Would the relative abundance of a certain species change with different nutrients concentrations like it does with pH and temperature? Does the nutrients addition enhance the bacterial growth rate, the specific iron assimilating capacity (bacterial activity), or both?

Moreover, literature achieved higher oxidation rates in continuous systems compared to batch systems. It is important to investigate the degree of enhancement that this switch in operating systems would achieve.

For the larger scale operation, more experiments are needed to evaluate and confirm the results achieved in this lab-scale study. Further optimization of pH and nutrients concentrations is necessary for cost-optimization purposes. Further testing of ammonium and phosphorus recovery techniques is also necessary to avoid eutrophication.

Moreover, the current pH at Truetown site is 5.26. Bringing it down to 2.5 by simply adding sulfuric acid then having to raise it back up to around pH 7 upon final discharge by adding sodium hydroxide is a costly step and defeats the purpose of reducing the usage of chemicals. Therefore, more tests are needed to figure out how to achieve this process economically and efficiently.

In addition to that, the after-iron-oxidation processes, including iron precipitation and settling were out of the scope of this study. These processes are crucial for the larger scale operation and need further investigation.

Finally, the current treatment method at TT site is relying on iron sludge as a valuable resource recovery to cover the operational costs of the treatment facility. For many years, researchers' efforts were invested in maximizing the iron sludge quality aiming to sell it as marketable and valuable pigment. Further tests are needed to evaluate the quality of the pigment resulting from biotic iron oxidation.

References

Acharya, B. S., & Kharel, G. (2020). Acid mine drainage from coal mining in the United States – An overview. *Journal of Hydrology*, *588*, 125061. https://doi.org/10.1016/J.JHYDROL.2020.125061

Ahonen't And, L., & Tuovinen2, O. H. (1989). Microbiological Oxidation of Ferrous Iron at Low Temperatures. *Applied and Environmental Microbiology*, *55*(2), 312–316. https://journals.asm.org/doi/abs/10.1128/aem.55.2.312-316.1989

Akcil, A., & Koldas, S. (2006). Acid Mine Drainage (AMD): causes, treatment and case studies. *Journal of Cleaner Production*, *14*(12-13 SPEC. ISS.), 1139–1145. https://doi.org/10.1016/J.JCLEPRO.2004.09.006

Avdalović, J., Beškoski, V., Gojgić-Cvijović, G., Mattinen, M. L., Stojanović, M., Zildžović, S., & Vrvić, M. M. (2015). Microbial solubilization of phosphorus from phosphate rock by iron-oxidizing Acidithiobacillus sp. B2. *Minerals Engineering*, *72*, 17–22. https://doi.org/10.1016/J.MINENG.2014.12.010

Aytar, P., Kay, C. M., Mutlu, M. B., Çabuk, A., & Johnson, D. B. (2015). Diversity of acidophilic prokaryotes at two acid mine drainage sites in Turkey. *Environmental Science and Pollution Research*, *22*(8), 5995–6003. https://doi.org/10.1007/S11356-014-3789-4/FIGURES/5

Blight, K. R., & Ralph, D. E. (2008). Aluminium sulphate and potassium nitrate effects on batch culture of iron oxidising bacteria. *Hydrometallurgy*, *92*(3–4), 130–134. https://doi.org/10.1016/J.HYDROMET.2008.02.010

Bologo, V., Maree, J. P., & Carlsson, F. (2012). Application of magnesium hydroxide and barium hydroxide for the removal of metals and sulphate from mine water. *Water SA*, *38*(1), 23–28. https://doi.org/10.4314/WSA.V38I1.4

Bonmati, M., Ceccanti, B., & Nannipieri, P. (1998). Protease extraction from soil by sodium pyrophosphate and chemical characterization of the extracts. *Soil Biology and Biochemistry*, *30*(14), 2113–2125. https://doi.org/10.1016/S0038-0717(98)00089-3

Boon, M., & Heijnen, J. J. (1998). Chemical oxidation kinetics of pyrite in bioleaching processes. *Hydrometallurgy*, *48*(1), 27–41. https://doi.org/10.1016/S0304-386X(97)00072-8

Boon, M., Ras, C., & Heijnen, J. J. (1999). The ferrous iron oxidation kinetics of Thiobacillus ferrooxidans in batch cultures. *Applied Microbiology and Biotechnology*, *51*(6), 813–819. https://doi.org/10.1007/s002530051467

Breed, A. W., Dempers, C. J. N., Searby, G. E., Gardner, M. N., Rawlings, D. E., & Hansford, G. S. (1999). The effect of temperature on the continuous ferrous-iron oxidation kinetics of a predominantly Leptospirillum ferrooxidans culture. *Biotechnology and Bioengineering*, *65*(1), 44–53. https://doi.org/10.1002/(SICI)1097-0290(19991005)65:1<44::AID-BIT6>3.0.CO;2-V

Breed, A. W., & Hansford, G. S. (1999a). Effect of pH on ferrous-iron oxidation kinetics of Leptospirillum ferrooxidans in continuous culture. *Biochemical Engineering Journal*, *3*(3), 193–201. https://doi.org/10.1016/S1369-703X(99)00018-2

Breed, A. W., & Hansford, G. S. (1999b). Studies on the mechanism and kinetics of bioleaching. *Minerals Engineering*, *12*(4), 383–392. https://doi.org/10.1016/S0892-6875(99)00018-7

Chemical Aspects of Acid Mine Drainage on JSTOR. (n.d.). Retrieved March 10, 2023, from https://www-jstor-org.proxy.library.ohio.edu/stable/25036044?seq=8

Chen, G., Ye, Y., Yao, N., Hu, N., Zhang, J., & Huang, Y. (2021). A critical review of prevention, treatment, reuse, and resource recovery from acid mine drainage. *Journal of Cleaner Production*, *329*. https://doi.org/10.1016/J.JCLEPRO.2021.129666

Clapa, T., Narozna, D., Siuda, R., Borkowski, A., Selwet, M., & Madrzak, C. (2019). Diversity of Bacterial Communities in the Acid Mine Drainage Ecosystem of an Abandoned Polymetallic Mine in Poland. *Polish Journal of Environmental Studies*, *28*(4), 2109–2119. https://doi.org/10.15244/PJOES/91785

Edward, C. J., Kotsiopoulos, A., & Harrison, S. T. L. (2022). Ferrous iron oxidation kinetics of Acidiplasma cupricumulans, a key archaeon in the mineral biooxidation consortium: Impact of nutrient availability, ferric iron and thiocyanate. *Hydrometallurgy*, *211*. https://doi.org/10.1016/J.HYDROMET.2022.105890

Edwards, K. J., Bond, P. L., & Banfield, J. F. (2000). Characteristics of attachment and growth of Thiobacillus caldus on sulphide minerals: a chemotactic response to sulphur minerals? *Environmental Microbiology*, *2*(3), 324–332. https://ami-journals.onlinelibrary.wiley.com/doi/full/10.1046/j.1462-2920.2000.00111.x

Falagán, C., & Johnson, D. B. (2014). Acidibacter ferrireducens gen. nov., sp. nov.: an acidophilic ferric iron-reducing gammaproteobacterium. *Extremophiles*, *18*(6), 1067–1073. https://link.springer.com/article/10.1007/s00792-014-0684-3

Fang, D., & Zhou, L. X. (2006). Effect of sludge dissolved organic matter on oxidation of ferrous iron and sulfur by Acidithiobacillus ferrooxidans and Acidithiobacillus thiooxidans. *Water, Air, and Soil Pollution*, *171*(1–4), 81–94. https://doi.org/10.1007/S11270-005-9014-9/METRICS

Filipe, C. D., & Grady, C. L., Jr. (1998). Biological Wastewater Treatment, second edition, Revised and Expanded. CRC Press. ISBN 0-82478919-9.

Frattini, C. J., Leduc, L. G., & Ferroni, G. D. (2000). Strain variability and the effects of organic compounds on the growth of the chemolithotrophic bacterium Thiobacillus ferrooxidans. *Antonie van Leeuwenhoek, International Journal of General and Molecular Microbiology*, *77*(1), 57–64. https://link.springer.com/article/10.1023/A:1002089001725

Gray, N. F. (1997). Environmental impact and remediation of acid mine drainage: A management problem. *Environmental Geology*, *30*(1–2), 62–71. https://doi.org/10.1007/S002540050133

Hallberg, K. B. (2010). New perspectives in acid mine drainage microbiology. *Hydrometallurgy*, *104*(3–4), 448–453. https://doi.org/10.1016/J.HYDROMET.2009.12.013

Hallberg, K. B., González-Toril, E., & Johnson, D. B. (2010). Acidithiobacillus ferrivorans, sp. nov.; facultatively anaerobic, psychrotolerant iron-, and sulfur-oxidizing acidophiles isolated from metal mine-impacted environments.

Extremophiles, *14*(1), 9–19. https://link.springer.com/article/10.1007/s00792-009-0282-y

Hallberg, K. B., & Johnson, D. B. (2001). Biodiversity of Acidophilic Prokaryotes. *Advances in Applied Microbiology*, *49*, 37–84. https://doi.org/10.1016/S0065-2164(01)49009-5

Hallberg, K. B., & Johnson, D. B. (2003). Novel acidophiles isolated from moderately acidic mine drainage waters. *Hydrometallurgy*, *71*(1–2), 139–148. https://doi.org/10.1016/S0304-386X(03)00150-6

Hedin, R., Environmental, H., & Hedin, R. S. (2003). *Land Contamination & Reclamation*. *11*(2). https://doi.org/10.2462/09670513.802

Herlihy, A. T., Kaufmann, P. R., Mitch, M. E., & Brown, D. D. (1990). Regional estimates of acid mine drainage impact on streams in the mid-atlantic and Southeastern United States. *Water, Air, and Soil Pollution*, *50*(1–2), 91–107. https://link.springer.com/article/10.1007/BF00284786

Holland, H. D., & Turekian, K. K. (2004). *Treatise on geochemistry*.

Hu, X., Yang, H., Tan, K., Hou, S., Cai, J., Yuan, X., Lan, Q., Cao, J., & Yan, S. (2022). Treatment and recovery of iron from acid mine drainage: a pilot-scale study. *Journal of Environmental Chemical Engineering*, *10*(1). https://doi.org/10.1016/J.JECE.2021.106974

Ingledew, W. J. (1982). Thiobacillus Ferrooxidans the bioenergetics of an acidophilic chemolithotroph. *Biochimica et Biophysica Acta (BBA) - Reviews on Bioenergetics*, *683*(2), 89–117. https://doi.org/10.1016/0304-4173(82)90007-6

Johnson, D. B., & Hallberg, K. B. (2005). Acid mine drainage remediation options: a review. *Science of The Total Environment*, *338*(1–2), 3–14. https://doi.org/10.1016/J.SCITOTENV.2004.09.002

Johnson, D. B., & McGinness, S. (1991). Ferric Iron Reduction by Acidophilic Heterotrophic Bacteria. *Applied and Environmental Microbiology*, *57*(1), 207–211. https://doi.org/10.1128/AEM.57.1.207-211.1991

Jones, A. A., & Bennett, P. C. (2017). Mineral ecology: Surface specific colonization and geochemical drivers of biofilm accumulation, composition, and phylogeny. *Frontiers in Microbiology*, *8*(MAR), 491. https://www.frontiersin.org/articles/10.3389/fmicb.2017.00491/full

Kefeni, K. K., Msagati, T. A. M., & Mamba, B. B. (2017). Acid mine drainage: Prevention, treatment options, and resource recovery: A review. *Journal of Cleaner Production*, *151*, 475–493. https://doi.org/10.1016/J.JCLEPRO.2017.03.082

Korehi, H., Blöthe, M., Sitnikova, M. A., Dold, B., & Schippers, A. (2013). Metal mobilization by iron- and sulfur-oxidizing bacteria in a multiple extreme mine tailings in the Atacama Desert, Chile. *Environmental Science and Technology*, *47*(5), 2189–2196. https://doi.org/10.1021/ES304056N/SUPPL_FILE/ES304056N_SI_001.PDF

Liljeqvist, M., Rzhepishevska, O. I., & Dopson, M. (2013). Gene identification and substrate regulation provide insights into sulfur accumulation during bioleaching with the psychrotolerant acidophile Acidithiobacillus ferrivorans. *Applied and Environmental Microbiology*, *79*(3), 951–957. https://doi.org/10.1128/AEM.02989-12/SUPPL_FILE/ZAM999104074SO1.PDF

Liljeqvist, M., Valdes, J., Holmes, D. S., & Dopson, M. (2011). Draft Genome of the Psychrotolerant Acidophile Acidithiobacillus ferrivorans SS3. *Journal of Bacteriology*, *193*(16), 4304–4305. https://journals.asm.org/doi/full/10.1128/jb.05373-11

Lobos, J. H., Chisolm, T. E., Bopp, L. H., & Holmes, D. S. (1986). Acidiphilium organovorum sp. nov., an acidophilic heterotroph isolated from a Thiobacillus ferrooxidans culture. *International Journal of Systematic Bacteriology*, *36*(2), 139–144. https://doi.org/10.1099/00207713-36-2-139/CITE/REFWORKS

Luther, G. W. (1987). Pyrite oxidation and reduction: Molecular orbital theory considerations. *Geochimica et Cosmochimica Acta*, *51*(12), 3193–3199. https://doi.org/10.1016/0016-7037(87)90127-X

Marchand, E. A., & Silverstein, J. (2010). The Role of Enhanced Heterotrophic Bacterial Growth on Iron Oxidation by Acidithiobacillus ferrooxidans, *20*(3), 231–244. https://doi.org/10.1080/01490450303878

Matlock, M. M., Howerton, B. S., & Atwood, D. A. (2002). Chemical precipitation of heavy metals from acid mine drainage. *Water Research*, *36*(19), 4757–4764. https://doi.org/10.1016/S0043-1354(02)00149-5

Mogashane, T. M., Maree, J. P., Mujuru, M., Mphahlele-Makgwane, M. M., & Modibane, K. D. (2023). Ferric Hydroxide Recovery from Iron-Rich Acid Mine Water with Calcium Carbonate and a Gypsum Scale Inhibitor. *Minerals 2023, Vol. 13, Page 167*, *13*(2), 167. https://doi.org/10.3390/MIN13020167

National Academies of Sciences, E. and M., Division, H. and M., Studies, D. on E. and L., Policy, B. on H. S., Toxicology, B. on E. S. and, Resources, B. on E. S. and, &

Mines, C. on the S. of the C. of R. C. M. D. E. in U. (2018). Coal Mining in the United States. *Monitoring and Sampling Approaches to Assess Underground Coal Mine Dust Exposures*. https://doi.org/10.17226/25111

Nemati, M., & Harrison, S. T. L. (2000). Comparative study on thermophilic and mesophilic biooxidation of ferrous iron. *Minerals Engineering*, *13*(1), 19–24. https://doi.org/10.1016/S0892-6875(99)00146-6

Norris, P. R., Burton, N. P., & Foulis, N. A. M. (2000). Acidophiles in bioreactor mineral processing. *Extremophiles*, *4*(2), 71–76. https://doi.org/10.1007/S007920050139/METRICS

Ojumu, T. V., Hansford, G. S., & Petersen, J. (2009). The kinetics of ferrous-iron oxidation by Leptospirillum ferriphilum in continuous culture: the effect of temperature. *Biochem Eng J*, *46*(2), 161–168. https://doi.org/10.1016/j.bej.2009.05.001

Ojumu, T. V., & Petersen, J. (2011). The kinetics of ferrous ion oxidation by Leptospirillum ferriphilum in continuous culture: The effect of pH. *Hydrometallurgy*, *106*(1–2), 5–11. https://doi.org/10.1016/J.HYDROMET.2010.11.007

Ortiz-Castillo, J. E., Mirazimi, M., Mohammadi, M., Dy, E., & Liu, W. (2021). The Role of Microorganisms in the Formation, Dissolution, and Transformation of Secondary Minerals in Mine Rock and Drainage: A Review. *Minerals 2021, Vol. 11, Page 1349*, *11*(12), 1349. https://doi.org/10.3390/MIN11121349

Özkaya, B., Nurmi, P., Sahinkaya, E., Kaksonen, A. H., & Puhakka, J. A. (2007). Temperature Effects on the Iron Oxidation Kinetics of a Leptospirillum ferriphilum

Dominated Culture at pH Below One. *Advanced Materials Research*, *20–21*, 465–468. https://doi.org/10.4028/WWW.SCIENTIFIC.NET/AMR.20-21.465

Peppas, A., Komnitsas, K., & Halikia, I. (2000). Use of organic covers for acid mine drainage control. *Minerals Engineering*, *13*(5), 563–574. https://doi.org/10.1016/S0892-6875(00)00036-4

Plumb, J. J., Muddle, R., & Franzmann, P. D. (2008). Effect of pH on rates of iron and sulfur oxidation by bioleaching organisms. *Minerals Engineering*, *21*(1), 76–82. https://doi.org/10.1016/J.MINENG.2007.08.018

Ryan, M. J., Kney, A. D., & Carley, T. L. (2017). A study of selective precipitation techniques used to recover refined iron oxide pigments for the production of paint from a synthetic acid mine drainage solution. *Applied Geochemistry*, *79*, 27–35. https://doi.org/10.1016/J.APGEOCHEM.2017.01.019

Sahoo, P. K., Kim, K., Equeenuddin, S. M., & Powell, M. A. (2013). Current approaches for mitigating acid mine drainage. *Reviews of Environmental Contamination and Toxicology*, *226*, 1–32. https://doi.org/10.1007/978-1-4614-6898-1_1/FIGURES/00017

Sand, W. (1989). Ferric iron reduction by Thiobacillus ferrooxidans at extremely low pH-values. *Biogeochemistry*, *7*(3), 195–201. https://doi.org/10.1007/BF00004217/METRICS

Schippers, A., Breuker, A., Blazejak, A., Bosecker, K., Kock, D., & Wright, T. L. (2010). The biogeochemistry and microbiology of sulfidic mine waste and bioleaching dumps and heaps, and novel Fe(II)-oxidizing bacteria. *Hydrometallurgy*, *104*(3–4), 342–350. https://doi.org/10.1016/J.HYDROMET.2010.01.012

Schnoor, J.L. 1996. Environmental Modeling. John... - Google Scholar. (n.d.). Retrieved June 28, 2023, from https://scholar.google.com/scholar?hl=en&as_sdt=0%2C36&q=Schnoor%2C+J.L.+1996.+Environmental+Modeling.+John+Wiley+%26+Sons%2C+New+York%2C+NY.+ISBN%3A+978-0471124368&btnG=

Seeger, M., & Jerez, C. A. (1993). Response of Thiobacillus ferrooxidans to phosphate limitation. *FEMS Microbiology Reviews*, *11*(1–3), 37–41. https://doi.org/10.1111/J.1574-6976.1993.TB00264.X

Sharma, S., Lee, M., Reinmann, C. S., Pumneo, J., Cutright, T. J., & Senko, J. M. (2020). Impact of acid mine drainage chemistry and microbiology on the development of efficient Fe removal activities. *Chemosphere*, *249*. https://doi.org/10.1016/J.CHEMOSPHERE.2020.126117

Sheng, Y., Bibby, K., Grettenberger, C., Kaley, B., Macalady, J. L., Wang, G., & Burgos, W. D. (2016). Geochemical and temporal influences on the enrichment of acidophilic iron-oxidizing bacterial communities. *Applied and Environmental Microbiology*, *82*(12), 3611–3621. https://doi.org/10.1128/AEM.00917-16/SUPPL_FILE/ZAM012167200SO1.PDF

Sheng, Y., Kaley, B., Bibby, K., Grettenberger, C., Macalady, J. L., Wang, G., & Burgos, W. D. (2017). Bioreactors for low-pH iron(ii) oxidation remove considerable amounts of total iron. *RSC Advances*, *7*(57), 35962–35972. https://doi.org/10.1039/C7RA03717A

Sheoran, V., Sheoran, A., & Poonia, P. (2010). Soil Reclamation of Abandoned Mine Land by Revegetation: A Review. *International Journal of Soil, Sediment and Water*, *3*(2). https://scholarworks.umass.edu/intljssw/vol3/iss2/13

Silva, R. de A., Secco, M. P., Lermen, R. T., Schneider, I. A. H., Hidalgo, G. E. N., & Sampaio, C. H. (2019). Optimizing the selective precipitation of iron to produce yellow pigment from acid mine drainage. *Minerals Engineering*, *135*, 111–117. https://doi.org/10.1016/J.MINENG.2019.02.040

Simate, G. S., & Ndlovu, S. (2014). Acid mine drainage: Challenges and opportunities. *Journal of Environmental Chemical Engineering*, *2*(3), 1785–1803. https://doi.org/10.1016/J.JECE.2014.07.021

Skousen, J. G., Ziemkiewicz, P. F., & McDonald, L. M. (2019). Acid mine drainage formation, control and treatment: Approaches and strategies. *The Extractive Industries and Society*, *6*(1), 241–249. https://doi.org/10.1016/J.EXIS.2018.09.008

Skousen, J., Zipper, C. E., Rose, A., Ziemkiewicz, P. F., Nairn, R., McDonald, L. M., & Kleinmann, R. L. (2017). Review of Passive Systems for Acid Mine Drainage Treatment. *Mine Water and the Environment*, *36*(1), 133–153. https://doi.org/10.1007/S10230-016-0417-1/FIGURES/11

Stumm, W., & Morgan, J. J. (1995). Aquatic Chemistry: Chemical Equilibria and Rates in Natural Waters. John Wiley & Sons. ISBN 0-471-51184-6.

Tabak, H. H., Scharp, R., Burckle, J., Kawahara, F. K., & Govind, R. (2003). Advances in biotreatment of acid mine drainage and biorecovery of metals: 1. Metal precipitation for recovery and recycle. *Biodegradation*, *14*(6), 423–436. https://doi.org/10.1023/A:1027332902740/METRICS

Tuovinen, O. H., Niemela, S. I., & Gyllenberg, H. G. (1971). Effect of mineral nutrients and organic substances on the development of Thiobacillus ferrooxidans. *Biotechnology and Bioengineering*, *13*(4), 517–527. https://doi.org/10.1002/BIT.260130406

Underground Coal Mining. (n.d.). Retrieved March 10, 2023, from https://www.dep.pa.gov/Business/Land/Mining/Pages/Underground-Coal-Mining.aspx

Vengosh, A. (2005). *Salinization and Saline Environments. In: Environmental Geochemistry, Editor: B.S. Lollar, Vol. 9 Treatise on Geochemistry, Executive Editors: H.D. Holland and K.K. Turekian*. 648. https://books.google.com/books/about/Environmental_Geochemistry.html?id=_NdjXZ4IU0EC

Vera, M., Guiliani, N., & Jerez, C. A. (2003). Proteomic and genomic analysis of the phosphate starvation response of Acidithiobacillus ferrooxidans. *Hydrometallurgy*, *71*(1–2), 125–132. https://doi.org/10.1016/S0304-386X(03)00148-8

Vera, M., Pagliai, F., Guiliani, N., & Jerez, C. A. (2008). The chemolithoautotroph Acidithiobacillus ferrooxidans can survive under phosphate-limiting conditions by expressing a C-P lyase operon that allows it to grow on phosphonates. *Applied and Environmental Microbiology*, *74*(6), 1829–1835. https://doi.org/10.1128/AEM.02101-07/ASSET/6184B096-0162-463A-B23F-24E765900446/ASSETS/GRAPHIC/ZAM0060886800004.JPEG

Vera, M., Schippers, A., & Sand, W. (2013). Progress in bioleaching: fundamentals and mechanisms of bacterial metal sulfide oxidation—part A. *Applied Microbiology and*

Biotechnology 2013 97:17, *97*(17), 7529–7541. https://doi.org/10.1007/S00253-013-4954-2

Wang, W., Zhenghe, X. U., & Finch, J. (1996). Fundamental study of an ambient temperature ferrite process in the treatment of acid mine drainage. *Environmental Science and Technology*, *30*(8), 2604–2608. https://pubs.acs.org/doi/abs/10.1021/es960006h

Water Quality Standards Program | Ohio Environmental Protection Agency. (n.d.). Retrieved May 28, 2023, from https://epa.ohio.gov/divisions-and-offices/surface-water/reports-data/water-quality-standards-program

Appendix

Ferrous Iron Oxidation at Other Iron Feeding Cycles

pH Test

WR AMD

Figure: Ferrous iron oxidation with WR AMD at pH 2.5, no nutrient addition (1st iron addition).

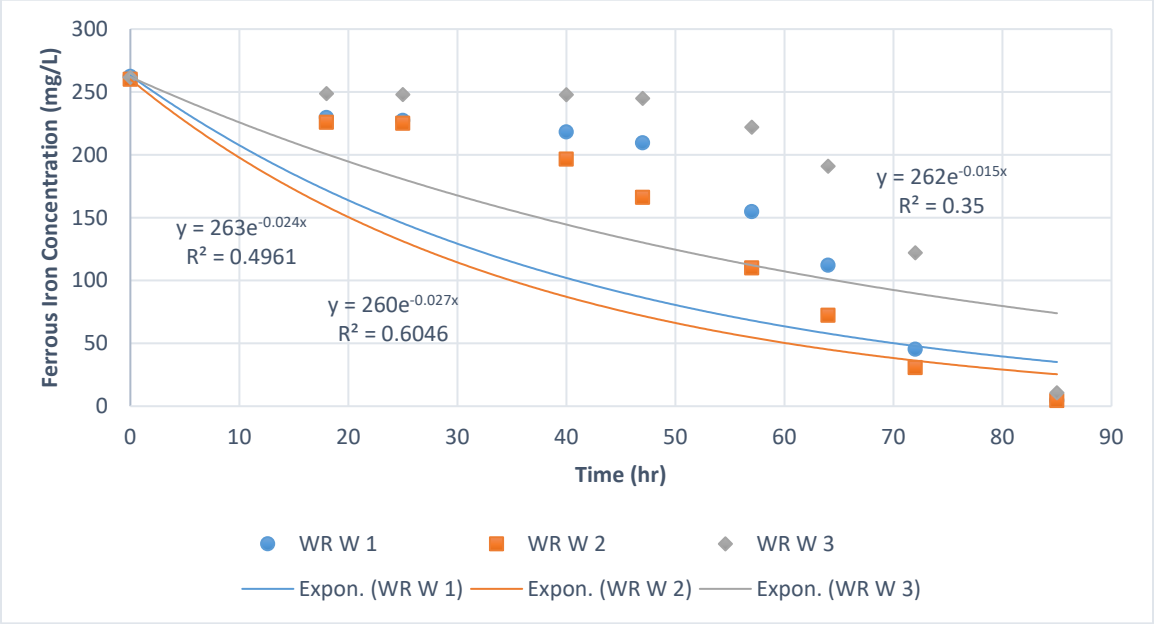

Ferrous iron oxidation with WR AMD and bacterial inoculum extracted from WR sediment at pH 3.0, no nutrient addition (1st addition)

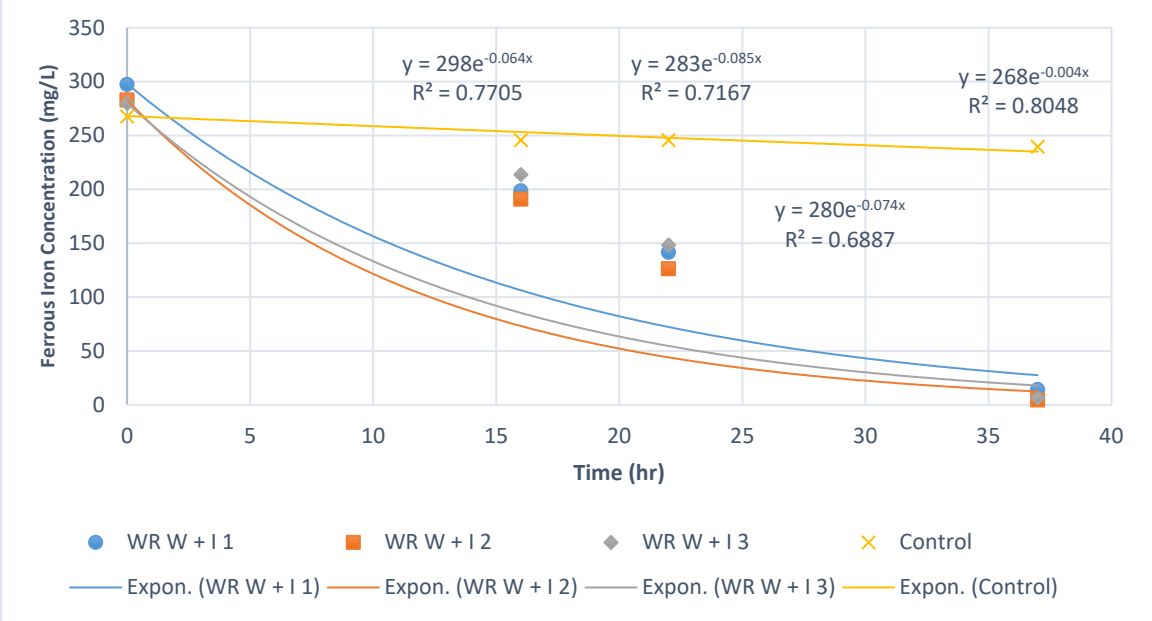

Ferrous iron oxidation with WR AMD and bacterial inoculum extracted from WR sediment at pH 3.0, no nutrient addition (3rd addition)

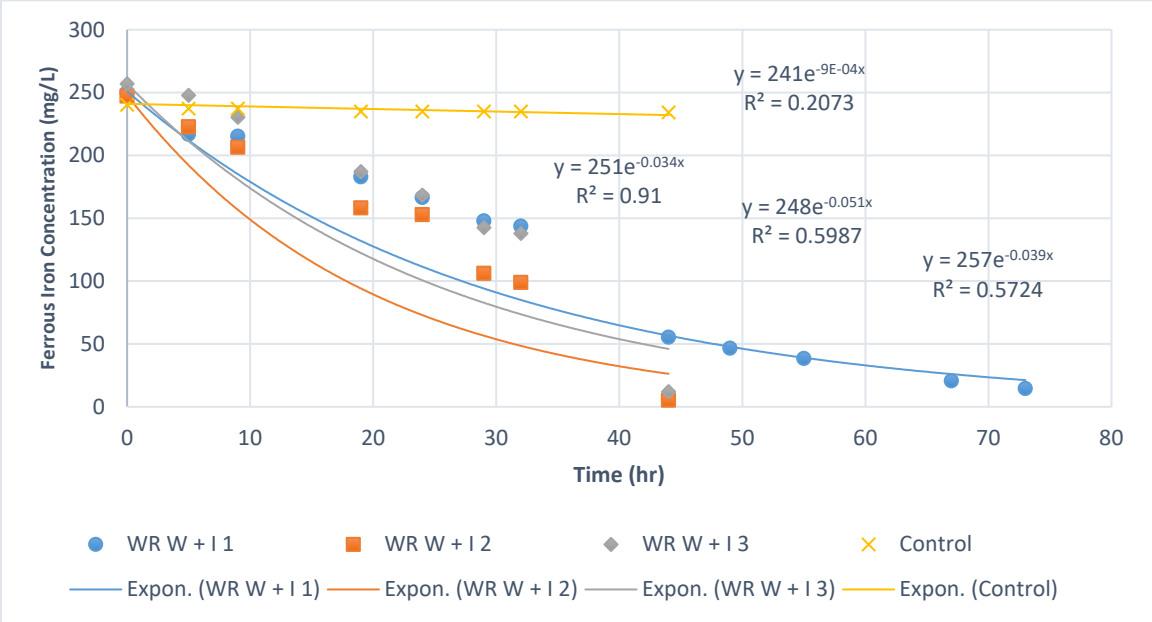

FR AMD

Figure: Ferrous iron oxidation with FR AMD and bacterial inoculum extracted from FR sediment at pH 2.5, no nutrient addition (1st iron addition)

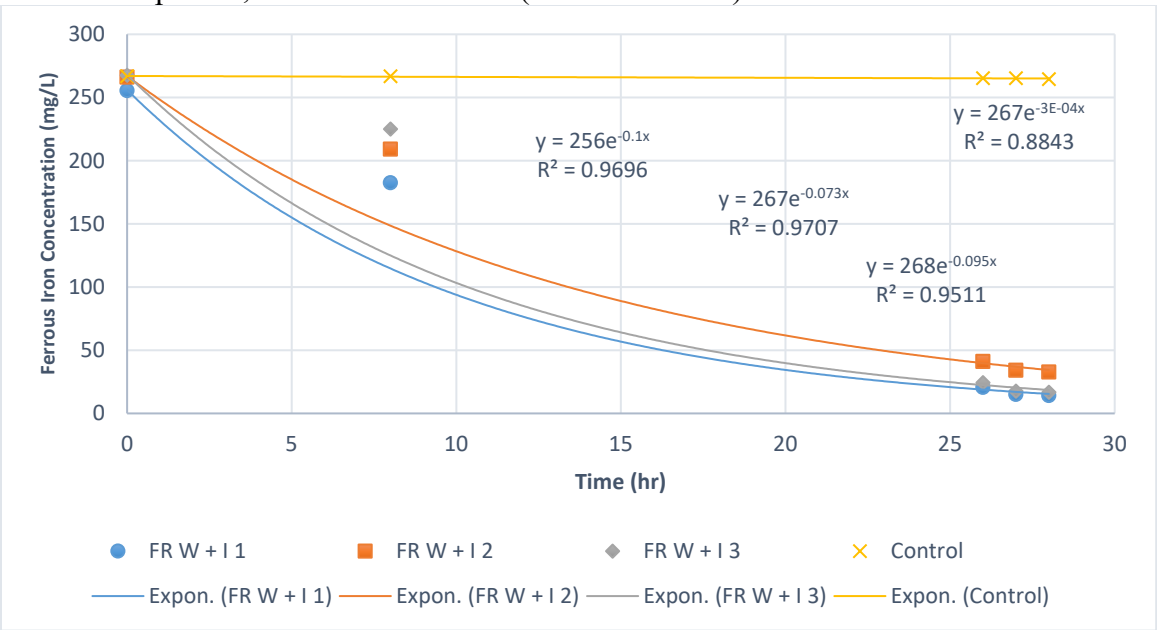

Figure: Ferrous iron oxidation with FR AMD and bacterial inoculum extracted from FR sediment at pH 2.5, no nutrient addition (3rd iron addition)

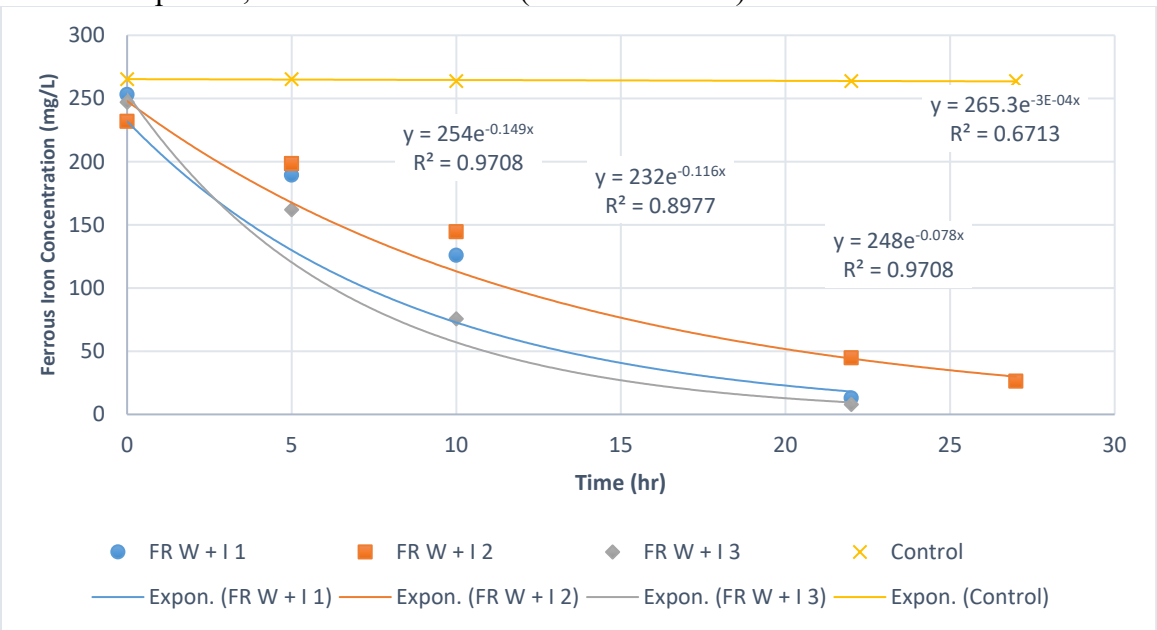

PA AMD

Figure: Ferrous iron oxidation with PA AMD and bacterial inoculum extracted from PA sediment at pH 2.0, no nutrient addition (2nd addition).

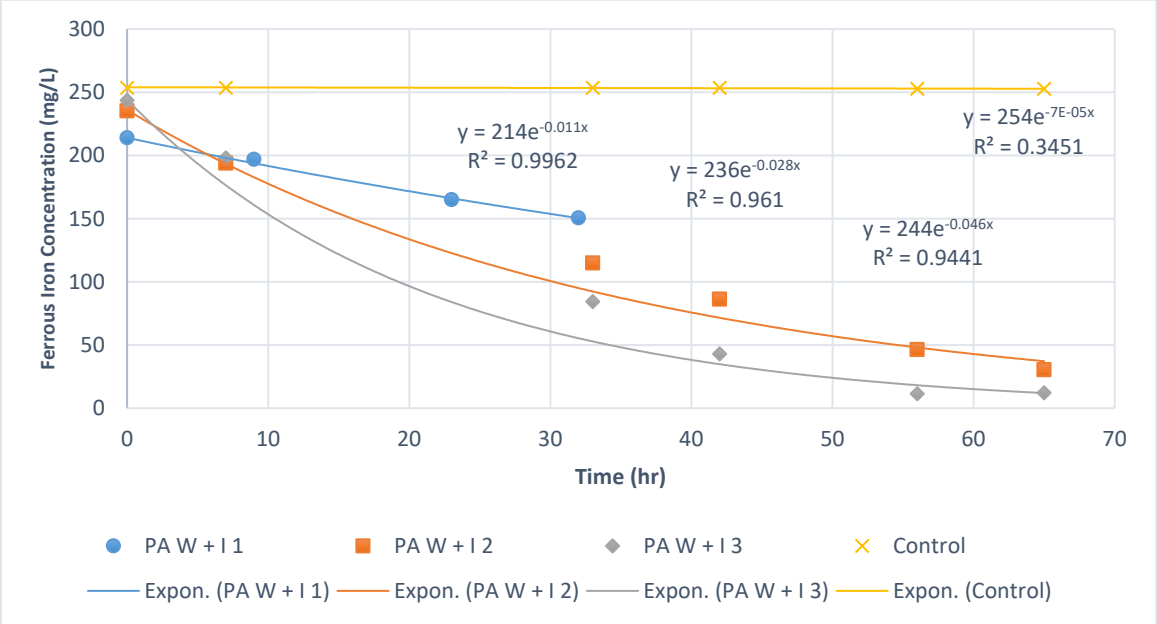

Figure: Ferrous iron oxidation with PA AMD and bacterial inoculum extracted from PA sediment at pH 2.0, no nutrient addition (3rd addition).

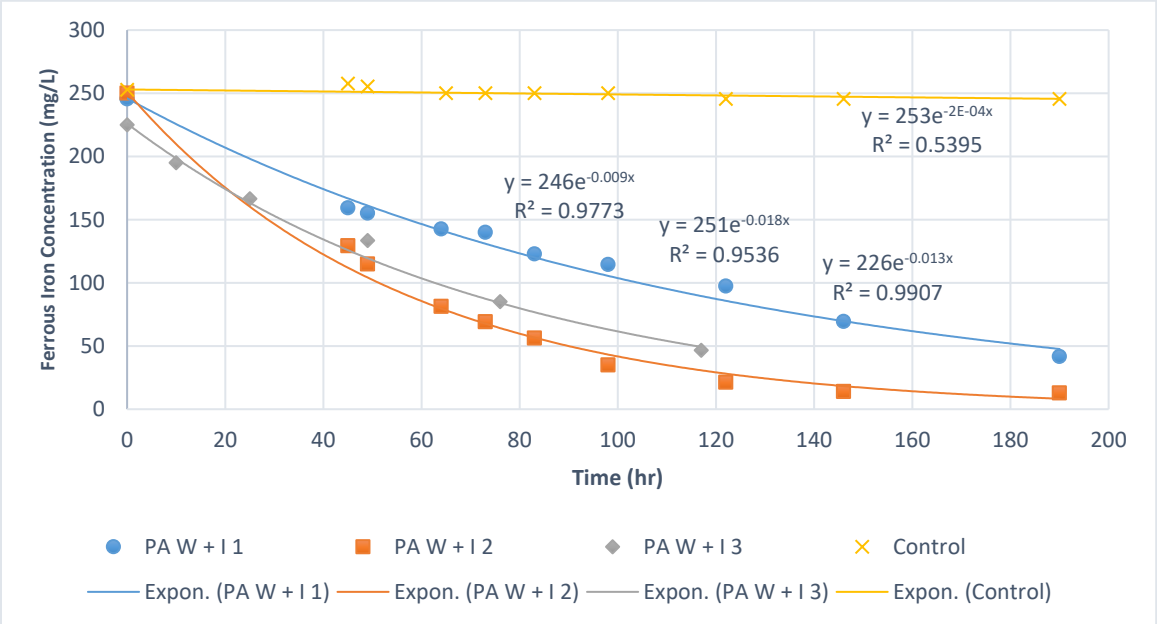

Figure: Ferrous iron oxidation with PA AMD and bacterial inoculum extracted from PA sediment at pH 4.0, no nutrient addition (1st addition).

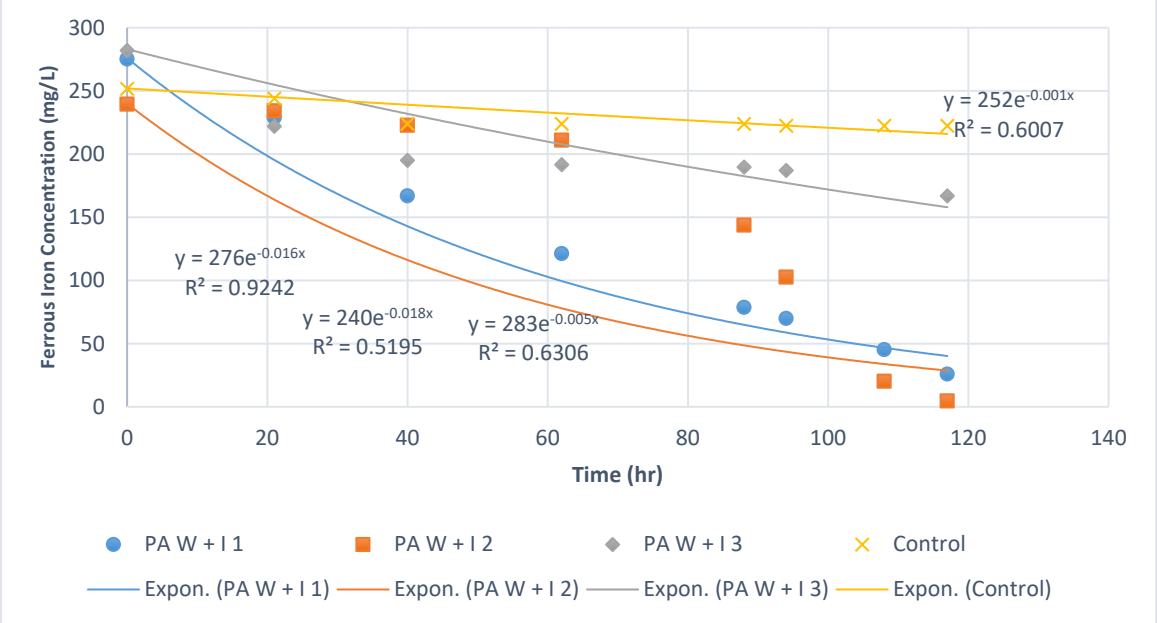

Nitrogen Test

Figure: Ferrous iron oxidation rates with WR inoculum in modified 9K media, 0.01 M N, 2.87 mM P, no C (1st iron addition)

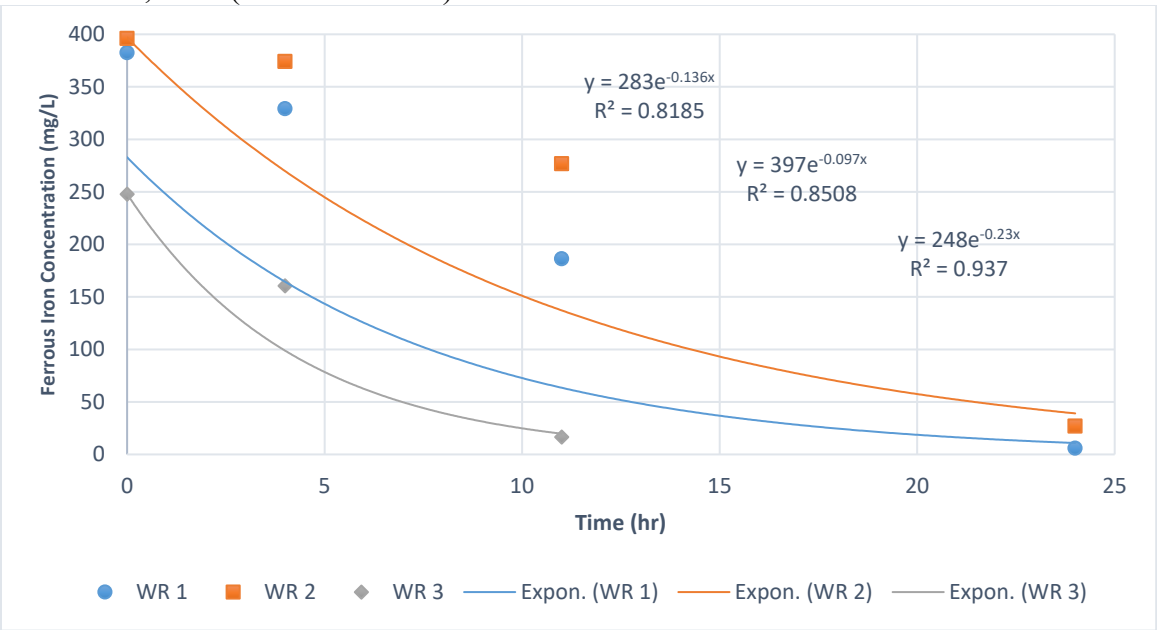

Figure: Ferrous iron oxidation rates with WR inoculum in modified 9K media, 0.01 M N, 2.87 mM P, no C (2nd iron addition)

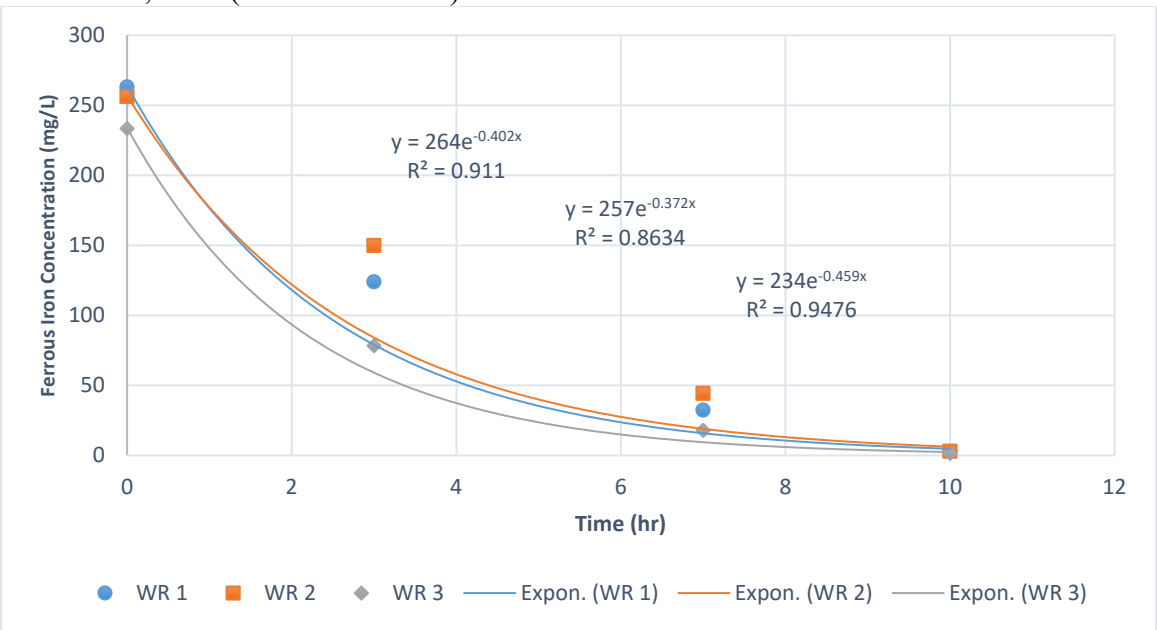

Figure: Ferrous iron oxidation rates with WR inoculum in modified 9K media, 0.05 M N, 2.87 mM P, no C (1st iron addition)

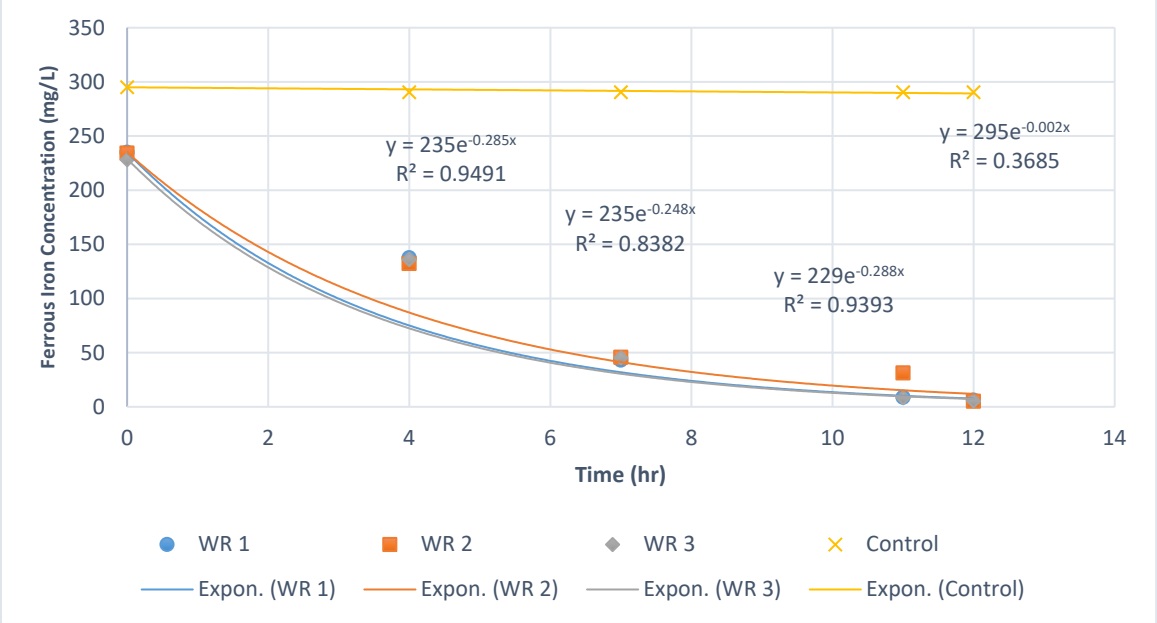

Figure: Ferrous iron oxidation rates with WR inoculum in modified 9K media, 0.05 M N, 2.87 mM P, no C (3rd iron addition)

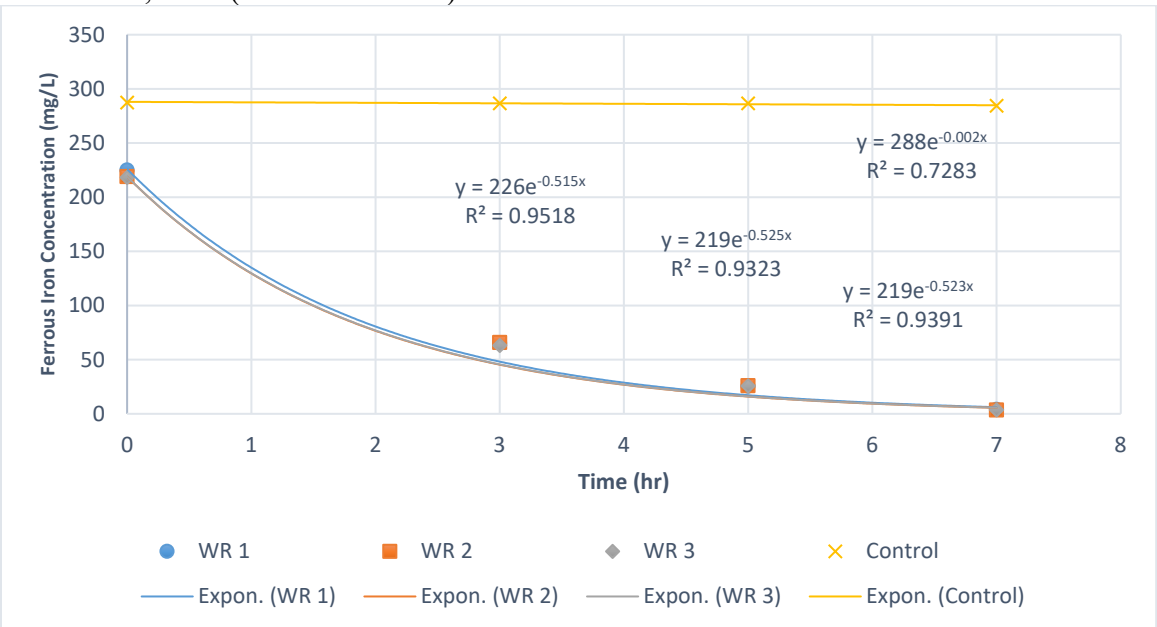

Figure: Ferrous iron oxidation rates with WR inoculum in modified 9K media, 0.1 M N, 2.87 mM P, no C (1st iron addition)

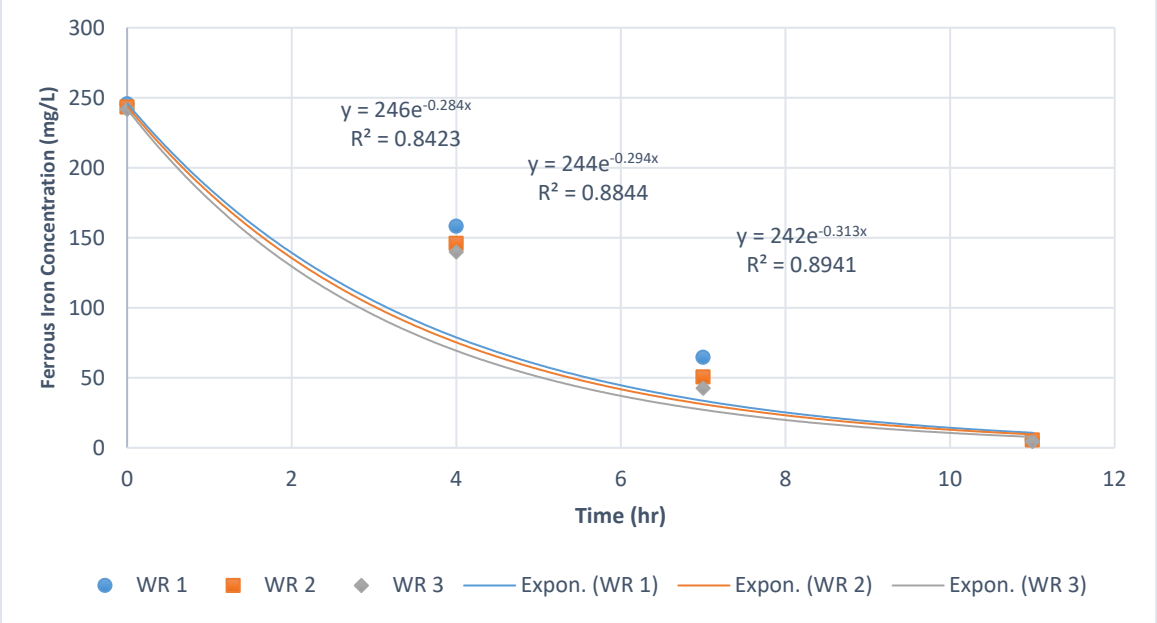

Figure: Ferrous iron oxidation rates with WR inoculum in modified 9K media, 0.1 M N, 2.87 mM P, no C (2nd iron addition)

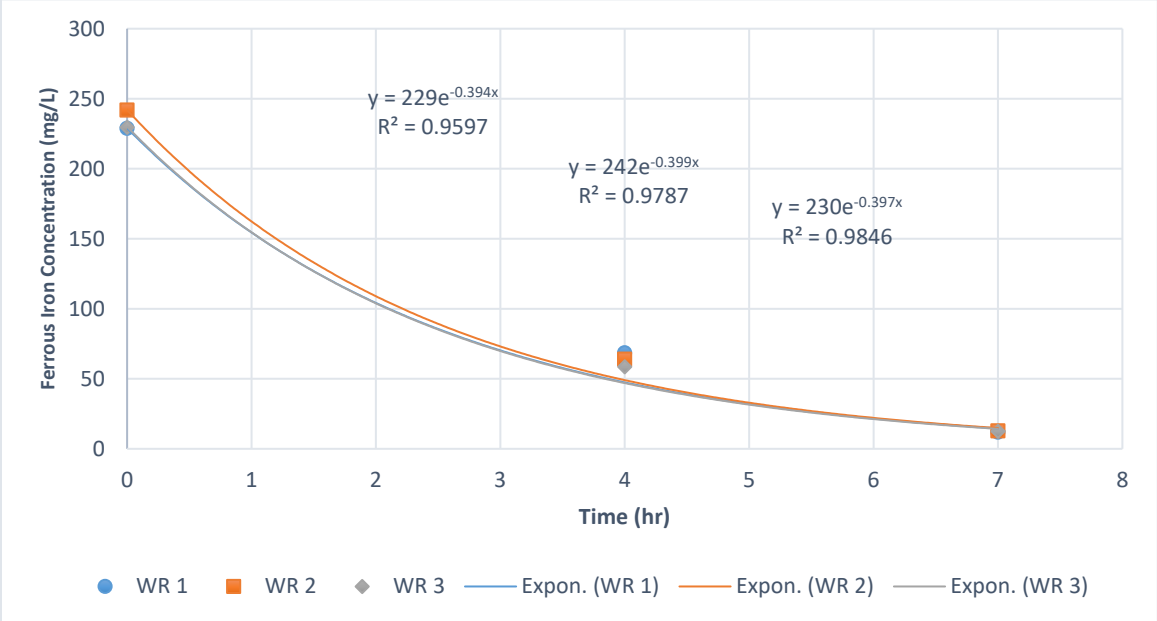

Figure: Ferrous iron oxidation rates with WR inoculum in modified 9K media, 0.5 M N, 2.87 mM P, no C (1st iron addition)

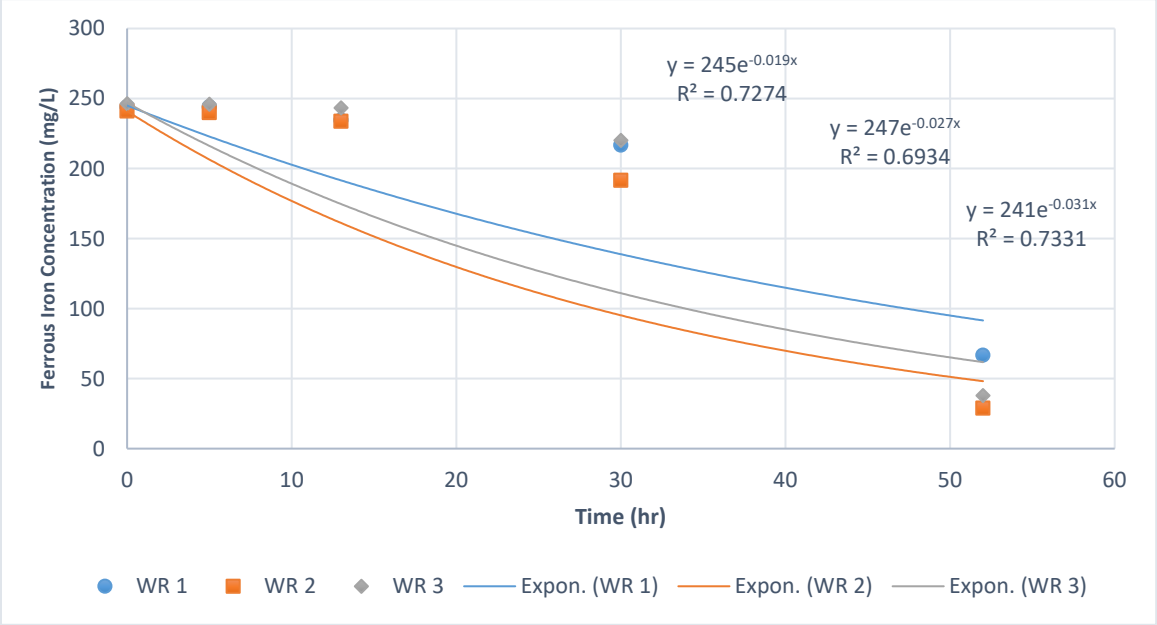

Figure: Ferrous iron oxidation rates with FR inoculum in modified 9K media, 0.01 M N, 2.87 mM P, no C (2nd iron addition)

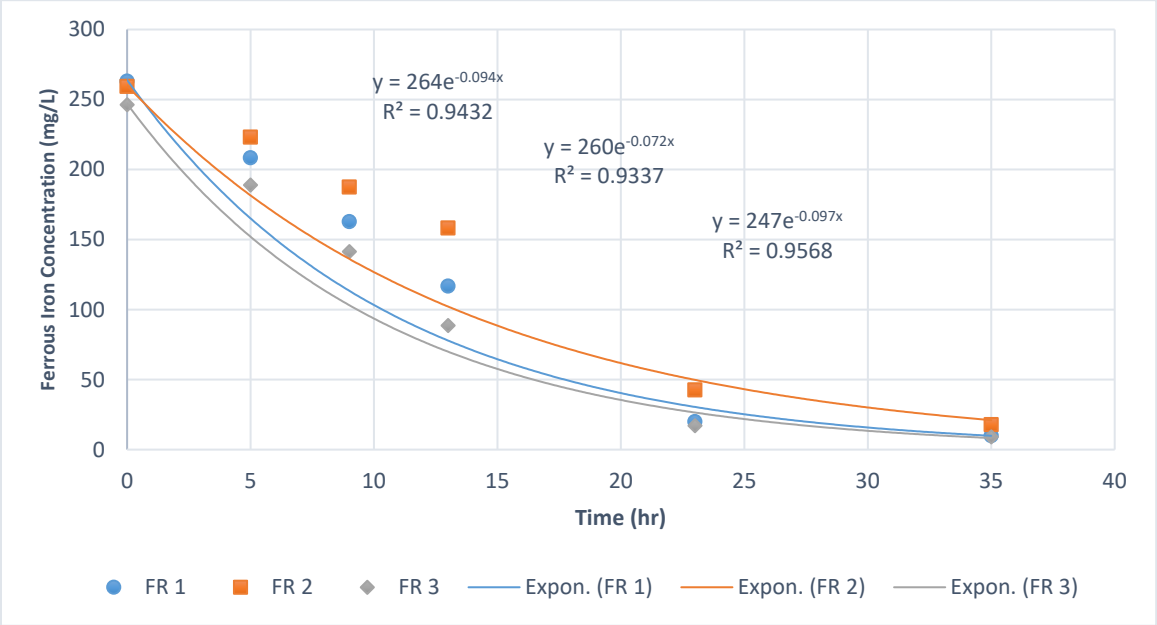

Figure: Ferrous iron oxidation rates with FR inoculum in modified 9K media, 0.05 M N, 2.87 mM P, no C (2nd iron addition)

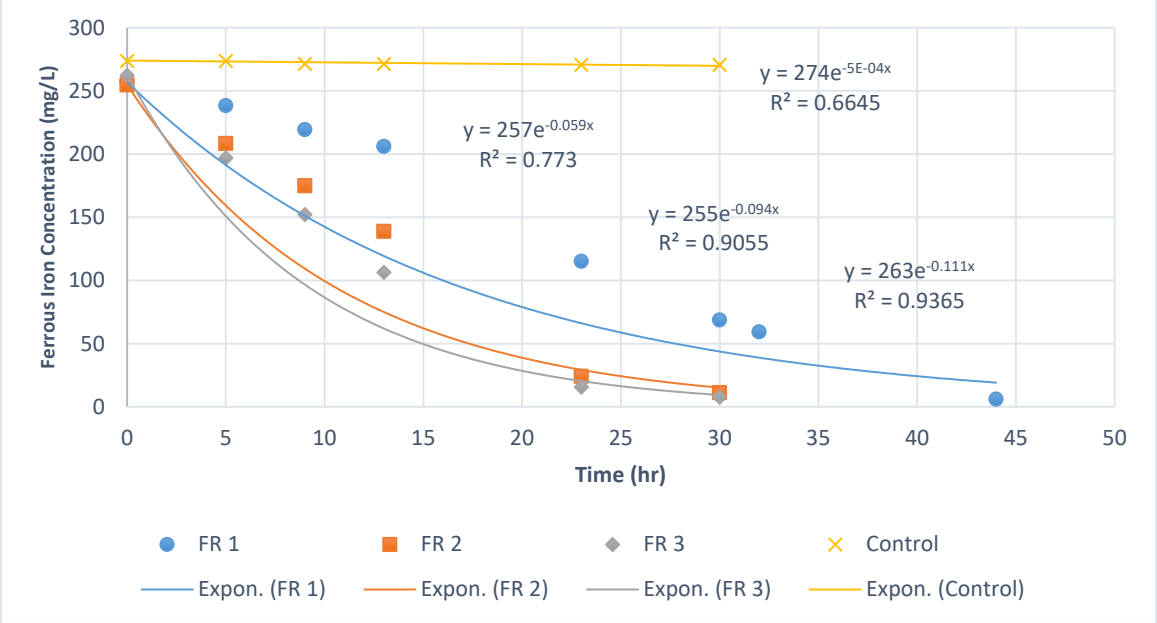

Figure: Ferrous iron oxidation rates with FR inoculum in modified 9K media, 0.1 M N, 2.87 mM P, no C (2nd iron addition)

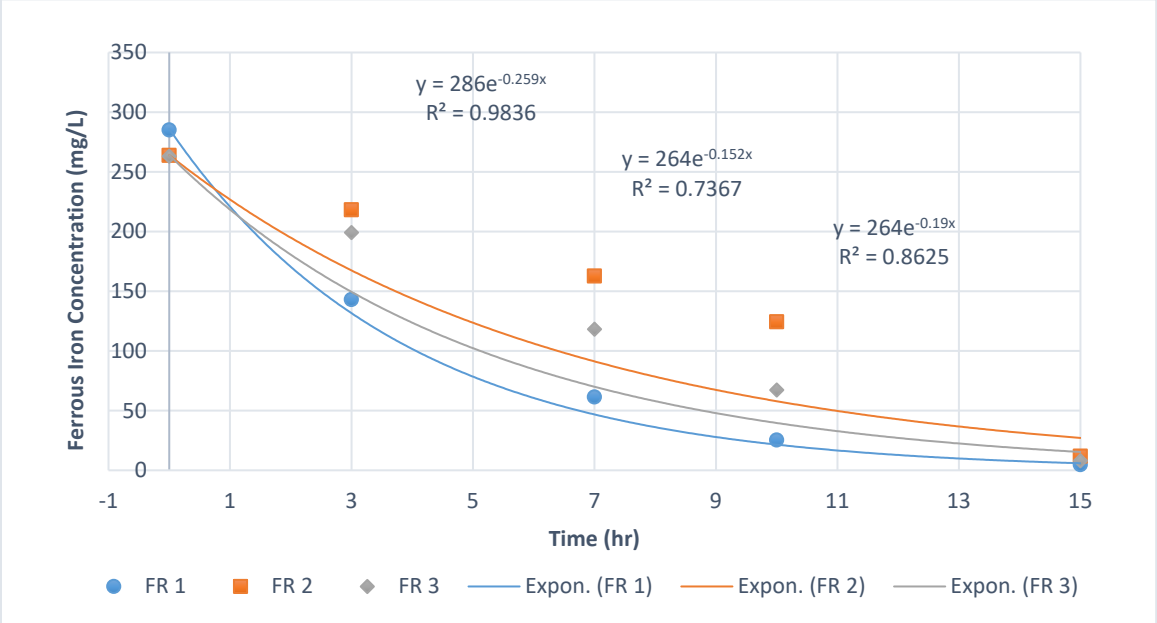

Phosphorus

Figure: Ferrous iron oxidation rates with WR inoculum in modified 9K media, 0.1 M N, 0.1 mM P, no C (1st iron addition)

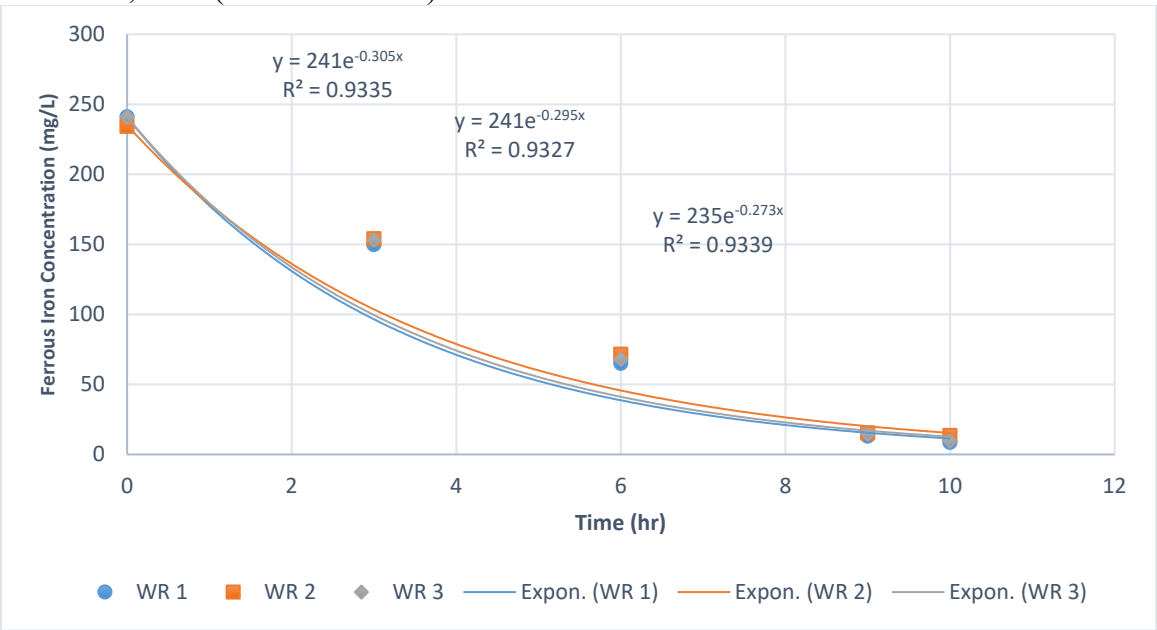

Figure: Ferrous iron oxidation rates with WR inoculum in modified 9K media, 0.1 M N, 0.5 mM P, no C (1st iron addition)

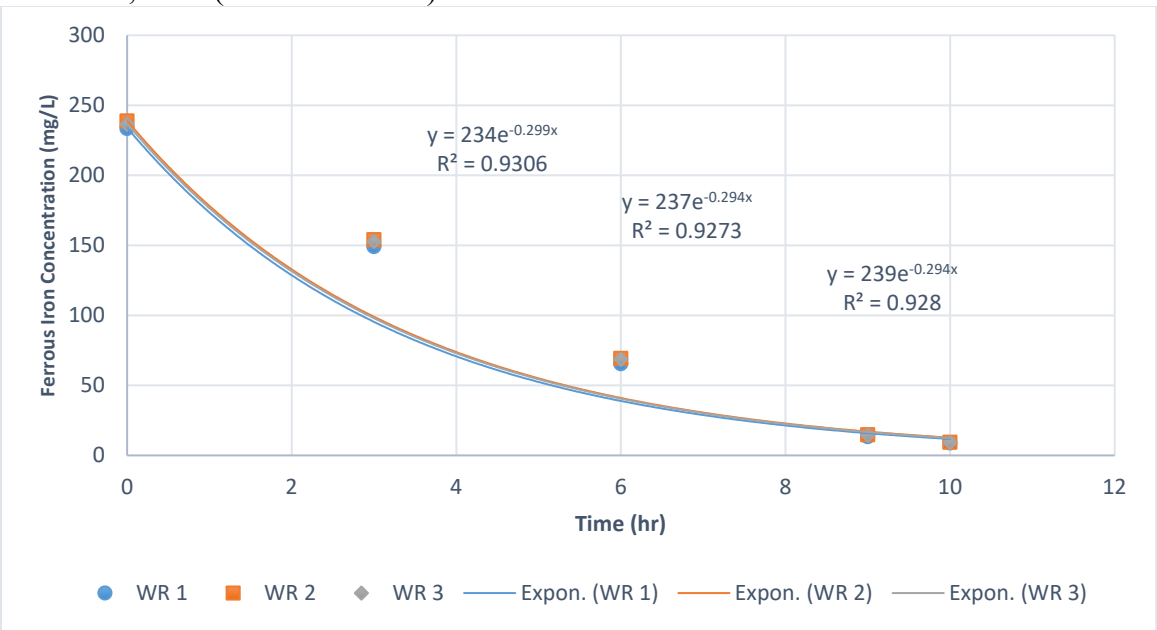

Figure: Ferrous iron oxidation rates with WR inoculum in modified 9K media, 0.1 M N, 1.0 mM P, no C (1st iron addition)

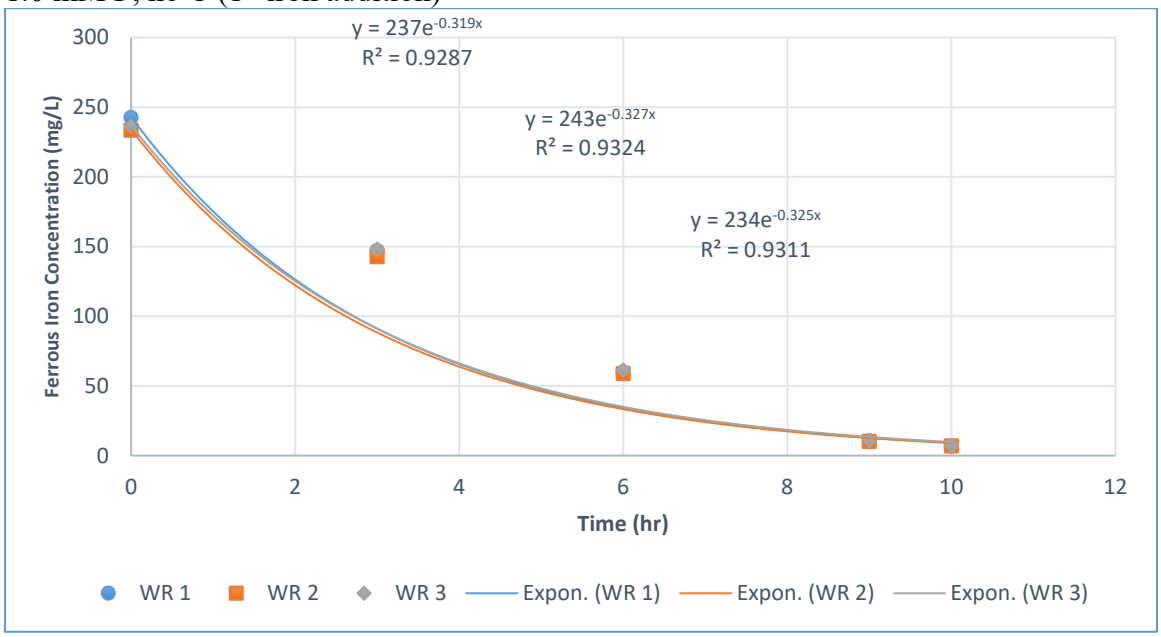

Figure: Ferrous iron oxidation rates with WR inoculum in modified 9K media, 0.1 M N, 5.0 mM P, no C (1st iron addition)

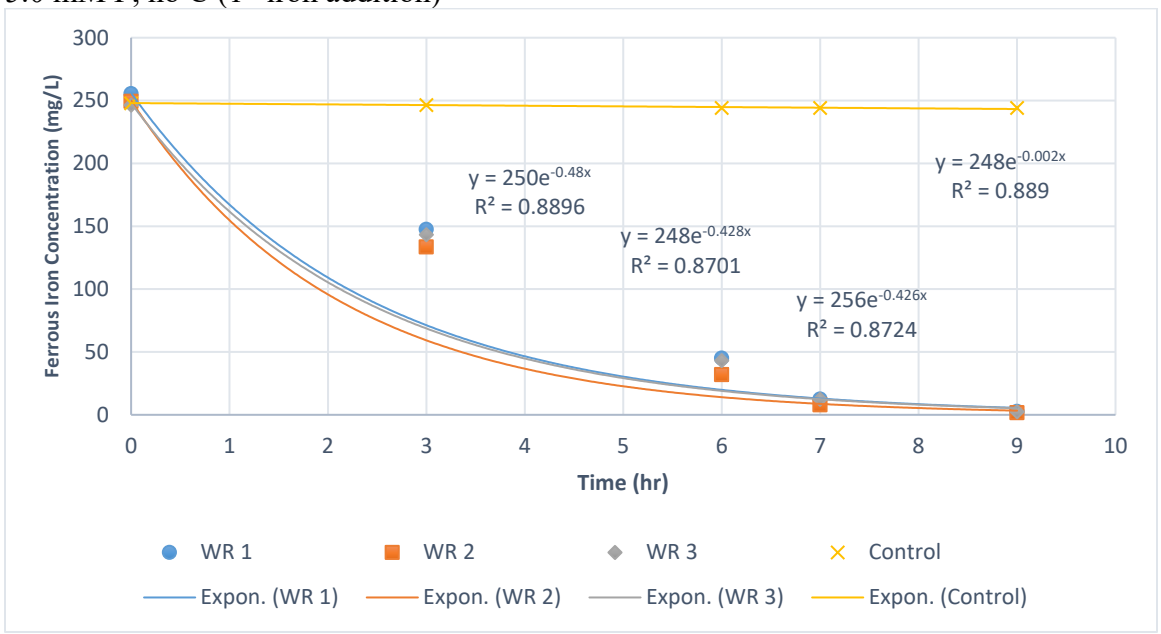

Figure: Ferrous iron oxidation rates with WR inoculum in modified 9K media, 0.1 M N, 10.0 mM P, no C (1st iron addition)

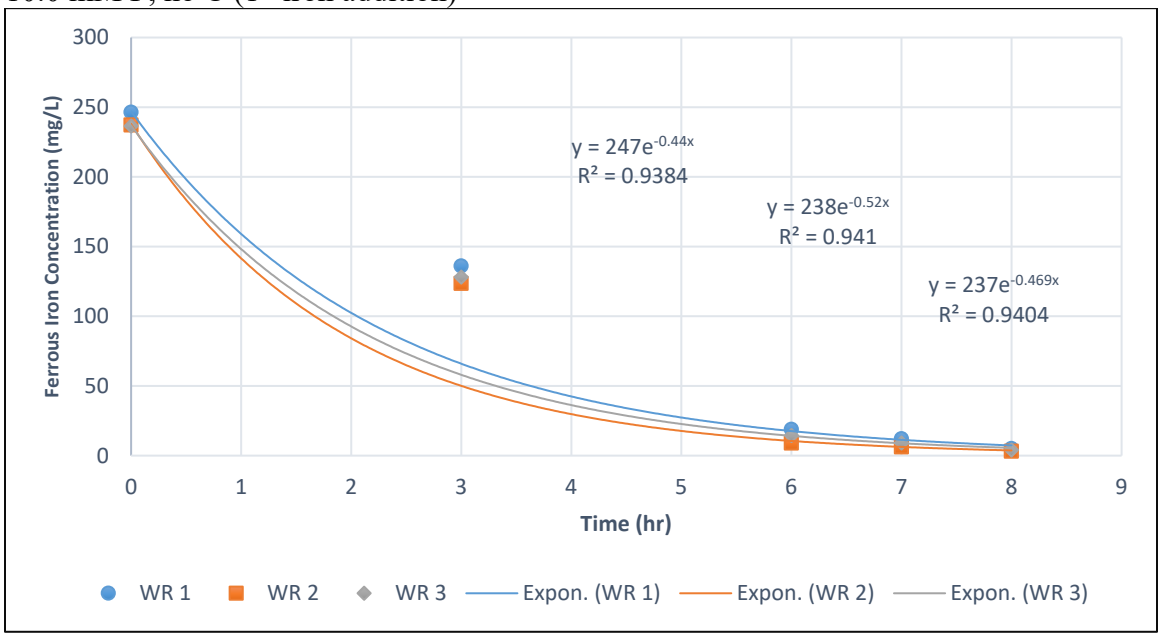

Carbon Test

Figure: Ferrous iron oxidation rates with WR inoculum in modified 9K media, 0.1 M N, 5.0 mM P, 0.05 M Glucose, first enrichment (1st iron addition)

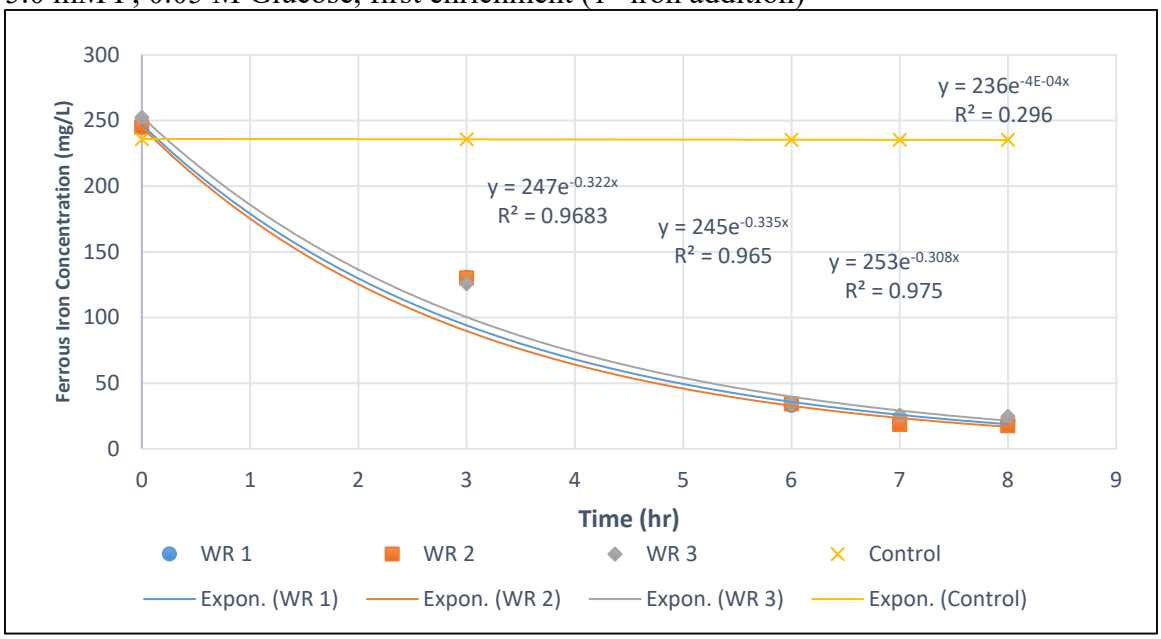

Figure: Ferrous iron oxidation rates with WR inoculum in modified 9K media, 0.1 M N, 5.0 mM P, 0.1 M Glucose, first enrichment (1st iron addition)

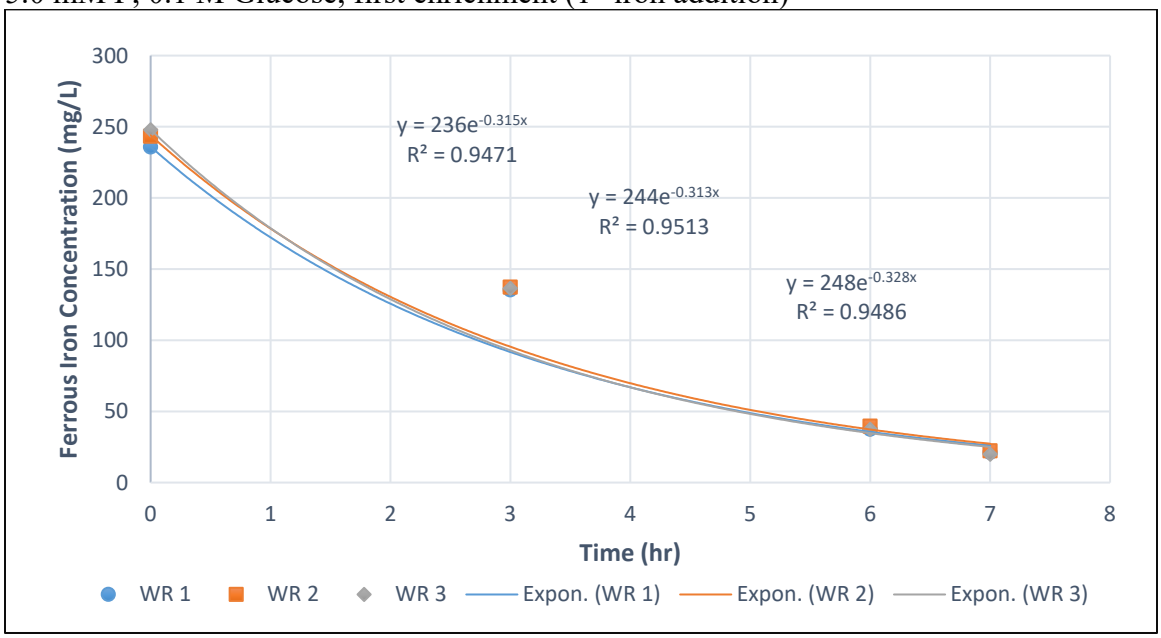

Figure: Ferrous iron oxidation rates with WR inoculum in modified 9K media, 0.1 M N, 5.0 mM P, 0.2 M Glucose, first enrichment (1st iron addition)

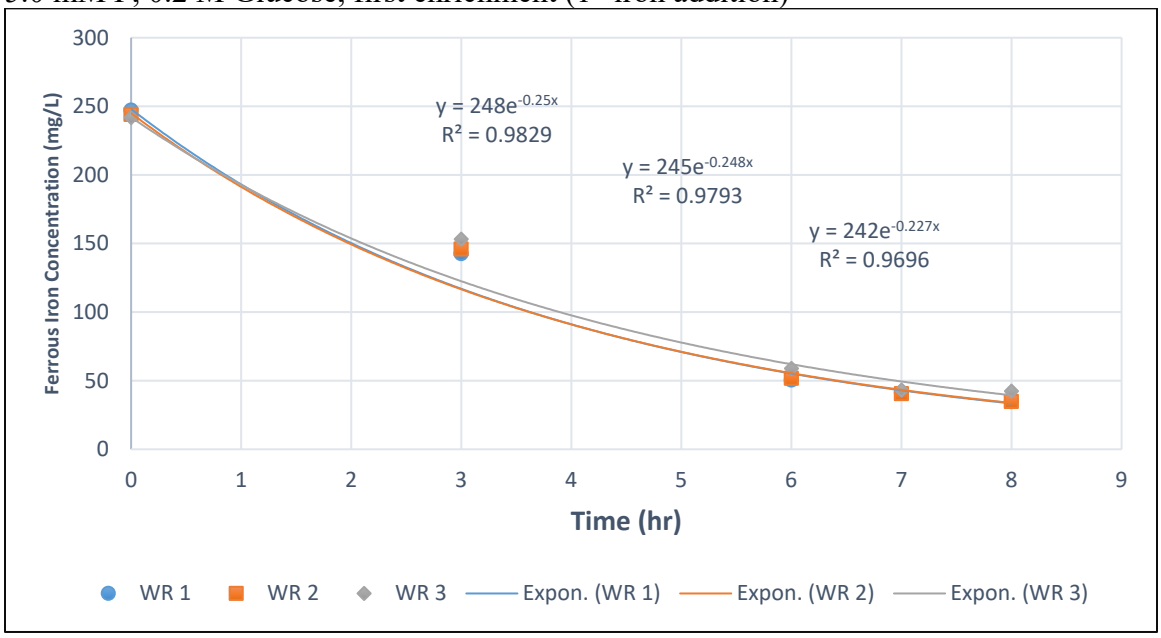

WR Culture

Figure: ferrous iron oxidation rates with WR AMD only at pH 2.5, no nutrient addition (2nd iron addition)

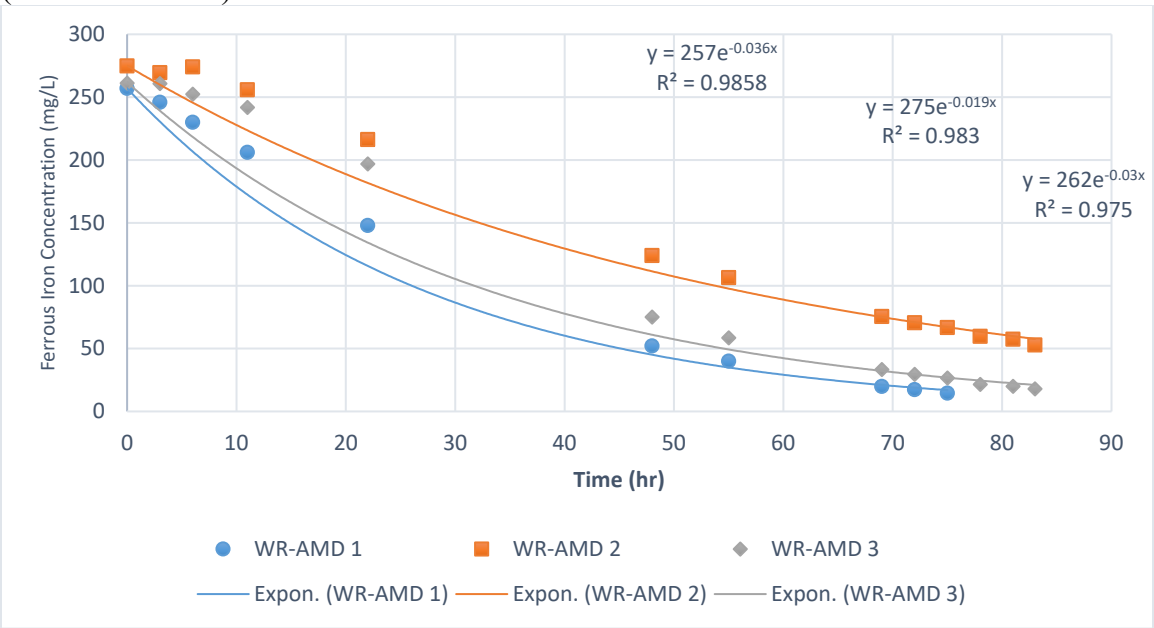

Figure: Ferrous iron oxidation with WR AMD and bacterial inoculum extracted from WR sediment at pH 2.5, no nutrient addition (1st iron addition)

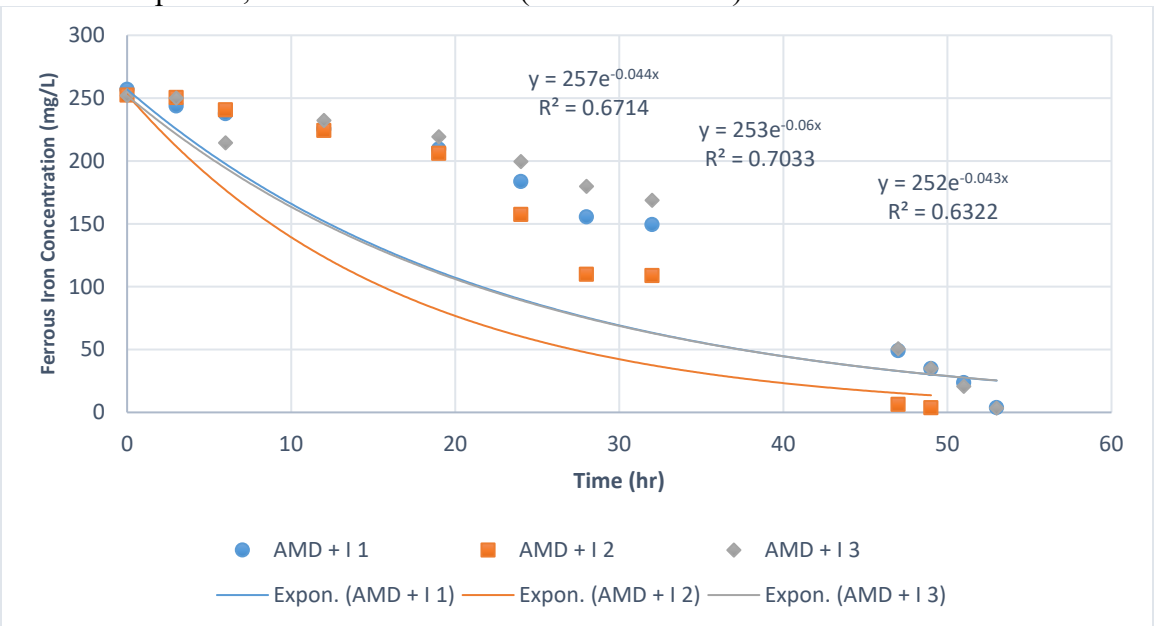

Figure: Ferrous iron oxidation with WR AMD and bacterial inoculum extracted from WR sediment at pH 2.5, no nutrient addition (2nd iron addition)

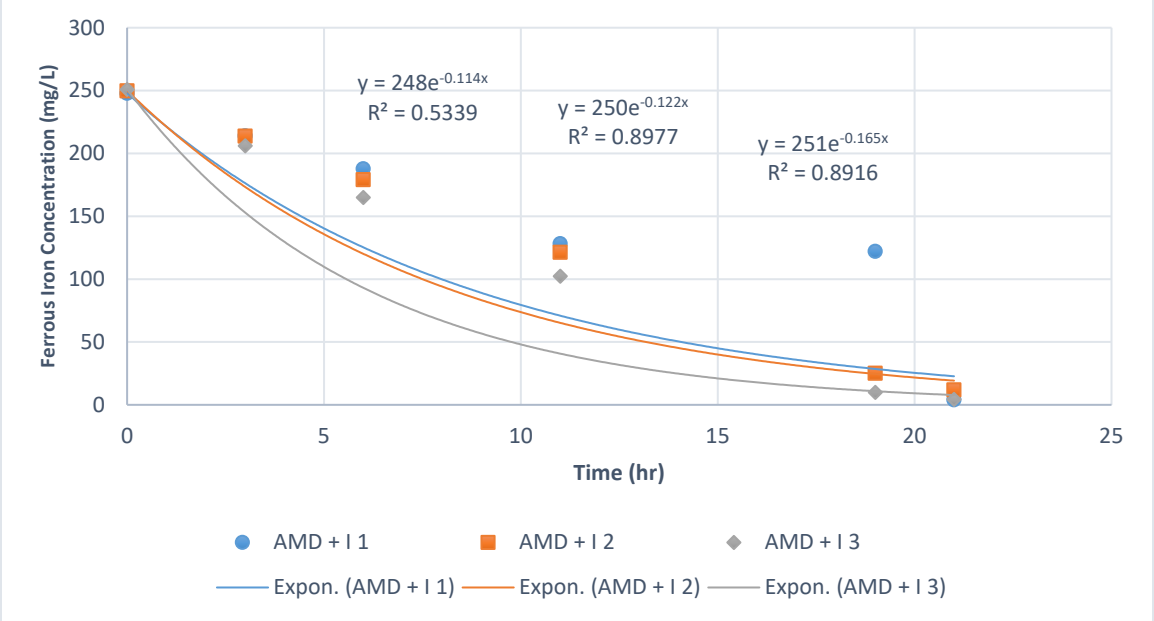

Figure: Ferrous iron oxidation with WR AMD and bacterial inoculum extracted from WR sediment at pH 2.5, 0.1 M N, no P, no C (1st iron addition)

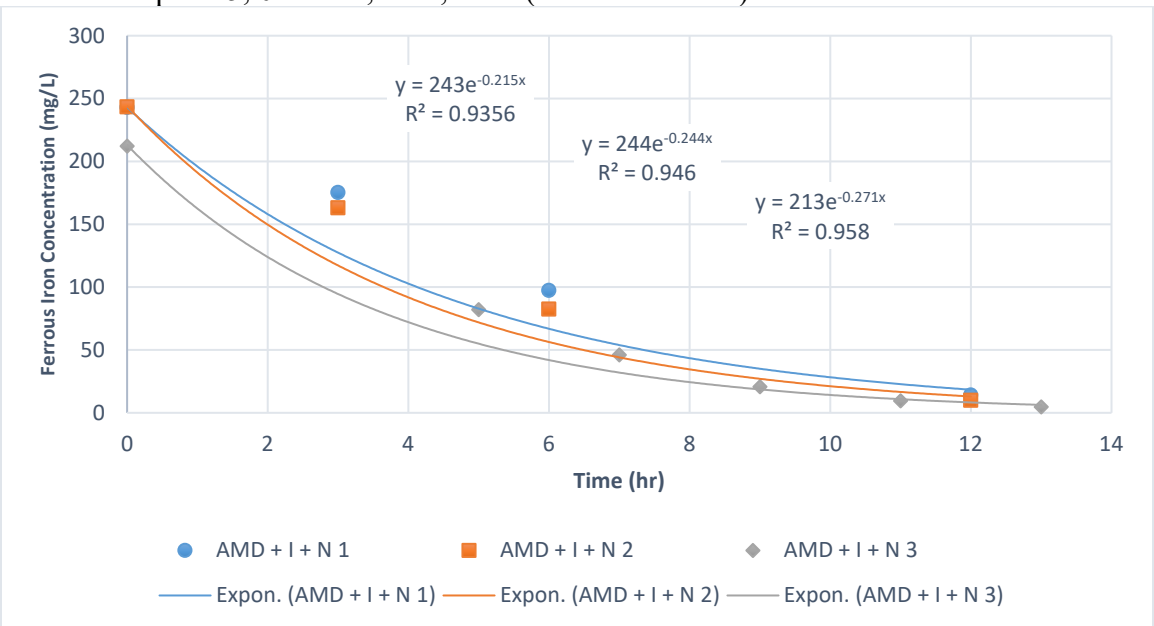

Figure: Ferrous iron oxidation with WR AMD and bacterial inoculum extracted from WR sediment at pH 2.5, 0.1 M N, no P, no C (3rd iron addition)

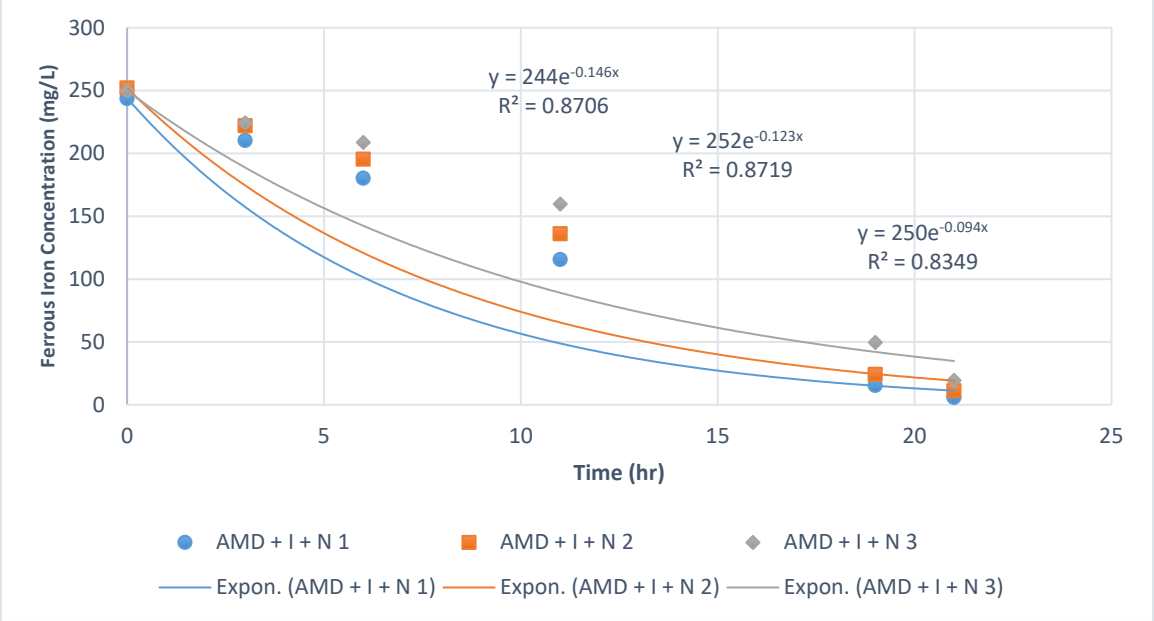

Figure: Ferrous iron oxidation with WR AMD and bacterial inoculum extracted from WR sediment at pH 2.5, 0.1 M N, no P, no C (4th iron addition)

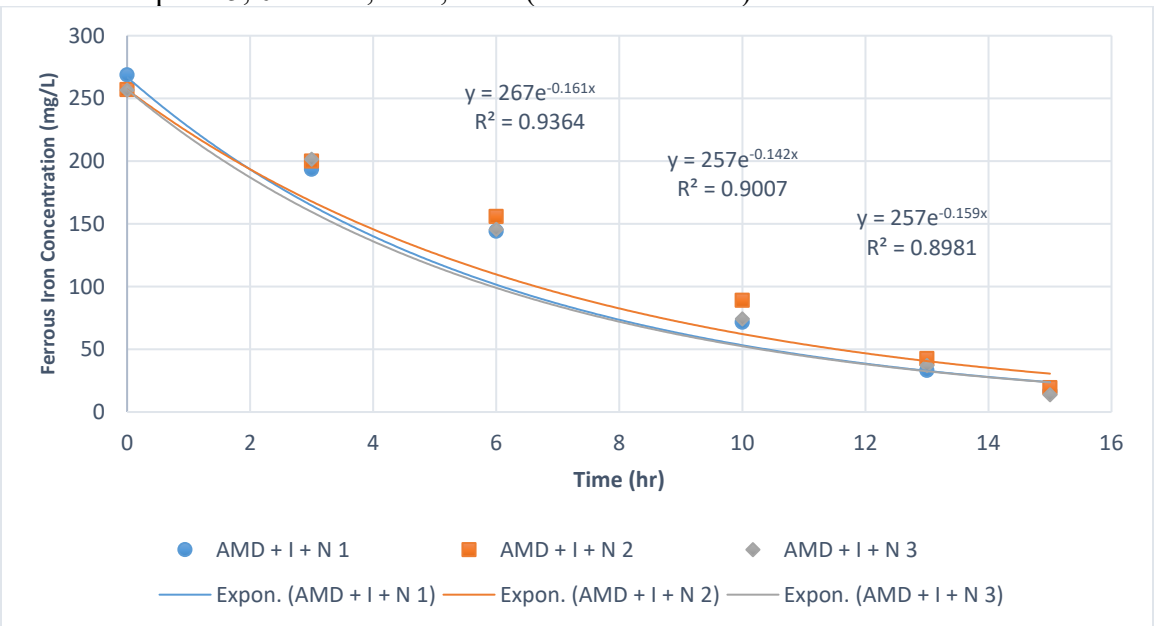

Figure: Ferrous iron oxidation with WR AMD and bacterial inoculum extracted from WR sediment at pH 2.5, 5.0 mM P, no N, no C (1st iron addition)

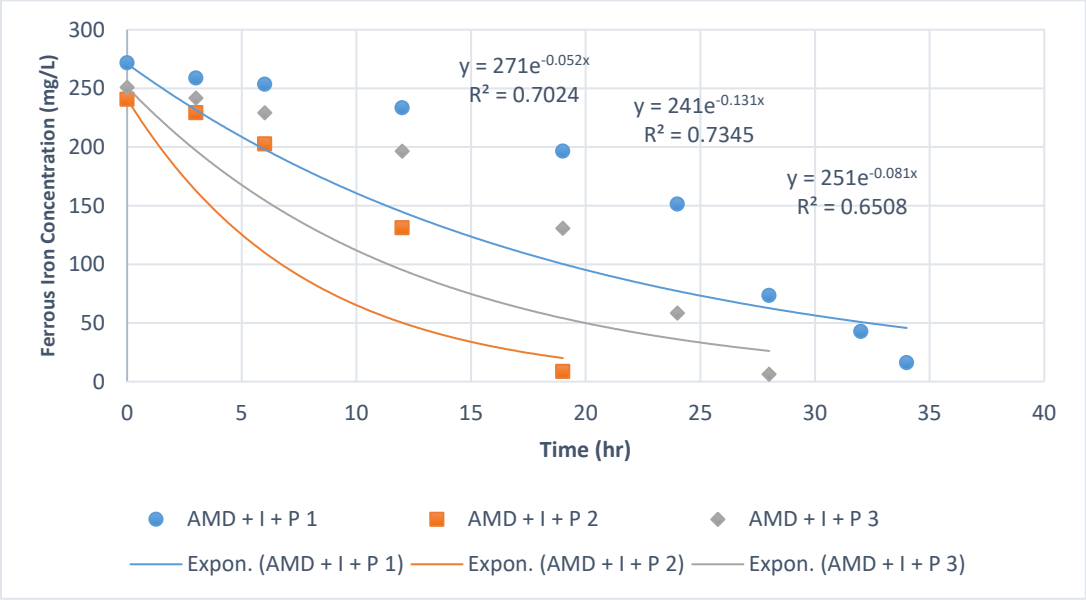

Figure: Ferrous iron oxidation with WR AMD and bacterial inoculum extracted from WR sediment at pH 2.5, 5.0 mM P, no N, no C (2nd iron addition)

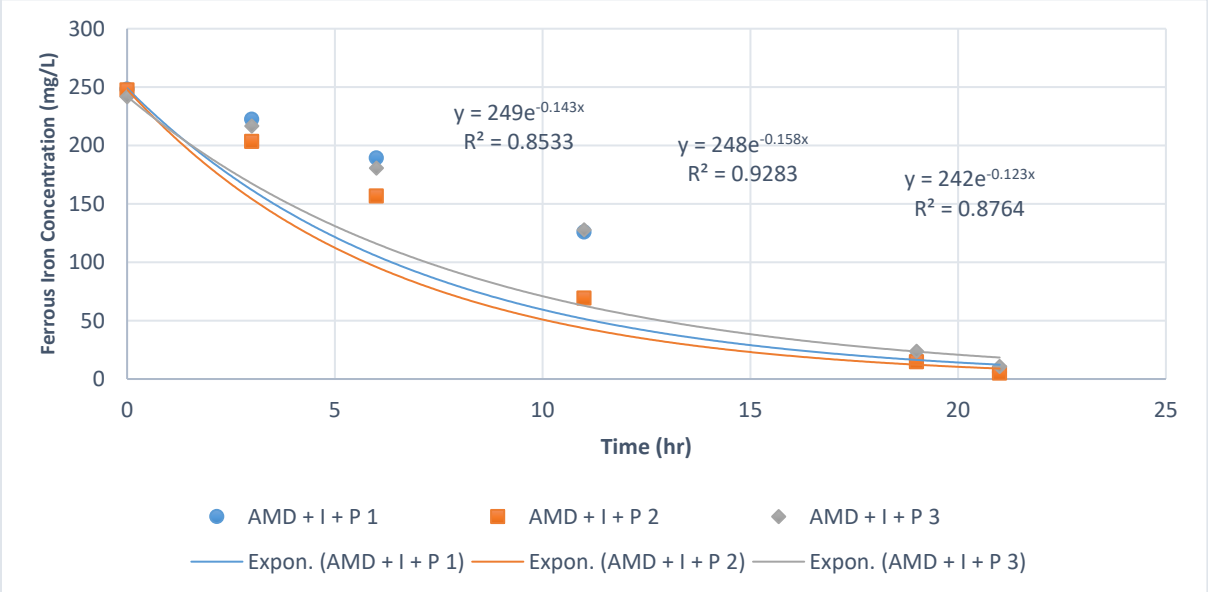

Figure: Ferrous iron oxidation with WR AMD at pH 2.5, 5.0 mM P, 0.1 M N, no C, no inoculum addition (1st iron addition)

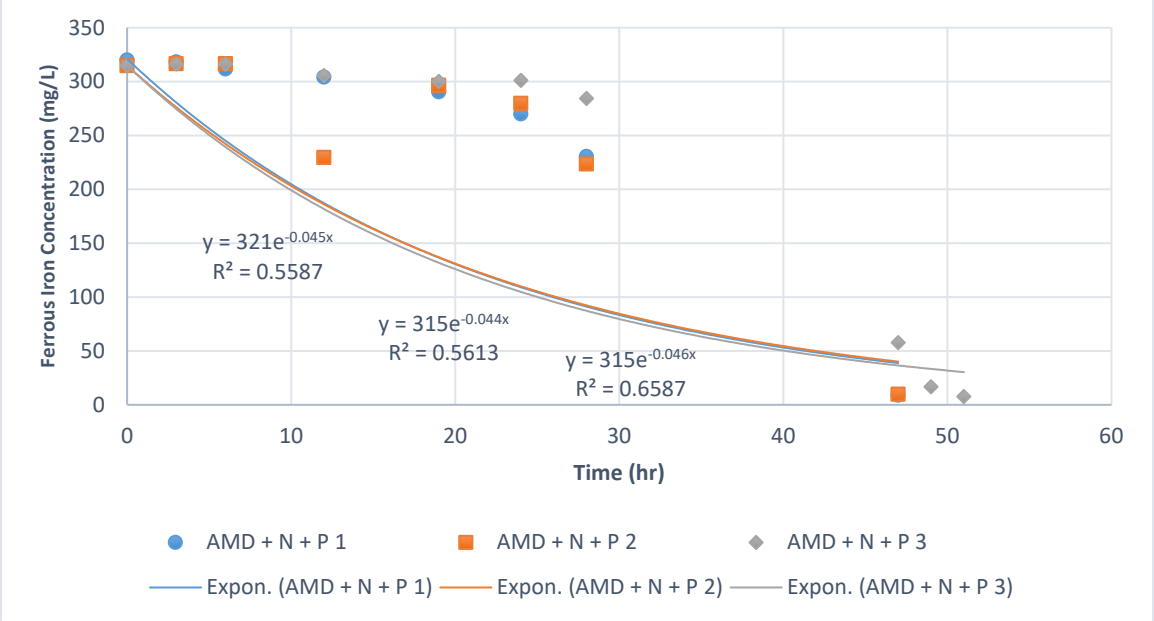

Figure: Ferrous iron oxidation with WR AMD at pH 2.5, 5.0 mM P, 0.1 M N, no C, no inoculum addition (3rd iron addition)

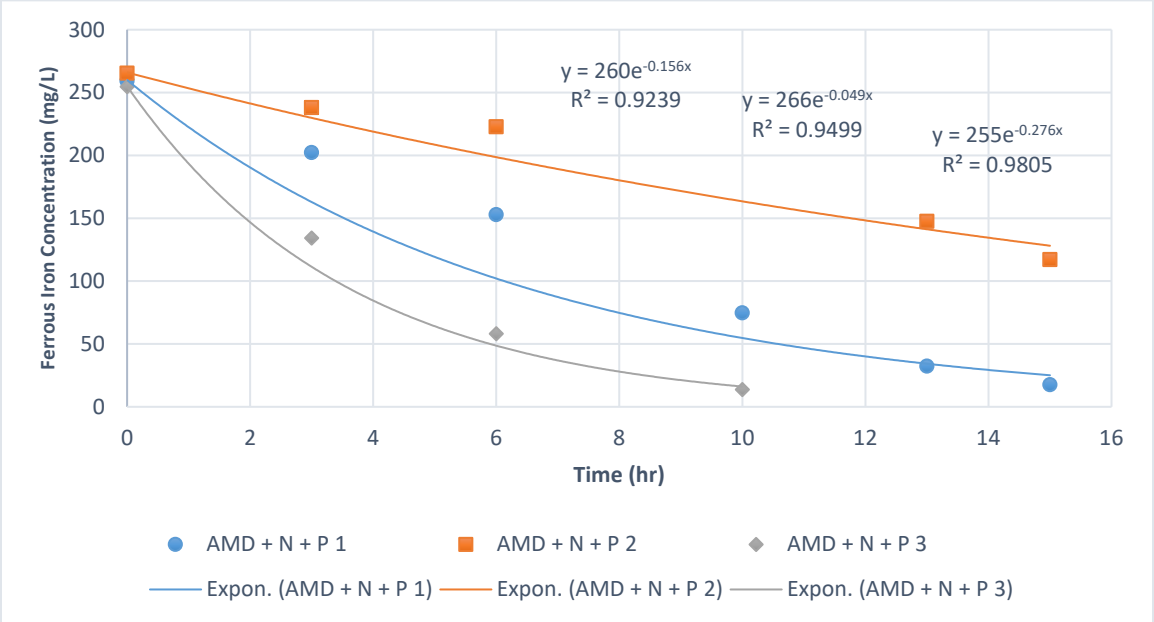

Figure: Ferrous iron oxidation with WR AMD and bacterial inoculum extracted from WR sediment at pH 2.5, 0.1 M N, 5.0 mM P, no C (1st iron addition)

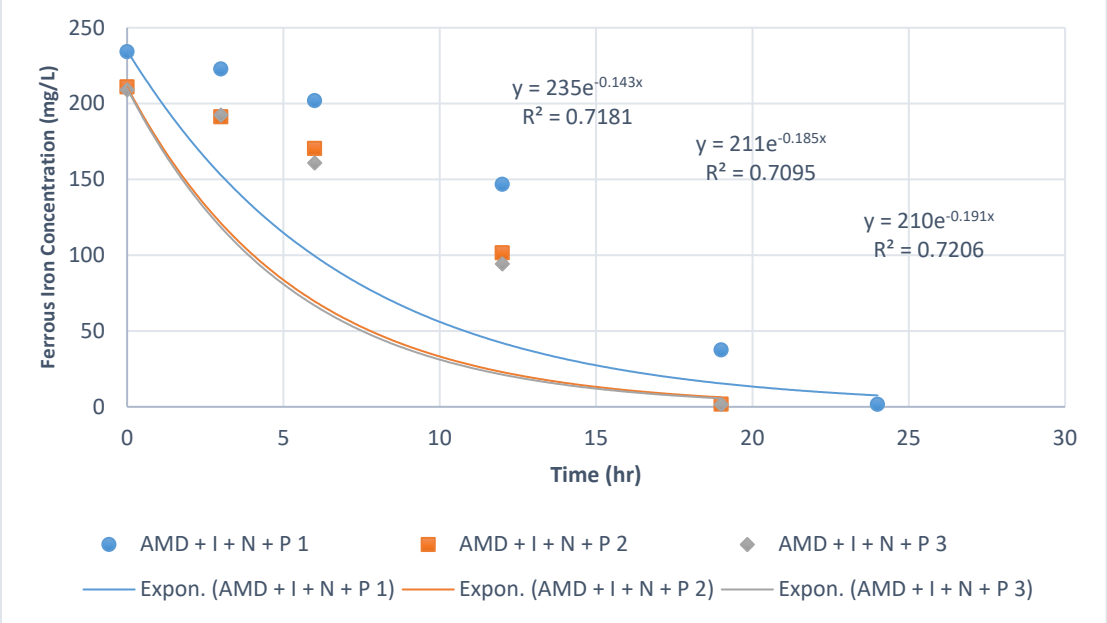

Figure: Ferrous iron oxidation with WR AMD and bacterial inoculum extracted from WR sediment at pH 2.5, 0.1 M N, 5.0 mM P, no C (2nd iron addition)

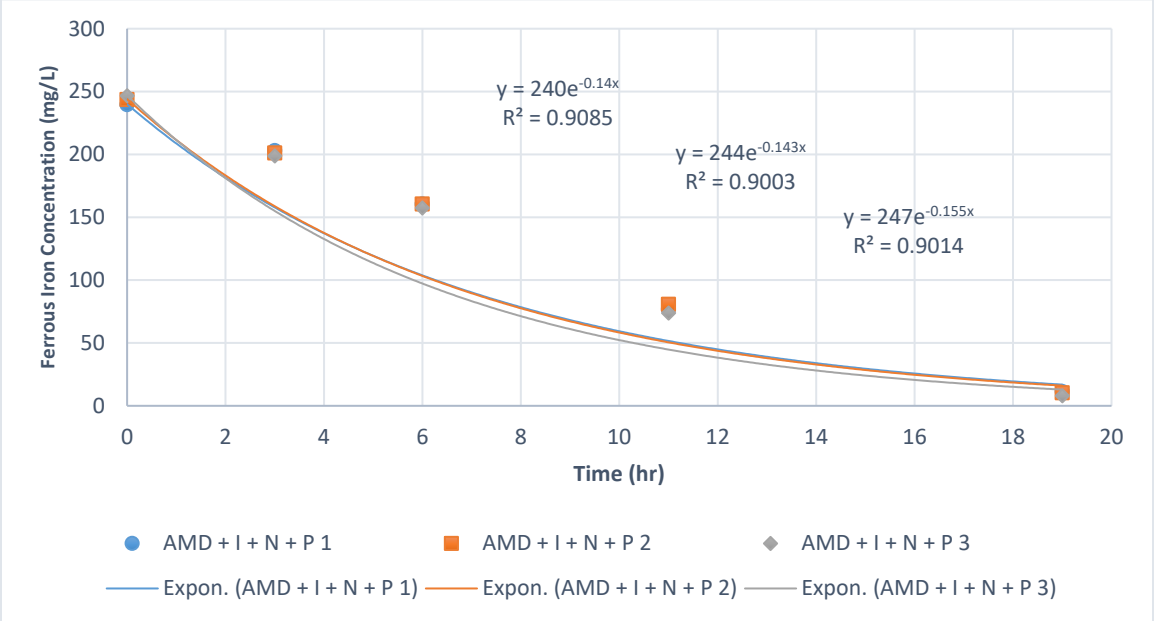

TT Culturing

Figure: Ferrous iron oxidation with TT AMD and bacterial inoculum extracted from WR sediment at pH 2.5, no nutrients addition (2nd iron addition)

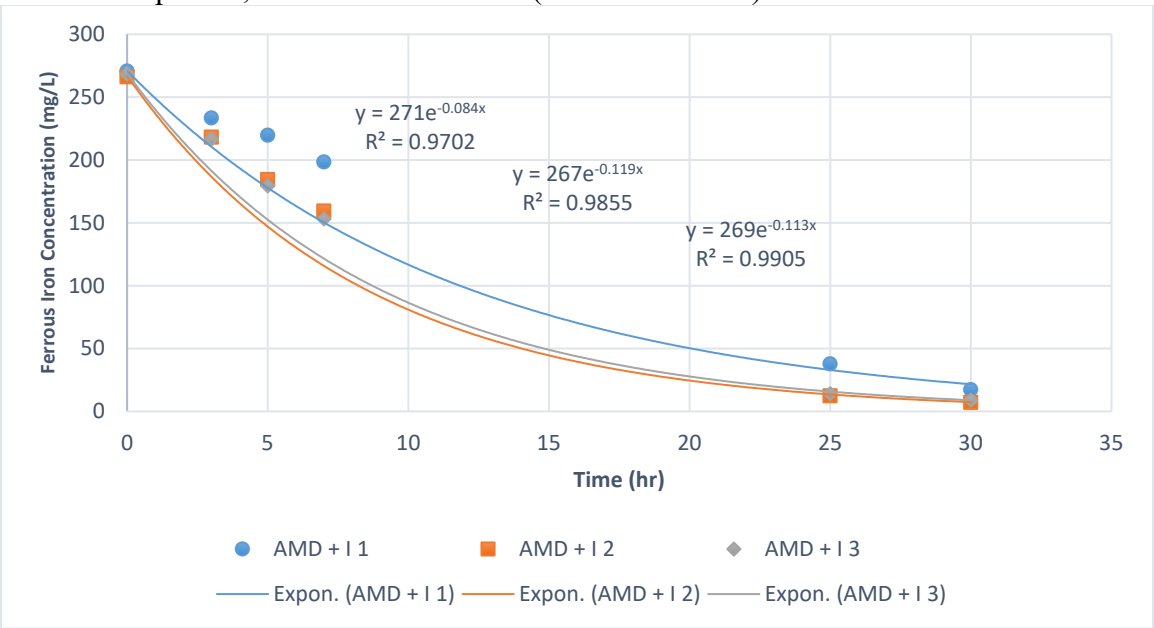

Figure: Ferrous iron oxidation with TT AMD and bacterial inoculum extracted from WR sediment at pH 2.5, no nutrients addition (3rd iron addition)

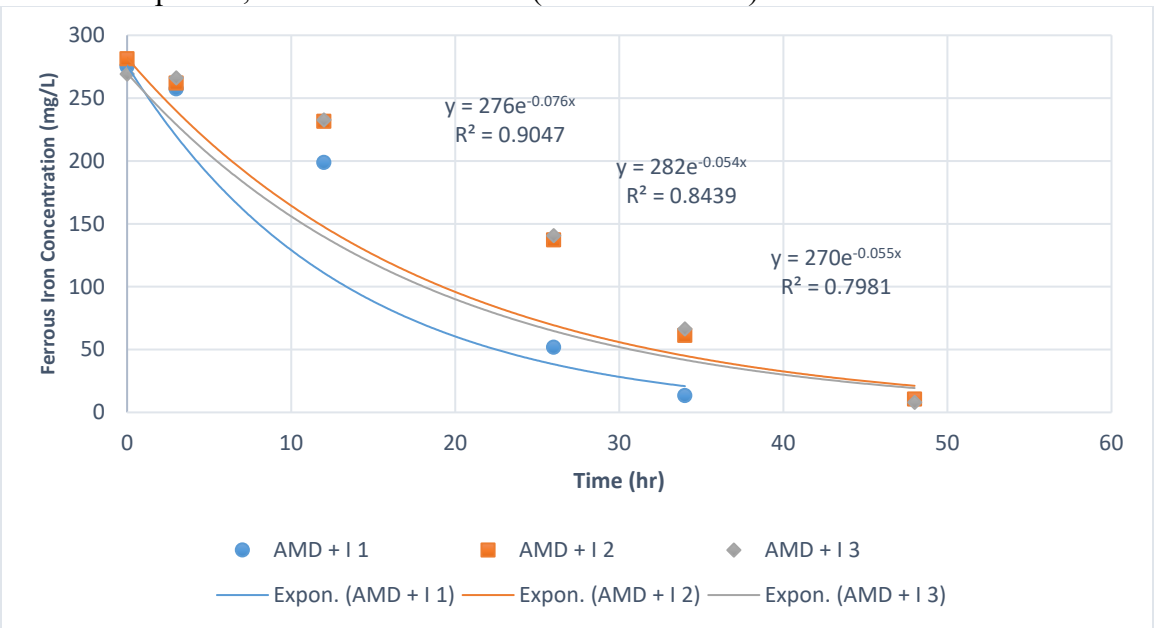

Figure: Ferrous iron oxidation with TT AMD and bacterial inoculum extracted from WR sediment at pH 2.5, 0.1 M N, no P, no C (2nd iron addition)

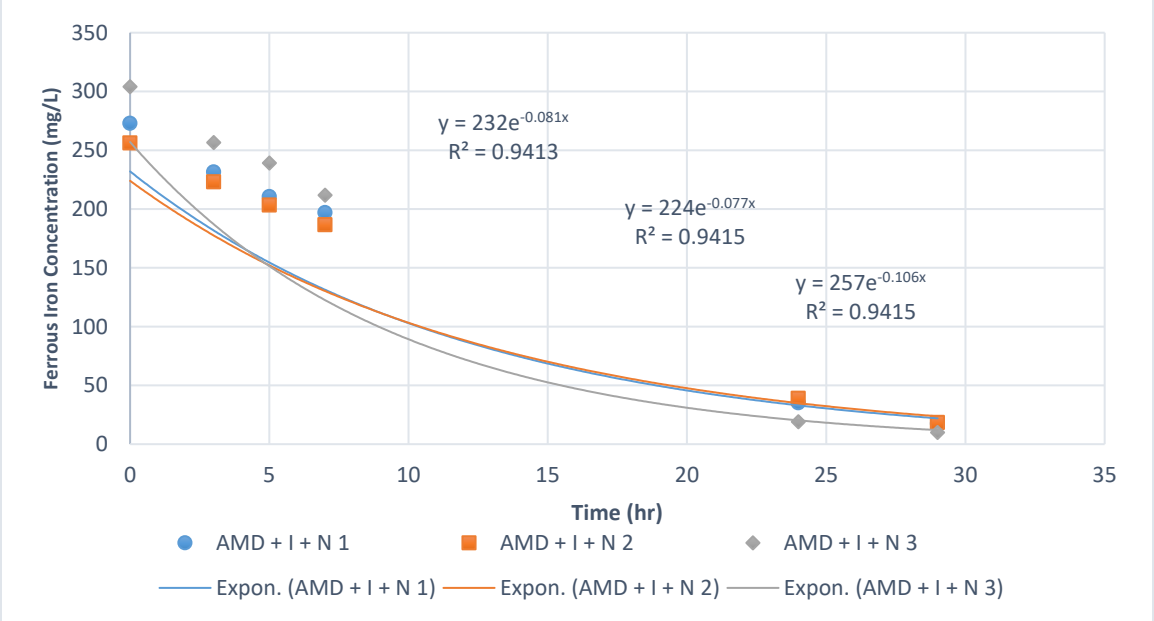

Figure: Ferrous iron oxidation with TT AMD and bacterial inoculum extracted from WR sediment at pH 2.5, 0.1 M N, no P, no C (3rd iron addition)

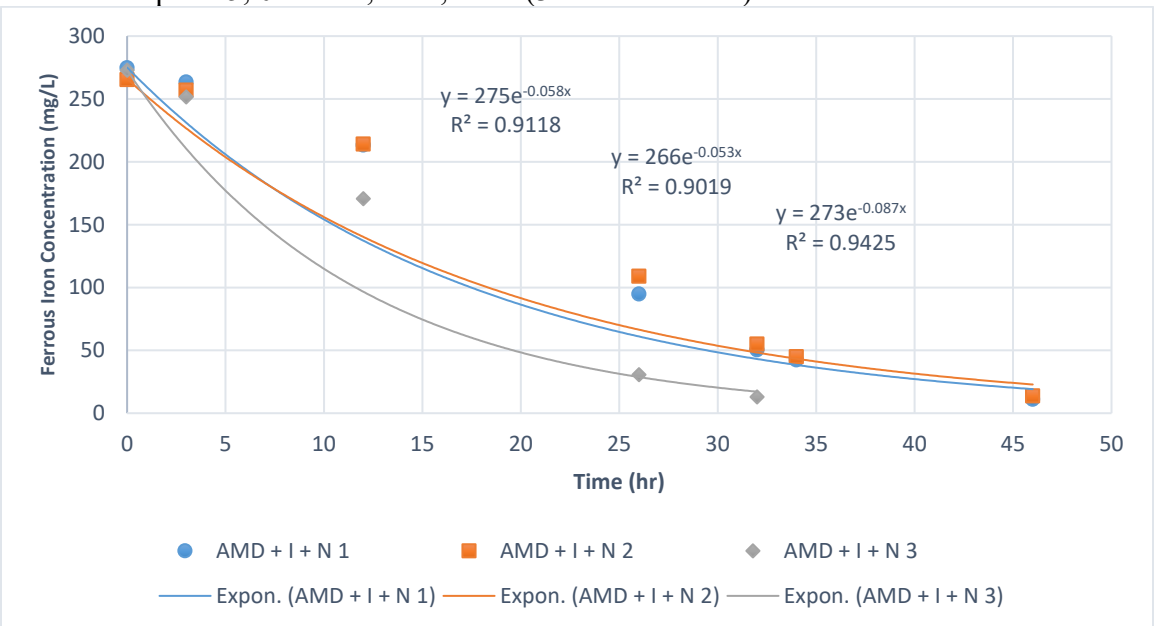

Figure: Ferrous iron oxidation with TT AMD and bacterial inoculum extracted from WR sediment at pH 2.5, 5.0 mM P, no N, no C (1st iron addition)

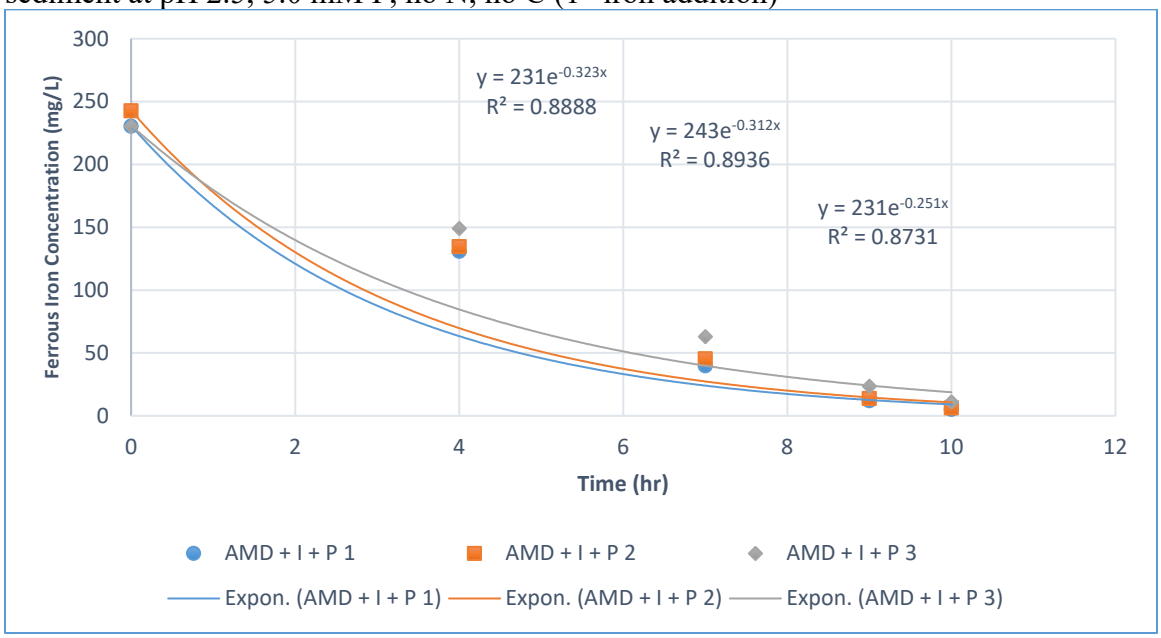

Figure: Ferrous iron oxidation with TT AMD and bacterial inoculum extracted from WR sediment at pH 2.5, 5.0 mM P, no N, no C (3rd iron addition)

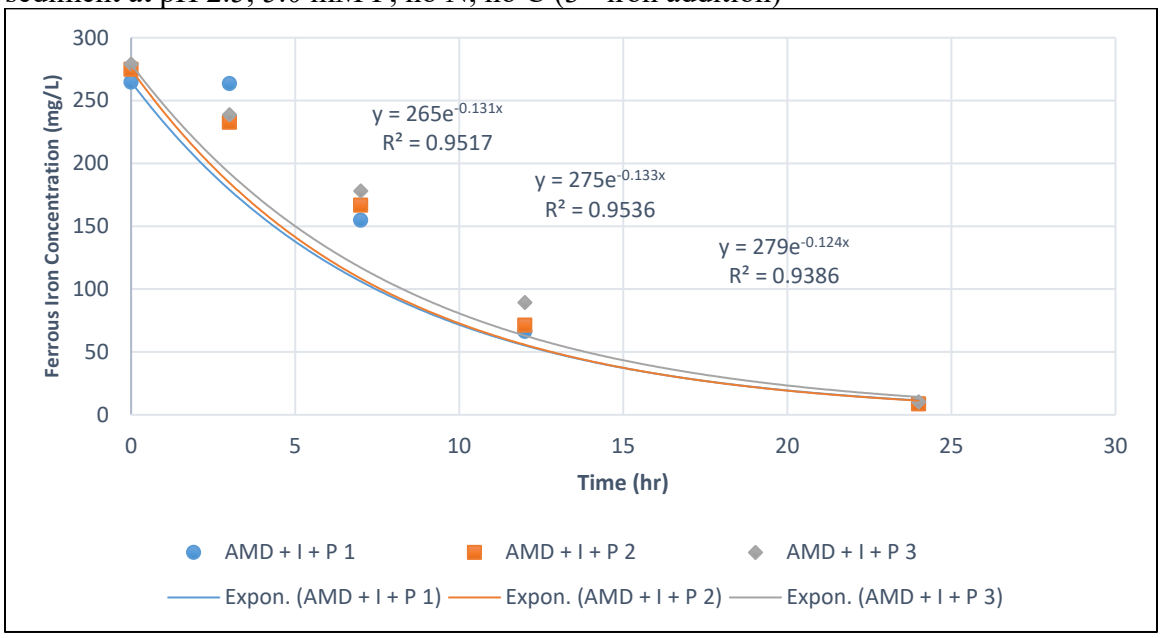

Figure: ferrous iron oxidation rates with TT AMD at pH 2.5, 5.0 mM P, no N, no C, no Inoculum addition (1st iron addition)

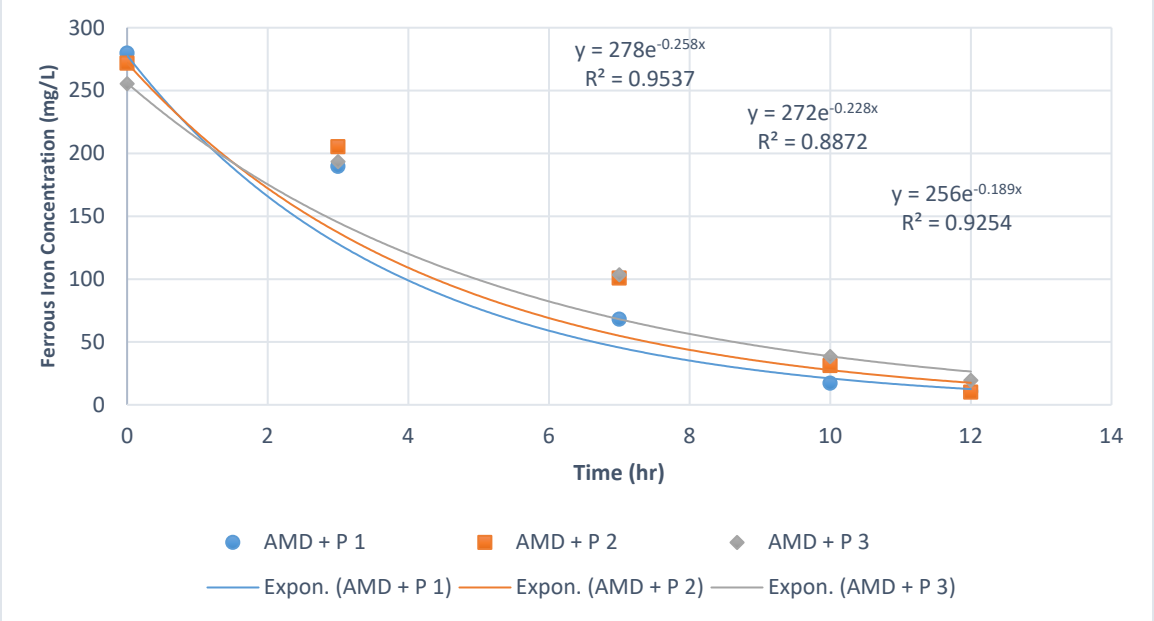

Figure: ferrous iron oxidation rates with TT AMD at pH 2.5, 5.0 mM P, no N, no C, no Inoculum addition (2nd iron addition)

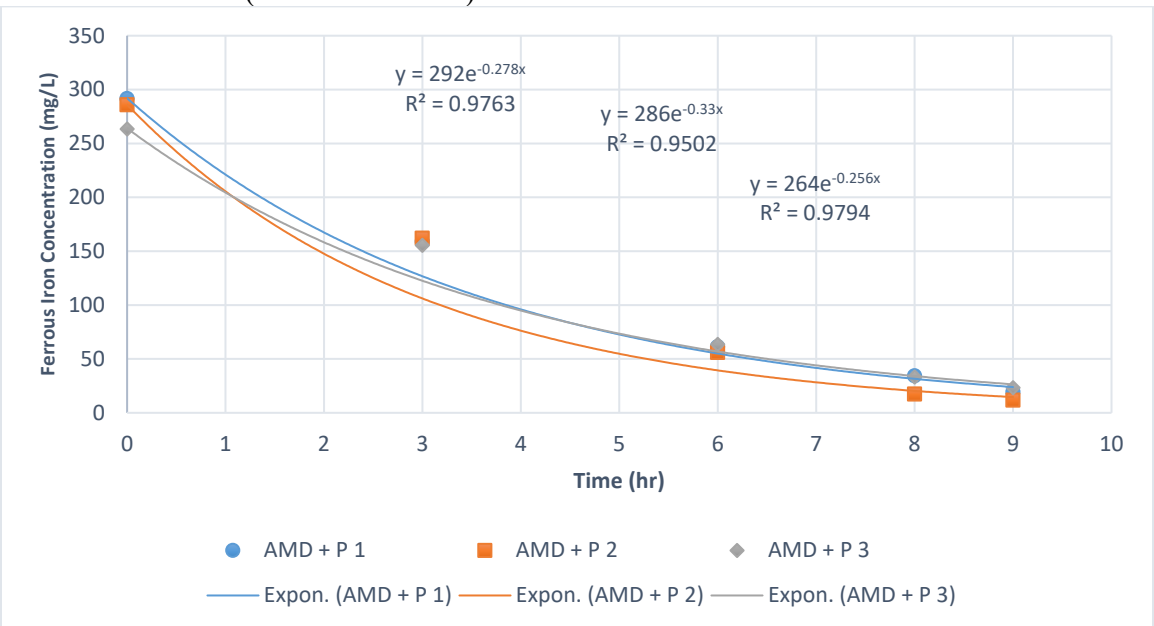

Figure: ferrous iron oxidation rates with TT AMD at pH 2.5, 0.1 M N, 5.0 mM P, no C, no Inoculum addition (1st iron addition)

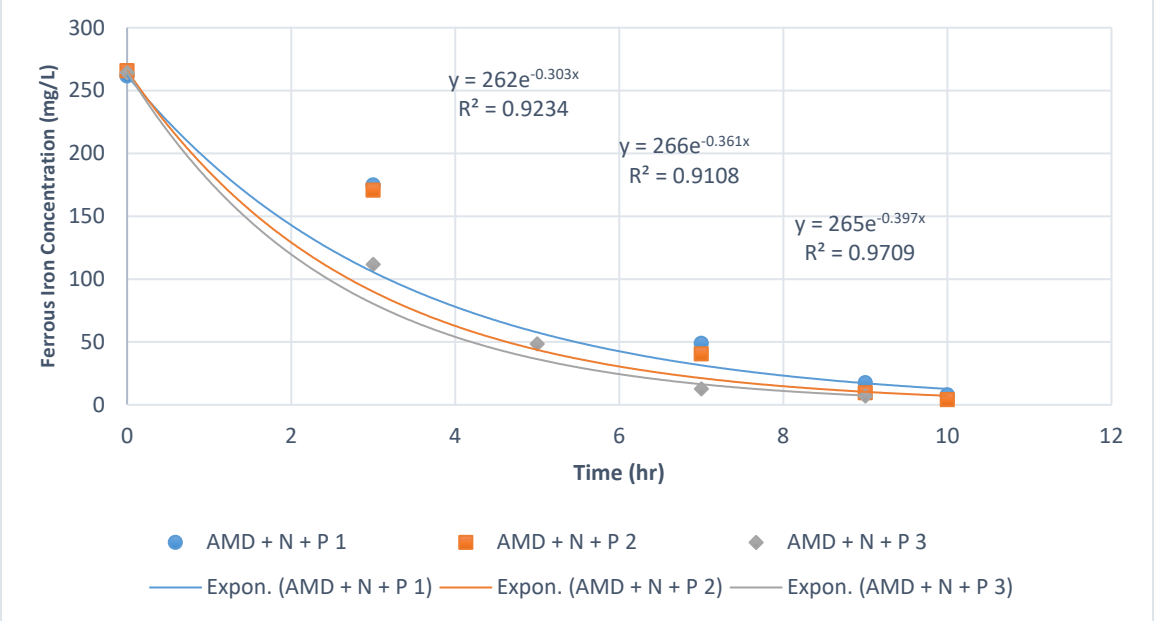

Figure: ferrous iron oxidation rates with TT AMD at pH 2.5, 0.1 M N, 5.0 mM P, no C, no Inoculum addition (2nd iron addition)

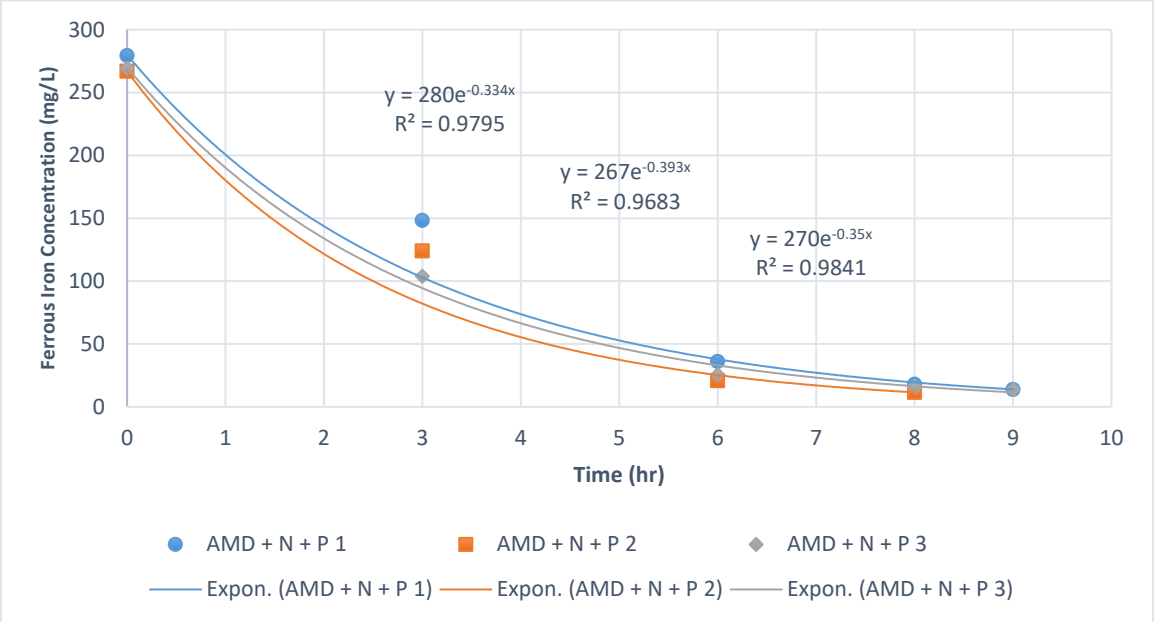

Figure: Ferrous iron oxidation with TT AMD and bacterial inoculum extracted from WR sediment at pH 2.5, 0.1 M N, 5.0 mM P, no C (2nd iron addition)

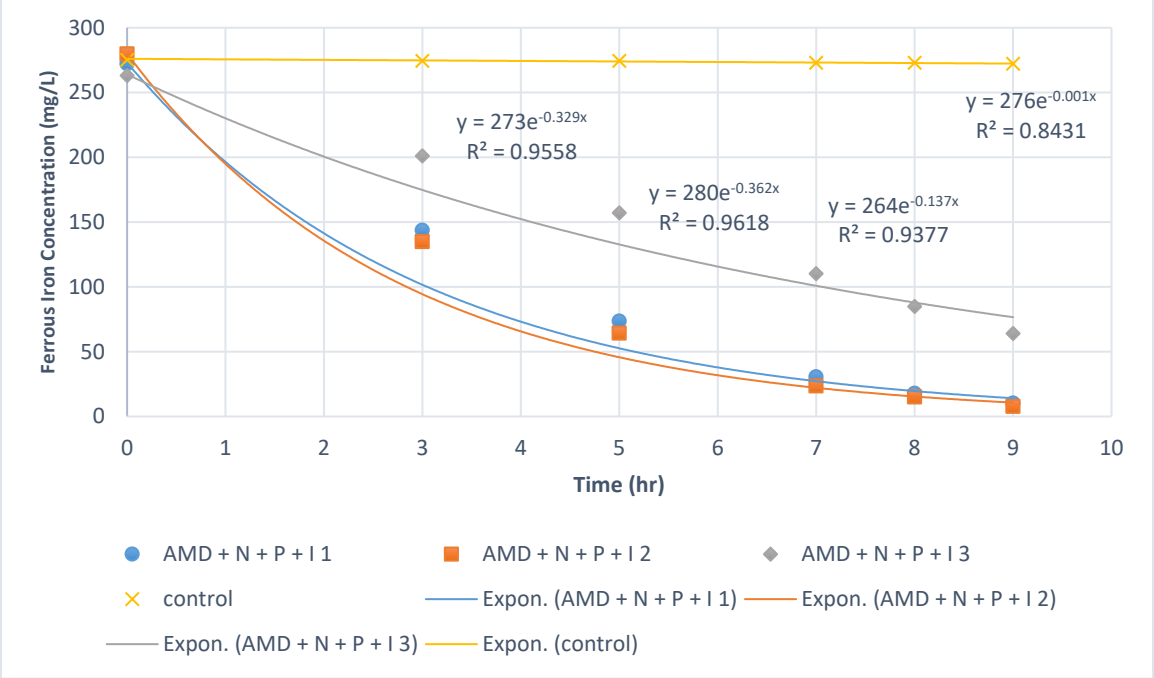

Figure: Ferrous iron oxidation with TT AMD and bacterial inoculum extracted from WR sediment at pH 2.5, 0.1 M N, 5.0 mM P, no C (3rd iron addition)

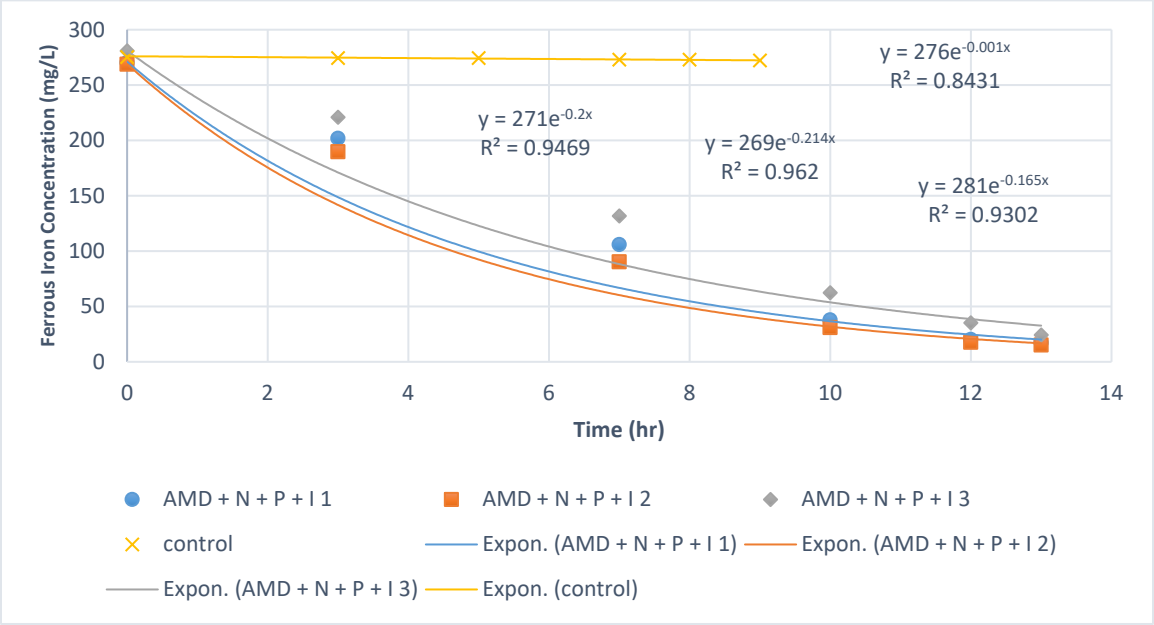

ANOVA Output Tables

pH Test

ANOVA

Culture_pH_test_data

	Sum of Squares	df	Mean Square	F	Sig.
Between Groups	.006	2	.003	1.224	.358
Within Groups	.014	6	.002		
Total	.020	8			

Tests of Homogeneity of Variances

		Levene Statistic	df1	df2	Sig.
Culture_pH_test_data	Based on Mean	3.994	2	6	.079
	Based on Median	.934	2	6	.443
	Based on Median and with adjusted df	.934	2	3.998	.465
	Based on trimmed mean	3.649	2	6	.092

Multiple Comparisons

Dependent Variable: Culture_pH_test_data

Bonferroni

(I) Culture_pH_test	(J) Culture_pH_test	Mean Difference (I-J)	Std. Error	Sig.	98.33% Confidence Interval	
					Lower Bound	Upper Bound
FR_WI_pH_2.5	WR_WI_pH_2.5	.006000	.039786	1.000	-.16186	.17386
	WR_WI_pH_3.0	.056667	.039786	.613	-.11119	.22453
WR_WI_pH_2.5	FR_WI_pH_2.5	-.006000	.039786	1.000	-.17386	.16186
	WR_WI_pH_3.0	.050667	.039786	.750	-.11719	.21853
WR_WI_pH_3.0	FR_WI_pH_2.5	-.056667	.039786	.613	-.22453	.11119
	WR_WI_pH_2.5	-.050667	.039786	.750	-.21853	.11719

Nitrogen Test

ANOVA

WR_NH4_data

	Sum of Squares	df	Mean Square	F	Sig.
Between Groups	.224	3	.075	62.712	<.001
Within Groups	.010	8	.001		
Total	.233	11			

Tests of Homogeneity of Variances

		Levene Statistic	df1	df2	Sig.
WR_NH4_data	Based on Mean	7.065	3	8	.012
	Based on Median	.916	3	8	.475
	Based on Median and with adjusted df	.916	3	3.796	.512
	Based on trimmed mean	6.088	3	8	.018

Multiple Comparisons

Dependent Variable: WR_NH4_data

Games-Howell

(I) WR_NH4	(J) WR_NH4	Mean Difference (I-J)	Std. Error	Sig.	98.75% Confidence Interval	
					Lower Bound	Upper Bound
WR 0.01 M NH4	WR 0.05 M NH4	-.093000	.021053	.110	-.37057	.18457
	WR 0.1 M NH4	-.120333	.039549	.141	-.40225	.16158
	WR 0.5 M NH4	.227000	.021179	.018	-.04157	.49557
WR 0.05 M NH4	WR 0.01 M NH4	.093000	.021053	.110	-.18457	.37057
	WR 0.1 M NH4	-.027333	.033731	.848	-.49019	.43552
	WR 0.5 M NH4	.320000*	.004714	<.001	.28992	.35008
WR 0.1 M NH4	WR 0.01 M NH4	.120333	.039549	.141	-.16158	.40225
	WR 0.05 M NH4	.027333	.033731	.848	-.43552	.49019
	WR 0.5 M NH4	.347333	.033810	.022	-.10922	.80389
WR 0.5 M NH4	WR 0.01 M NH4	-.227000	.021179	.018	-.49557	.04157
	WR 0.05 M NH4	-.320000*	.004714	<.001	-.35008	-.28992
	WR 0.1 M NH4	-.347333	.033810	.022	-.80389	.10922

*. The mean difference is significant at the 0.0125 level.

ANOVA

FR_NH4_data

	Sum of Squares	df	Mean Square	F	Sig.
Between Groups	.023	2	.012	33.600	<.001
Within Groups	.002	6	.000		
Total	.026	8			

Tests of Homogeneity of Variances

		Levene Statistic	df1	df2	Sig.
FR_NH4_data	Based on Mean	3.303	2	6	.108
	Based on Median	1.091	2	6	.394
	Based on Median and with adjusted df	1.091	2	3.399	.430
	Based on trimmed mean	3.091	2	6	.119

Multiple Comparisons

Dependent Variable: FR_NH4_data

Bonferroni

(I) FR_NH4	(J) FR_NH4	Mean Difference (I-J)	Std. Error	Sig.	98.33% Confidence Interval	
					Lower Bound	Upper Bound
FR 0.01 M NH4+	FR 0.05 M NH4+	-.011000	.015249	1.000	-.07534	.05334
	FR 0.1 M NH4+	-.113333*	.015249	<.001	-.17767	-.04900
FR 0.05 M NH4+	FR 0.01 M NH4+	.011000	.015249	1.000	-.05334	.07534
	FR 0.1 M NH4+	-.102333*	.015249	.002	-.16667	-.03800
FR 0.1 M NH4+	FR 0.01 M NH4+	.113333*	.015249	<.001	.04900	.17767
	FR 0.05 M NH4+	.102333*	.015249	.002	.03800	.16667

*. The mean difference is significant at the 0.0167 level.

Phosphorous test

Tests of Homogeneity of Variances

		Levene Statistic	df1	df2	Sig.
WR_PO4_test_data	Based on Mean	4.748	3	8	.035
	Based on Median	1.175	3	8	.378
	Based on Median and with adjusted df	1.175	3	2.837	.454
	Based on trimmed mean	4.381	3	8	.042

ANOVA

WR_PO4_test_data

	Sum of Squares	df	Mean Square	F	Sig.
Between Groups	.072	3	.024	74.729	<.001
Within Groups	.003	8	.000		
Total	.074	11			

Multiple Comparisons

Dependent Variable: WR_PO4_test_data

Games-Howell

(I) WR_PO4_test	(J) WR_PO4_test	Mean Difference (I-J)	Std. Error	Sig.	98.75% Confidence Interval Lower Bound	98.75% Confidence Interval Upper Bound
WR_PO4_0.5mM	WR_PO4_1mM	-.031000*	.002867	.007	-.05554	-.00646
	WR_PO4_5mM	-.197000	.017499	.019	-.43941	.04541
	WR_PO4_10mM	-.120667	.010750	.018	-.26560	.02427
WR_PO4_1mM	WR_PO4_0.5mM	.031000*	.002867	.007	.00646	.05554
	WR_PO4_5mM	-.166000	.017651	.025	-.39660	.06460
	WR_PO4_10mM	-.089667	.010995	.027	-.21827	.03894
WR_PO4_5mM	WR_PO4_0.5mM	.197000	.017499	.019	-.04541	.43941
	WR_PO4_1mM	.166000	.017651	.025	-.06460	.39660
	WR_PO4_10mM	.076333	.020467	.085	-.07074	.22340
WR_PO4_10mM	WR_PO4_0.5mM	.120667	.010750	.018	-.02427	.26560
	WR_PO4_1mM	.089667	.010995	.027	-.03894	.21827
	WR_PO4_5mM	-.076333	.020467	.085	-.22340	.07074

*. The mean difference is significant at the 0.0125 level.

Carbon Test

Tests of Homogeneity of Variances

		Levene Statistic	df1	df2	Sig.
WR_Glucose_test_data	Based on Mean	.833	3	8	.512
	Based on Median	.232	3	8	.872
	Based on Median and with adjusted df	.232	3	6.932	.872
	Based on trimmed mean	.766	3	8	.545

ANOVA

WR_Glucose_test_data

	Sum of Squares	df	Mean Square	F	Sig.
Between Groups	.002	3	.001	.877	.493
Within Groups	.006	8	.001		
Total	.008	11			

WR enrichment

Tests of Homogeneity of Variances

		Levene Statistic	df1	df2	Sig.
WR_AMD_enrichment_data	Based on Mean	3.326	4	10	.056
	Based on Median	.574	4	10	.688
	Based on Median and with adjusted df	.574	4	3.791	.699
	Based on trimmed mean	2.987	4	10	.073

ANOVA

WR_AMD_enrichment_data

	Sum of Squares	df	Mean Square	F	Sig.
Between Groups	.017	4	.004	2.910	.078
Within Groups	.015	10	.001		
Total	.032	14			

Group Statistics

	WR_AMD_enrichment	N	Mean	Std. Deviation	Std. Error Mean
WR_AMD_enrichment_data	WR_AMD_I	3	.13567	.039107	.022578
	WR_AMD_N_P_I	3	.19100	.009165	.005292

Independent Samples Test

		Levene's Test for Equality of Variances		t-test for Equality of Means							
						Significance				95% Confidence Interval of the Difference	
		F	Sig.	t	df	One-Sided p	Two-Sided p	Mean Difference	Std. Error Difference	Lower	Upper
WR_AMD_enrichment_data	Equal variances assumed	2.823	.168	-2.386	4	.038	.075	-.055333	.023190	-.119719	.009053
	Equal variances not assumed			-2.386	2.219	.064	.127	-.055333	.023190	-.146243	.035577

Group Statistics

	WR_AMD_enrichment	N	Mean	Std. Deviation	Std. Error Mean
WR_AMD_enrichment_data	WR_AMD_N_P	3	.16567	.066078	.038150
	WR_AMD_N_P_I	3	.19100	.009165	.005292

Independent Samples Test

		Levene's Test for Equality of Variances		t-test for Equality of Means							
						Significance				95% Confidence Interval of the Difference	
		F	Sig.	t	df	One-Sided p	Two-Sided p	Mean Difference	Std. Error Difference	Lower	Upper
WR_AMD_enrichment_data	Equal variances assumed	10.145	.033	-.658	4	.273	.547	-.025333	.038516	-.132270	.081603
	Equal variances not assumed			-.658	2.077	.288	.576	-.025333	.038516	-.185307	.134640

Group Statistics

	WR_AMD_enrichment	N	Mean	Std. Deviation	Std. Error Mean
WR_AMD_enrichment_data	WR_AMD_N_I	3	.23700	.029715	.017156
	WR_AMD_P_I	3	.19600	.021000	.012124

Independent Samples Test

		Levene's Test for Equality of Variances		t-test for Equality of Means							
						Significance				95% Confidence Interval of the Difference	
		F	Sig.	t	df	One-Sided p	Two-Sided p	Mean Difference	Std. Error Difference	Lower	Upper
WR_AMD_enrichment_data	Equal variances assumed	.869	.404	1.952	4	.061	.123	.041000	.021008	-.017327	.099327
	Equal variances not assumed			1.952	3.599	.065	.131	.041000	.021008	-.019983	.101983

Group Statistics

	WR_AMD_enrichment	N	Mean	Std. Deviation	Std. Error Mean
WR_AMD_enrichment_data	WR_AMD_N_P	3	.16567	.066078	.038150
	WR_AMD_N_I	3	.23700	.029715	.017156

Independent Samples Test

		Levene's Test for Equality of Variances		t-test for Equality of Means							
						Significance				95% Confidence Interval of the Difference	
		F	Sig.	t	df	One-Sided p	Two-Sided p	Mean Difference	Std. Error Difference	Lower	Upper
WR_AMD_enrichment_data	Equal variances assumed	3.498	.135	-1.705	4	.082	.163	-.071333	.041830	-.187473	.044806
	Equal variances not assumed			-1.705	2.777	.097	.194	-.071333	.041830	-.210709	.068042

TT enrichment

Tests of Homogeneity of Variances

		Levene Statistic	df1	df2	Sig.
TT_AMD_enrichment_data	Based on Mean	1.864	3	8	.214
	Based on Median	.350	3	8	.790
	Based on Median and with adjusted df	.350	3	4.637	.792
	Based on trimmed mean	1.673	3	8	.249

ANOVA

TT_AMD_enrichment_data

	Sum of Squares	df	Mean Square	F	Sig.
Between Groups	.061	3	.020	412.706	<.001
Within Groups	.000	8	.000		
Total	.061	11			

Multiple Comparisons

Dependent Variable: TT_AMD_enrichment_data

Bonferroni

(I) TT_AMD_enrichment	(J) TT_AMD_enrichment	Mean Difference (I-J)	Std. Error	Sig.	98.75% Confidence Interval Lower Bound	98.75% Confidence Interval Upper Bound
TT_AMD_I	TT_AMD_N_I	-.044000*	.005720	<.001	-.06957	-.01843
	TT_AMD_P_I	-.129000*	.005720	<.001	-.15457	-.10343
	TT_AMD_N_P_I	-.182333*	.005720	<.001	-.20790	-.15676
TT_AMD_N_I	TT_AMD_I	.044000*	.005720	<.001	.01843	.06957
	TT_AMD_P_I	-.085000*	.005720	<.001	-.11057	-.05943
	TT_AMD_N_P_I	-.138333*	.005720	<.001	-.16390	-.11276
TT_AMD_P_I	TT_AMD_I	.129000*	.005720	<.001	.10343	.15457
	TT_AMD_N_I	.085000*	.005720	<.001	.05943	.11057
	TT_AMD_N_P_I	-.053333*	.005720	<.001	-.07890	-.02776
TT_AMD_N_P_I	TT_AMD_I	.182333*	.005720	<.001	.15676	.20790
	TT_AMD_N_I	.138333*	.005720	<.001	.11276	.16390
	TT_AMD_P_I	.053333*	.005720	<.001	.02776	.07890

*. The mean difference is significant at the 0.0125 level.

Thesis and Dissertation Services